

# Aspects of particle cosmology with an emphasis on baryogenesis

---

Graham Albert White



MONASH University

School of Physics, Monash University

A thesis submitted in partial fulfillment for the  
degree of Doctor of Philosophy

in the

Department of Physics and Astronomy  
Monash University

Supervisor: Csaba Balazs

May 2017

## **Copyright Notices**

### **Notice 1**

Under the Copyright Act 1968, this thesis must be used only under the normal conditions of scholarly fair dealing. In particular no results or conclusions should be extracted from it, nor should it be copied or closely paraphrased in whole or in part without the written consent of the author. Proper written acknowledgement should be made for any assistance obtained from this thesis

### **Notice 2**

I certify that I have made all reasonable efforts to secure copyright permissions for third-party content included in this thesis and have not knowingly added copyright content to my work without the owner's permission.

---

# Contents

---

<b>1</b>	<b>Introduction</b>	<b>11</b>
<b>2</b>	<b>The Standard Model, the hierarchy problem and cosmology</b>	<b>13</b>
2.1	The Standard Model . . . . .	13
2.1.1	Gauge symmetry . . . . .	14
2.1.2	Symmetry breaking and the Higgs sector . . . . .	15
2.1.3	Standard Model Lagrangian . . . . .	15
2.1.4	The hierarchy problem . . . . .	16
2.1.5	Some cosmological shortcomings of the Standard Model . . . . .	17
2.2	Supersymmetry . . . . .	18
2.2.1	Superspace . . . . .	19
2.2.2	Non Interacting Supersymmetric Theories . . . . .	20
2.2.3	Examples of supersymmetric theories . . . . .	21
2.2.4	A brief summary of supersymmetric cosmology . . . . .	22
2.3	The relaxion mechanism: another solution to the hierarchy problem	23
2.3.1	Declaration for thesis chapter 2 . . . . .	23
2.3.2	Published material for chapter 2: Naturalness of the relaxion mechanism . . . . .	26
<b>3</b>	<b>Baryogenesis</b>	<b>53</b>
3.1	Sakharov Conditions . . . . .	53
3.2	Introductory remarks for published material in thesis chapter 3 . . . . .	54
3.3	Declaration for thesis chapter 3 . . . . .	55
3.4	Published material for chapter 3: A pedagogical introduction to electroweak baryogenesis . . . . .	57
3.5	A brief review of thermal field theory . . . . .	97
3.6	The effective potential at finite temperature . . . . .	98
3.6.1	Bubble nucleation . . . . .	99
3.6.2	Transport equations . . . . .	100
<b>4</b>	<b>Solving transport equations during a cosmic phase transitions</b>	<b>101</b>
4.1	Introductory remarks . . . . .	101
4.2	Declaration for thesis chapter 4 . . . . .	101
4.3	Published material for Chapter 4: General analytic methods for solving coupled transport equations: From cosmology to beyond . . . . .	103

<b>5</b>	<b>Solving bubble wall profiles</b>	<b>119</b>
5.1	Introductory remarks . . . . .	119
5.2	Declaration for thesis chapter 5 . . . . .	119
5.3	Published material for chapter 5: Semi-analytic techniques for calculating bubble wall profiles . . . . .	122
<b>6</b>	<b>Particle cosmology in the NMSSM</b>	<b>133</b>
6.1	Introductory remarks . . . . .	133
6.2	Declaration for thesis chapter 6 . . . . .	133
6.3	Published material for chapter 6: Baryogenesis, dark matter and inflation in the Next-to-Minimal Supersymmetric Standard Model . . . . .	136
<b>7</b>	<b>Gravitational waves as a probe of vacuum stability via high scale phase transitions</b>	<b>163</b>
7.1	Introductory remarks . . . . .	163
7.2	Declaration for thesis chapter 7 . . . . .	164
7.3	Published material for chapter 7: Gravitational waves at aLIGO and vacuum stability with a scalar singlet extension of the Standard Model . . . . .	166
<b>8</b>	<b>Effective field theory, electric dipole moments and electroweak baryogenesis</b>	<b>177</b>
8.1	Introductory remarks . . . . .	177
8.2	Declaration for thesis chapter 8 . . . . .	178
8.3	Published material for chapter 8: Effective field theory, electric dipole moments and electroweak baryogenesis . . . . .	180
<b>9</b>	<b>Conclusions and future work</b>	<b>205</b>
	<b>Bibliography</b>	<b>207</b>

# Abstract

Cosmology provides some compelling reasons to expect physics beyond the Standard Model on top of theoretical concerns such as the hierarchy problem and grand unification. In this thesis I explore some of the intersection between particle physics and cosmology with an emphasis on electroweak baryogenesis. I will present original work on whether the relaxion mechanism solves the hierarchy problem, a pedagogical review of electroweak baryogenesis and present research on computational and phenomenological aspects of electroweak baryogenesis and cosmic phase transitions including gravitational wave signals. I also present a new testable paradigm for producing the baryon asymmetry of the Universe as well as an application of effective field theory to directly use experimental constraints to put bounds on CP violating operators.

# List of research outputs

1. G. A. White *A Pedagogical Introduction to Electroweak Baryogenesis* Morgan & Claypool Publishers, IOC concise physics series. 2016 ISBN: 978-1-6817-4457-5
2. C. Balazs, G. White and J. Yue, *JHEP* **1703**, 030 (2017) doi:10.1007/JHEP03(2017)030 [arXiv:1612.01270 [hep-ph]].
3. C. Balazs, A. Fowlie, A. Mazumdar and G. White, *Phys. Rev. D* **95**, no. 4, 043505 (2017) doi:10.1103/PhysRevD.95.043505 [arXiv:1611.01617 [hep-ph]].
4. S. Akula, C. Balázs and G. A. White, *Eur. Phys. J. C* **76**, no. 12, 681 (2016) doi:10.1140/epjc/s10052-016-4519-5 [arXiv:1608.00008 [hep-ph]].
5. A. Fowlie, C. Balazs, G. White, L. Marzola and M. Raidal, “Naturalness of the relaxion mechanism,” *JHEP* **1608**, 100 (2016) doi:10.1007/JHEP08(2016)100 [arXiv:1602.03889 [hep-ph]].
6. G. A. White, “General analytic methods for solving coupled transport equations: From cosmology to beyond,” *Phys. Rev. D* **93**, no. 4, 043504 (2016) doi:10.1103/PhysRevD.93.043504 [arXiv:1510.03901 [hep-ph]].
7. C. Balazs, A. Mazumdar, E. Pukartas and G. White, “Baryogenesis, dark matter and inflation in the Next-to-Minimal Supersymmetric Standard Model,” *JHEP* **1401**, 073 (2014) doi:10.1007/JHEP01(2014)073 [arXiv:1309.5091 [hep-ph]].
8. J. P. Straley, G. A. White and E. B. Kolomeisky, “Casimir energy of a cylindrical shell of elliptical cross section,” *Phys. Rev. A* **87**, no. 2, 022503 (2013) doi:10.1103/PhysRevA.87.022503 [arXiv:1403.3439 [cond-mat.stat-mech]]
9. G. A. White, “Higher entanglement and fidelity with a uniformly accelerated partner via non-orthogonal states,” *Phys. Rev. A* **86**, 032340 (2012) doi:10.1103/PhysRevA.86.032340 [arXiv:1210.3040 [quant-ph]].
10. M. Ramsey-Musolf, G. A. White and P. Winslow “Colour Breaking Baryogenesis,” Anticipated February 2017.
11. S. Akula, C. Balazs and G. A. White, “Exploring baryogenesis in the  $\mathcal{Z}_3$  invariant NMSSM,” Anticipated February 2017.

# General declarations

Monash University

**Declaration for thesis based or partly based on conjointly published or unpublished work**

## General Declaration

In accordance with Monash University Doctorate Regulation 17.2 Doctor of Philosophy and Research Master's regulations the following declarations are made: I hereby declare that this thesis contains no material which has been accepted for the award of any other degree or diploma at any university or equivalent institution and that, to the best of my knowledge and belief, this thesis contains no material previously published or written by another person, except where due reference is made in the text of the thesis. This thesis includes x original papers published in peer reviewed journals. The core theme of the thesis is the study of particle cosmology with an emphasis on electroweak baryogenesis. The ideas, development and writing up of all the papers in the body of the thesis were the principal responsibility of myself, the candidate, working within the School of Physics under the supervision of Csaba Balázs. The inclusion of co-authors reflects the fact that the work came from active collaboration between researchers and acknowledges input into team-based research. My contribution to each of the included works is declared overleaf.

Signed:

A black rectangular box redacting the signature of the candidate.

Graham Albert White

Date:

<i>Thesis Chapter</i>	<i>Publication Title</i>	<i>Status</i>	<i>Nature and % of student contribution</i>	<i>Names and contributions of Monash student coauthors</i>
2	Naturalness of the relaxation mechanism	Published	25% including coding analytic sections, writing some sections and editing the paper. Contributed to ideas throughout	N/A
3	A pedagogical introduction to electroweak baryogenesis	Published	100% (single author)	N/A
4	General analytic methods for solving coupled transport equations: From cosmology to beyond	Published	100% (single author)	N/A
5	Semi-analytic techniques for calculating bubble wall profiles	Published	70% including original concepts and derivation as well as numerical implementation.	N/A
6	Baryogenesis, dark matter and inflation in the Next-to-Minimal Supersymmetric Standard Model	Published	50% involved with numerical implementation as well as analytic derivation and writeup	N/A
7	Gravitational waves at aLIGO and vacuum stability with a scalar singlet extension of the Standard Model	Published	50% involved with numerical implementation as well as analytic derivation and writeup	N/A
8	Effective field theory, electric dipole moments and electroweak baryogenesis	Published	60% including formulating idea and plan for the project. Doing the numerical calculations for the BAU and deriving the major concepts and theorems in the paper.	N/A

## Acknowledgements

I'd like to acknowledge my wife for putting up with me often being preoccupied with research and frequently working late nights and weekends. You are a very kind, patient, gentle and understanding wife and I know this PhD has been difficult for you at times.

I would like to acknowledge Csaba Balazs for his fantastic supervision. He has a great way of talking you up in order to build your confidence. He initially surveyed my skill set and interests and chose a great subject in baryogenesis. He then helped me work through all messy literature on the subject before connecting me with one of the leaders of the field and giving me the confidence to apply for the prestigious American Australian Award. He also gave me the confidence to work independently and pursue ideas I had and convinced me that my work was strong enough to write a review book on the subject.

I would like to thank Michael Ramsey-Musolf for accepting me as a guest scholar and teaching me so many subtle points on baryogenesis.

I would then like to thank my many collaborators: Ernestas Pukartas, Andrew Fowlie, Liam Dunn, Luca Marzola, Jason Yue, Martti Raidal, Sujeet Akula, Peter Winslow, Anupam Mazumdar, Basem El-menoufi and Oleg Popov. I have learnt so much from so many of them and I would not be able to write this thesis without them. I would in particular like to acknowledge Joseph Straley who offered me a very nice RA at a time when they were tricky to find. This allowed me to get a Masters and a paper which resulted in my acceptance into Monash University.

Finally I would like to thank the funding agencies that have made this work possible. In particular I would like to thank the American Australian Association who awarded me the Keith Murdoch Fellowship, the J. L. William Fellowship and the Australian Post Graduate award. I would also like to acknowledge the Center of Excellence for Particle Physics at the Tera Scale (CoEPP) for funding my travel to multiple conferences and workshops.



## *Chapter 1*

---

# Introduction

---

Motivated by the hierarchy problem, theorists have proposed a landscape of models predicting new physics at the weak, or TeV, scale [1, 2, 3, 4, 5]. At the high energy frontier experiments will continue to probe weak and TeV scale physics both at the Large Hadron Collider (LHC) and, hopefully, at higher energy colliders [6]. The Standard Model has thus far survived incredible examination, well beyond the expectations of many. This can lead one to ask if any of the proposed solutions to the hierarchy problem are correct. A no answer would, surprisingly, shatter our notion of the naturalness of our Universe. Whereas a yes answer could lead to one of the richest discovery periods in the history of particle physics.

On the other hand, cosmological data is already decisive in its rejection of the Standard Model. Of the four major pillars of particle cosmology - the baryon asymmetry, dark matter, dark energy and inflation - not one can be explained within the Standard Model. From a certain perspective, the Universe and everything in it including our existence is the data from a "particle accelerator" that reached energies one can never achieve here on Earth. The results are striking! The vast majority of the universe is made up of a combination of dark energy and dark matter - neither of which are accommodated within the Standard Model. Even the abundance of baryonic matter presents a puzzle [7]. The Universe is far more flat and the cosmic microwave background (CMB) is far too isothermal than one would expect and as such inflation has been proposed as necessary ingredient in our cosmic history [8]. However, inflation will washout any initial baryon asymmetry and the Standard Model Cabibbo–Kobayashi–Maskawa (CKM) matrix provides too feeble CP violation and the mass of the Higgs is too heavy to produce the baryon asymmetry of the Universe.

To solve these puzzles, particle physics and cosmology have developed a rich dialogue of late. Electroweak precision studies at both the energy and precision frontier are beginning to make a dent in the parameter space where extra scalar fields can catalyze a strongly first order electroweak phase transition - a key ingredient in electroweak baryogenesis - and a 100 TeV collider might decisively answer this question [9]. Experiments that search for permanent electric dipole moments have improved in their sensitivity very rapidly and all but rule out some popular models of electroweak baryogenesis. Even gravitational waves at eLISA and aLIGO are probing the possibility of electroweak phase transition being strongly first order or multi-step [10, 11, 12].

For dark matter, gravitational lensing in the CMB[13] as well as studies of bullet clusters [14] indeed point to a particle solution to the dark matter problem. The DAMA experiment gives a striking signal [15] whereas the LUX and PANDA experiments are nearing the neutrino background in their search for WIMPs [16, 17]. As to inflation, searches for B modes in the CMB probe inflation, while improved precision in such searches will be able to probe physics at the inflaton scale by examining correlations in density fluctuations. Remarkably particle cosmology might even give insight to physics at the Grand Unification Theory (GUT) scale! [18]

Finally, the precision frontier is also starting to give promising hints - from the flavour anomalies in LHCb and Belle [19, 20, 21, 22] to the anomalous results in  $g-2$  experiments and perhaps these intriguing signals are cracks in the Standard Model [23]. If these cracks widen they could also shed some light into our cosmological history. In other words just about every signal or negative search in any fundamental physical experiment has consequences for the interplay between particle physics and cosmology. It is a young field where many type of research whether it is formal progress, model building, phenomenology or numerical tool is possible.

In this thesis I will look at particular aspects of the interplay between particle physics and cosmology with an emphasis on electroweak baryogenesis. I will begin with a review of the Standard Model and the hierarchy problem in chapter 2 and its most popular solution - supersymmetry - before discussing a particle cosmology inspired solution known as the relaxion method where I will present some of my work (a copyright agreement limits how much I can put into this thesis). I will then focus more closely on baryogenesis in chapter 3 presenting an overview of the subject including the review given in my book before discussing some technical and phenomenological work I have done. Specifically, I will present some work on how to analytically solve sets of coupled transport equations in chapter 4 before applying these techniques to calculating bubble wall profiles in chapter 5. I will then shift gears to focus more exclusively on phenomenology analysing the compatibility of the collider constraints on the NMSSM with particle cosmology constraints in chapter 6 and then in chapter 7 I look at gravitational wave signatures at aLIGO due to high scale phase transitions and how they are physically motivated by vacuum stability. I explore the use of effective field theory in baryogenesis in chapter 8 before concluding in chapter 9

## Chapter 2

---

# The Standard Model, the hierarchy problem and cosmology

---

The Standard Model of particle physics is perhaps the most successful physical model ever tested [24]. It is of course known to be incomplete as it does not describe gravity. This fact requires the Standard Model to be modified at energy levels where gravitational effects become important; the so called "Planck scale". Unfortunately, physics at the Planck scale is potentially well beyond anything that can feasibly be tested on Earth in the foreseeable future. On the other hand, there is some evidence that the Standard Model may be incomplete at energies much lower than the Planck scale. For example, numerous observations show that the Universe is much more massive than the (directly) observable matter of the Universe would suggest [25], the energy scale of the electroweak force in the Standard Model is in a region that requires incredible fine tuning [26], there is more matter than anti-matter in the Universe, and finally there is evidence that the Universe began with a period of incredibly rapid expansion known as "inflation" [8]. There was once hope that the Standard Model could explain the matter/antimatter asymmetry in the universe. However, the recent discovery of a Higgs particle at 125 GeV is far too heavy for electroweak baryogenesis to be viable in the Standard Model. Further, there is little hope that any of the other problems can be solved within the Standard Model.

## 2.1 The Standard Model

For the sake of completeness, let us briefly review the Standard Model before commenting on aspects of its incompleteness. (I will ignore in this thesis the strong CP problem, the existence of neutrino masses, dark energy, quantum gravity and a number of intriguing hints in experimental data). The components of the Standard Model are fermions, scalar fields and gauge bosons which facilitate forces as well as interactions between the scalar and fermionic sectors. The fermions come in two varieties, quarks with non-zero baryon number and leptons with non-zero lepton number. Each fermion has three generations or flavours.

## 2.1.1 Gauge symmetry

The Standard Model is most conveniently formulated in such a way where one introduces redundant degrees of freedom. Physically equivalent states are then related through gauge transformations. The simplest example of this is quantum electrodynamics (QED) where for example it can be convenient to express the electric field as the gradient of a scalar field as well as representing the magnetic field as the curl of a vector field. The cost of this is that one has introduced a redundancy in the theory. For the QED case, the theory is redundant under local phase transformations where fields transform

$$\psi(x) \rightarrow e^{i\alpha(x)}\psi(x). \quad (2.1)$$

The generalization of this is to consider replacing such a local phase transformation with a general set of local transformations belonging to a Lie group.

### Lie groups and the exponential map

In general a continuous symmetry of Nature is described by a Lie group - a group that is also a smooth manifold. The smooth nature of the manifold ensures that the group indeed describes a continuous transformation. Using the fact that

$$e^X = 1 + X + \frac{X^2}{2} + \dots \quad (2.2)$$

and

$$\det[e^X] = e^{\text{Tr}[X]} \quad (2.3)$$

for  $X$  being any square matrix, one can generate elements of a group from the properties of the group. For example, special groups require that the determinant of all members of the group is equal to one. From the above equation I see that this is achieved for the set of matrices,  $X \in \tau$ , that are traceless. It is well known that orthogonal groups have the property that the transpose of a matrix is its inverse. A member of the orthogonal group is generated by the exponential of an antisymmetric matrix. Here, the set  $\tau$  is known as the "Lie algebra" which generates the Lie group by the exponential map. Unfortunately the exponential of  $\tau$  does not generate the entire group. However one can observe that the commutator between any two elements of a Lie algebra is itself a member of the algebra. For example, for a unitary group whose Lie algebra is the set of antihermitian matrices (or equivalently  $i$  multiplied by a hermitian matrix as is convention amongst physicists) one can see that

$$\text{let } A = [X_1, X_2] \quad (2.4)$$

$$A^\dagger = (X_1 X_2)^\dagger - (X_2 X_1)^\dagger \quad (2.5)$$

$$= X_2^\dagger X_1^\dagger - X_1^\dagger X_2^\dagger \quad (2.6)$$

$$= X_2 X_1 - X_1 X_2 = -[X_1, X_2] = -A \in \tau. \quad (2.7)$$

Next we make use of the Baker-Campbell-Herstoff theorem, which states that

$$e^A e^B = \exp\left[A + B + \frac{1}{2}[A, B] + \dots\right] \quad (2.8)$$

where all terms in the unwritten sum are just functions of the commutators between  $A$  and  $B$ . Therefore if  $\exp[A]$  and  $\exp[B]$  are members of the Lie group,  $\mathcal{G}$  then

$\exp[A] \times \exp[B] \in \mathcal{G}$ . One can then use the set  $\exp[\alpha A]$  where  $A \in \tau$  to completely map a finite region of the group around the identity. It is customary for  $\alpha$  to be infinitesimal and this region to therefore also be infinitesimal but this need not be the case. If one can completely cover a region around the identity then one can use a series of products to generate the entire connected region of the group. The proof of this will not be repeated here. For an example consider the case of SU(2) which is one of the gauge groups of the Standard Model. Since it is a special group the Lie algebra generators must be traceless and Hermitian (since I will include a factor of  $i$  in the exponential). The 2 in SU(2) implies that the generating matrices are  $2 \times 2$  matrices. Specifically they are the Pauli matrices

$$\sigma_i = \left[ \begin{pmatrix} 0 & 1 \\ 1 & 0 \end{pmatrix}, \begin{pmatrix} 0 & i \\ -i & 0 \end{pmatrix}, \begin{pmatrix} 1 & 0 \\ 0 & -1 \end{pmatrix} \right]. \quad (2.9)$$

It is easy to see that these matrices obey the commutation relations

$$[\sigma_i, \sigma_j] = 2i\epsilon_{ijk}\sigma_k. \quad (2.10)$$

Therefore the product of two elements of the SU(2) group is also an element of the group.

## 2.1.2 Symmetry breaking and the Higgs sector

The Standard Model gauge product group is  $SU(3)_C \times SU(2)_L \times U(1)_Y$ , and its terms are known as colour, weak isospin and hypercharge group, respectively. It is difficult to give Standard Model particles a tree level mass without violating gauge symmetry. One mechanism to do this though is known as the Anderson-Higgs mechanism [27, 28] where a scalar field with gauge symmetries  $SU(2)_L$  and  $U(1)_Y$  acquires a vacuum expectation value (vev). Specifically, if the Higgs field has an effective potential

$$V(H) = -\mu^2|H|^2 + \lambda|H|^4 \quad (2.11)$$

with  $H = (H^+, H^0)^T$ , the potential has a minimum that is not invariant under  $SU(2)_L$  and  $U(1)_Y$  transformations. I am free to choose the direction of the vev within the Higgs internal space. Let us choose the vev  $v$  such that

$$H = \begin{pmatrix} H^+ \\ (h_r + h_I + v)/\sqrt{2} \end{pmatrix}. \quad (2.12)$$

Fermions acquire masses through Yukawa interactions where the Yukawa coupling times the vev are an effective mass term. Three linear combinations of gauge bosons acquire a mass through the kinetic term in the Lagrangian. Specifically, these particles are the  $W_{\pm}$ , and  $Z$  bosons.

## 2.1.3 Standard Model Lagrangian

I now have all the necessary pieces to form the Standard Model Lagrangian

$$\mathcal{L}_{\text{SM}} = \mathcal{L}_{\text{Kinetic}} + \mathcal{L}_{\text{gauge}} + \mathcal{L}_{\text{Yukawa}} + V(H) \quad (2.13)$$

where  $V(H)$  is given in equation (2.11). The kinetic terms are given by

$$\mathcal{L}_{\text{Kinetic}} \equiv \sum_f \bar{f} \not{D} f + D_\mu H D^\mu H \quad (2.14)$$

with  $D_\mu \equiv \partial_\mu + ig\tau^a A_\mu^a$  is the covariant derivative for the gauge group with Lie generators  $\tau^a$ . The covariant derivatives for the Higgs and left handed fermions contain gauge bosons for weak isospin ( $SU(2)_L$ ) whereas right handed fermions do not. The covariant derivative of all Standard Model fermions and the Higgs boson include gauge bosons for hypercharge ( $U(1)_Y$ ) and finally the covariant derivative of both left and right handed quark fields have gauge bosons for colour ( $SU(3)_C$ ). The full set of fermions are three generations of quark doubles ( $(U_{Li}, D_{Li})^T$ ) and their right handed counter parts as well as three generations of Lepton doublets ( $(\nu_{Li}, e_{Li})$ ) and the right handed partner of the three generations of the electrons ( $e_{Ri}$ ). The gauge sector terms have the form

$$\mathcal{L}_{\text{gauge}} \equiv \frac{1}{4} \text{Tr}[G_{\mu\nu}^a G^{a,\mu\nu}] + \frac{1}{4} \text{Tr}[B_{\mu\nu}^a B^{a,\mu\nu}] + \frac{1}{4} Y_{\mu\nu} Y^{\mu\nu} \quad (2.15)$$

with  $G_{\mu\nu}$ ,  $B_{\mu\nu}$  and  $Y_{\mu\nu}$  being the field strength tensors for the Standard Model gauge groups  $SU(3)_C$ ,  $SU(2)_L$  and  $U(1)_Y$  respectively. Generically the field strength tensors have the form

$$\tau^a G_{\mu\nu}^a = \frac{1}{g_s} [D_\mu, D_\nu] \quad (2.16)$$

and similarly for the other gauge groups. Finally the Yukawa terms have the form

$$\mathcal{L}_{\text{Yukawa}} \equiv Y_u \bar{U}_L U_R H_0 - Y_u \bar{D}_L U_R \phi^- + Y_d \bar{U}_L D_R \phi^+ + Y_d \bar{D}_L D_R \phi_0 \quad (2.17)$$

where  $Y_d$  and  $Y_u$  are  $3 \times 3$  matrices in flavour space.

## 2.1.4 The hierachy problem

The Higgs boson should receive corrections to its mass from any new physics particles via radiative corrections. Suppose new physics appears at some scale  $\Lambda$  and couples to the Standard Model with some coupling  $g_{f,b}$ , the mass of the Higgs acquires quadratic corrections of the form

$$\Delta m_H^2 = c_{f,b} \frac{g_{f,b}^2}{16\pi^2} \Lambda^2 + \dots \quad (2.18)$$

where  $c_{f,b} = (-2, 1)$  for fermions and bosons respectively [26]. One does have a tree level bare mass term to cancel against the quadratic corrections. However, if the scale of new physics is  $n$  orders of magnitude above the weak scale, the first  $\sim 2n$  decimal places must cancel the loop corrections in order for the mass to be weak scale. There is expected to be new physics at the Planck scale – a full 17 orders of magnitude higher than the weak scale! Aside from the stability of the Higgs mass, the weak scale value of the vacuum expectation value is also unstable because it receives tree level corrections from any other scalar particles that might acquire a vacuum expectation value. For example, suppose there is an additional scalar field,  $S$ , that is a singlet under the Standard Model gauge group. In principle there can be many such scalar particles each with a vev at an arbitrary scale. Such a particle

couples to the Higgs via portal couplings  $g_{hs}H^2S^2$ . Replacing  $S$  with its vev, this portal coupling becomes an effective correction to  $\mu^2$ . Again, it requires a fine tuned cancellation for the Higgs vev to be weak scale (of course it is also possible that no new scalar singlets exist).

### 2.1.5 Some cosmological shortcomings of the Standard Model

Outside the hierarchy problem some of the most convincing reasons to look beyond the Standard Model are cosmological. Of particular interest to particle physicists are inflation, dark matter and baryogenesis.

#### Inflation

One of the strongest pieces of evidence for the Big Bang cosmological model is that it correctly predicts cosmic microwave background radiation (CMB). However, measurements of the CMB show that the universe is very much in thermal equilibrium. The troubling aspect of this is that in the expansion of the universe regions of the universe which one observes to be in thermal equilibrium are causally disconnected. This is known as the horizon problem. A solution was proposed by Alan Guth who noted that as the Universe expands, the Higgs field undergoes a phase transition as it cools [8]. If the Higgs field supercools, in a process similar to the supercooling of water, the Higgs field will not undergo the phase transition when the temperature falls below the critical temperature at which the change of phase normally occurs. During the phase of supercooling a large negative pressure drives the universe to expand exponentially fast. Then, once the phase transition occurs, latent heat is released into the Universe. This solves the horizon problem by allowing the Universe to obtain thermal equilibrium before the period of inflation occurs. Unfortunately, there are many problems with using the Higgs field as the driver of inflation. This motivates the need to look beyond the Standard Model to facilitate inflation.

#### Dark matter

It was first observed by Zwicky [29] that velocity dispersions in the Coma and Virgo galaxy clusters were large than expected based on their visible mass. Later, Rubin and others confirmed the missing mass [30, 31, 32]. This has traditionally inspired two explanations: some modification of Newton's law at large distance, or some new form of matter that does not interact with light commonly referred to as dark matter. Several observations contribute substantially to the popularity of the dark matter explanation. First the behaviour of two colliding galaxy clusters known as the Bullet cluster is consistent with dark matter but inconsistent with the most popular modified gravity models. Second the scale of angular fluctuations in the CMB has a spectrum consisting of a peak for baryonic matter followed by successive peaks. This is predicted by dark matter but difficult to explain through modified gravity [33]. Finally there is the circumstantial evidence known as the so called "WIMP miracle" where if one assumes that the dark matter particle has a weak scale mass the right dark matter relic abundance is achieved for a weak scale cross section [34]. The Standard Model does not have a viable dark matter candidate so to explain this part of cosmology one needs to go beyond the Standard Model. Furthermore the

simplest extension of the Standard Model, massive neutrinos, can be a component of dark matter. However, they will not have enough mass density to explain all of dark matter.

## Baryogenesis

If one has a cosmic history that includes inflation, then one cannot have an asymmetry between baryons and anti-baryons as an initial condition as any initial baryon asymmetry would be washed out by inflation. Therefore one must produce it dynamically.<sup>1</sup> I will be primarily interested in electroweak baryogenesis which occurs during the electroweak phase transition [35]. As I will explain in later chapters the Standard Model fails to provide an explanation for this observed asymmetry.

## 2.2 Supersymmetry

The Higgs sector of the Standard Model is unique in that it describes the dynamics of a *scalar* quantum field. The superficial degree of divergence of a scalar field theory with a quartic interaction term is quadratic in the momentum cutoff which is a much more dramatic divergence than the rest of the Standard Model which diverges only logarithmically. However, since the masses of the weak gauge bosons (as well as the Higgs mass itself) depend upon the quadratically divergent Higgs mass, their masses should be of the order of the square of the momentum cutoff. Not only would this give masses well outside what is observed experimentally, the weak scale masses are strongly constrained to within about an order of magnitude of what is observed by the "unitarity bound" and the "perturbativity bound". The Standard Model is inconsistent outside this region. Strictly speaking it is actually possible within the Standard Model to achieve renormalized masses within these bounds as one has a free parameter, the bare mass, which one can fine tune to get the required values [26].

Much like the fact that once upon a time Geocentric models of the Universe needed to be fine tuned in order to be consistent with observation was actually a hint of new physics, the fine tuning required in the Standard Model may have given us hints at how to extend it [36]

That the *superficial* degree of divergence is worse than logarithmic for a quartic scalar field theory is not unique. Quantum electrodynamics, for example, superficially diverges worse than logarithmically. However, both Lorentz and gauge symmetries conspire to reduce the actual degree of divergence. The fact that the Higgs field does not have a local gauge symmetry in essence means that the actual degree of divergence remains quadratic [24]. Naturally, if one could find a new symmetry of nature one could reduce the degree of divergence. Historically, there were many attempts to extend the Poincare group, in particular to find a symmetry group that would contain space time symmetries and internal symmetries in a single group. Ultimately all of these failed and in 1967, Coleman and Mandula proved a "no go" theorem that showed that you cannot extend the symmetries of the Standard Model in a non-trivial way [37]. The theorem was flawed however as it failed to take into account the spinor like nature of quantum particles [38]. Even still, through this

---

<sup>1</sup>Note that with arbitrarily large fine tuning one can evade this claim.

came the realization that there is only one unique extension to spacetime, the theory now known as "supersymmetry".

## 2.2.1 Superspace

### Graded Lie groups and a violation of the Coleman-Mandula theorem

The symmetry that describes supersymmetry is in fact not a Lie group but a “graded” Lie group [39]. A graded Lie group differs from a Lie group in that its associated Lie algebra is closed under anti-commutation rather than commutation. The full graded group is semi-simple and is described by the set of charges  $\{P_\mu, M_{\mu\nu}, Q\}$ . These charges obey the following relations

$$[P_\mu, P_\nu] = 0, \quad (2.19)$$

$$[M_{\mu\nu}, P_\lambda] = i(\eta_{\nu\lambda}P_\mu - \eta_{\lambda\mu}P_\nu), \quad (2.20)$$

$$[M_{\mu\nu}, M_{\nu\rho}] = i(\eta_{\nu\rho}M_{\mu\sigma} - \eta_{\nu\sigma}M_{\mu\rho} - \eta_{\nu\rho}M_{\eta\sigma} + \eta_{\nu\sigma}M_{\nu\rho}), \quad (2.21)$$

$$\{Q_a, Q_b\} = \{Q_a^\dagger, Q_b^\dagger\} = 0, \quad (2.22)$$

$$\{Q_a, Q_b^\dagger\} = \sigma_{ab}^\mu P_\mu, \quad (2.23)$$

$$[Q_a, P_\mu] = [Q_a^\dagger, P_\mu] = 0, \quad (2.24)$$

$$[Q_a, M_{\mu\nu}] = (\sigma_{\mu\nu})_a^b Q_b. \quad (2.25)$$

From the above equations one can see that the entire algebra is closed under commutation and anti commutation. I therefore consider a set of infinitesimal supersymmetry transformations generated by the exponential of the Lie algebra to follow the same recipes as for Lie groups

$$e^{i\bar{\alpha}Q} \approx 1 + i\bar{\alpha}Q. \quad (2.26)$$

Although the charges  $Q_a$  obey anticommutation relations, I can still use the Baker Campbell Horstoff theorem if the infinitesimal parameter that they are multiplied by,  $\bar{\alpha}$ , is a Grassmann valued number. Therefore if I can completely cover a region around the identity I can use products of infinitesimal transformations to map the entire connected region of the graded Lie group. Since  $\bar{\alpha}$  is Grassmann and I “begin” around the identity, the entire space that these transformations connect is a Grassmann valued space. Here and in Eq. (2.23) one sees the radical nature of supersymmetry. A supersymmetric transformation is something like the square root of a space time translation! Supersymmetry is something like a spinorial extension to space time such that one now has the usual 3+1 space time dimensions,  $x^\mu$  as well as four extra quantum dimensions,  $\theta_i$ . Even stranger, the dimensions  $\theta_i$  are Grassmann numbers that anticommute with each other and commute with ordinary numbers. It appears occasionally in the literature that “Superspace” is just a mathematical trick. However, as shown in the discussion above, if Eqs. (2.19-2.25) are the generators of the symmetries that describe our world then our world *literally* has four extra Grassmann valued dimensions. Of course I cannot directly observe these anti-commuting variables. However, one is convinced of curved space time because general relativity works and if supersymmetry works I will be convinced of anti commuting dimensions. Supersymmetry is a radical idea!

## 2.2.2 Non Interacting Supersymmetric Theories

In quantum field theory, one considers functions of the ordinary space time variables,  $x^\mu$ . However, if the world is supersymmetric then I must consider functions of both the space time and the Grassmann coordinates. I begin with a scalar superfield (where by superfield I mean a function of  $x^\mu$  and  $\theta_i$ ). Any product of  $\theta$ 's that contains more than four terms is then by definition zero. I can therefore write the most general scalar function as the sum

$$\begin{aligned}\hat{\Phi}(x, \theta) &= \mathcal{S} - i\sqrt{2}\bar{\theta}\gamma_5\psi - \frac{i}{2}(\bar{\theta}\gamma_5\theta)\mathcal{M} + \frac{1}{2}(\bar{\theta}\theta)\mathcal{N} \\ &+ \frac{1}{2}(\bar{\theta}\gamma_5\gamma_\mu\theta)V^\mu + i(\bar{\theta}\gamma_5\theta)\left[\bar{\theta}\left(\lambda + \frac{i}{\sqrt{2}}\not{\theta}\psi\right)\right] \\ &- \frac{1}{4}(\bar{\theta}\gamma_5\theta)^2\left[\mathcal{D} - \frac{1}{2}\square\mathcal{S}\right].\end{aligned}\quad (2.27)$$

If  $\hat{\Phi}$  transforms like a scalar and  $Q_a$  transforms like a spinor then  $Q\hat{\Phi}$  transforms as a spinor. Clearly a transformation that multiplies or removes a  $\theta$  to each term in  $\hat{\Phi}$  satisfies this condition. That is

$$\begin{aligned}e^{[i\bar{\alpha}Q]} &\approx 1 + i\bar{\alpha}Q \\ &= 1 + i\left(\bar{\alpha}\frac{\partial}{\partial\theta} + i\bar{\alpha}\not{\theta}\right).\end{aligned}\quad (2.28)$$

This set of transformations completely covers the Lie group around the identity and all other transformations that obey the correct transformation properties can be expressed as product of such infinitesimal transformations. Therefore Eq. (2.28) is sufficient to generate the entire set of supersymmetric transformations. Applying  $Q$  to Eq. (2.27) I can match powers of  $\theta$  to get the following set of transformations for the components of the superfield

$$\delta\mathcal{S} = i\sqrt{2}\bar{\alpha}\gamma_5\psi, \quad (2.29)$$

$$\delta\psi = -\frac{\alpha\mathcal{M}}{\sqrt{2}} - i\frac{\gamma_5\alpha\mathcal{N}}{\sqrt{2}} - i\frac{\gamma_\mu\alpha V^\mu}{\sqrt{2}} - \frac{\gamma_5\not{\theta}\mathcal{S}\alpha}{\sqrt{2}}, \quad (2.30)$$

$$\delta\mathcal{M} = \bar{\alpha}\left(\lambda + i\sqrt{2}\not{\theta}\psi\right), \quad (2.31)$$

$$\delta\mathcal{N} = i\bar{\alpha}\gamma_5\left(\lambda + i\sqrt{2}\not{\theta}\psi\right), \quad (2.32)$$

$$\delta V^\mu = -i\bar{\alpha}\gamma^\mu\lambda + \sqrt{2}\bar{\alpha}\partial^\mu\psi, \quad (2.33)$$

$$\delta\lambda = -i\gamma_5\alpha\mathcal{D} - \frac{1}{2}[\not{\theta}, \gamma_\mu]V^\mu\alpha, \quad (2.34)$$

$$\delta\mathcal{D} = \bar{\alpha}\not{\theta}\gamma_5\lambda. \quad (2.35)$$

In order to create a supersymmetric theory the action must be invariant under supersymmetric transformations. As seen in the earlier discussion it is sufficient for a theory to be invariant under infinitesimal supersymmetry transformations. Since I integrate our Lagrangian density over all space, a theory is still supersymmetric if the Lagrangian density transforms as a total derivative under supersymmetry transformations. Consider Eq. (2.35). One sees that the  $\mathcal{D}$  term of any Lagrangian, that is, the coefficient of  $(\bar{\theta}\gamma_5\theta)^2$ , will transform the correct way. Setting  $\lambda = \mathcal{D} = 0$  in

Eqs. (2.29-2.35) I see that the coefficient of the term  $\mathcal{M} + i\mathcal{M}$  also transforms as a total derivative. Such a field one calls a left chiral superfield for reasons that will not be explained here and these coefficients are called “F” terms. The product of any left chiral superfields will also give a left chiral superfield that also has an F term. This is obvious from the additivity of the left chiral derivative (which again will not be explained here). I can project out F terms and  $\mathcal{D}$  terms by integrating over two and four Grassmann variables respectively. I can also limit the types of F terms and  $\mathcal{D}$  terms that can appear in the Lagrangian if I insist that our theory is renormalizable. A general noninteracting supersymmetric theory can then be written as

$$S = \int d^4x d^4\theta \mathcal{L}_D + \int d^4x d^2\theta \mathcal{L}_F \quad (2.36)$$

and from renormalizability one finds that the most general form of  $\mathcal{L}_D$  is

$$\mathcal{L}_D = \sum_{n=1}^N \hat{S}_i^\dagger \hat{S}_i \quad (2.37)$$

whereas the most general form of  $\mathcal{L}_F$  is

$$\begin{aligned} \mathcal{L}_F = & -i \sum_i \left. \frac{\partial f}{\partial \hat{S}_i} \right|_{\hat{S}=\mathcal{S}} \mathcal{F}_i - \frac{1}{2} \sum_{i,j} \left. \frac{\partial^2 f}{\partial \hat{S}_i \partial \hat{S}_j} \right|_{\hat{S}=\mathcal{S}} \bar{\psi}_i P_L \psi_j \\ & + i \sum_i \left. \frac{\partial f}{\partial \hat{S}_i} \right|_{\hat{S}=\mathcal{S}} \mathcal{F}_i^\dagger - \frac{1}{2} \sum_{i,j} \left. \frac{\partial^2 f}{\partial \hat{S}_i \partial \hat{S}_j} \right|_{\hat{S}=\mathcal{S}} \bar{\psi}_i P_R \psi_j . \end{aligned} \quad (2.38)$$

This master Lagrangian gives us an interesting phenomenological prediction of supersymmetry. Consider  $\mathcal{L}_D$  for the case of a single superfield. The D term can be evaluated to be

$$\int d^4\theta \hat{S}_L^\dagger \hat{S}_L = \partial_\mu \mathcal{S}^\dagger \partial^\mu \mathcal{S} + \frac{1}{2} \bar{\psi} \not{\partial} \psi + \mathcal{F}^\dagger \mathcal{F} . \quad (2.39)$$

I see that every particle has a corresponding superpartner! It turns out that this feature is how the quadratic divergences of the higgs masses are cancelled out. This justifies our motivation for supersymmetry in the first place.

### 2.2.3 Examples of supersymmetric theories

Our master Lagrangian is still missing some key features of a theory that can plausibly describe anything to do with the real world. Such a theory would need spontaneous symmetry breaking to give particles a mass, they would also need supersymmetry breaking terms to ensure that the supersymmetric partners of Standard Model do not have the same mass as Standard Model particles (someone would have observed them otherwise!) and of course the fields in the theory would need to interact. Recall that to create an interacting theory in standard quantum field theories one makes the fields invariant under a space time dependent “gauge transformation”. To generalize this to supersymmetric theories one needs to make the gauge transformations superspace-time dependent. The result of this is that every gauge boson has a fermion

superpartner called a “gaugino” [39]. In order to make the masses of the superpartners much greater than their Standard Model partners I need to add mass terms to the Lagrangian for the superpartners. However, doing so breaks supersymmetry. Even though supersymmetry is a broken symmetry of nature in any theory that describes the real world, nonetheless the quadratic divergences that plagued the Standard Model are still canceled out if one merely adds mass terms to the Lagrangian [40]. Finally, electroweak symmetry breaking is done the same way as in the Standard Model, however, I have the added complication that to get a supersymmetric theory I require at least two Higgs bosons. This is another prediction of supersymmetry.

A theory that is just like the Standard Model, save for the fact that it has two Higgs bosons and every particle has a heavier superpartner, is known as the “minimally supersymmetric Standard Model” (or MSSM). The second Higgs doublet is necessary for anomaly cancellation. Another model I will consider is the NMSSM to which the Lagrangian contains the superpotential [41]

$$\begin{aligned}
W = & \lambda \hat{S} \hat{H}_1 \cdot \hat{H}_2 + \frac{\kappa}{3} \hat{S}^3 \\
& + y_u \hat{Q} \cdot \hat{H}_2 \hat{U}^c + y_d \hat{Q} \cdot \hat{H}_1 \hat{D}^c + y_e \hat{L} \cdot \hat{H}_1 \hat{E}^c
\end{aligned} \tag{2.40}$$

where  $\hat{S}$  is a singlet under  $SU(3) \times SU(2) \times U(1)$ ,  $\hat{H}_i$  are the superfields that generate the two higgs fields,  $\hat{Q}$  corresponds to your quark doublet,  $\hat{L}$  corresponds to the lepton doublet and  $\hat{U}^c$ ,  $\hat{D}^c$  and  $\hat{E}^c$  correspond to the right handed fermion singlets. The 125 GeV Higgs mass is difficult to reproduce in the MSSM with light superpartners [42, 43, 44, 45, 46], consequently the baryogenesis window is extremely narrow in the MSSM [47]. I will therefore in this research be considering the NMSSM.

I conclude with a comment on the large non conservation of baryon number in supersymmetric models which tends to sharply contradict observation due to strict bounds on the violation baryon and lepton number conservation. This is solved by proposing a new  $\mathbb{Z}_2$  symmetry known as  $R$  parity which forbids tree level baryon and lepton number violation. Specifically,  $R$  parity is defined by

$$P_R = (-1)^{3B-L+2s} \tag{2.41}$$

where  $B$ ,  $L$  and  $s$  are the baryon number, lepton number and spin respectively. All Standard Model particles has  $R$  parity of  $+1$  whereas the super partners have  $R$  parity of  $-1$ . The result of this is that any interaction must conserve the number of supersymmetric particles. This means that the lightest supersymmetric partner is completely stable.

## 2.2.4 A brief summary of supersymmetric cosmology

Supersymmetry has incredible cosmological benefits. There are many new flat scalar directions in field space which can facilitate inflation [48, 49, 50, 51, 52, 53, 54, 55]. Under  $R$  parity the lightest supersymmetric partner is completely stable which provides a very good dark matter candidate [34, 56, 57, 58, 59, 60, 61, 62, 63, 64, 65]. As for baryogenesis, supersymmetry naturally provides two mechanisms: during inflation one has the Affleck-Dine mechanism [66] which won't be reviewed here (but is reviewed in my book). The other mechanism is electroweak baryogenesis. Supersymmetry facilitates this in a number of ways. First the presence of coloured

scalar particles (stops) in the plasma provides a strong source of friction that slows the expansion of bubble walls [67] – which is ideal for baryogenesis. Second the presence of new scalar particles that interact with the Higgs potentially catalyse a strongly first order phase transition in contrast with the Standard Model [25]. Finally there are many new sources of CP violation through new coupling terms. I will examine how well electroweak baryogenesis is supported by simple supersymmetric models in later chapters.

## 2.3 The relaxion mechanism: another solution to the hierarchy problem

I previously discussed a dichotomy of explanations to explain fine tuning - the anthropic principle can be invoked if there is an anthropic reason why an observable is fine tuned otherwise one needs new physics. If the anthropic principle is invoked then one is conceding that something about our world cannot be explained by examining current local physics. There has been another very clever category of explanation that has been proposed recently where the anthropic principle is not invoked to explain the hierarchy problem but still the explanation is not found in current local physics as the explanation is cosmological. This proposal is known as the relaxion mechanism [5] where the Higgs couples to an axion field with a periodic potential. These periodic barriers form at the same time when electroweak symmetry breaking occurs and large Hubble friction during inflation prevents the Higgs vev from rolling past the first minimum.

To determine whether this is indeed a solution to the hierarchy problem I invoke a rigorous Bayesian model comparison framework. The Bayesian framework has a fine tuning penalty and Occam’s razor automatically built in to the formalism. I find that, unfortunately, the simplest versions of relaxion method do not solve the hierarchy problem since one requires an unnaturally small Hubble parameter during inflation to allow periodic barriers to form. Remarkably this problem is so acute that the Standard Model turns out to be less fine tuned. Nonetheless relaxion is an interesting scenario and perhaps more exotic inflationary scenarios can overcome this difficulty.

### 2.3.1 Declaration for thesis chapter 2

#### Declaration by candidate

In the case of the paper present contained in chapter 7, the nature and extent of my contribution was as follows:

Publication	Nature of contribution	Extent of contribution
2	Worked on analytic derivations throughout. Wrote a number of sections and edited all sections. Contributed to discussions throughout.	25%

The following coauthors contributed to the work. If the coauthor is a student at Monash, their percentage contribution is given:

<b>Author</b>	<b>Nature of contribution</b>	<b>Extent of contribution</b>
Csaba Balazs	Involved in conceptual development and contributed to discussions throughout	
Andrew Fowlie	Developed the concept, worked on analytic derivations and implemented numerical scan. Wrote and edited sections. Contributed to discussions throughout	
Luca Marzola	Heavily responsible for conceptual development. Involved heavily in writeup. Contributed to discussions throughout.	
Martti Raidal	Contributed to discussions throughout.	

The undersigned hereby certify that the above declaration correctly reflects the nature and extent of the candidate and co-authors' contributions to this work.

**Signatures:**

Graham White



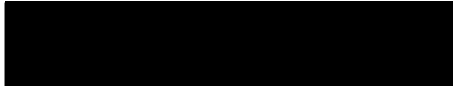
Csaba Balazs



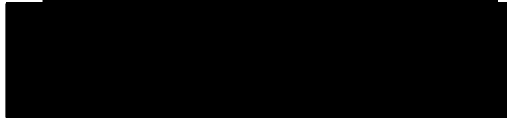
Andrew Fowlie



Luca Marzola



Martti Raidal



**Date:**

3.04.2017

### **2.3.2 Published material for chapter 2: Naturalness of the relaxation mechanism**

## Naturalness of the relaxion mechanism

---

Andrew Fowlie,<sup>a</sup> Csaba Balazs,<sup>a</sup> Graham White,<sup>a</sup> Luca Marzola<sup>b,c</sup> and Martti Raidal<sup>b,c</sup>

<sup>a</sup>*ARC Centre of Excellence for Particle Physics,  
School of Physics and Astronomy, Monash University,  
Wellington Road, Melbourne, Victoria 3800, Australia*

<sup>b</sup>*National Institute of Chemical Physics and Biophysics,  
Rüvala 10, Tallinn 10143, Estonia*

<sup>c</sup>*Institute of Physics, University of Tartu,  
Ravila 14c, Tartu 50411, Estonia*

*E-mail:* [andrew.fowlie@monash.edu](mailto:andrew.fowlie@monash.edu), [csaba.balazs@monash.edu](mailto:csaba.balazs@monash.edu),  
[graham.white@monash.edu](mailto:graham.white@monash.edu), [luca.marzola@ut.ee](mailto:luca.marzola@ut.ee), [martti.raidal@cern.ch](mailto:martti.raidal@cern.ch)

**ABSTRACT:** The relaxion mechanism is a novel solution to the hierarchy problem. In this first statistical analysis of the relaxion mechanism, we quantify the relative plausibility of a QCD and a non-QCD relaxion model versus the Standard Model with Bayesian statistics, which includes an automatic penalty for fine-tuning. We find that in light of the hierarchy between the weak and Planck scales, relaxion models are favoured by colossal Bayes-factors. Constraints upon e.g., the vacuum energy during relaxation, however, shrink the Bayes-factors such that relaxion models are only slightly favoured. Including the bounds on  $|\theta_{\text{QCD}}|$  shatters the plausibility of the QCD relaxion model as it typically yields  $|\theta_{\text{QCD}}| \gg 0$ . Finally, we augment our models with scalar-field inflation and consider measurements of inflationary observables from BICEP/Planck. We find that, all told, the Standard Model is favoured by huge Bayes-factors as the relaxion models require fine-tuning such that the Hubble parameter is less than the height of the periodic barriers. Thus, whilst we confirm that relaxion models could solve the hierarchy problem, we find that their unconventional cosmology is at odds with their plausibility.

**KEYWORDS:** Beyond Standard Model, Higgs Physics

ARXIV EPRINT: [1602.03889](https://arxiv.org/abs/1602.03889)

---

**Contents**

<b>1</b>	<b>Introduction</b>	<b>1</b>
<b>2</b>	<b>Bayesian fine-tuning</b>	<b>3</b>
<b>3</b>	<b>Analysis of relaxion potential</b>	<b>4</b>
3.1	$ \theta_{\text{QCD}} $ in relaxion models	6
3.2	Finite-temperature effects	7
3.3	Baryon asymmetry	7
<b>4</b>	<b>Description of models</b>	<b>8</b>
4.1	The Standard Model with scalar-field inflation	8
4.1.1	Calculation of observables	9
4.2	Relaxion models	9
4.2.1	Relaxion physicality conditions	10
4.2.2	Calculation of (electroweak and QCD) observables	11
<b>5</b>	<b>Bayesian analysis</b>	<b>11</b>
5.1	Evidences	14
5.2	Observables	15
<b>6</b>	<b>Discussion and conclusions</b>	<b>17</b>

---

**1 Introduction**

Graham et al. [1] recently proposed a relaxation mechanism [2–4] that solves the hierarchy problem [5–8] by utilising the dynamics of an axion-like field, dubbed the relaxion. In the Standard Model (SM), the hierarchy problem originates from quadratic corrections to the weak scale. Whereas supersymmetry cancels them with new quadratic corrections involving supersymmetric particles [9], the relaxion mechanism cancels them with the vacuum expectation value (VEV) of a relaxion field.

The ingenuity of the relaxion mechanism is that the dynamics of the relaxion field ensure a precise cancellation without patent fine-tuning of parameters or initial conditions. Within the relaxion paradigm, interactions between a complex Higgs doublet,  $h$ , and an axion-like field,  $\phi$ , govern the weak scale via the scalar potential [1]

$$V = (\mu^2 - \kappa \langle a \rangle \phi) h^2 - m_b^3 \langle h \rangle \cos\left(\frac{\phi}{f}\right) - m^2 \langle a \rangle \phi + \lambda h^4, \quad (1.1)$$

where, because of quadratic corrections, we expect that the masses should be close to the cut-off  $\Lambda$ , i.e.,  $\mu^2 \sim m^2 \sim \Lambda^2$ ,  $m_b$  and  $f$  are coupling constants of dimension mass,  $\langle a \rangle$  is

the VEV of a spurion field that breaks a shift symmetry  $\phi \rightarrow \phi + 2\pi f$ ,  $\kappa$  is a dimensionless coupling, and  $\langle h \rangle$  is the VEV of the Higgs field, which is a function of the relaxion field  $\phi$ .

Let us label the co-efficient of  $h^2$  in the relaxion potential

$$m_h^2(\phi) \equiv \mu^2 - \kappa \langle a \rangle \phi, \tag{1.2}$$

for convenience, such that the Higgs VEV may be written

$$\langle h \rangle = \begin{cases} \sqrt{\frac{-m_h^2(\phi)}{2\lambda}} & m_h^2(\phi) < 0, \\ 0 & \text{otherwise.} \end{cases} \tag{1.3}$$

If the Higgs VEV is non-zero, the cosine term provides a periodic barrier for the relaxion field with barriers separated by  $2\pi f$ . In the unbroken phase in which  $\langle h \rangle = 0$ , the barrier is down and the relaxion field slowly rolls down a linear potential. Once  $m_h^2(\phi) < 0$ , however, the potential is such that the Higgs field acquires a VEV,  $\langle h \rangle \neq 0$ , breaking electroweak symmetry (EWSB) and raising the periodic barrier. The now-raised periodic barrier traps the relaxion field in a minimum. If the relaxion field cannot roll past a local minimum, it results in a weak scale of about

$$\langle h \rangle \gtrsim f \frac{m^2 \langle a \rangle}{m_b^3}. \tag{1.4}$$

Thus this mechanism could result in  $\langle h \rangle \ll M_P$ .

We require, inter alia, that the relaxion field dissipates energy as it rolls or else it would have sufficient kinetic energy to surmount the periodic barriers. In the relaxion paradigm, this is ensured by Hubble friction — a term analogous to a friction term in the Euler-Lagrange equation for the relaxion field originating from the expansion of the Universe see e.g. ref. [10]:

$$\ddot{\phi} + 3H\dot{\phi} + \frac{\partial V}{\partial \phi} = 0, \tag{1.5}$$

where  $H$  is the Hubble parameter. If Hubble friction is substantial, the relaxion field could be in a slow-roll regime in which the acceleration  $\ddot{\phi}$  can be neglected.

Ostensibly, the relaxion mechanism ameliorates fine-tuning associated with the weak scale, but Raidal et al. [11] stress that it could require a fine-tuned inflationary sector if the relaxion is the QCD axion because of constraints upon the Hubble parameter during inflation. Unfortunately, there is no consensus in high-energy physics on the appropriate measure of fine-tuning or about the logical foundations of fine-tuning arguments, despite their prominence. In earlier work to judge fine-tuning in relaxion models, Jaeckel et al. [12] developed a new formalism based on their intuition, whereas Raidal et al. [11] utilised common Barbieri-Giudice style measures [13, 14]. In section 2, we critique Jaeckel’s approach and instead advocate a Bayesian methodology, discussed numerous times over the last decade in the context of fine-tuning in supersymmetric models [15–22]. In this methodology, in light of experimental data about the weak scale and inflation, we update our belief in a model with a Bayesian evidence. We further analyse the relaxion potential in section 3. We describe our models — minimal relaxion models and the SM augmented by scalar-field inflation — in section 4 and calculate their Bayesian evidences in section 5. This is the

first statistical analysis of a relaxation model. We close in section 6 with a brief discussion of our findings.

## 2 Bayesian fine-tuning

Bayesian statistics provides a logical framework for updating beliefs in scientific theories in light of data see e.g. ref. [23–25]. This methodology is becoming increasingly common in high-energy physics see e.g. ref. [26–69] and cosmology see e.g. ref. [70–72], and arguably captures the essence of the hierarchy problem [15–22] and the principle of Occam’s razor see e.g. ref. [73]. We briefly recapitulate the essential details.

The Bayesian framework enables one to assign numerical measures to degrees of belief. To assess two models,  $M_a$  and  $M_b$ , one begins by quantifying one’s relative degree of belief in the models, prior to considering any experimental data. This is known as the prior odds,

$$\text{Prior odds} \equiv \frac{P(M_a)}{P(M_b)}, \tag{2.1}$$

where  $P(M)$  is one’s prior belief in a model  $M$ . From the prior odds, we can calculate the posterior odds — one’s relative degree of belief in the models updated with experimental data,

$$\text{Posterior odds} \equiv \frac{P(M_a | D)}{P(M_b | D)}, \tag{2.2}$$

where  $D$  represents experimental data e.g., in this work data from BICEP/Planck. The prior odds and the posterior odds are related by a so-called Bayes-factor:

$$\text{Posterior odds} = \text{Bayes-factor} \times \text{Prior odds}. \tag{2.3}$$

By applying Bayes’ theorem, it can be readily shown that the Bayes-factor is a ratio of probability densities,

$$\text{Bayes-factor} \equiv \frac{p(D | M_a)}{p(D | M_b)}, \tag{2.4}$$

where the probability densities in question are known as Bayesian evidences or just evidences. The evidence for a model  $M$  can be calculated by Bayes’ theorem and marginalisation,

$$\mathcal{Z} \equiv p(D | M) = \int p(D | M, \mathbf{p}) \cdot p(\mathbf{p} | M) \prod d\mathbf{p} \tag{2.5}$$

where  $\mathbf{p}$  are the model’s parameters,  $p(D | M, \mathbf{p})$  is a so-called likelihood function — the probability density of our observed data given parameters  $\mathbf{p}$  — and  $p(\mathbf{p} | M)$  is our prior density for the model’s parameters  $\mathbf{p}$ .

The likelihood function is uncontroversial as its form is dictated by the nature of an experiment and it is a critical ingredient in Bayesian and frequentist statistics. The role and form of the prior density, however, remain contentious issues. In as much as it is possible, we pick objective priors that reflect our knowledge or ignorance about a parameter and respect rational constraints from e.g., symmetries.

We calculate Bayes-factors for the SM augmented with scalar-field inflation (SM +  $\sigma$ ) versus relaxion models. The final step — that of updating one’s prior odds with a Bayes-factor to find one’s posterior odds — is left to the reader. That is not to say that a Bayes-factor is independent of any prior choices — it is in fact a functional of the priors for the parameters of the models in question.

Before closing, we briefly discuss attempts to quantify fine-tuning in a relaxion model by Jaeckel et al. [12] and by Raidal et al. [11]. Raidal et al. employed Barbieri-Giudice style measures of fine-tuning [13, 14]. Whilst intuitive, such measures lack a logical foundation, though emerge in intermediate steps in a calculation of the Bayesian evidence [15–22]. Jaeckel et al. developed a novel measure of electroweak fine-tuning,  $F$ , based on the fraction of a model’s parameter space,  $\mathbf{p}$ , that predicts a weak scale less than that observed:

$$\frac{1}{F} \equiv \frac{V_{v(\mathbf{p}) \leq v}}{V} = \frac{\int \theta(v - v(\mathbf{p})) \prod d\mathbf{p}}{\int \prod d\mathbf{p}}. \quad (2.6)$$

This measure contrasts with Barbieri-Giudice measures in that it considers a model’s entire parameter space rather than a single point in it. Jaeckel’s measure, however, depends on one’s choice of parameterisation or measure for the parameter space.<sup>1</sup>

Curiously, Jaeckel’s measure in eq. (2.6) is reminiscent of the Bayesian evidence if one considers measurements of the weak scale, especially if one writes (unnecessary) normalisation factors for the priors,

$$\mathcal{Z} = \frac{\int p(v | M, \mathbf{p}) \cdot p(\mathbf{p} | M) \prod d\mathbf{p}}{\int p(\mathbf{p} | M) \prod d\mathbf{p}} \quad \text{vs.} \quad \frac{1}{F} = \frac{\int \theta(v - v(\mathbf{p})) \prod d\mathbf{p}}{\int \prod d\mathbf{p}}. \quad (2.7)$$

The differences are that Jaeckel et al. pick a step-function for the likelihood for the weak scale,  $v$ , and omit a measure for the volume of parameter space, i.e., a prior. In other words, by following their noses and attempting to formulate fine-tuning in a logical manner, Jaeckel et al. create an ersatz Bayesian evidence.

### 3 Analysis of relaxion potential

Let us further analyse the relaxion potential in eq. (1.1),

$$V = (\mu^2 - \kappa \langle a \rangle \phi) h^2 - m_b^3 \langle h \rangle \cos\left(\frac{\phi}{f}\right) - m^2 \langle a \rangle \phi + \lambda h^4.$$

As in ref. [74], for simplicity we consider only linear terms in the relaxion field  $\phi$ . The equations  $\partial V / \partial \phi = 0$  and  $\partial V / \partial h = 0$  result in a transcendental equation,

$$\sin(\phi/f) = \frac{f \kappa \langle a \rangle}{m_b^3} \left( \frac{m^2 / \kappa + \langle h \rangle^2}{\langle h \rangle} \right). \quad (3.1)$$

By graphing as in figure 1, one finds that if there is a solution, it lies in the interval  $\langle h \rangle_{\min} \leq \langle h \rangle \leq \langle h \rangle_{\max}$  where

$$\langle h \rangle_{\min} = \frac{m_b^3 - \sqrt{m_b^6 - 4\kappa m^2 \langle a \rangle^2 f^2}}{2\kappa \langle a \rangle f} \quad \text{and} \quad \langle h \rangle_{\max} = \sqrt{\frac{-\mu^2 + \kappa \langle a \rangle \langle \phi \rangle_{\max}}{2\lambda}}, \quad (3.2)$$

---

<sup>1</sup>However, Jaeckel et al. [12] includes a general discussion of parameterisation in the context of fine-tuning.

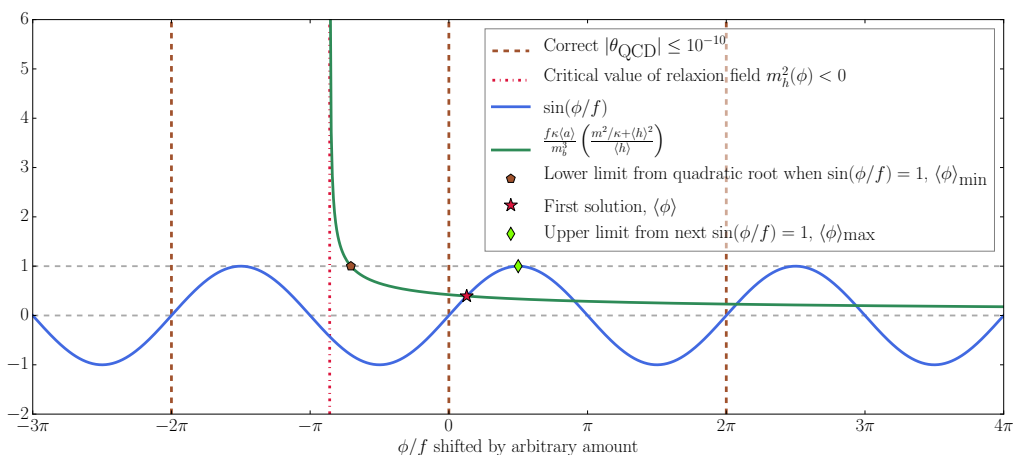


**Figure 1.** Graphing the left-hand side (blue line) and right-hand side (green line) of the transcendental equation in eq. (3.1). The solution (red star) lies in the interval in eq. (3.2), marked by a brown pentagon and a green diamond. In unusual cases, the second point at which the right-hand side equals plus one (not shown) may be a sharper bound. The  $\phi/f$ -axis is shifted such that correct  $|\theta_{\text{QCD}}|$  occurs at small multiples of  $2\pi$  (vertical brown dashed lines) close to the solution. EWSB is broken once the critical value of the relaxion field is surpassed (vertical red dot-dashed line).

and

$$\langle\phi\rangle_{\min} = \frac{2\lambda\langle h\rangle_{\min}^2 + \mu^2}{\kappa\langle a\rangle} \quad \text{and} \quad \langle\phi\rangle_{\max} = (2n + 1/2)\pi f \quad (3.3)$$

where  $n$  is the smallest integer such that  $\langle\phi\rangle_{\max} > \langle\phi\rangle_{\min}$ . If the square-root is imaginary, there are no solutions, otherwise, there are zero to four solutions inside the interval, which must be identified numerically. The interval results from recognising that a solution must lie between the point at which the right-hand side of eq. (3.1) equals plus one, matching the maximum of the left-hand side, and the subsequent point at which the latter is again maximal. If required, one can improve this interval with piece-wise expressions by graphing. In some cases, the positive quadratic root, similar to that for  $\langle h\rangle_{\min}$ , is a sharper bound for  $\langle h\rangle_{\max}$ . If the barrier height is substantial, the lower bound reduces to the approximation for  $\langle h\rangle$  in eq. (1.2), that is,

$$\langle h\rangle_{\min} \approx f \frac{m^2\langle a\rangle}{m_b^3} \quad \text{if} \quad \frac{4\kappa m^2\langle a\rangle^2 f^2}{m_b^6} \ll 1. \quad (3.4)$$

This implies that  $\kappa\langle a\rangle \ll m_b^3/(4f\langle h\rangle)$ . A necessary (though not sufficient) condition for solutions to the transcendental equation is that the root in eq. (3.2) must be real,

$$\frac{4\kappa m^2\langle a\rangle^2 f^2}{m_b^6} \leq 1. \quad (3.5)$$

In other words, the relaxion mechanism ensures that the weak scale is independent of quadratic corrections to the Higgs mass from a cut-off or unknown high-scale physics,

solving the hierarchy problem. In fact, the Higgs VEV is bounded by an expression that is independent of the Higgs mass,

$$\langle h \rangle_{\min} \leq \langle h \rangle \leq \langle h \rangle_{\max} \leq \sqrt{\langle h \rangle_{\min}^2 + \kappa \langle a \rangle f \pi / \lambda}. \quad (3.6)$$

The Higgs mass  $\mu^2$  and any corrections affect the position of  $\langle h \rangle$  inside this interval, but not the interval itself. The width of this interval is typically small such that numerically solving for the VEV of the Higgs field inside the interval may be unnecessary.

Unfortunately, if the relaxion is the QCD axion, we expect that barrier height  $m_b^3$  is connected to QCD, such that  $m_b \sim \Lambda_{\text{QCD}}$ , resulting in

$$\langle a \rangle \lesssim \langle h \rangle \times 10^{-18} \simeq 10^{-16} \text{ GeV}, \quad (3.7)$$

where we impose an experimental limit on the QCD decay constant,  $f \gtrsim 10^9 \text{ GeV}$ , and pick  $m \simeq 1 \text{ TeV}$  in eq. (3.4). Thus achieving a small weak scale requires a tiny spurion VEV,  $\langle a \rangle \lll M_{\text{P}}$ . Such a small coupling may be natural as it breaks a shift-symmetry see e.g. ref. [75]; however, there may be issues due to the gauge symmetry at the basis of the construction [76, 77].

### 3.1 $|\theta_{\text{QCD}}|$ in relaxion models

Let us investigate whether a relaxion model might resolve the strong-CP problem [78] by explaining  $|\theta_{\text{QCD}}| \lesssim 10^{-10}$  [79]. Prima facie, the expression for  $|\theta_{\text{QCD}}|$  is simple see e.g. ref. [80],

$$|\theta_{\text{QCD}}| = |\langle \phi \rangle / f \quad \text{on } -\pi \text{ to } \pi|. \quad (3.8)$$

Numerically, however, this cannot be used for calculating  $|\theta_{\text{QCD}}|$  — as  $\langle \phi \rangle / f$  is substantial, there is a breakdown in numerical precision in expressions such as  $\langle \phi \rangle / f \pmod{2\pi}$ . Instead, we find the principal solution for  $|\theta_{\text{QCD}}|$ ,

$$|\theta_{\text{QCD}}| = \arcsin \left| \frac{f \kappa \langle a \rangle}{m_b^3} \left( \frac{m^2 / \kappa + \langle h \rangle^2}{\langle h \rangle} \right) \right|, \quad (3.9)$$

by utilising eq. (3.1).

The minimum  $|\theta_{\text{QCD}}|$  obtainable occurs at the minimum of the right-hand side of eq. (3.1), such that, if there is a solution at that point,  $\sin(\phi/f)$  is as close to zero as possible. Thus we find that

$$\min |\theta_{\text{QCD}}| = \begin{cases} \arcsin \left| \frac{2 \langle a \rangle f m \sqrt{\kappa}}{m_b^3} \right| & \text{if } \langle h \rangle_{\min} \leq \langle h \rangle_{\max}, \\ \arcsin \left| 1 - \frac{\kappa \langle a \rangle f \pi}{2 \lambda \langle h \rangle_{\min}^2} + \dots \right| = \pi/2 - \sqrt{2\epsilon} + \dots & \text{otherwise,} \end{cases} \quad (3.10)$$

where  $\langle h \rangle_{\min} = m / \sqrt{\kappa}$  which minimises the right-hand side of eq. (3.1) and the second line is never less than the first line. The terms represented by the ellipses are higher powers of  $\eta$  and  $\epsilon$ ,

$$\langle h \rangle_{\max} \approx \langle h \rangle_{\min} (1 + \epsilon) \quad \text{where} \quad \epsilon \equiv \frac{\kappa \langle a \rangle f \pi}{2 \lambda \langle h \rangle_{\min}^2} \ll 1 \quad \text{and} \quad \eta \equiv \frac{\kappa \langle h \rangle_{\min}^2}{m^2} \ll 1. \quad (3.11)$$

We expand to first order in  $\epsilon$  and neglect all powers of  $\eta$ . Eq. (3.10) originates from considering that the minimum possible  $|\theta_{\text{QCD}}|$  would occur at the minimum of the right-hand side of eq. (3.1) if that minima occurred at  $\phi/f \approx 2n\pi$  and not  $\phi/f \approx (2n+1)\pi$ , such that  $|\theta_{\text{QCD}}| \approx 0$  and not  $|\theta_{\text{QCD}}| \approx \pi$ . If that minima occurs, however, outside the interval for the possible solutions for  $\langle h \rangle$ , it is impossible. In that case, the right-hand side of eq. (3.1) is monotonic inside the interval for the possible solutions for  $\langle h \rangle$  and we consider the right-hand side evaluated at  $\langle h \rangle_{\text{max}}$  from eq. (3.6). As the general expression is rather complicated, we apply the approximations in eq. (3.11), which are reasonable for phenomenologically viable points. In fact, phenomenologically viable points are always in the second regime in which  $\langle h \rangle_{\text{minima}} = m/\sqrt{\kappa} \gg \langle h \rangle_{\text{max}}$ , such that  $\min |\theta_{\text{QCD}}| \approx \arcsin 1 = \pi/2$ . This is confirmed in our numerical analysis.

### 3.2 Finite-temperature effects

In this paper and in the literature so far, the relaxion mechanism was analysed at zero temperature.<sup>2</sup> Finite-temperature effects could, however, non-trivially affect the relaxion potential in eq. (1.1):

- Non-perturbative effects responsible for the induced effective potential of the relaxion are temperature dependent [82]. However, since this affects only the heights of the barriers and not their spacing and since Hubble friction during inflation is typically substantial, it is unclear whether finite-temperature effects would impact the viability of the relaxion mechanism.
- Finite-temperature corrections to the effective potential would alter the shape of the potential (increasing the gradients of the slopes), possibly delaying the onset of EWSB [83]. If EWSB is delayed until a late time (corresponding to a lower temperature after reheating), it could constrain when inflation must start through the requirement that it lasts at least 50  $e$ -folds after EWSB. Furthermore, the flat regions of the zero-temperature inflaton potential are strongly modified by finite-temperature effects.
- We find that the reheating temperature in our relaxion models is typically of order  $10^{10}$  GeV. At such a high temperature, electroweak symmetry could be easily restored, with the effect of further hindering the viability of the model.

Clearly all the mentioned finite-temperature effects have the potential to impose further constraints on the relaxion model parameter space, to an extent that will be quantified in following projects.

### 3.3 Baryon asymmetry

We observe a significant baryon asymmetry in our Universe. Sakharov [84] demonstrated that generating this asymmetry — baryogenesis — would require a departure from thermal

---

<sup>2</sup>We note, however, that ref. [81] considers finite-temperature effects in an alternative relaxion mechanism.

equilibrium,  $\mathcal{C}$  and  $\mathcal{CP}$  violation, and baryon number violation. In the relaxion paradigm, however, the final 50 or so  $e$ -folds of inflation occur during or immediately after EWSB and inevitably wash-out any potential net baryon number generated in this process see e.g. ref. [85]. Novel mechanisms that invoke multi-step phase transitions are also ruled out since the fields must be in the final SM vacuum at the end of inflation.<sup>3</sup> Scenarios in which the inflaton itself could generate the required baryon asymmetry see e.g. ref. [86, 87] also appear to be incompatible with the relaxion mechanism because of the further constraints implied by the already heavily constrained dynamics of the inflaton. Finally weak sphalerons are also exponentially VEV suppressed [88] after the electroweak phase transition which means that any subsequent baryogenesis scenario would have to rely on a different source of baryon and lepton number violation. As we shall see, these difficulties would strengthen our conclusions about the viability of inflation in the present framework.

## 4 Description of models

We apply Bayesian model comparison to three models: the SM augmented with single-field scalar-field inflation (SM +  $\sigma$ ), a QCD relaxion model and a general relaxion model. For other relaxion models, see e.g., ref. [74, 89–96]. Ultimately, we wish to find whether the relaxion mechanism ensures that a relaxion model is favoured by the Bayesian evidence versus the SM. In each model, all scalar-fields receive quadratic corrections to their masses from a cut-off,  $\Lambda$ , which lies close to the Planck scale.

### 4.1 The Standard Model with scalar-field inflation

The SM Higgs sector is described by two bare Lagrangian parameters —  $\mu^2$  and  $\lambda$  — in the SM Higgs potential,

$$V_h = \mu^2 |h|^2 + \lambda |h|^4, \tag{4.1}$$

and a cut-off at which the bare parameters are specified,  $\Lambda$ . We augment the SM with mixed inflation, a canonical model of scalar-field inflation see e.g. ref. [97]. Mixed inflation is described by an inflaton mass,  $m_\sigma^2$ , and quartic coupling,  $\lambda_\sigma$ , in a potential

$$V_\sigma = \frac{1}{2} m_\sigma^2 \sigma^2 + \lambda_\sigma \sigma^4 \tag{4.2}$$

and the number of  $e$ -folds,  $N_{e\text{-fold}}$ . We denote this model by SM +  $\sigma$ .

Note that in the SM +  $\sigma$  model, the evidence approximately factorises into a factor for the weak scale and a factor for the inflationary observables,  $r$ ,  $n_s$  and  $A_s$ ,

$$\begin{aligned} \mathcal{Z} &= p(M_Z, r, n_s, A_s | \text{SM} + \sigma) \\ &\approx p(M_Z | \text{SM} + \sigma) \cdot p(r, n_s, A_s | \text{SM} + \sigma) \\ &= p(M_Z | \text{SM}) \cdot p(r, n_s, A_s | \sigma) \end{aligned} \tag{4.3}$$

as the measurements are independent and model parameters that affect inflationary observables do not affect the weak scale and vice-versa, with the exception of the cut-off,  $\Lambda$ , which results in quadratic corrections to the inflaton mass and the Higgs mass.

---

<sup>3</sup>One could in principle have a multi-step phase transition that departed from the SM vacuum for baryogenesis and later returned to it but this somewhat undermines the motivation for relaxion models.

### 4.1.1 Calculation of observables

For comparison with measurements from Planck in our statistical analysis, we calculate inflationary observables via the so-called slow-roll parameters [98]:

$$\epsilon(\sigma) \equiv \frac{M_{\text{P}}^2}{16\pi} \left( \frac{V'(\sigma)}{V(\sigma)} \right)^2 \quad \text{and} \quad \eta(\sigma) \equiv \frac{M_{\text{P}}^2}{8\pi} \frac{V''(\sigma)}{V(\sigma)} \quad (4.4)$$

where a prime indicates a derivative with respect to the inflaton field  $\sigma$ . Inflation finishes once the inflaton field reaches a value  $\sigma_f$  such that  $\epsilon(\sigma_f) = 1$ . The number of  $e$ -folds desired before inflation ends (and in the case of the relaxion, after EWSB),

$$N_{e\text{-fold}} \simeq \frac{-8\pi}{M_{\text{P}}^2} \int_{\sigma_i}^{\sigma_f} \frac{V(\sigma)}{V'(\sigma)} d\sigma, \quad (4.5)$$

determines the inflaton field at the beginning of inflation,  $\sigma_i$ . The number of  $e$ -folds desired should be  $N_{e\text{-fold}} \gtrsim 50$ . The spectral index,  $n_s$ , and the ratio of scalar to tensor perturbations,  $r$ , may be written to first order in the slow-roll parameters as see e.g. ref. [99]

$$n_s = 1 - 6\epsilon(\sigma_i) + 2\eta(\sigma_i) \quad \text{and} \quad r = 4\pi\epsilon(\sigma_i). \quad (4.6)$$

The normalisation of the potential governs the amplitude of scalar perturbations and the Hubble parameter,

$$A_s = \frac{1}{M_{\text{P}}^6} \frac{128\pi}{3} \frac{V(\sigma_i)^3}{|V'(\sigma_i)|^2}, \quad (4.7)$$

$$H = \sqrt{\frac{V(\sigma_i)}{3M_{\text{P}}^2}}, \quad (4.8)$$

but cannot affect  $r$  or  $n_s$ . The normalisation of the scalar perturbations is arbitrary and varies in the literature. For comparison with Planck data, we pick that of the Planck experiment see e.g. ref. [100]. We include a quadratic correction to the inflaton mass — to include a dominant quantum contribution to fine-tuning — but otherwise our formulas are tree-level. We solve for the inflaton field at the beginning and end of inflation,  $\sigma_i$  and  $\sigma_f$ , with numerical methods.

The mass of the  $Z$  boson — which represents the weak scale — is calculated in the usual manner,

$$M_Z^2 = \frac{-g^2}{2\lambda} (\mu^2 + \beta\Lambda^2), \quad (4.9)$$

where  $\beta$  is a loop factor. The QCD phase is an input parameter.

## 4.2 Relaxion models

We consider two relaxion models described by the potential in eq. (1.1). In the first model, we do not identify the relaxion with the Peccei-Quinn axion that solves the strong CP problem [78], whereas in the second model, the relaxion is indeed the Peccei-Quinn axion.

For a necessary epoch of low-scale inflation after the relaxion mechanism, we extend the relaxion potential in eq. (1.1) by the most general renormalisable single-field inflaton potential see e.g. ref. [11] with an inflaton field  $\sigma$ ,

$$V = m_3^3 \sigma + \frac{1}{2} m_2^2 \sigma^2 + \frac{1}{3} m_1 \sigma^3 + \frac{1}{4} \lambda_\sigma \sigma^4. \quad (4.10)$$

We suppose that pre-inflation multi-field dynamics dictate that inflation begins at the origin,  $\sigma = 0$ , as in Raidal et al. [11]. This introduces only four parameters: four couplings in the potential — the desired number of  $e$ -folds,  $N_{e\text{-fold}}$ , is not an input parameter. We, furthermore, tune a dressed vacuum energy,  $\rho$ , such that the cosmological constant vanishes in the vacuum, i.e.,  $V(\langle\sigma\rangle, \dots) + \rho = 0$ . Thus, low-scale inflation with  $H \lll M_{\text{P}}$  is achieved provided  $V(\sigma = 0) = \rho \lll M_{\text{P}}^4$ . This implies that the potential must be fine-tuned such that  $|V(\langle\sigma\rangle)| \lll M_{\text{P}}^4$ .

The cosmological constant poses an infamous fine-tuning problem see e.g. ref. [101]. In almost all known models, agreement with measurements of the cosmological constant requires extreme fine-tuning between a bare cosmological constant in the Lagrangian,  $\rho_0$ , quantum corrections and contributions from spontaneous symmetry breaking i.e.,  $V(\langle\sigma\rangle, \dots)$ . Because all models that we consider suffer from this fine-tuning problem, fine-tuning penalties from the cosmological constant would approximately cancel in ratios of Bayesian evidences. We ensure that the second epoch of inflation cannot spoil the relaxion mechanism by applying conditions on the Hubble parameter during inflation.

### 4.2.1 Relaxion physicality conditions

There are parameter points for which the back-reaction to EWSB fails to trap the relaxion field in a minimum. If that were the case, the relaxion mechanism would fail and the point would be in severe disagreement with observations. Graham et al. list conditions required for a successful relaxion mechanism [1]:

$$H^2 M_{\text{P}}^2 > \frac{\mu^2 m^2}{\kappa} \quad (\text{vacuum energy}) \quad (4.11)$$

$$H < m_b \quad (\text{barriers form}) \quad (4.12)$$

$$H^3 < m^2 \langle a \rangle \quad (\text{classical beats quantum}) \quad (4.13)$$

We assign zero likelihood to a point that violates the resulting condition,

$$\sqrt{\frac{\mu^2 m^2}{\kappa}} < M_{\text{P}} \min(m_b, m^{2/3} \langle a \rangle^{1/3}). \quad (4.14)$$

Graham et al. also list the conditions

$$N_{e\text{-fold}} \gtrsim \frac{H^2}{\kappa \langle a \rangle^2} \quad (\text{inflation lasts long enough}) \quad (4.15)$$

$$\kappa \langle a \rangle \mu^2 f \sim m_b^3 \langle h \rangle \quad (\text{barrier heights}) \quad (4.16)$$

We assume that a first epoch of inflation is provided by the slow-rolling relaxion fields, and cosmological constant later cancelled when the Higgs and relaxion fields acquire VEVs, and

that this epoch provides an acceptable Hubble parameter, as described in ref. [11]. The latter condition is unnecessary as we solve the potential with numerical methods, checking whether a solution exists. To avoid destroying the periodic barriers, the second epoch of inflation must, however, satisfy,

$$H < m_b \tag{4.17}$$

where, as before,  $m_b$  is related to the height of the periodic barriers. The barriers result from a phase-transition to a QCD condensate (or a condensate associated with similar non-QCD dynamics). A Hubble parameter  $H > m_b$  would reverse that transition, destroying the barriers see e.g. ref. [1].

#### 4.2.2 Calculation of (electroweak and QCD) observables

We calculated the VEVs of the Higgs and relaxion fields with numerical methods based on bisecting the interval in eq. (3.2), from which we calculated the mass of the  $Z$ -boson,

$$M_Z = g\langle h \rangle \tag{4.18}$$

and  $|\theta_{\text{QCD}}|$  (see section 3.1). In the non-QCD relaxion model,  $|\theta_{\text{QCD}}|$  is an input parameter. The calculations for the inflationary observables were identical to those in the SM+ $\sigma$  model.

### 5 Bayesian analysis

We calculated Bayesian evidences for our SM +  $\sigma$  model and relaxion models with (Py)-MultiNest [102–105], which utilises the nested sampling algorithm [106, 107] for Monte-Carlo integration in Bayesian evidences in eq. (2.5) (though delta-functions were first integrated by hand).<sup>4</sup> This requires two ingredients: a likelihood function and a set of priors. Our likelihood function, summarised in table 1, was a product of at most five factors:

- **weak-scale:** a likelihood function for measurements of the mass of the  $Z$ -boson [79]. In the SM, this is approximated by a delta-function and integrated by hand. In a relaxion model, this is impossible, as there is no analytic expression for the  $Z$ -boson mass as a function of the Lagrangian parameters.
- **conditions:** if a relaxion model (i.e., a point in a relaxion model’s parameter space) violates physicality conditions in section 4.2.1, we assign a likelihood of zero, since it would be in stark disagreement with observations.
- **decay:** a likelihood function for the experimental lower-limit on  $f_a$ , the axion decay constant, approximated by a step-function see e.g. ref. [108].
- **theta:** a likelihood function for the experimental upper-limit on  $|\theta_{\text{QCD}}|$ , approximated by a step-function [79].

---

<sup>4</sup>We utilised importance sampling, picked 1000 live points and a stopping criteria of 0.01 in MultiNest.

Parameter	Measurement	Likelihood function
<b>weak-scale</b>		
$M_Z$	$91.1876 \pm 0.0021 \text{ GeV}$ [79]	Dirac in SM, Gaussian in relaxion
<b>decay</b>		
$f_a$	$f_a \gtrsim 10^9 \text{ GeV}$ [108]	Step-function
<b>theta</b>		
$ \theta_{\text{QCD}} $	$ \theta_{\text{QCD}}  \lesssim 10^{-10}$ [79]	Step-function
<b>inflation</b>		
$r$	$r < 0.12$ at 95% [109]	Step-function
$n_s$	$0.9645 \pm 0.0049$ [110]	Gaussian
$\ln(10^{10} A_s)$	$3.094 \pm 0.034$ [110]	Gaussian

**Table 1.** Likelihoods included in our Bayesian evidences for the scale of electroweak symmetry breaking, the axion decay constant,  $|\theta_{\text{QCD}}|$  and BICEP/Planck measurements of inflationary observables. Note that we neglect statistical correlations in Planck measurements of inflationary observables.

- **inflation:** a likelihood for the spectral index,  $n_s$ , the ratio of scalar to tensor perturbations,  $r$ , and the amplitude of scalar perturbations,  $A_s$ , from Planck and BICEP measurements [109, 110]. For simplicity, we neglect correlations amongst Planck measurements and impose an upper-limit for the scalar-to-tensor ratio.

We applied the likelihoods incrementally in five calculations per model: only **weak-scale**; adding **conditions**; adding a lower-bound on the axion decay constant, **decay**; adding an upper bound on  $|\theta_{\text{QCD}}|$ , **theta**; and finally adding BICEP/Planck measurements in **inflation**. This enabled us to assess the individual impacts of the constraints.

We picked uninformative scale-invariant priors for the dimensionful Lagrangian parameters and cut-off because we are ignorant of their scale, a linear prior for  $|\theta_{\text{QCD}}|$ , reflecting a shift-symmetry, and a linear prior for  $N_{e\text{-fold}}$  because the number of  $e$ -folds is already a logarithmic quantity. Our prior ranges are summarised in table 2. All massive parameters —  $\mu^2$  and  $m^2$  and inflaton masses — receive quadratic corrections from a cut-off, such that we expect that without fine-tuning  $\mu^2 \sim m^2 \sim \Lambda^2$ . The main difference between the priors for our QCD relaxion model and general relaxion model is that in the former, the barrier height is related to the QCD scale, whilst in the latter, it is no greater than about the weak scale. Furthermore, we assigned zero prior weight to corners of parameter space in which a relaxion Lagrangian parameter with dimension mass exceeded the cut-off scale,  $\Lambda$ , as in an effective field theory such corners may be considered inconsistent or implausible. This eliminated approximately 18% of the prior volume in table 2.

By picking scale-invariant priors for the Lagrangian parameters, we implicitly acknowledge our lack of information about a possible UV theory that might generate them. If there were sufficient reason to believe that a particular mechanism might generate them, imprint-

Parameter	Prior	
SM + $\sigma$		
$\mu^2$	Log	$10^{-40}, 1$
$\lambda$	Log	$10^{-4}, 4\pi$
$\Lambda^2$	Log	$10^{-4}, 1$
$m_\sigma^2$	Log	$10^{-40}, 1$
$\lambda_\sigma$	Log	$10^{-20}, 4\pi$
$N_{e\text{-fold}}$	Linear	50, 500
$ \theta_{\text{QCD}} $	Linear	0, $\pi$
QCD relaxion		
$\mu^2$	Log	$10^{-40}, 1$
$\lambda$	Log	$10^{-4}, 4\pi$
$\Lambda^2$	Log	$10^{-4}, 1$
$\kappa$	Log	$10^{-4}, 4\pi$
$\langle a \rangle$	Log	$10^{-50}, 1$
$m_b$	Log	$10^{-1}\Lambda_{\text{QCD}}, 10\Lambda_{\text{QCD}}$
$m^2$	Log	$10^{-40}, 1$
$f$	Log	$10^{-50}, 1$
$m_1$	Log	$10^{-100}, 1$
$m_2^2$	Log	$10^{-100}, 1$
$m_3^3$	Log	$10^{-100}, 1$
$\lambda_\sigma$	Log	$10^{-40}, 4\pi$
Non-QCD relaxion, as for QCD relaxion except		
$m_b$	Log	$10^{-6}\langle h \rangle, 10^{-1}\langle h \rangle$
$ \theta_{\text{QCD}} $	Linear	0, $\pi$

**Table 2.** Priors for parameters in SM augmented with scalar-field inflation (SM +  $\sigma$ ) and relaxion models. Masses are in Planck units. Furthermore, regions in parameter space in which a dimensionful relaxion Lagrangian parameter exceeded a cut-off were assigned zero prior weight.

ing distinguishing correlations between parameters, it should be reflected in one's choice of priors. In supersymmetric models, for instance, the knowledge of particular breaking mechanisms such as minimal supergravity (mSUGRA) results in relations between Lagrangian parameters at the GUT scale that must be acknowledged in the choice of suitable priors. Likewise, the identification of a UV-completion of the relaxion model could, in principle, ameliorate the fine-tuning of the scenario as the Bayes-factor is a functional of the priors, however, to-date we know of no compelling reason to pick anything other than scale-invariant priors.

## 5.1 Evidences

The evidences and Bayes-factors for the SM +  $\sigma$  and relaxion models are summarised in table 3. We find that, considering only a measurement of the weak scale (i.e., **weak-scale**), relaxion models are favoured by colossal Bayes-factors of about  $10^{30}$ . This is similar to findings for the constrained minimal supersymmetric SM versus the SM [17], and was expected, as the SM with a Planck-scale cut-off makes an egregious generic prediction for the weak scale.

The physicality conditions (**conditions** in section 4.2.1) dramatically impact the preference for relaxion models. The conditions wipe-out a fraction of the relaxion models' parameter spaces and shrink the Bayes-factors by about  $10^{-28}$ . The preference for relaxion models versus the SM almost entirely disappears. In other words, despite their success in solving the hierarchy problem, relaxion models are hamstrung by severe fine-tuning associated with their physicality conditions.

The preference for the QCD relaxion model is further damaged by measurements of the axion decay constant, **decay**, and the  $|\theta_{\text{QCD}}|$ , **theta**. The latter results in approximately zero preference for the QCD relaxion model as it predicts that  $|\theta_{\text{QCD}}| \approx \pi/2$  (see eq. (3.10)). The preference of about  $10^2$  for a non-QCD relaxion model versus the SM is unaffected by **decay** and **theta**.

The final data-set of inflationary observables (**inflation**) also impairs the credibility of the considered relaxion models. Low-scale inflation, required in the relaxion paradigm, suffers severe fine-tuning as it requires a light scalar, and thus results in partial Bayes-factors of about  $10^{-30}$  for relaxion models versus the SM. Thus, all data considered, the SM +  $\sigma$  model is favoured by a Bayes-factor of at least about  $10^{25}$ . We note that eq. (4.14) results in an approximate limit of  $\mu^2 \sim m^2 \lesssim (10^8 \text{ GeV})^2$ , such that by chance

$$\frac{\mu^2}{\beta M_{\text{P}}^2} \frac{m^2}{\beta M_{\text{P}}^2} \sim \frac{M_Z^2}{\beta M_{\text{P}}^2}. \tag{5.1}$$

The factors are in fact approximately the fractions of parameter space in which a scalar mass is fine-tuned to be so light versus a cut-off,  $M_{\text{P}}$ . Thus tuning two scalar masses —  $\mu^2$  and  $m^2$  — in a relaxion model to be  $\mu^2 \sim m^2 \sim (10^8 \text{ GeV})^2$  results in a similar fine-tuning penalty as tuning a single scalar mass such that  $M_Z \sim 100 \text{ GeV}$ . This, in essence, explains why the evidence for the SM and relaxion models are similar, if one considers only **weak + conditions**. Note that lowering the quadratic corrections by supersymmetrizing the SM and relaxion models see e.g. ref. [94] could favour relaxion models, as from eq. (5.1) a Bayes-factor might scale as the cut-off squared. Lowering the Planck mass, on the other hand, might help slightly less, as it would lower the bounds on scalar masses from eq. (4.14).

To further investigate this issue, we relaxed the Planck-scale cut-off, plotting evidence as a function of the cut-off in the SM and our QCD relaxion model in figure 2. By doing so, we wish to confirm that our QCD relaxion model would be favoured versus the SM, were the cut-off much lower than the Planck scale. We find in figure 2 that, although we previously found that the relaxion model was not favoured versus the SM with a Planck-scale cut-off, if the cut-off were lowered in each model to about  $10^8 \text{ GeV}$ , the relaxion

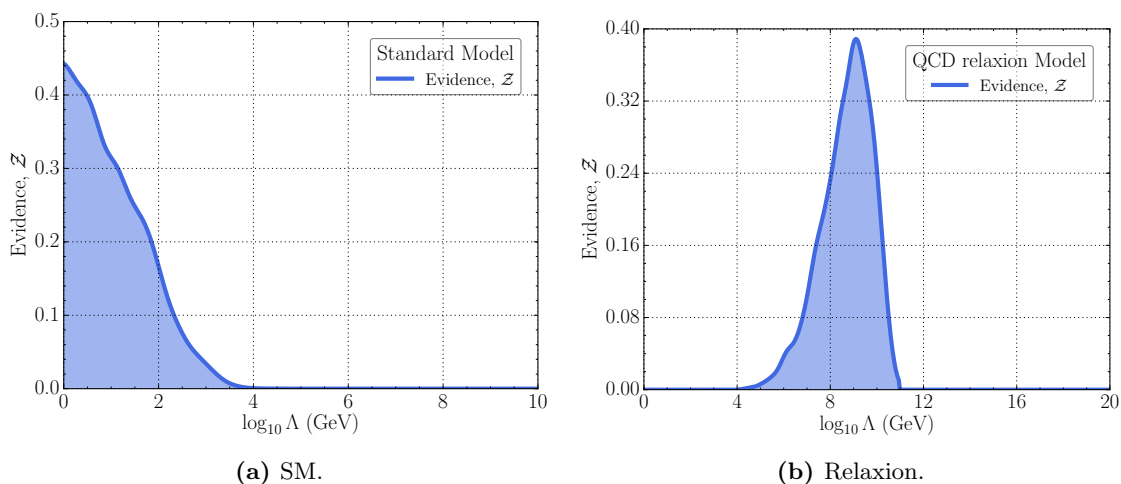


**Figure 2.** The evidence as a function of the cut-off,  $\Lambda$ , in (a) the SM and (b) a relaxion model. The evidence includes **weak-scale** and **conditions**. This illustrates that a relaxion model could be significantly favoured if the cut-off were lowered from the Planck scale to about  $10^8$  GeV e.g., by supersymmetrizing the SM and relaxion model. The evidences are plotted in arbitrary units.

model could be significantly favoured. In other words, the relaxion mechanism may solve the little-hierarchy problem in a supersymmetric model with soft-breaking masses at about  $10^8$  GeV, but not the hierarchy problem by itself. Hence, in isolation, our QCD relaxion model cannot improve fine-tuning compared to the SM.

With a cut-off allowed to be as low as 10 TeV, considering **weak-scale**, **conditions** and **decay**, the Bayes-factor favours our QCD relaxion model by  $10^6$  versus the SM and about  $10^{31}$  versus the SM with Planck-scale quadratic corrections. Including low-scale inflation in e.g., a supersymmetrized relaxion model, however, might necessitate an inflaton mass  $m_\sigma \ll M_{\text{SUSY}}$ . This little-hierarchy problem could scotch the Bayes-factor of  $10^6$  in favour of the supersymmetrized relaxion model.

## 5.2 Observables

To illustrate the resolution of the hierarchy problem, in figure 3 we plot the priors for the  $Z$ -boson mass in the SM and our QCD relaxion model that result from the non-informative priors for Lagrangian parameters in table 2, that is,

$$p(\log M_Z | M) = \int \delta(\log M_Z - \log M_Z(\mathbf{p})) p(\mathbf{p} | M) \prod d\mathbf{p}. \quad (5.2)$$

This illustrates their generic predictions for the weak scale. This would be numerically equivalent to the Bayesian evidence if our data were  $\log M_Z$  and we approximated our measurement with a Dirac function. Whereas the SM favours a weak scale close to the Planck scale, the relaxion model results in considerable probability mass at scales much less than the Planck scale, resolving the hierarchy problem. We find that if the relaxion is the QCD axion, the posterior probability that  $|\theta_{\text{QCD}}| \lesssim 10^{-10}$  is negligible, confirming our expectations.

Data-set	weak-scale	+=conditions	+=decay	+=theta	+=inflation
$\mathcal{Z}$ (SM + $\sigma$ ) · GeV	$10^{-34}$			$10^{-45}$	$10^{-53}$
$\mathcal{Z}$ (relaxion) · GeV	$10^{-4}$	$10^{-32}$		$10^{-42}$	$10^{-77}$
$\mathcal{Z}$ (QCD relaxion) · GeV	$10^{-4}$	$10^{-34}$	$10^{-39}$	$\lll 10^{-39}$	$\lll 10^{-81}$
$B$ (relaxion/SM + $\sigma$ )	$10^{30}$	$10^2$		$10^2$	$10^{-25}$
$B$ (QCD relaxion/SM + $\sigma$ )	$10^{30}$	1	$10^{-5}$	$\lll 10^5$	$\lll 10^{-28}$
$B$ (QCD relaxion/relaxion)	1	$10^{-2}$	$10^{-7}$	$\lll 10^3$	$\lll 10^{-3}$
$P$ (relaxion/SM + $\sigma$ )		$10^{-28}$		1	$10^{-27}$
$P$ (QCD relaxion/SM + $\sigma$ )		$10^{-30}$	$10^{-6}$	$\lll 1$	$10^{-33}$
$P$ (QCD relaxion/relaxion)		$10^{-2}$	$10^{-6}$	$\lll 1$	$10^{-6}$

**Table 3.** Evidences,  $\mathcal{Z}$ , Bayes-factors,  $B$  and partial Bayes-factors,  $P$ , for the SM augmented with scalar-field inflation (SM +  $\sigma$ ), a relaxion toy-model and a QCD relaxion toy-model. We apply data incrementally in five data-sets: (i) the  $Z$ -boson mass (**weak-scale**), (ii) physicality conditions in relaxion models (**conditions**), (iii) constraints on the axion decay constant (**decay**), (iv)  $|\theta_{\text{QCD}}|$  (**theta**) and (v) BICEP/Planck measurements of inflationary observables (**inflation**). A Bayes-factor is a ratio of evidences, indicating the change in relative plausibility of two models in light of all data considered thus far. A partial Bayes-factor is a ratio of Bayes-factors, indicating the change in relative plausibility of two models in light of incrementing the data by a single data-set. A ratio of greater than one indicates that a relaxion toy-model is favoured. We highlight our most important findings in blue: that relaxion toy-models are favoured by about  $10^{30}$  by the  $Z$ -boson mass, but that once all constraints are included, that preference is reversed to about  $10^{-25}$  against relaxion toy-models.

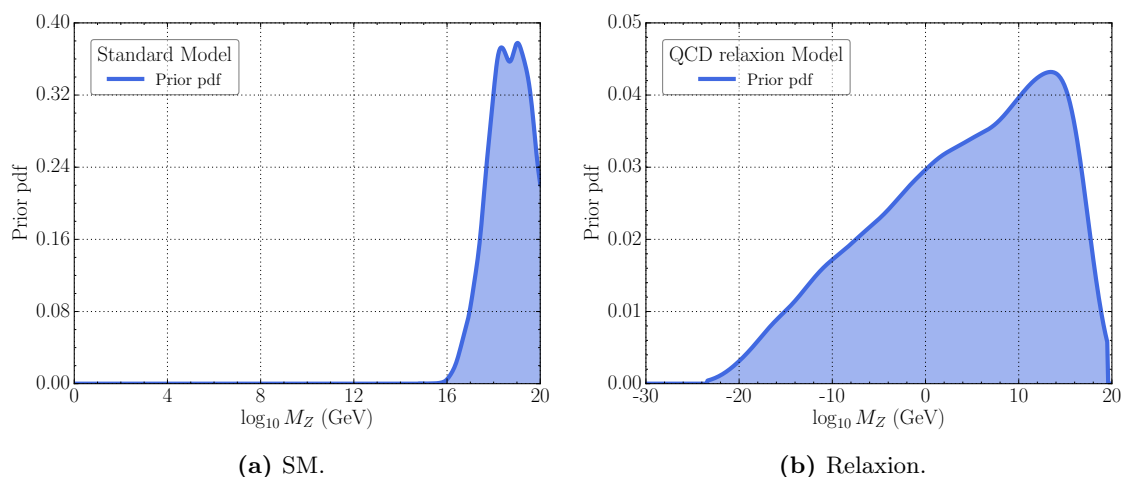


**Figure 3.** Prior distribution of  $\log_{10}$  of the  $Z$ -boson mass in (a) the SM and (b) a QCD relaxion model including no data. The density at the correct weak scale in the relaxion model is much greater than that in the SM. This illustrates that the relaxion mechanism improves fine-tuning of the weak scale with respect to the SM. The densities are plotted in arbitrary units.

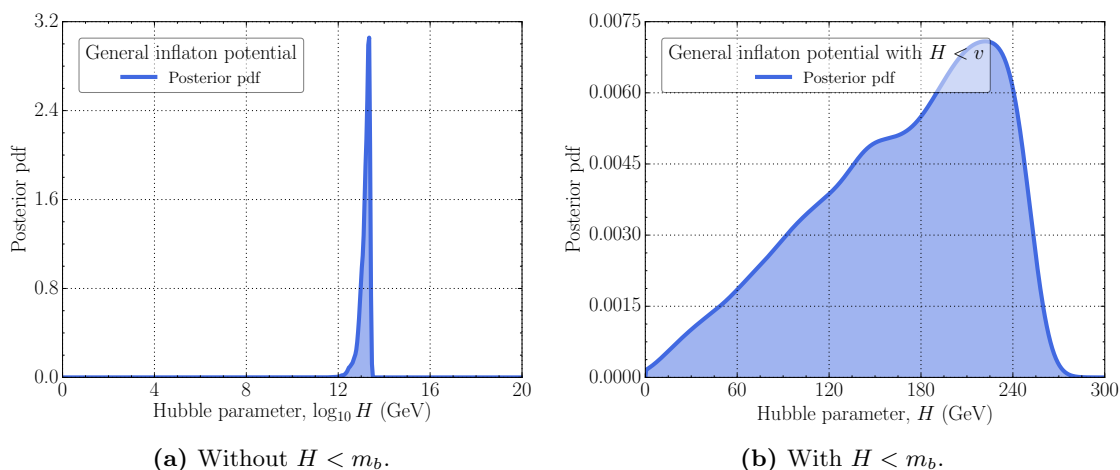


**Figure 4.** Posterior distribution for the Hubble parameter,  $H$ , for a general renormalisable inflationary potential (eq. (4.10)). In (a), the constraint that the Hubble parameter is less than the height of the periodic barriers,  $H < m_b$  (eq. (4.17)), is not applied; whereas in (b), it is applied. Both plots include Planck/BICEP measurements of  $r$ ,  $n_s$  and  $A_s$ .

To illustrate the fine-tuning required in the second epoch of inflation in a relaxation scenario, in figure 4 we plot the posterior distribution of the Hubble parameter  $H$  with and without constraint that the Hubble parameter is less than the height of the periodic barriers,  $H < m_b$  (eq. (4.17)), but with Planck/BICEP measurements of  $r$ ,  $n_s$  and  $A_s$ . In the unconstrained case in figure 4a, the posterior shows preference for  $H \gg m_b$ , as expected, resulting in a tiny evidence once  $H < m_b$  is applied. Consequently, the Bayes-factor significantly favours inflation in the SM +  $\sigma$  model.

This can be understood analytically. As discussed in section 4.2, for  $H \ll M_P$ , we must have that  $V(\langle\sigma\rangle) \ll M_P^4$ , where the potential is an order-four polynomial. The mass-squared term is typically Planckian as it received a quadratic correction. The general solution involves roots of a cubic equation. For simplicity, instead consider that  $m_3^3 = m_1 = 0$ . By dimensional analysis, the result must be that  $V(\langle\sigma\rangle) = f(\lambda)m_2^4 \sim M_P^4$ . In fact, the result is that  $V(\langle\sigma\rangle) = m_2^4/(4\lambda\sigma)$ . Other than by extreme fine-tuning of the mass-squared (which might not agree with Planck/BICEP measurements of  $r$ ,  $n_s$  and  $A_s$ ), there is no chance that  $H \ll m_b$ . On the other hand, consider that all dimensional parameters are equal to the mass-squared term,  $|m_1| = |m_2| = |m_3|$ . Again, it must be that  $V(\langle\sigma\rangle) = f(\lambda)m_2^4 \sim M_P^4$ , though in this case the function  $f$  is rather complicated. In any case, one must still require fine-tuning such that  $V(\langle\sigma\rangle) \sim M_P^4$  is avoided.

## 6 Discussion and conclusions

We constructed models that utilised a relaxation mechanism recently proposed by Graham et al. to solve the hierarchy problem. Unfortunately, finding the weak scale in relaxation models involves solving a transcendental equation with numerical methods. We presented

an analytic expression for an interval bounding the weak scale and an analytic expression for a lower bound on  $|\theta_{\text{QCD}}|$ , confirming that  $|\theta_{\text{QCD}}| \approx \pi/2$  if the relaxion is the QCD axion.

We performed the first statistical analysis of a relaxion model by scanning relaxion models' parameter spaces with the nested sampling algorithm, considering data from measurements of the weak scale, the axion decay constant,  $|\theta_{\text{QCD}}|$  and BICEP/Planck measurements of inflationary observables  $r$ ,  $n_s$  and  $A_s$ . This resulted in so-called Bayesian evidences for our relaxion models augmented with scalar-field inflation. In a similar manner, we calculated Bayesian evidences for the SM augmented with scalar-field inflation.

We found that the Bayes-factors — ratios of Bayesian evidences that indicate how one ought to update one's relative prior belief in two models — favoured relaxion models versus the SM by a colossal factor of about  $10^{30}$  if one considered only the weak scale. Once we included physicality conditions upon inflation during relaxation, however, the Bayes-factors were decimated to about 100 for the non-QCD relaxion model and about 1 for the QCD relaxion model. The physicality condition on the energy density during the relaxion mechanism results, in fact, in a fine-tuning penalty similar to that for the hierarchy problem in the SM, as demonstrated in eq. (5.1). The resulting Bayes-factors are then of order unity.

Constraints upon the QCD relaxion decay constant and  $|\theta_{\text{QCD}}|$  severely impair the plausibility of the QCD relaxion model, whereas inflationary observables measured by BICEP/Planck demolish that of the surviving, non-QCD relaxion model. In this regard, we find that the SM augmented with scalar-field inflation is favoured by a Bayes-factor of about  $10^{25}$  with respect to the non-QCD relaxion model. This stems from a constraint upon the Hubble parameter during inflation: within the relaxion framework the Hubble parameter must be fine-tuned to  $H \lll M_{\text{P}}$ , in order to prevent inflation from destroying the periodic barriers in the relaxion potential. In contrast, the polynomial inflationary potentials supported by current observations generically predict that  $H \lesssim M_{\text{P}}$ , as explained in figure 4 and the accompanying discussion.

Thus, whilst the analysed relaxion models indeed solve the hierarchy problem leading to Bayes-factors of about  $10^{30}$  in their favour, the same Bayes-factors are scotched by constraints upon parameters in the relaxion potential and the Hubble parameter during inflation, ultimately leading to a Bayes-factor of about  $10^{25}$  in favour of the SM augmented with scalar-field inflation. We anticipate, furthermore, that detailed consideration of baryogenesis and thermal effects (including the disastrous possibility of reheating restoring electroweak symmetry) would further damage the plausibility of relaxion models and conclude that the required unconventional cosmology is the Achilles' heel of the relaxion mechanism.

To conclude, we also remark that our results stand in the absence of a clear UV-completion for the considered relaxion models and that the lack of information regarding the origins of the parameters in the relaxion Lagrangian was encoded in the adopted uninformative priors. If such a UV-completion were available, it would possibly dictate a different choice of priors that could re-establish the plausibility of the relaxion framework.

## Acknowledgments

We thank Kristjan Kannike for helpful discussions. LM and MR are supported by the grants IUT23-6, PUTJD110 and by EU through the ERDF CoE program. AF, GW and CB are in part supported by the ARC Centre of Excellence for Particle Physics at the Tera-scale.

**Open Access.** This article is distributed under the terms of the Creative Commons Attribution License ([CC-BY 4.0](https://creativecommons.org/licenses/by/4.0/)), which permits any use, distribution and reproduction in any medium, provided the original author(s) and source are credited.

## References

- [1] P.W. Graham, D.E. Kaplan and S. Rajendran, *Cosmological relaxation of the electroweak scale*, *Phys. Rev. Lett.* **115** (2015) 221801 [[arXiv:1504.07551](https://arxiv.org/abs/1504.07551)] [[INSPIRE](#)].
- [2] L.F. Abbott, *A mechanism for reducing the value of the cosmological constant*, *Phys. Lett. B* **150** (1985) 427 [[INSPIRE](#)].
- [3] G. Dvali and A. Vilenkin, *Cosmic attractors and gauge hierarchy*, *Phys. Rev. D* **70** (2004) 063501 [[hep-th/0304043](https://arxiv.org/abs/hep-th/0304043)] [[INSPIRE](#)].
- [4] G. Dvali, *Large hierarchies from attractor vacua*, *Phys. Rev. D* **74** (2006) 025018 [[hep-th/0410286](https://arxiv.org/abs/hep-th/0410286)] [[INSPIRE](#)].
- [5] S. Weinberg, *Implications of dynamical symmetry breaking*, *Phys. Rev. D* **13** (1976) 974 [[INSPIRE](#)].
- [6] S. Weinberg, *Implications of dynamical symmetry breaking: an addendum*, *Phys. Rev. D* **19** (1979) 1277 [[INSPIRE](#)].
- [7] L. Susskind, *Dynamics of spontaneous symmetry breaking in the Weinberg-Salam theory*, *Phys. Rev. D* **20** (1979) 2619 [[INSPIRE](#)].
- [8] E. Gildener, *Gauge symmetry hierarchies*, *Phys. Rev. D* **14** (1976) 1667 [[INSPIRE](#)].
- [9] E. Witten, *Dynamical breaking of supersymmetry*, *Nucl. Phys. B* **188** (1981) 513 [[INSPIRE](#)].
- [10] V. Mukhanov, *Physical foundations of cosmology*, Cambridge University Press, Oxford U.K. (2005).
- [11] S. Di Chiara, K. Kannike, L. Marzola, A. Racioppi, M. Raidal and C. Spethmann, *Relaxion cosmology and the price of fine-tuning*, *Phys. Rev. D* **93** (2016) 103527 [[arXiv:1511.02858](https://arxiv.org/abs/1511.02858)] [[INSPIRE](#)].
- [12] J. Jaeckel, V.M. Mehta and L.T. Witkowski, *Musings on cosmological relaxation and the hierarchy problem*, *Phys. Rev. D* **93** (2016) 063522 [[arXiv:1508.03321](https://arxiv.org/abs/1508.03321)] [[INSPIRE](#)].
- [13] R. Barbieri and G.F. Giudice, *Upper bounds on supersymmetric particle masses*, *Nucl. Phys. B* **306** (1988) 63 [[INSPIRE](#)].
- [14] J.R. Ellis, K. Enqvist, D.V. Nanopoulos and F. Zwirner, *Observables in low-energy superstring models*, *Mod. Phys. Lett. A* **1** (1986) 57 [[INSPIRE](#)].
- [15] B.C. Allanach, K. Cranmer, C.G. Lester and A.M. Weber, *Natural priors, CMSSM fits and LHC weather forecasts*, *JHEP* **08** (2007) 023 [[arXiv:0705.0487](https://arxiv.org/abs/0705.0487)] [[INSPIRE](#)].
- [16] M.E. Cabrera, J.A. Casas and R. Ruiz de Austri, *Bayesian approach and naturalness in MSSM analyses for the LHC*, *JHEP* **03** (2009) 075 [[arXiv:0812.0536](https://arxiv.org/abs/0812.0536)] [[INSPIRE](#)].

- [17] A. Fowlie, *CMSSM, naturalness and the “fine-tuning price” of the Very Large Hadron Collider*, *Phys. Rev. D* **90** (2014) 015010 [[arXiv:1403.3407](#)] [[INSPIRE](#)].
- [18] S. Fichet, *Quantified naturalness from Bayesian statistics*, *Phys. Rev. D* **86** (2012) 125029 [[arXiv:1204.4940](#)] [[INSPIRE](#)].
- [19] M.E. Cabrera, *Bayesian study and naturalness in MSSM forecast for the LHC*, in *Proceedings, 45<sup>th</sup> Rencontres de Moriond on Electroweak Interactions and Unified Theories*, (2010) [[arXiv:1005.2525](#)] [[INSPIRE](#)].
- [20] A. Fowlie, *The little-hierarchy problem is a little problem: understanding the difference between the big- and little-hierarchy problems with Bayesian probability*, [arXiv:1506.03786](#) [[INSPIRE](#)].
- [21] D. Kim, P. Athron, C. Balázs, B. Farmer and E. Hutchison, *Bayesian naturalness of the CMSSM and CNMSSM*, *Phys. Rev. D* **90** (2014) 055008 [[arXiv:1312.4150](#)] [[INSPIRE](#)].
- [22] A. Fowlie, *Is the CNMSSM more credible than the CMSSM?*, *Eur. Phys. J. C* **74** (2014) 3105 [[arXiv:1407.7534](#)] [[INSPIRE](#)].
- [23] J. Earman, *Bayes or bust?: a critical examination of Bayesian confirmation theory*, MIT Press, U.S.A. (1992).
- [24] E.T. Jaynes, *Probability theory: the logic of science*, Cambridge University Press, Cambridge U.K. (2003).
- [25] P. Gregory, *Bayesian logical data analysis for the physical sciences*, Cambridge University Press, Cambridge U.K. (2005).
- [26] D.E. Lopez-Fogliani, L. Roszkowski, R. Ruiz de Austri and T.A. Varley, *A Bayesian analysis of the constrained NMSSM*, *Phys. Rev. D* **80** (2009) 095013 [[arXiv:0906.4911](#)] [[INSPIRE](#)].
- [27] K. Kowalska, S. Munir, L. Roszkowski, E.M. Sessolo, S. Trojanowski and Y.-L.S. Tsai, *Constrained next-to-minimal supersymmetric Standard Model with a 126 GeV Higgs boson: a global analysis*, *Phys. Rev. D* **87** (2013) 115010 [[arXiv:1211.1693](#)] [[INSPIRE](#)].
- [28] A.J. Williams, *Explaining the Fermi galactic centre excess in the CMSSM*, [arXiv:1510.00714](#) [[INSPIRE](#)].
- [29] R. Diamanti, M.E.C. Catalan and S. Ando, *Dark matter protohalos in a nine parameter MSSM and implications for direct and indirect detection*, *Phys. Rev. D* **92** (2015) 065029 [[arXiv:1506.01529](#)] [[INSPIRE](#)].
- [30] M.E. Cabrera-Catalan, S. Ando, C. Weniger and F. Zandanel, *Indirect and direct detection prospect for TeV dark matter in the nine parameter MSSM*, *Phys. Rev. D* **92** (2015) 035018 [[arXiv:1503.00599](#)] [[INSPIRE](#)].
- [31] J.A. Casas, J.M. Moreno, S. Robles, K. Rolbiecki and B. Zaldivar, *What is a natural SUSY scenario?*, *JHEP* **06** (2015) 070 [[arXiv:1407.6966](#)] [[INSPIRE](#)].
- [32] L. Roszkowski, E.M. Sessolo and A.J. Williams, *What next for the CMSSM and the NUHM: improved prospects for superpartner and dark matter detection*, *JHEP* **08** (2014) 067 [[arXiv:1405.4289](#)] [[INSPIRE](#)].
- [33] C. Strece et al., *Profile likelihood maps of a 15-dimensional MSSM*, *JHEP* **09** (2014) 081 [[arXiv:1405.0622](#)] [[INSPIRE](#)].

- [34] A. Fowlie and M. Raidal, *Prospects for constrained supersymmetry at  $\sqrt{s} = 33$  TeV and  $\sqrt{s} = 100$  TeV proton-proton super-colliders*, *Eur. Phys. J. C* **74** (2014) 2948 [[arXiv:1402.5419](#)] [[INSPIRE](#)].
- [35] S.S. AbdusSalam, *Stop-mass prediction in naturalness scenarios within MSSM-25*, *Int. J. Mod. Phys. A* **29** (2014) 1450160 [[arXiv:1312.7830](#)] [[INSPIRE](#)].
- [36] M.E. Cabrera, A. Casas, R. Ruiz de Austri and G. Bertone, *LHC and dark matter phenomenology of the NUGHM*, *JHEP* **12** (2014) 114 [[arXiv:1311.7152](#)] [[INSPIRE](#)].
- [37] C. Arina and M.E. Cabrera, *Multi-lepton signatures at LHC from sneutrino dark matter*, *JHEP* **04** (2014) 100 [[arXiv:1311.6549](#)] [[INSPIRE](#)].
- [38] R. Ruiz de Austri and C. Pérez de los Heros, *Impact of nucleon matrix element uncertainties on the interpretation of direct and indirect dark matter search results*, *JCAP* **11** (2013) 049 [[arXiv:1307.6668](#)] [[INSPIRE](#)].
- [39] A. Fowlie, K. Kowalska, L. Roszkowski, E.M. Sessolo and Y.-L.S. Tsai, *Dark matter and collider signatures of the MSSM*, *Phys. Rev. D* **88** (2013) 055012 [[arXiv:1306.1567](#)] [[INSPIRE](#)].
- [40] M.E. Cabrera, J.A. Casas and R. Ruiz de Austri, *The health of SUSY after the Higgs discovery and the XENON100 data*, *JHEP* **07** (2013) 182 [[arXiv:1212.4821](#)] [[INSPIRE](#)].
- [41] C. Stenge, G. Bertone, F. Feroz, M. Fornasa, R. Ruiz de Austri and R. Trotta, *Global fits of the CMSSM and NUHM including the LHC Higgs discovery and new XENON100 constraints*, *JCAP* **04** (2013) 013 [[arXiv:1212.2636](#)] [[INSPIRE](#)].
- [42] C. Balázs and S.K. Gupta, *Peccei-Quinn violating minimal supergravity and a 126 GeV Higgs boson*, *Phys. Rev. D* **87** (2013) 035023 [[arXiv:1212.1708](#)] [[INSPIRE](#)].
- [43] A. Fowlie et al., *The CMSSM favoring new territories: the impact of new LHC limits and a 125 GeV Higgs*, *Phys. Rev. D* **86** (2012) 075010 [[arXiv:1206.0264](#)] [[INSPIRE](#)].
- [44] C. Balázs, A. Buckley, D. Carter, B. Farmer and M. White, *Should we still believe in constrained supersymmetry?*, *Eur. Phys. J. C* **73** (2013) 2563 [[arXiv:1205.1568](#)] [[INSPIRE](#)].
- [45] L. Roszkowski, E.M. Sessolo and Y.-L.S. Tsai, *Bayesian implications of current LHC supersymmetry and dark matter detection searches for the constrained MSSM*, *Phys. Rev. D* **86** (2012) 095005 [[arXiv:1202.1503](#)] [[INSPIRE](#)].
- [46] C. Stenge, G. Bertone, D.G. Cerdeno, M. Fornasa, R. Ruiz de Austri and R. Trotta, *Updated global fits of the CMSSM including the latest LHC SUSY and Higgs searches and XENON100 data*, *JCAP* **03** (2012) 030 [[arXiv:1112.4192](#)] [[INSPIRE](#)].
- [47] A. Fowlie, A. Kalinowski, M. Kazana, L. Roszkowski and Y.L.S. Tsai, *Bayesian implications of current LHC and XENON100 search limits for the constrained MSSM*, *Phys. Rev. D* **85** (2012) 075012 [[arXiv:1111.6098](#)] [[INSPIRE](#)].
- [48] G. Bertone, D.G. Cerdeno, M. Fornasa, L. Pieri, R. Ruiz de Austri and R. Trotta, *Complementarity of indirect and accelerator dark matter searches*, *Phys. Rev. D* **85** (2012) 055014 [[arXiv:1111.2607](#)] [[INSPIRE](#)].
- [49] M.E. Cabrera, J.A. Casas, V.A. Mitsou, R. Ruiz de Austri and J. Terron, *Histogram comparison as a powerful tool for the search of new physics at LHC. Application to CMSSM*, *JHEP* **04** (2012) 133 [[arXiv:1109.3759](#)] [[INSPIRE](#)].

- [50] B.C. Allanach and M.J. Dolan, *Supersymmetry with prejudice: fitting the wrong model to LHC data*, *Phys. Rev. D* **86** (2012) 055022 [[arXiv:1107.2856](#)] [[INSPIRE](#)].
- [51] G. Bertone, D.G. Cerdeno, M. Fornasa, R. Ruiz de Austri, C. Strece and R. Trotta, *Global fits of the CMSSM including the first LHC and XENON100 data*, *JCAP* **01** (2012) 015 [[arXiv:1107.1715](#)] [[INSPIRE](#)].
- [52] D.T. Cumberbatch, D.E. Lopez-Fogliani, L. Roszkowski, R. Ruiz de Austri and Y.-L.S. Tsai, *Is light neutralino as dark matter still viable?*, [arXiv:1107.1604](#) [[INSPIRE](#)].
- [53] A. Fowlie and L. Roszkowski, *Reconstructing ATLAS  $SU_3$  in the CMSSM and relaxed phenomenological supersymmetry models*, [arXiv:1106.5117](#) [[INSPIRE](#)].
- [54] B.C. Allanach, *Impact of CMS multi-jets and missing energy search on CMSSM fits*, *Phys. Rev. D* **83** (2011) 095019 [[arXiv:1102.3149](#)] [[INSPIRE](#)].
- [55] F. Feroz, K. Cranmer, M. Hobson, R. Ruiz de Austri and R. Trotta, *Challenges of profile likelihood evaluation in multi-dimensional SUSY scans*, *JHEP* **06** (2011) 042 [[arXiv:1101.3296](#)] [[INSPIRE](#)].
- [56] J. Ripken, J. Conrad and P. Scott, *Implications for constrained supersymmetry of combined H.E.S.S. observations of dwarf galaxies, the galactic halo and the galactic centre*, *JCAP* **11** (2011) 004 [[arXiv:1012.3939](#)] [[INSPIRE](#)].
- [57] M.E. Cabrera, J.A. Casas, R. Ruiz de Austri and R. Trotta, *Quantifying the tension between the Higgs mass and  $(g-2)_\mu$  in the CMSSM*, *Phys. Rev. D* **84** (2011) 015006 [[arXiv:1011.5935](#)] [[INSPIRE](#)].
- [58] Y. Akrami, C. Savage, P. Scott, J. Conrad and J. Edsjo, *Statistical coverage for supersymmetric parameter estimation: a case study with direct detection of dark matter*, *JCAP* **07** (2011) 002 [[arXiv:1011.4297](#)] [[INSPIRE](#)].
- [59] M.E. Cabrera, J.A. Casas and R. Ruiz d Austri, *MSSM forecast for the LHC*, *JHEP* **05** (2010) 043 [[arXiv:0911.4686](#)] [[INSPIRE](#)].
- [60] Y. Akrami, P. Scott, J. Edsjo, J. Conrad and L. Bergstrom, *A profile likelihood analysis of the constrained MSSM with genetic algorithms*, *JHEP* **04** (2010) 057 [[arXiv:0910.3950](#)] [[INSPIRE](#)].
- [61] L. Roszkowski, R. Ruiz de Austri and R. Trotta, *Efficient reconstruction of CMSSM parameters from LHC data: a case study*, *Phys. Rev. D* **82** (2010) 055003 [[arXiv:0907.0594](#)] [[INSPIRE](#)].
- [62] L. Roszkowski, R. Ruiz de Austri, R. Trotta, Y.-L.S. Tsai and T.A. Varley, *Global fits of the non-universal Higgs model*, *Phys. Rev. D* **83** (2011) 015014 [*Erratum* *ibid.* **83** (2011) 039901] [[arXiv:0903.1279](#)] [[INSPIRE](#)].
- [63] R. Trotta, F. Feroz, M.P. Hobson, L. Roszkowski and R. Ruiz de Austri, *The impact of priors and observables on parameter inferences in the constrained MSSM*, *JHEP* **12** (2008) 024 [[arXiv:0809.3792](#)] [[INSPIRE](#)].
- [64] F. Feroz, B.C. Allanach, M. Hobson, S.S. AbdusSalam, R. Trotta and A.M. Weber, *Bayesian selection of sign  $\mu$  within  $mSUGRA$  in global fits including WMAP5 results*, *JHEP* **10** (2008) 064 [[arXiv:0807.4512](#)] [[INSPIRE](#)].
- [65] B.C. Allanach and D. Hooper, *Panglossian prospects for detecting neutralino dark matter in light of natural priors*, *JHEP* **10** (2008) 071 [[arXiv:0806.1923](#)] [[INSPIRE](#)].

- [66] B.C. Allanach, M.J. Dolan and A.M. Weber, *Global fits of the large volume string scenario to WMAP5 and other indirect constraints using Markov chain Monte Carlo*, *JHEP* **08** (2008) 105 [[arXiv:0806.1184](#)] [[INSPIRE](#)].
- [67] B.C. Allanach, *SUSY predictions and SUSY tools at the LHC*, *Eur. Phys. J. C* **59** (2009) 427 [[arXiv:0805.2088](#)] [[INSPIRE](#)].
- [68] L. Roszkowski, R. Ruiz de Austri and R. Trotta, *Implications for the constrained MSSM from a new prediction for  $b \rightarrow s\gamma$* , *JHEP* **07** (2007) 075 [[arXiv:0705.2012](#)] [[INSPIRE](#)].
- [69] L. Roszkowski, R. Ruiz de Austri and R. Trotta, *On the detectability of the CMSSM light Higgs boson at the Tevatron*, *JHEP* **04** (2007) 084 [[hep-ph/0611173](#)] [[INSPIRE](#)].
- [70] R. Trotta, *Bayes in the sky: Bayesian inference and model selection in cosmology*, *Contemp. Phys.* **49** (2008) 71 [[arXiv:0803.4089](#)] [[INSPIRE](#)].
- [71] J. Martin, C. Ringeval, R. Trotta and V. Vennin, *The best inflationary models after Planck*, *JCAP* **03** (2014) 039 [[arXiv:1312.3529](#)] [[INSPIRE](#)].
- [72] J. Martin, C. Ringeval, R. Trotta and V. Vennin, *Compatibility of Planck and BICEP2 in the light of inflation*, *Phys. Rev. D* **90** (2014) 063501 [[arXiv:1405.7272](#)] [[INSPIRE](#)].
- [73] W. Jefferys and J. Berger, *Sharpening Occam's razor on a Bayesian stop*, *Bull. Amer. Astron. Soc.* **23** (1991) 1259.
- [74] J.R. Espinosa, C. Grojean, G. Panico, A. Pomarol, O. Pujolàs and G. Servant, *Cosmological Higgs-axion interplay for a naturally small electroweak scale*, *Phys. Rev. Lett.* **115** (2015) 251803 [[arXiv:1506.09217](#)] [[INSPIRE](#)].
- [75] G. 't Hooft, *Naturalness, chiral symmetry, and spontaneous chiral symmetry breaking*, *NATO Sci. Ser. B* **59** (1980) 135 [[INSPIRE](#)].
- [76] R.S. Gupta, Z. Komargodski, G. Perez and L. Ubaldi, *Is the relaxion an axion?*, *JHEP* **02** (2016) 166 [[arXiv:1509.00047](#)] [[INSPIRE](#)].
- [77] L.E. Ibáñez, M. Montero, A. Uranga and I. Valenzuela, *Relaxion monodromy and the weak gravity conjecture*, *JHEP* **04** (2016) 020 [[arXiv:1512.00025](#)] [[INSPIRE](#)].
- [78] R.D. Peccei and H.R. Quinn, *CP conservation in the presence of instantons*, *Phys. Rev. Lett.* **38** (1977) 1440 [[INSPIRE](#)].
- [79] PARTICLE DATA GROUP collaboration, K.A. Olive et al., *Review of particle physics*, *Chin. Phys. C* **38** (2014) 090001 [[INSPIRE](#)].
- [80] J.F. Donoghue, *CP violation and the limits of the Standard Model: (TASI-94) Proceedings of the 1994 Theoretical Advanced Study Institute in Elementary Particle Physics*, World Scientific, Singapore (1995).
- [81] E. Hardy, *Electroweak relaxation from finite temperature*, *JHEP* **11** (2015) 077 [[arXiv:1507.07525](#)] [[INSPIRE](#)].
- [82] D.J. Gross, R.D. Pisarski and L.G. Yaffe, *QCD and instantons at finite temperature*, *Rev. Mod. Phys.* **53** (1981) 43 [[INSPIRE](#)].
- [83] M. Quirós, *Finite temperature field theory and phase transitions*, in *High energy physics and cosmology. Proceedings, Summer School, Trieste Italy June 29–July 17 1998*, pg. 187 [[hep-ph/9901312](#)] [[INSPIRE](#)].

- [84] A.D. Sakharov, *Violation of CP invariance, c asymmetry and baryon asymmetry of the universe*, *Pisma Zh. Eksp. Teor. Fiz.* **5** (1967) 32 [*JETP Lett.* **5** (1967) 24] [*Sov. Phys. Usp.* **34** (1991) 392] [*Usp. Fiz. Nauk* **161** (1991) 61] [INSPIRE].
- [85] A. Riotto, *Theories of baryogenesis*, in *High energy physics and cosmology. Proceedings, Summer School, Trieste Italy June 29–July 17 1998*, pg. 326 [hep-ph/9807454] [INSPIRE].
- [86] R. Rangarajan and D.V. Nanopoulos, *Inflationary baryogenesis*, *Phys. Rev. D* **64** (2001) 063511 [hep-ph/0103348] [INSPIRE].
- [87] S. H.-S. Alexander, M.E. Peskin and M.M. Sheikh-Jabbari, *Leptogenesis from gravity waves in models of inflation*, *Phys. Rev. Lett.* **96** (2006) 081301 [hep-th/0403069] [INSPIRE].
- [88] H.H. Patel and M.J. Ramsey-Musolf, *Baryon washout, electroweak phase transition and perturbation theory*, *JHEP* **07** (2011) 029 [arXiv:1101.4665] [INSPIRE].
- [89] S.P. Patil and P. Schwaller, *Relaxing the electroweak scale: the role of broken dS symmetry*, *JHEP* **02** (2016) 077 [arXiv:1507.08649] [INSPIRE].
- [90] O. Matsedonskyi, *Mirror cosmological relaxation of the electroweak scale*, *JHEP* **01** (2016) 063 [arXiv:1509.03583] [INSPIRE].
- [91] D.E. Kaplan and R. Rattazzi, *Large field excursions and approximate discrete symmetries from a clockwork axion*, *Phys. Rev. D* **93** (2016) 085007 [arXiv:1511.01827] [INSPIRE].
- [92] K. Choi and S.H. Im, *Realizing the relaxion from multiple axions and its UV completion with high scale supersymmetry*, *JHEP* **01** (2016) 149 [arXiv:1511.00132] [INSPIRE].
- [93] O. Antipin and M. Redi, *The half-composite two Higgs doublet model and the relaxion*, *JHEP* **12** (2015) 031 [arXiv:1508.01112] [INSPIRE].
- [94] B. Batell, G.F. Giudice and M. McCullough, *Natural heavy supersymmetry*, *JHEP* **12** (2015) 162 [arXiv:1509.00834] [INSPIRE].
- [95] N. Fonseca, L. de Lima, C.S. Machado and R.D. Matheus, *Large field excursions from a few site relaxion model*, *Phys. Rev. D* **94** (2016) 015010 [arXiv:1601.07183] [INSPIRE].
- [96] J.L. Evans, T. Gherghetta, N. Nagata and Z. Thomas, *Naturalizing supersymmetry with a two-field relaxion mechanism*, [arXiv:1602.04812] [INSPIRE].
- [97] J. Martin, C. Ringeval and V. Vennin, *Encyclopædia inflationaris*, *Phys. Dark Univ.* **5-6** (2014) 75 [arXiv:1303.3787] [INSPIRE].
- [98] A.R. Liddle and D.H. Lyth, *COBE, gravitational waves, inflation and extended inflation*, *Phys. Lett. B* **291** (1992) 391 [astro-ph/9208007] [INSPIRE].
- [99] A.R. Liddle and D.H. Lyth, *Cosmological inflation and large scale structure*, Cambridge University Press, Cambridge U.K. (2000).
- [100] PLANCK collaboration, P.A.R. Ade et al., *Planck 2013 results. XXII. Constraints on inflation*, *Astron. Astrophys.* **571** (2014) A22 [arXiv:1303.5082] [INSPIRE].
- [101] R. Bousso, *TASI lectures on the cosmological constant*, *Gen. Rel. Grav.* **40** (2008) 607 [arXiv:0708.4231] [INSPIRE].
- [102] J. Buchner et al., *X-ray spectral modelling of the AGN obscuring region in the CDFS: Bayesian model selection and catalogue*, *Astron. Astrophys.* **564** (2014) A125 [arXiv:1402.0004] [INSPIRE].

- [103] F. Feroz, M.P. Hobson, E. Cameron and A.N. Pettitt, *Importance nested sampling and the MultiNest algorithm*, [arXiv:1306.2144](#) [INSPIRE].
- [104] F. Feroz and M.P. Hobson, *Multimodal nested sampling: an efficient and robust alternative to MCMC methods for astronomical data analysis*, *Mon. Not. Roy. Astron. Soc.* **384** (2008) 449 [[arXiv:0704.3704](#)] [INSPIRE].
- [105] F. Feroz, M.P. Hobson and M. Bridges, *MultiNest: an efficient and robust Bayesian inference tool for cosmology and particle physics*, *Mon. Not. Roy. Astron. Soc.* **398** (2009) 1601 [[arXiv:0809.3437](#)] [INSPIRE].
- [106] J. Skilling, *Nested sampling*, *AIP Conf. Proc.* **735** (2004) 395.
- [107] J. Skilling, *Nested sampling for general Bayesian computation*, *Bayesian Anal.* **1** (2006) 833.
- [108] M. Dine, *Supersymmetry and string theory: beyond the Standard Model*, Cambridge University Press, Cambridge U.K. (2007).
- [109] BICEP2 and PLANCK collaborations, P.A.R. Ade et al., *Joint analysis of BICEP2/Keck Array and Planck data*, *Phys. Rev. Lett.* **114** (2015) 101301 [[arXiv:1502.00612](#)] [INSPIRE].
- [110] PLANCK collaboration, P.A.R. Ade et al., *Planck 2015 results. XIII. Cosmological parameters*, [arXiv:1502.01589](#) [INSPIRE].

## Chapter 3

---

# Baryogenesis

---

I have argued that particle cosmology provides some of the most compelling reasons to believe that there is physics beyond the Standard Model. Baryonic matter makes up a small fraction 4.9% of the Universe's energy budget meaning that 95% of the Universe is made up of stuff everyone is yet to understand [33]. However, as I will argue, from a cosmological perspective no one even understands the baryonic component. So 100% of the Universe is unexplained! Indeed, the three pillars of the Standard Model of particle cosmology – inflation, the production of dark matter and the generation of a baryon asymmetry – all require physics beyond the Standard Model. That being said, some striking confirmations of the Standard Model of cosmology gives a strong argument that its the Standard Model of particle physics that needs modification rather than cosmology.

The cosmic baryon abundance can be measured through two completely independent methods. First through baryon acoustic oscillations in the cosmic microwave background and second through the Deuterium abundance which is very sensitive to the baryon abundance. It is convenient to express the cosmic baryon abundance as a fraction of the entropy density as this gives a number that does not change as the Universe expands [68]

$$Y_B = \frac{n_B}{s} = 8.59 \pm 0.11 . \quad (3.1)$$

This agreement is a triumph of modern cosmology as it is highly non-trivial for two independent measures to agree. One sees very few anti-baryons in the Universe. The few experiments observe is consistent with secondary production [69]. This baryon asymmetry is much too large to be a consequences of some initial condition as inflation will dilute any initial asymmetry. Specifically if one has a Planckian energy density pre-inflation, the maximum baryon asymmetry one can have assuming constant entropy is about five orders of magnitude too small.

### 3.1 Sakharov Conditions

Well before all this was known, it was shown by Sakharov that any mechanism that spontaneously produced the BAU would have to satisfy three conditions [70, 71]

- Violation of baryon (and lepton) number conservation,
- C and CP violation,

- Departure from equilibrium.

The first condition can be satisfied either through electroweak sphalerons, explicit B violation occurring in grand unified theories or through anomalous currents in Cherns Simons gravity. Electroweak sphalerons have the added advantage of converting P violating electroweak processes into C violating processes. This in conjunction with CP violating three body couplings (Yukawa or tri-scalar) can satisfy the second Sakharov condition. Satisfying the third option is where there has been the most variety in suggestions – from inflation, to the decay of heavy particles to a cosmic phase transition. One can mix and match different mechanisms for satisfying these three conditions and arrive at the major paradigms for generating the BAU. For example combining heavy particle decay (heavy neutrinos) mixed with electroweak sphalerons and neutrino sector CP violation is the essential ingredients of leptogenesis. I will focus our attention on electroweak baryogenesis which utilizes electroweak sphalerons during the electroweak phase transition. Electroweak baryogenesis has the significant advantage of being testable as the new physics it requires is generally weak scale.

The Standard Model in principle has all three ingredients – electroweak sphalerons provide a source of baryon number violation at high temperature, the CKM matrix is a source of CP violation and as the Universe cools the Higgs field acquires a vev in the electroweak phase transition. However, on a quantitative level the Standard Model fails to fulfil the last two Sakharov conditions. For a Higgs mass of 125 GeV, the electroweak phase transition does not proceed by bubble nucleation so the departure from equilibrium is not dramatic enough to facilitate enough baryon production. Furthermore the CKM matrix provides too feeble a source of CP violation.

## 3.2 Introductory remarks for published material in thesis chapter 3

Electroweak baryogenesis is a subject that has lacked a comprehensive reference that is self contained and includes everything (although some very fine reviews exist that include some very useful information see [72, 73]). As such I wrote a book that covers enough to take one from a graduate level to being able to perform state of art calculations focusing on the vev insertion approach.<sup>1</sup> I partially include this book here. Unfortunately IOP does not give permission for more than two chapters to be shared so I will also presented abbreviated summary of some of the content throughout this section focusing on the background most needed for later chapters in this thesis. This review contains a self contained summary on the baryon number violation in the Standard Model, finite temperature quantum field theory, phase transitions in quantum field theory, the derivation and solution to transport equations using the closed time path formalism, details of relevant thermal parameters such as thermal masses, widths, diffusion coefficients etc., and electric dipole moments.

---

<sup>1</sup>for a nice explanation of the WKB approach see [74, 75] and the references therein

### 3.3 Declaration for thesis chapter 3

#### Declaration by candidate

In the case of the paper present contained in chapter 3, the nature and extent of my contribution was as follows:

<b>Publication</b>	<b>Nature of contribution</b>	<b>Extent of contribution</b>
3	Single author paper	100%

The undersigned hereby certify that the above declaration correctly reflects the nature and extent of the candidate and co-authors' contributions to this work.

**Signatures:**

Graham White



**Date:**

3, 04. 2017

### **3.4 Published material for chapter 3: A pedagogical introduction to electroweak baryogenesis**

This content has been downloaded from IOPscience. Please scroll down to see the full text.

Download details:

IP Address: 130.194.20.173

This content was downloaded on 01/02/2017 at 01:58

Please note that [terms and conditions apply](#).

You may also be interested in:

[The baryon asymmetry in the standard model with a low cut-off](#)

Dietrich Bödeker, Lars Fromme, Stephan J. Huber et al.

[Non-gaussianity from baryon asymmetry](#)

Masahiro Kawasaki, Kazunori Nakayama and Fuminobu Takahashi

[Affleck-Dine \(pseudo\)-Dirac neutrino genesis](#)

Steven Abel and Véronique Pagé

[Quantum and medium effects in \(resonant\) leptogenesis](#)

Andreas Hohenegger

[Baryogenesis in the two-Higgs doublet model](#)

Lars Fromme, Stephan J. Huber and Michael Seniuch

[On Higgs and sphaleron effects during the leptogenesis era](#)

Enrico Nardi, Yosef Nir, Juan Racker et al.

[SO\(10\) unified models and soft leptogenesis](#)

Eung-Jin Chun and Liliana Velasco-Sevilla

[Neutrino masses, Baryon asymmetry, dark matter and the moduli problem — A complete framework](#)

Piyush Kumar

[Triplet seesaw model: from inflation to asymmetric dark matter and leptogenesis](#)

Chiara Arina

# A Pedagogical Introduction to Electroweak Baryogenesis



# A Pedagogical Introduction to Electroweak Baryogenesis

**Graham Albert White**

*ARC Centre of Excellence for Particle Physics at the Tera-scale, School of Physics  
and Astronomy, Monash University, Melbourne, Victoria 3800 Australia*  
*and*

*Monash Centre for Astrophysics, School of Physics and Astronomy,  
Monash University, Melbourne, Victoria 3800 Australia*

Morgan & Claypool Publishers

Copyright © 2016 Morgan & Claypool Publishers

All rights reserved. No part of this publication may be reproduced, stored in a retrieval system or transmitted in any form or by any means, electronic, mechanical, photocopying, recording or otherwise, without the prior permission of the publisher, or as expressly permitted by law or under terms agreed with the appropriate rights organization. Multiple copying is permitted in accordance with the terms of licences issued by the Copyright Licensing Agency, the Copyright Clearance Centre and other reproduction rights organisations.

#### Rights & Permissions

To obtain permission to re-use copyrighted material from Morgan & Claypool Publishers, please contact [info@morganclaypool.com](mailto:info@morganclaypool.com).

ISBN 978-1-6817-4457-5 (ebook)

ISBN 978-1-6817-4456-8 (print)

ISBN 978-1-6817-4459-9 (mobi)

DOI 10.1088/978-1-6817-4457-5

Version: 20161101

IOP Concise Physics

ISSN 2053-2571 (online)

ISSN 2054-7307 (print)

A Morgan & Claypool publication as part of IOP Concise Physics

Published by Morgan & Claypool Publishers, 40 Oak Drive, San Rafael, CA, 94903 USA

IOP Publishing, Temple Circus, Temple Way, Bristol BS1 6HG, UK

*For Samuel White*



# Contents

<b>Preface</b>	<b>x</b>
<b>Acknowledgements</b>	<b>xi</b>
<b>Author biography</b>	<b>xii</b>
<b>1 Introduction</b>	<b>1-1</b>
References	1-4
<b>2 The Sakharov conditions</b>	<b>2-1</b>
References	2-2
<b>3 Baryon number violation in the Standard Model</b>	<b>3-1</b>
3.1 The axial anomaly	3-1
3.1.1 Dimensional regularization	3-2
3.1.2 The Fujikawa method	3-4
3.1.3 Baryon and lepton number violation	3-7
3.2 The Chern–Simons form, baryon number violation, and the winding number	3-8
3.3 Winding number and non-abelian gauge groups	3-10
3.4 Solitons and instantons	3-12
3.5 The sphaleron	3-15
References	3-21
<b>4 Phase transitions</b>	<b>4-1</b>
4.1 Closed time path formalism	4-3
4.2 A brief review of the effective potential at zero temperature	4-8
4.3 The effective potential at finite temperature	4-12
4.3.1 The Standard Model example	4-15
4.3.2 Issues of gauge invariance	4-16
4.3.3 Daisy re-summation	4-19
4.3.4 The sphaleron rate at high temperature	4-19
4.4 The bounce solution	4-21
4.5 Analytic techniques for the single field case	4-22
4.5.1 Single field approximation	4-22
4.5.2 Developing ansatz solutions	4-24

4.6	Path deformation method	4-26
4.7	Perturbative method	4-28
4.7.1	Observations on convergence	4-31
4.7.2	A numerical example	4-32
4.7.3	Wall width and variation in $\beta$	4-33
4.8	Baryon washout condition	4-34
	References	4-36
<b>5</b>	<b>CP violation</b>	<b>5-1</b>
	References	5-4
<b>6</b>	<b>Particle dynamics during a phase transition</b>	<b>6-1</b>
6.1	Particle current divergences and self-energy	6-1
6.2	Transport coefficients and sources	6-4
6.2.1	A biscalar with VEV insertions	6-5
6.2.2	Dirac fermions with VEV insertions	6-11
6.2.3	Chiral fermions with VEV insertions	6-13
6.2.4	Triscalar and Yukawa interactions	6-15
6.2.5	Four-body interactions	6-22
6.3	Local equilibrium approximations	6-23
6.4	Gauge and supergauge equilibrium	6-23
6.5	Fast rate approximations	6-24
	References	6-25
<b>7</b>	<b>Plasma and bubble dynamics</b>	<b>7-1</b>
7.1	Imaginary time formalism	7-1
7.2	Diffusion coefficients	7-2
7.3	Thermal widths	7-6
7.4	Thermal masses	7-7
7.5	Bubble wall velocity	7-8
	References	7-12
<b>8</b>	<b>Transport equations</b>	<b>8-1</b>
8.1	The MSSM under supergauge equilibrium	8-1
8.2	Solution using fast rates, diffusion approximation, and ultrathin wall approximations	8-3
8.3	Solution without fast rates	8-5

8.4	Deriving the analytic solution	8-5
8.5	Beyond ultrathin walls	8-10
	References	8-11
<b>9</b>	<b>The baryon asymmetry</b>	<b>9-1</b>
	References	9-2
<b>10</b>	<b>A brief phenomenological summary</b>	<b>10-1</b>
	References	10-3
<b>11</b>	<b>Other mechanisms for producing the baryon asymmetry</b>	<b>11-1</b>
11.1	Leptogenesis	11-2
11.2	Affleck–Dine	11-3
11.3	Using inflation	11-4
	References	11-6
<b>12</b>	<b>Discussion and outlook</b>	<b>12-1</b>
	References	12-2

# Preface

We present a mostly self-contained pedagogical review of the theoretical background to electroweak baryogenesis as well as a brief summary of some of the other prevailing mechanisms for producing the asymmetry between matter and antimatter using the minimal supersymmetric Standard Model as a pedagogical tool whenever appropriate. This book covers an in-depth look at baryon number violation in the Standard Model, the necessary background in finite temperature field theory, plasma dynamics, and how to calculate the out-of-equilibrium evolution of particle number densities throughout a phase transition.

# Acknowledgements

A lot of what I learnt about Baryogenesis was from Michael Ramsey Musolf and Csaba Balazs. I would also like to acknowledge the post-doctorates and students that answered many questions of mine especially Peter Winslow and Huaike Guo. I would also like to acknowledge David Paganin, Jonathan Kozaczuk, Giancarlo Pozzo, Kaori Fuyuto and Andrew Fowlie for useful comments regarding this work. Finally I would like to acknowledge my wife for enduring many nights of me working late during this project.

# Author biography

## **Graham Albert White**

---



Graham White grew up in north Queensland, Australia. He developed a love of physics after reading some popular science books as a teenager and decided he wanted to become a physicist shortly after. Graham White is a Doctoral Student at Monash University studying Baryogenesis and holds a masters degree from University of Kentucky and has studied Baryogenesis at the Amherst Center for fundamental interactions (University of Massachusetts Amherst) as a guest scholar. He currently lives in Melbourne with his wife and son.

# A Pedagogical Introduction to Electroweak Baryogenesis

Graham Albert White

---

## Chapter 1

### Introduction

The origin of the baryon asymmetry of the Universe (BAU) is one of the deepest short-comings of our understanding of particle physics, as it cannot be explained within the Standard Model. For instance, one cannot simply set the baryon asymmetry as an initial condition as this would be washed out by inflation<sup>1</sup>. On the other hand, coinciding estimates of the baryon asymmetry using different techniques are a triumph of modern cosmology. The baryon asymmetry can be estimated by the deuterium abundance and from the cosmic microwave background (CMB), where the relative sizes of Doppler peaks in the temperature anisotropy are sensitive to the BAU. These two methods give the overlapping estimates of the baryon to entropy ratio<sup>2</sup> [2–4]

$$Y_B = \frac{n_B - \bar{n}_B}{s} \approx \frac{n_B}{s} = \begin{cases} (7.3 \pm 2.5) \times 10^{-11}, \text{ BBN} \\ (9.2 \pm 1.1) \times 10^{-11}, \text{ WMAP} \\ (8.59 \pm 0.11) \times 10^{-11}, \text{ Planck.} \end{cases} \quad (1.1)$$

This remarkable overlap in the estimates of the BAU from light element abundances (particularly deuterium) and baryon acoustic oscillations are shown in figure 1.1 and figure 1.2 respectively. Reproducing this estimate using particle physics makes one of the three pillars of the Standard Model of particle cosmology, the other two being inflation [5] and dark matter [6]. Like inflation and dark matter, it requires at least some additions to the Standard Model. Furthermore, like the other two pillars of the Standard Model of particle cosmology, there are a very large variety of models to explain this peculiar fact about our Universe. Two of the most elegant explanations

---

<sup>1</sup>For a recent attempted exception to this, albeit a fine-tuned one, see [1].

<sup>2</sup>Sometimes the baryon asymmetry is compared to the photon density,  $n_B/n_\gamma \approx 7.04 Y_B$ , rather than the entropy. However during the early Universe many particles are expected to be in thermal equilibrium making  $Y_B$  more convenient.

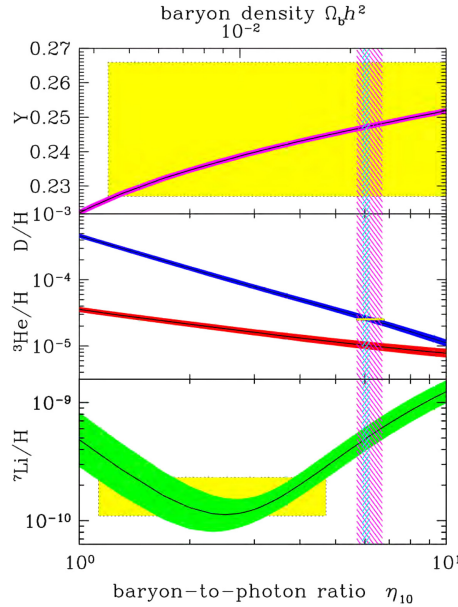


**Figure 1.1.** The abundances predicted by the Standard Model of Big Bang nucleosynthesis (BBN) [7] for  $^4\text{He}$ , D,  $^3\text{He}$ , and  $^7\text{Li}$ . Here the bands show the range for the 95% confidence level and the boxes indicate the light element abundances—the smaller boxes show  $2.75\sigma$  statistical errors; the larger boxes  $2.75\sigma$  statistical and systematic errors. The wide band indicates the BBN concordance range, whereas the vertical narrow band indicates the baryon asymmetry measured via the CMB given at the 95% confidence level. Reproduced from [2].

are leptogenesis [9] and the Affleck–Dine mechanism [10]. Unfortunately both tend to be well out of reach of the particle colliders of today and of the foreseeable future.

The focus of this review will be electroweak baryogenesis, which is the term for any mechanism that produces the matter–antimatter asymmetry during the electroweak phase transition. Such a scenario requires physics beyond the Standard Model that must couple relatively strongly to Standard Model particles and have masses that are not too far above the weak scale. Therefore, unlike Affleck–Dine baryogenesis or leptogenesis, electroweak baryogenesis has the tantalizing prospect of being tested, at least indirectly, by weak and TeV scale searches at the large hadron collider (LHC).

Apart from testability, electroweak baryogenesis has the attractive feature that coincides the breaking of the symmetry between particles and anti-particles with the spontaneous breaking of the one symmetry we know to be broken—electroweak symmetry. Unfortunately the literature on this exciting subject is somewhat opaque to newcomers. There are some very nice pedagogical introductions to small parts of the theoretical foundations of baryogenesis scattered throughout the literature if one digs hard enough<sup>3</sup>. However, the study of baryogenesis is arguably too decoupled

<sup>3</sup>For recent reviews see [11–14].

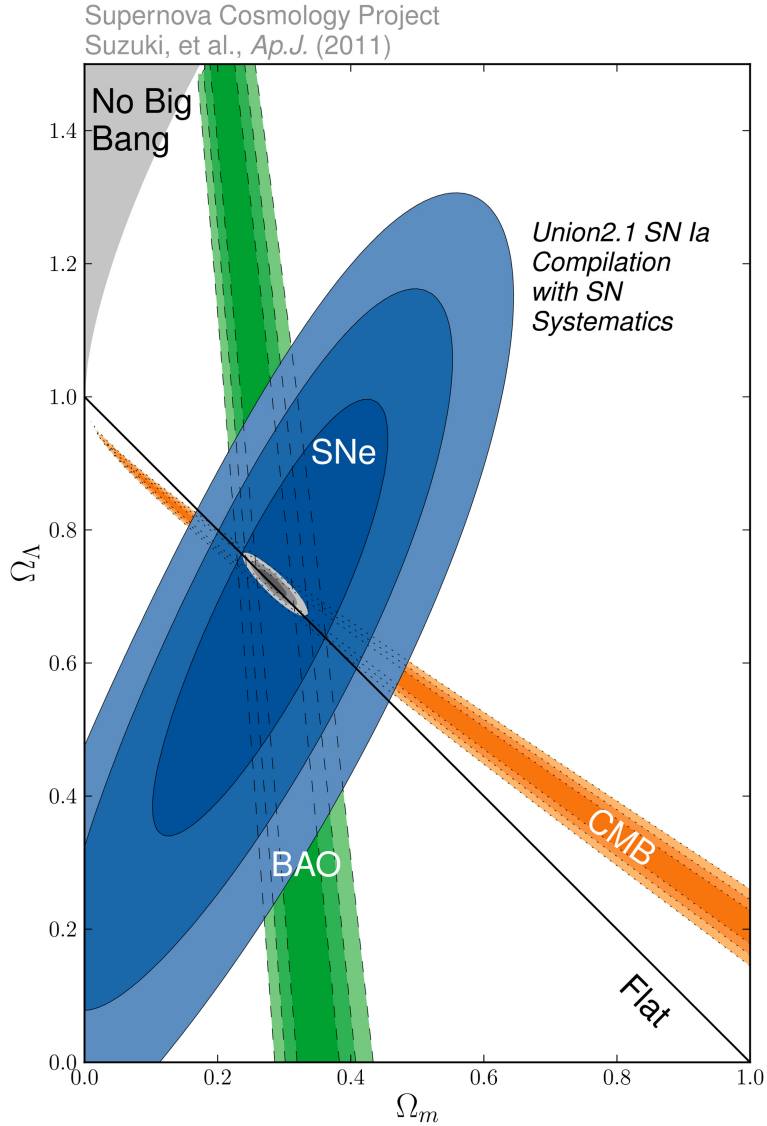


**Figure 1.2.**  $\Omega_M - \Omega_\Lambda$  constraints due to CMB, baryon acoustic oscillations, and Supernova Cosmology Project Union2.1 SN constraints including SN systematic errors. Reproduced from [8].

from the rest of high energy physics given its promising phenomenological implications and the fundamental nature of the question it attempts to answer. Furthermore, the techniques one needs to learn to research in the field of electroweak baryogenesis have a large cross-over with other calculations in particle cosmology—including other models of producing the baryon asymmetry such as leptogenesis.

This primer will therefore give a mostly self-contained introduction to the field of *electroweak* baryogenesis, assuming the reader has a graduate level knowledge of

particle physics, including dimensional regularization, some basic path integral techniques, the computation of amplitudes at tree and loop level, the Standard Model Lagrangian, and Big Bang cosmology, as well as a rudimentary knowledge of effective field theory and the minimal supersymmetric Standard Model (MSSM),<sup>4</sup> which we will use as a pedagogical tool where appropriate. There are of course many candidates for producing the BAU, but it is my hope that the theoretical foundations given in this book should make learning such mechanisms significantly more tractable.

## References

- [1] Krnjaic G 2016 Can the baryon asymmetry arise from initial conditions? arXiv: [1606.05344](#)
- [2] Eidelman S *et al* 2004 (Particle Data Group Collaboration) *Review of Particle Physics Phys. Lett. B* **592** 1
- [3] Spergel D N *et al* 2003 (WMAP Collaboration) First year wilkinson microwave anisotropy Probe (WMAP) observations: determination of cosmological parameters *Astrophys. J. Suppl.* **148** A16
- [4] Ade P A R *et al* 2014 Planck 2013 results. XVI. cosmological parameters *Astron. Astrophys.* **571** A16
- [5] Bassett B A, Tsujikawa S and Wands D 2006 Inflation dynamics and reheating *Rev. Mod. Phys.* **78** 2
- [6] Feng J L 2010 Dark matter candidates from particle physics and methods of detection *Annu. Rev. Astron. Astrophys.* **48** 495–545
- [7] Cyburt R H *et al* 2008 An update on the big bang nucleosynthesis prediction for  ${}^7\text{Li}$ : the problem worsens *J. Cosmol. Astropart. Phys.* [JCAP11\(2008\)012](#)
- [8] Suzuki N *et al* 2012 The Hubble Space Telescope Cluster Supernova Survey. V. Improving the dark-energy constraints above  $z > 1$  and building an early-type-hosted supernova sample **756** 85
- [9] Fukugita M and Yanagida T 1986 Baryogenesis without grand unification *Phys. Lett. B* **174** 1
- [10] Affleck I and Dine M 1985 A new mechanism for baryogenesis *Nucl. Phys. B* **249** 361
- [11] Morrissey D E and Ramsey-Musolf M J 2010 Electroweak baryogenesis *New J. Phys.* **14** 12
- [12] Cline J M 2012 *Baryogenesis* arXiv: [0609145\(hep-ph\)](#)
- [13] Riotto A and Trodden M 1999 Recent progress in baryogenesis *Annu. Rev. Nucl. Part. Sci.* **49** 46
- [14] Trodden M 1999 Electroweak baryogenesis *Rev. Mod. Phys.* **71** 5
- [15] Kuroda M 1999 Complete lagrangian of MSSM arXiv: [9902340\(hep-ph\)](#)
- [16] Csaki C 1996 The minimal supersymmetric standard model (MSSM) *Mod. Phys. Lett. A* **11.08** 599–613

---

<sup>4</sup>If you lack knowledge of the MSSM see [[15](#),[16](#)] for an introduction.

## Chapter 3

### Baryon number violation in the Standard Model

The baryon number is a classically conserved quantity in the Standard Model as can be demonstrated by Noether's theorem or even a cursory look at the available interactions. This intuition breaks down when one quantizes the Standard Model, due to so-called anomalous processes, which will be described in this chapter. That some fundamental symmetries may not survive the process of quantization is highly counter-intuitive. This is not just a feature of field theory. It was shown in [1, 2] that even standard quantum mechanics with certain potentials—specifically a delta function or a  $1/r^2$  potential—have anomalous violations of conservation laws. The key anomaly of interest is the so-called chiral or axial anomaly. This anomaly, combined with the fact that the SU(2) gauge symmetry is a symmetry of left-handed particles only, will conspire to fulfil Sakharov's baryon number violation condition.

#### 3.1 The axial anomaly

Let us warm up, however, by considering the simplest possible fermionic field theory, a single massless, free fermion field with a U(1) gauge symmetry. Such a theory has a global phase symmetry. Less obvious is that such a model's Lagrangian is also invariant under the following transformation

$$\psi \rightarrow e^{i\theta\gamma_5} \psi. \quad (3.1)$$

From these symmetries we can of course use Noether's theorem to derive conserved currents. The Noether currents associated with these two symmetries are

$$J_\mu = \bar{\psi} \gamma_\mu \psi \quad (3.2)$$

$$J_{5\mu} = \bar{\psi} \gamma_5 \gamma_\mu \psi, \quad (3.3)$$

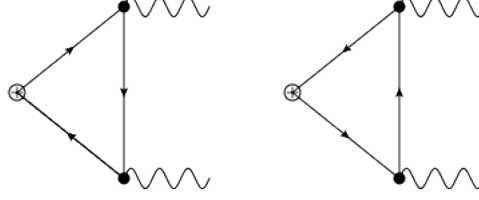


**Figure 3.1.** The famous triangle diagram responsible for anomalous quantum violations of classical chiral symmetry. The circle denotes a  $\gamma_5$  on the vertex.

which implies Ward identities  $\partial^\mu J_\mu = 0$  and  $\partial^\mu J_{5\mu} = 0$ . Obviously we expect the product of conserved currents to also be a conserved quantity. Therefore we should not even need to bother to calculate the divergence of the following quantity:

$$-i\Gamma_{\mu\nu\lambda}(x_1, x_2, x_3) = \langle 0|T(J_{5\mu}(x_3)J_\nu(x_1)J_\lambda(x_2))|0\rangle. \quad (3.4)$$

Amazingly this quantity is not zero. This remarkable result is known as the ‘triangle anomaly’ [3, 4] due to the fact that the Feynman diagram related to this amplitude has three vertices, as shown in figure 3.1. In the author’s opinion the most effective way to learn the axial anomaly is through direct calculation. We present a review of what we believe is probably the simplest derivation in the literature using operator methods with dimensional regularization, followed by the Fujikawa method which is a path integral derivation.

### 3.1.1 Dimensional regularization

Let us calculate this example using the ever-familiar dimensional regularization. A potential ambiguity that can arise in such a calculation is that there is no clear way to generalize the matrix  $\gamma_5$  to  $4 - 2\epsilon$  dimensions although various proposals exist [5]. We follow the approach of [6], which demonstrated that no knowledge of any of  $\gamma_5$  properties is needed to calculate the triangle anomaly<sup>1</sup>. The axial current to one-loop order due to the triangle anomaly is given by

$$\langle 0|J_5^\mu(x)|0\rangle = \int \frac{d^D p}{(2\pi)^D} \frac{d^D k}{(2\pi)^D} e^{iq \cdot x} A_\nu(p) A_\lambda(k) \mathcal{M}^{\mu\nu\lambda}, \quad q = k + p. \quad (3.5)$$

The above amplitude relates to the two diagrams in figure 3.1, and the second diagram is obtained from the first by merely interchanging  $(p, \nu)$  and  $(k, \lambda)$ . Hence, it suffices to compute one diagram

$$\mathcal{M}_{(1)}^{\mu\nu\lambda}(k, p) = -ie^2 \int \frac{d^D l}{(2\pi)^D} \left\{ \gamma^\mu \gamma_5 \frac{\not{l} - \not{k}}{(l - k)^2 + i\epsilon} \gamma^\lambda \frac{\not{l}}{l^2 + i\epsilon} \gamma^\nu \frac{\not{l} + \not{p}}{(l + p)^2 + i\epsilon} \right\}, \quad (3.6)$$

<sup>1</sup>Part of this calculation has some cross-over with the calculation in [7].

where the curly brackets denote a trace operation and the photon momenta are on-shell. Although we introduced this section stating that we are considering a massless fermion model, we will use a mass to regularize the integrals and take the limit  $m^2 \rightarrow 0$  at the end. Let us integrate over loop momentum and contract with  $q_\mu$ . The result we can write as the sum of two terms

$$iq_\mu \mathcal{M}_{(1)}^{\mu\nu\lambda} = \mathcal{A}^{\nu\lambda}(k, p) + \mathcal{B}^{\nu\lambda}(k, p), \quad (3.7)$$

where

$$\begin{aligned} \mathcal{A}^{\nu\lambda}(k, p) &= \frac{ie^2}{32\pi^2} \int_0^1 dx \int_0^{1-x} dy \left[ \frac{1}{\bar{\epsilon}} - \ln\left(\frac{\Delta}{\mu^2}\right) \right] \\ &\times \left\{ \not{q} \gamma_3 \gamma^\alpha \gamma^\lambda \gamma_\alpha \gamma^\nu (x \not{k} + (1-y) \not{p}) - \not{q} \gamma_3 (y \not{p} + (1-x) \not{k}) \right. \\ &\times \left. \gamma^\lambda \gamma^\alpha \gamma^\nu \gamma_\alpha - \not{q} \gamma_3 \gamma^\alpha \gamma^\lambda (y \not{p} - x \not{k}) \gamma^\nu \gamma_\alpha \right\} \end{aligned} \quad (3.8)$$

and

$$\begin{aligned} \mathcal{B}^{\nu\lambda}(k, p) &= -\frac{ie^2}{16\pi^2} \int_0^1 dx \int_0^{1-x} dy \\ &\times \frac{\left\{ \not{q} \gamma_3 ((x-1) \not{k} - y \not{p}) \gamma^\lambda (x \not{k} - y \not{p}) \gamma^\nu (x \not{k} + (1-y) \not{p}) \right\}}{\Delta}. \end{aligned} \quad (3.9)$$

In the above we have defined the parameters

$$\Delta = -q^2 xy + m^2, \quad \frac{1}{\bar{\epsilon}} = \frac{1}{\epsilon} - \gamma + \ln 4\pi. \quad (3.10)$$

The tensor  $\mathcal{A}^{\nu\lambda}$  contains a divergent piece. If we employ the identities

$$\gamma^\alpha \gamma^\mu \gamma_\alpha = (-2 + 2\epsilon) \gamma^\mu, \quad \gamma^\alpha \gamma^\mu \gamma^\lambda \gamma^\nu \gamma_\alpha = -2\gamma^\nu \gamma^\lambda \gamma^\mu + 2\epsilon \gamma^\mu \gamma^\lambda \gamma^\nu \quad (3.11)$$

along with the cyclic property of traces, we can reduce this tensor to the form

$$\begin{aligned} \mathcal{A}_{\text{div}}^{\nu\lambda} &= \frac{ie^2}{96\pi^2 \bar{\epsilon}} \left[ 4p^\lambda \{ \gamma^\nu \not{q} \gamma_3 \} - 4k^\nu \{ \gamma^\lambda \not{q} \gamma_3 \} - 2p^\nu \{ \gamma^\lambda \not{q} \gamma_3 \} + 2k^\lambda \{ \gamma^\nu \not{q} \gamma_3 \} \right. \\ &\left. + 2g^{\nu\lambda} \{ \not{k} \not{p} \gamma_3 - \not{p} \not{k} \gamma_3 \} \right]. \end{aligned} \quad (3.12)$$

So all traces with four Dirac matrices have already canceled and we are left with a series of terms that are zero in four dimensions. However, we need not make an assumption about the value of these traces. The term multiplying  $1/\bar{\epsilon}$  is anti-symmetric under the interchange  $(p, \nu)$  and  $(k, \lambda)$  so it cancels when the two diagrams are added, giving

$$\mathcal{A}_{\text{div}}^{\nu\lambda}(k, p) + \mathcal{A}_{\text{div}}^{\lambda\nu}(p, k) = 0. \quad (3.13)$$

The finite part of  $\mathcal{A}^{\nu\lambda}$  comes from the  $\mathcal{O}(\epsilon)$  part of equation (3.11) and the  $\ln \Delta$  part in equation (3.8). The result in the massless limit reads

$$\lim_{\epsilon \rightarrow 0} [\mathcal{A}^{\nu\lambda}(k, p) + \mathcal{A}^{\lambda\nu}(p, k)]_{m=0} = \frac{e^2}{6\pi^2} \epsilon^{\lambda\nu\alpha\beta} p_\alpha k_\beta. \quad (3.14)$$

Note that the above tensor is infrared finite, so the inclusion of a mass regulator was a convenient calculation tool. Moving to  $\mathcal{B}^{\nu\lambda}(k, p)$ , we find that the potentially singular terms cancel identically so we can take the limit  $D \rightarrow 4$  and write

$$\lim_{\epsilon \rightarrow 0} [\mathcal{B}^{\nu\lambda}(k, p) + \mathcal{B}^{\lambda\nu}(p, k)]_{m=0} = \frac{e^2}{3\pi^2} \epsilon^{\lambda\nu\alpha\beta} p_\alpha k_\beta. \quad (3.15)$$

Putting everything together yields the well-known, but non-zero result

$$\langle 0 | \partial \cdot J_S | 0 \rangle = \frac{e^2}{2\pi^2} \epsilon^{\mu\nu\alpha\beta} \int \frac{d^D p}{(2\pi)^D} \frac{d^D k}{(2\pi)^D} e^{iq \cdot x} A_\nu(p) A_\lambda(k) p_\alpha k_\beta. \quad (3.16)$$

Thus we have found by explicit calculation the anomalous violation of chiral current conservation. We have chosen a particular way of performing the calculation that makes it maximally clear that the anomaly is not some ill effect of how we regulate our integrals. Indeed the anomaly is experimentally demonstrated in predicting the correct rate for pion decay  $\pi^0 \rightarrow \gamma\gamma$ . Furthermore, as remarked in the previous section, it has been shown to happen in ordinary quantum mechanics and the above calculation has been repeated with multiple different regularization schemes. Nonetheless we present one more derivation in the next subsection, since it naturally organizes the anomalies in the Standard Model such that it is straightforward to show that lepton and baryon currents have anomalous currents.

### 3.1.2 The Fujikawa method

Since the anomaly is independent of the regularization scheme we will calculate the anomalies using the path integral method with a hard cutoff regularization scheme. The regularization free nature of the anomaly is more opaque in this scheme, so I will assume that the reader understood the results of the previous section where things were more clear. The cost of this opaqueness will be justified by the simplicity of the calculation that follows. Let us begin by returning to the anomalous chiral current

$$J_\mu^5 = \bar{\psi} \gamma_5 \gamma_\mu \psi. \quad (3.17)$$

As in the previous section, the triangle diagram anomalously violates the classical conservation law derived through Noether's theorem. This time our fermions interact with Standard Model gauge bosons. Path integral techniques are far more efficient and systematic than trying to find all anomalous operators and hoping you have not missed any. The path integral's approach begins with simply adding the current to the Lagrangian [8, 9]

$$W[a_\mu, A_\lambda^c] = \int [d\psi][d\bar{\psi}] e^{i \int d^4x \mathcal{L}_{\text{QCD}} - a_\mu J_5^\mu}. \quad (3.18)$$

We then vary  $W$  with respect to  $a_\mu$  by an infinitesimal function  $\partial_\mu \beta$  in order to test whether  $W$  is invariant under such a change. Using the definition of functional derivatives

$$\begin{aligned} \delta[\ln W] &= \ln \left[ W(a_\mu - \partial_\mu \beta, A_\mu^b) \right] - \ln \left[ W(a_\mu, A_\mu^b) \right] \\ &= - \int d^4x \frac{\delta \ln W}{\delta a^\mu} \\ &= i \int d^4x \bar{J}_5^\mu \partial_\mu \beta \\ \delta[\ln W] &= -i \int d^4x \partial_\mu \bar{J}_5^\mu \beta(x). \end{aligned} \quad (3.19)$$

So if  $\delta[\ln W] = 0$ ,  $\partial_\mu J_5^\mu = 0$  and the chiral current is conserved. To test for an anomaly one determines if the statement

$$W[a_\mu - \partial_\mu \beta, A_\lambda^c] = W[a_\mu, A_\lambda^c] \quad (3.20)$$

holds true. Let us begin by seeing if there is a change of variables that takes our primed Lagrangian back to the original form. That is

$$L'_{\text{QCD}}(\psi', \bar{\psi}', A_\mu^a) \equiv L_{\text{QCD}}(\psi', \bar{\psi}', A_\mu^a) - (\partial_\mu \beta) J_5^\mu \rightarrow L_{\text{QCD}}(\psi, \bar{\psi}, A_\mu^a). \quad (3.21)$$

The appropriate set of transformations is

$$\psi' = (1 - i\beta\gamma_5)\psi \sim e^{-i\beta\gamma_5}\psi \quad (3.22)$$

$$\bar{\psi}' = \bar{\psi}(1 - i\beta\gamma_5) \sim \bar{\psi}e^{-i\beta\gamma_5}. \quad (3.23)$$

This can be verified by direct substitution in which one ignores all terms  $\mathcal{O}(\beta^2)$  and uses the anti-commutivity of the gamma matrices. The only other modification to make to our function  $W$  is the measure

$$[d\psi][d\bar{\psi}] \rightarrow [d\psi'][d\bar{\psi}'] \quad (3.24)$$

in which we will pick up a Jacobian determinant  $\mathcal{J}$ . We will later verify that  $\mathcal{J}$  is independent of  $\psi$  and  $\bar{\psi}$  so we can take it out of the integral

$$\begin{aligned} W[a_\mu - \partial_\mu \beta, A_\mu^a] &= \int [d\psi'][d\bar{\psi}'] \mathcal{J} e^{i \int d^4x L_{\text{QCD}} - a_\mu J_5^\mu} \\ &= \mathcal{J} \int [d\psi][d\bar{\psi}] e^{i \int d^4x L_{\text{QCD}} - a_\mu J_5^\mu} \\ &= \mathcal{J} W[a_\mu, A_\mu^a]. \end{aligned} \quad (3.25)$$

Therefore we can write the variation of  $\ln W$  exclusively in terms of the Jacobian

$$\begin{aligned}\delta[\ln W] &= \ln\left[W(a_\mu - \partial_\mu\beta, A_\mu^a)\right] - \ln\left[W(a_\mu, A_\mu^a)\right] \\ &= \ln\left[\mathcal{J}W(a_\mu, A_\mu^a)\right] - \ln\left[W(a_\mu, A_\mu^a)\right] \\ &= \ln \mathcal{J}.\end{aligned}\tag{3.26}$$

Our Jacobian is of Grassman valued functions so it is given by the inverse of the functional determinant of our transformations

$$\mathcal{J} = \text{Det}[e^{i\beta\gamma_5} e^{i\beta\gamma_5}]^{-1}.\tag{3.27}$$

We can use a simple identity,  $\text{Det } C = \exp[\text{Tr} \ln C]$ , to write this determinant in terms of a trace

$$\mathcal{J} = e^{-2i\text{Tr}\beta\gamma_5}.\tag{3.28}$$

This determinant diverges so we need to introduce a regulator. Let us first separate the divergent part of the trace

$$\text{Tr} \beta\gamma_5 = \text{Tr}' \int d^4x \langle x | \beta\gamma_5 \rangle,\tag{3.29}$$

where the primed trace is over internal degrees of freedom. To regularize the integral we rewrite it as

$$\text{Tr} \beta\gamma_5 = \lim_{M \rightarrow \infty} \text{Tr}' \int d^4x \langle x | \beta\gamma_5 e^{-\left(\frac{\mathcal{D}}{M}\right)^2} | x \rangle.\tag{3.30}$$

The square in the regulator can be expanded

$$\left(\frac{\mathcal{D}}{M}\right)^2 = \frac{1}{M^2} \left( \partial_\mu \partial^\mu + \frac{1}{4} g_3 \lambda^a \sigma^{\mu\nu} F_{\mu\nu}^a \right) \equiv \frac{1}{M^2} (D^2 + g_3 \sigma \cdot F).\tag{3.31}$$

Here the definition of  $\sigma \cdot F$  is given implicitly. To calculate the trace of the regulator we introduce the complete set of states

$$\begin{aligned}\text{Tr} \beta\gamma_5 &= \lim_{M \rightarrow \infty} \text{Tr}' \int d^4x \frac{d^d p}{(2\pi)^{d/2}} \frac{d^d p'}{(2\pi)^{d/2}} \langle x | p \rangle \langle p | \beta\gamma_5 e^{-\left(\frac{\mathcal{D}}{M}\right)^2} | p' \rangle \langle p' | x \rangle \\ &= \lim_{M \rightarrow \infty} \text{Tr}' \int d^4x \frac{d^d p}{(2\pi)^d} \beta\gamma_5 e^{-(ip_\mu + D_\mu)^2 + g_3 \sigma \cdot F} / M^2 \\ &= \lim_{M \rightarrow \infty} \text{Tr}' \int d^4x \frac{d^d p}{(2\pi)^d} \beta\gamma_5 e^{p^2/M^2} e^{-(D^2 + g_3 \sigma \cdot F + 2ip \cdot D)/M^2}.\end{aligned}\tag{3.32}$$

We will now Taylor expand the right-hand side up to  $\mathcal{O}(1/M^4)$  keeping in mind that each factor of  $p^2$  is of order  $\mathcal{O}(M^2)$

$$\begin{aligned}
\text{Tr } \beta\gamma_5 &= \lim_{M \rightarrow \infty} \text{Tr}' \int d^4x \frac{d^d p}{(2\pi)^d} \beta\gamma_5 e^{\frac{p^2}{M^2}} \left[ 1 - \frac{1}{M^2} (D^2 + g_3 \sigma \cdot F) \right. \\
&\quad + \frac{1}{2M^4} \left( \{D^2 + g_3 \sigma \cdot F\}^2 - 4p \cdot D \right) + \frac{2}{3M^6} \\
&\quad \times \left( p \cdot D p \cdot D \{D^2 + g_3 \sigma \cdot F\} + p \cdot D \{D^2 + g_3 \sigma \cdot F\} p \cdot D \right. \\
&\quad \left. + \{D^2 + g_3 \sigma \cdot F\} p \cdot D p \cdot D \right) + \frac{4}{M^8} (p \cdot D)^4 \left. \right] \\
&= \lim_{M \rightarrow \infty} \text{Tr}' i \int d^4x \beta\gamma_5 \frac{iM^4}{(4\pi)^2} \times \left[ 1 - \frac{g_3 \sigma \cdot F}{M^2} \right. \\
&\quad \left. + \frac{1}{M^4} \left( \frac{1}{2} (g_3 \sigma \cdot F)^2 + \frac{1}{12} [D_\mu, D_\nu]^2 + \frac{1}{6} [D_\mu, [D_\mu, \sigma \cdot F]] \right) \right].
\end{aligned} \tag{3.33}$$

The only trace that survives is the one with a product of two  $\sigma$ . Recalling that

$$\text{Tr } \gamma_5 \sigma^{\mu\nu} \sigma^{\alpha\beta} = -4i \epsilon^{\mu\nu\alpha\beta}, \tag{3.34}$$

it is then easy to take the trace over the internal degrees of freedom to show that

$$\mathcal{J} = \exp \left[ -i \int d^4x \beta \frac{3\alpha_S}{8\pi} F^{\mu\nu} \tilde{F}_{\mu\nu} \right]. \tag{3.35}$$

We therefore have

$$\partial_\mu J_5^\mu = \frac{3\alpha_S}{8\pi} F^{\mu\nu} \tilde{F}_{\mu\nu}. \tag{3.36}$$

This effective operator generates the amplitude given in equation (3.15) which was derived using operator techniques and dimensional regularization.

### 3.1.3 Baryon and lepton number violation

At this stage we have rederived the chiral anomaly using functional techniques and taking into account the gauge symmetries of the Standard Model. The SU(2) gauge bosons couple only to left-handed particles so the chiral anomaly interferes with lepton and baryon number conservation. Consider the classically conserved currents

$$J_{L,R}^\mu = \frac{1}{2} \bar{\psi} \gamma^\mu (1 \mp \gamma^5) \psi. \tag{3.37}$$

Let us first couple the left-handed current to the Standard Model. Following the procedure as before we consider the term  $W[a_\mu + \partial_\mu \beta, A_\mu, B_\mu, G_\mu]$  where  $L = L_{\text{SM}} + (a_\mu + \partial_\mu \beta) J_L^\mu$ . This can be related to the term  $W[a_\mu, A_\mu, B_\mu, G_\mu]$  by the transformations

$$\psi' = (1 - i\beta\gamma_5)\psi \sim e^{-i\beta\gamma_5}\psi \tag{3.38}$$

$$\bar{\psi}' = \bar{\psi}(1 - i\beta\gamma_5) \sim \bar{\psi}e^{-i\beta\gamma_5}. \quad (3.39)$$

We then can use the method outlined before to derive an expression for  $\partial_\mu J_L^\mu$  with associated regulator  $\exp\{[(\partial_\mu + gA_\mu + g'B_\mu + g_s G_\mu)\gamma^\mu]^2/M^2\} \equiv \exp[\mathcal{D}_L^2/M^2]$ . Similarly we can couple the right-handed current to our Lagrangian. The transformation required to bring us back to our original  $W$  function is

$$\psi' = (1 + i\beta\gamma_5)\psi \sim e^{+i\beta\gamma_5}\psi \quad (3.40)$$

$$\bar{\psi}' = \bar{\psi}(1 + i\beta\gamma_5) \sim \bar{\psi}e^{+i\beta\gamma_5}. \quad (3.41)$$

Our Jacobian will acquire an extra minus sign. This time the associated regulator is  $\exp\{[(\partial_\mu + gA_\mu + g_s G_\mu)\gamma^\mu]^2/M^2\} \equiv \exp[\mathcal{D}_R^2/M^2]$ . Following the previous calculation one finds for quarks

$$\partial_\mu [J_L^\mu - J_R^\mu] \equiv \partial_\mu J_5^\mu = \frac{3\alpha_S}{8\pi} G^{\mu\nu} \tilde{G}_{\mu\nu} \quad (3.42)$$

$$\partial_\mu J_L^\mu = \frac{3\alpha_W}{8\pi} B^{\mu\nu} \tilde{B}_{\mu\nu}. \quad (3.43)$$

When one performs the calculation for leptons there is only the anomalous left-handed current which is equal to one third the above equation since one does not perform a trace over colour. Noting that the baryon number of a quark is 1/3 we can write the exact symmetry

$$\partial_\mu B^\mu = \partial_\mu L^\mu. \quad (3.44)$$

### 3.2 The Chern–Simons form, baryon number violation, and the winding number

We have now demonstrated that both lepton and baryon number are violated in the Standard Model through these strange anomalous currents. In this subsection we will try and find the sort of field configuration that violates baryon and lepton number. This is one part of the background theory which can quickly get unnecessarily formal, so we will be taking an approach to make things only as formal as is useful to understanding the subject at the level needed to do research in this field<sup>2</sup>. Let us first make some manipulations to our effective action. Recall that

<sup>2</sup> We do not follow any particular reference as they often lack details in the areas we need and are too formal or too detailed in areas orthogonal to this analysis. Nonetheless, some useful resources for more information are [10–12].

$$\begin{aligned}
\partial_\mu L^\mu &= \partial_\mu B^\mu = \frac{g^2}{32\pi^2} \int d^4x \epsilon^{\mu\nu\alpha\beta} \text{Tr}[F_{\mu\nu} F_{\alpha\beta}] \\
&= \frac{g^2}{32\pi^2} \int d^4x \epsilon^{\mu\nu\alpha\beta} \partial_\mu \text{Tr} \left[ \partial_\nu A_\mu^a - \partial_\nu A_\mu^a + f^{abc} A_\mu^b A_\nu^c \right] \\
&\quad \times \left[ \partial_\alpha A_\beta - \partial_\beta A_\alpha^a + f^{ade} A_\alpha^d A_\beta^e \right] \\
&= \frac{g^2}{8\pi^2} \int d^4x \epsilon^{\mu\nu\alpha\beta} \partial_\mu \text{Tr} \left[ A_\nu \partial_\alpha A_\beta - \frac{2i}{3} A_\nu A_\alpha A_\beta \right] \\
&\quad + f^{abc} f^{ade} \epsilon^{\mu\nu\alpha\beta} \text{Tr} \left[ [A_\mu^a, A_\nu^b] [A_\alpha^d A_\beta^e] \right] \\
&= \frac{g^2}{8\pi^2} \int d^4x \epsilon^{\mu\nu\alpha\beta} \partial_\mu \text{Tr} \left[ A_\nu \partial_\alpha A_\beta - \frac{2i}{3} A_\nu A_\alpha A_\beta \right] \\
&= \frac{g^2}{8\pi^2} \int_{S^3} \text{Tr} \left[ A \wedge dA + \frac{1}{3} A \wedge A \wedge A \right].
\end{aligned} \tag{3.45}$$

Note we used the Jacobi identity in the above derivation. Also in the last line we have used the divergence theorem and wrote the result in a compact notation using wedge products. If you are unfamiliar with this notation rest assured we will use them sparingly. The integrand here is known as the ‘Chern–Simons action’ as it is the surface integral of the Chern–Simons form [13]. The field configurations that will be relevant are finite-energy solutions, so we require them to be well-behaved at infinity

$$A_\mu \rightarrow ig\partial_\mu g^{-1} + \mathcal{O}\left(\frac{1}{r^2}\right). \tag{3.46}$$

That is, we require that in some gauge the field vanishes at a rate faster than  $1/r^2$  up to ‘pure gauge’ contributions. Field configurations that do not satisfy the finite-energy condition make no contribution to the functional integral so they can be ignored. We note that the integral of the Chern–Simons form is the volume integral of a total divergence. We can then use Gauss’ divergence theorem to turn this into an integral over the surface at spatial infinity. If we enter the pure gauge part into equation (3.45) we obtain

$$\begin{aligned}
\partial_\mu L^\mu &= \frac{g^2}{8\pi^2} \int dS_\mu \epsilon^{\mu\nu\alpha\beta} \text{Tr} \left[ i^2 g \partial_\nu g^{-1} (\partial_\alpha g \partial_\beta g^{-1}) - \frac{2i^4}{3} g \partial_\mu g^{-1} g \partial_\alpha g^{-1} g \partial_\beta g^{-1} \right] \\
&= \frac{g^2}{8\pi^2} \int dS_\mu \epsilon^{\mu\nu\alpha\beta} \text{Tr} \left[ -g \partial_\nu g^{-1} (\partial_\alpha g (g g^{-1}) \partial_\beta g^{-1}) - \frac{2}{3} g \partial_\mu g^{-1} g \partial_\alpha g^{-1} g \partial_\beta g^{-1} \right] \\
&= \frac{g^2}{8\pi^2} \int dS_\mu \epsilon^{\mu\nu\alpha\beta} \text{Tr} \left[ g \partial_\mu g^{-1} g \partial_\alpha g^{-1} g \partial_\beta g^{-1} - \frac{2}{3} g \partial_\mu g^{-1} g \partial_\alpha g^{-1} g \partial_\beta g^{-1} \right] \\
&= \frac{g^2}{24\pi^2} \int dS_\mu \epsilon^{\mu\nu\alpha\beta} \text{Tr} \left[ g \partial_\mu g^{-1} g \partial_\alpha g^{-1} g \partial_\beta g^{-1} \right],
\end{aligned} \tag{3.47}$$

where in the second line we used the identity

$$\partial_x 1 = 0 = \partial_x (gg^{-1}) = (\partial_x g)g^{-1} + g(\partial_x g^{-1}). \quad (3.48)$$

The form of this is very interesting. Consider the volume element for the internal group

$$d\Omega_V = \frac{1}{24\pi^2} \int \text{Tr}[(dgg^{-1}) \wedge (dgg^{-1}) \wedge (dgg^{-1})]. \quad (3.49)$$

So the particle current divergence is proportional to the volume integral over the internal group pulled back onto Euclidean space-time. In other words it is proportional to the number of times the field winds around the group at the three-dimensional surface at spatial infinity. If the integral of the Chern-Simons form is non-zero we therefore denote it with a ‘non-zero’ Chern-Simons number due to the connection with the winding number.

### 3.3 Winding number and non-abelian gauge groups

The kind of field configuration that violates baryon number conservation is one with a non-zero ‘Chern-Simons number’, which we argued in the previous section is satisfied if the winding number is non-zero. In this section we will make things a little more concrete. The winding number is a concept from topology. As we only need surface level understanding of the concept we will only give a few examples to build intuition toward the subject. First consider the case where the internal space of a gauge field is a simple circle. Now consider the following mapping:

$$g^\nu(\theta) = e^{i\nu\theta}. \quad (3.50)$$

The winding number is defined as how often this function winds around the circle. It is easy to show that the following equation is the winding number:

$$\frac{i}{2\pi} \int_0^{2\pi} d\theta dg^{-1}/d\theta. \quad (3.51)$$

What is obvious also from explicit calculation is that the product of two mappings gives a winding number that is the sum of the winding numbers of each mapping. That is, if the winding number of one function,  $f(\theta)$  is  $\nu_1$  and the winding number of  $g(\theta)$  is  $\nu_2$ , then the winding number of  $f(\theta)g(\theta)$  is  $\nu_1 + \nu_2$ . This just follows from the properties of exponential functions. However, let us prove this in a way that may seem needlessly complicated for this simple example, but will be useful for the more complicated case we are interested in. First we consider a small change in the winding number

$$\delta g = i(\delta\lambda). \quad (3.52)$$

It is easy to show that  $\delta\nu = 0$ ,

$$\begin{aligned}
\nu + \delta\nu &= \frac{i}{2\pi} \int_0^{2\pi} d\theta (g + \delta g) \frac{d(g^{-1} - \delta g)}{d\theta} d\theta \\
&= \nu + \frac{1}{2\pi} \int_0^{2\pi} \left( \delta g \frac{dg^{-1}}{d\theta} - i \frac{d\delta\lambda g^{-1}}{d\theta} \right) \\
&= \nu + \frac{1}{2\pi} \int_0^{2\pi} d\theta \frac{d\delta\lambda}{d\theta} \\
&= \nu.
\end{aligned} \tag{3.53}$$

Thus we have shown that the winding number is invariant under continuous transformations. So we see that the winding number of the product of two functions is just the sum of the two winding numbers. Now consider the case where the gauge field has a local SU(2) symmetry. In the previous section we claimed that the winding number for this group is given by

$$\nu = \frac{1}{24\pi^2} \int dS_\nu \epsilon^{\nu\mu\alpha\beta} \text{Tr} [g \partial_\mu g^{-1} g \partial_\alpha g^{-1} g \partial_\beta g^{-1}], \tag{3.54}$$

which we will prove to be the winding number in a way completely analogous to the case of a circle. It is straightforward by direct substitution to take a configuration with winding number of unity,  $g = \sigma \cdot \mathbf{x}/r$  (where of course  $\sigma^4 = 1_2$ ), and show that it indeed gives one when inserted into the above equation. So we can prove it is the winding number by demonstrating that winding number of two maps is the sum of their individual winding numbers using the same techniques we used for the circle. Once again we begin with considering a small change in the winding number. Recall the identity that

$$(\partial_x g) g^{-1} = -g (\partial_x g^{-1}), \tag{3.55}$$

which we can use to write

$$\delta\nu = \int d\sigma_\nu \epsilon^{\nu\mu\alpha\beta} \text{Tr} [\partial_\mu g^{-1} \partial_\alpha g \partial_\beta \delta\lambda^a(x) \tau^a]. \tag{3.56}$$

This vanishes upon integration by parts. It is then trivial to see that our expression for  $\nu$  is indeed the winding number as one can then continuously deform our expression for  $g$  such that it is equal to one for the upper part of the hypersphere, and deform another mapping of winding number one such that it is equal to one for the lower part of the hypersphere. The winding number of the product of these two mappings is then 2. A similar process can produce a mapping  $g_\nu$  with winding number  $\nu$ . So what does this mean? If we consider the SU(2) gauge fields in four dimensional Euclidean space and track their value as we walk around spatial infinity, if the field winds around its internal group at least once in this walk then baryon and lepton number is violated. So to understand the process of baryon number violation we will then seek to understand these topologically interesting processes. Specifically we will find in the following sections that we are interested in

lumps of field, from the perspective of four-dimensional Euclidean space, called instantons, and unstable temporally localized lumps called sphalerons.

### 3.4 Solitons and instantons

In the previous sections we demonstrated that field configurations that violate baryon or lepton number must be topologically non-trivial—that is they must have non-zero Chern–Simons number. In this section we will demonstrate that topologically interesting field configurations generically are associated with quasi-particles.

Let us begin with the simplest example. Consider a simple scalar field in 1 + 1 dimensions with degenerate minima. For simplicity and clarity we will set a bunch of parameters in this theory to one to avoid them cluttering our equations as we only wish to discuss some qualitative features of the theory. The ‘uncluttered’ version of the Lagrangian for 1 + 1-dimensional scalar field theory is

$$\mathcal{L} = \frac{1}{2} \left( \frac{d\phi}{dt} \right)^2 - \frac{1}{2} \left( \frac{d\phi}{dx} \right)^2 - \frac{1}{4} (\phi^2 - 1)^2. \quad (3.57)$$

Now consider finite-energy solutions to the action that are stationary in time (that is we set the  $d\phi/dt$  term to zero). Without putting pen to paper we can already make remarks about the types of solutions we will find. The key to this is knowing that if the solution is finite then the field must take the value of one of the minima at plus and minus spatial infinity. This gives us two types of solution, a field that has the same minima at  $\pm\infty$  and a field that goes from one minimum at  $-\infty$  to another at  $+\infty$ . The second class of solutions is topologically non-trivial. Consider a specific example of the second type of solution to the classical equations of motion

$$\phi(x) = \pm \tanh \left[ (x - x_0) / \sqrt{2} \right]. \quad (3.58)$$

The energy profile of this solution is a highly localized lump of field. This can be seen if we write the energy density of the solution

$$\epsilon(x) = \frac{1}{2} \operatorname{sech}^2 \left[ (x - x_0) / \sqrt{2} \right] \quad (3.59)$$

which we depict in figure 3.2. This is known as a classical lump or a soliton. It is a quasi-particle whose existence derives from a degeneracy in the ground state. Although the solution given above is stationary, we can easily boost to a moving frame to obtain moving soliton solutions. Recalling that under a Lorentz transformation,  $\phi(x) \rightarrow \phi(\Lambda x)$ , we can write the following class of moving solitons

$$\phi(x, t) = \tanh \left[ \frac{1}{\sqrt{2}} \left( \frac{(x - x_0) - vt}{\sqrt{1 - u^2}} \right) \right]. \quad (3.60)$$

In the Standard Model we have a very large degeneracy in the ground state since one can have different winding numbers. Field configurations that are topologically interesting in an analogous way to the soliton described above will also look like

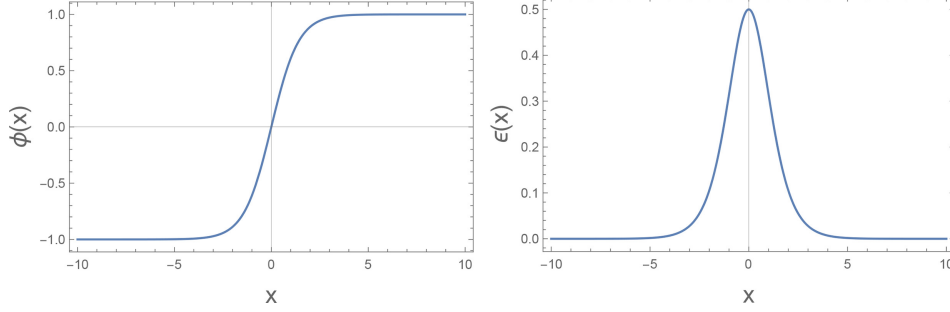


**Figure 3.2.** Depiction of a soliton in a single spatial dimension for the simple case of two degenerate minima at  $\pm 1$ . The energy profile is highly localized which justifies its status as a quasi-particle.

localized lumps in the field except in all four Euclidean dimensions. These lumps are known as instantons since they are localized in time. If you reverse the Wick rotation, returning to  $3 + 1$  dimensions, these instantons look like tunneling processes [14]. Having more dimensions and a more complicated degeneracy means we cannot immediately write down the instanton solution as we did with the soliton. In the case where we have  $SU(2)$  gauge symmetry, it helps to first show that the instanton is a solution to the classical equations of motion—it is a local minimum of the action. First take the field strength tensor and make use of the trivial identity

$$\begin{aligned} \int d^4x \operatorname{Tr} F_{\mu\nu} F^{\mu\nu} &= \int d^4x \operatorname{Tr} \left[ \sqrt{F_{\mu\nu} F^{\mu\nu} \tilde{F}_{\alpha\beta} \tilde{F}^{\alpha\beta}} \right] \\ &\geq \int d^4x \operatorname{Tr} \left[ |F_{\mu\nu} \tilde{F}^{\mu\nu}| \right]. \end{aligned} \quad (3.61)$$

This means that

$$\int d^4x \operatorname{Tr} F_{\mu\nu} F^{\mu\nu} \geq \frac{8\pi^2}{g^2} |\nu| \quad (3.62)$$

with the equality being satisfied for  $F = \tilde{F}$ . To construct an ansatz for an instanton we have the conditions that the winding number is 1, the configuration is finite-energy and the solution is a local extrema of the action. For simplicity let us ignore the gauge coupling constant by setting it to 1 and write the ansatz

$$A_\mu = if(r^2)g(x)\partial_\mu g^{-1}(x), \quad (3.63)$$

where  $f$  is a radial function that goes to 1 as  $r \rightarrow \infty$  faster than  $1/r^2$ . We can substitute this ansatz into the classical equations of motion (or equivalently the equation  $F = \tilde{F}$ ) to find

$$f(r^2)^2 - f(r^2) = -r^2 f'(r^2), \quad (3.64)$$

which is satisfied for

$$f(r^2) = \frac{r^2}{r^2 + \rho^2}. \quad (3.65)$$

The instanton is then [15, 16]

$$\begin{aligned} A_\mu(x) &= g^{-1}(x - a) [\partial_\mu g(x - a)] \frac{|(x - a)|^2}{|(x - a)|^2 + \rho^2} \\ \phi(x) &= 1 + \frac{\rho^2}{(x - a)^2}. \end{aligned} \quad (3.66)$$

That  $A_\mu(x)$  winds around the group once is clear from the fact that it is a radial function times the pure gauge form for the  $\nu = 1$  gauge configuration. This can also be seen by explicitly putting the above solution into the Chern–Simons form (3.47). The above instanton tunnels between two neighboring vacua and in the process produces three leptons and three baryons. If all particles are Standard Model this means nine quarks and three leptons. Calculating the energy density of this solution once again shows a clump of field highly localized in space and time, as can be seen in figure 3.3.

The amplitude for an instanton rate at zero temperature can be found by simply inserting the instanton solution into the path integral and making a saddle-point approximation. Doing so one finds that the instanton amplitude is proportional to  $\exp[-8\pi^2/g^2] \sim 10^{-173}$  [14] which is an incredible suppression! So at zero temperature it cannot possibly be important to explain the baryon asymmetry. Finally let us see how the ground state of the Standard Model can be thought of as a periodic potential [17–19]. Let an eigenstate of definite winding number be denoted by  $|n\rangle$ .

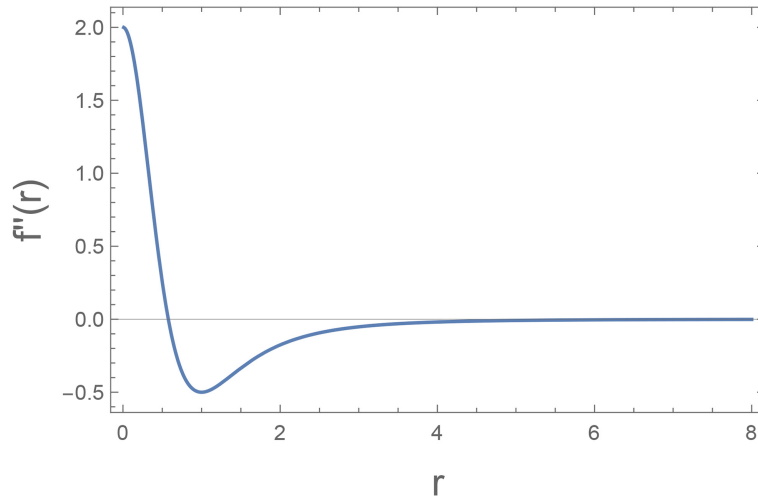


**Figure 3.3.** The energy profile of an instanton as a function of  $r^2$  is also highly localized. This is the motivation behind thinking of the instanton as a quasi-particle in Euclidean space. Here the parameter  $\rho = 1$ .

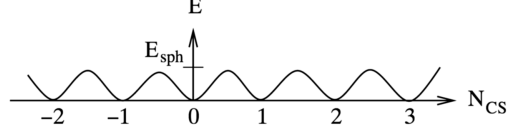


**Figure 3.4.** Standard Model ground state is actually periodic with a potential height of  $E_{\text{sph}}$ . Each degenerate minimum corresponds to a different Chern–Simons number. A shift to the right from one minimum to another is the instanton, whereas the local maxima are the sphalerons. Each degenerate ground state has a different Chern–Simons number,  $N_{\text{CS}}$ . Instantons move one to the right from one ground state to another with a higher Chern–Simons number whereas anti-instantons move one to the left.

The conjugate variable to  $n$  will then be a phase variable. An eigenstate of phase can be written as

$$|\theta\rangle = \sum_{n=-\infty}^{\infty} e^{in\theta}|n\rangle. \quad (3.67)$$

Let us consider the term  $\langle\theta'|\exp[-HT]|\theta\rangle$ . We of course have calculated the term  $\langle n+1|\exp[-HT]|n\rangle - \langle n+1|HT|n\rangle \approx AT \exp[-8\pi^2/g^2]$ . We can make the approximation where we ignore multiple tunneling events and consider only single tunneling transitions. Defining  $E(\theta)\delta(\theta - \theta') = \langle\theta'|H|\theta\rangle$  we have

$$E(\theta) = E_0 - 2A \exp\left[\frac{-8\pi^2}{g^2}\right] \cos \theta. \quad (3.68)$$

The ground state can be approximated as a periodic potential with a potential height proportional to the tunneling amplitude as depicted in figure 3.4.

Let us conclude the section by summarizing what we have learned so far about baryon number violation in the Standard Model:

- Classical conservation laws can be anomalously broken.
- Triangle anomalies in the Standard Model result in an anomalous violation of both baryon and lepton number conservation.
- The field configurations that anomalously violate baryon/lepton number are ones with a non-zero Chern–Simons number. This means they wrap around the internal space at the surface at spatial infinity in Euclidean space.
- Fields with integer winding number at infinity are solutions to the classical equations of motion.
- Fields with integer winding number look like localized lumps in Euclidean space.

### 3.5 The sphaleron

Let us now try and bootstrap another topologically interesting quasi-particle that is a good candidate for baryon number violation. Specifically, the quasi-particle we will discuss is the sphaleron whose etymology is from the Greek word that means to ‘go down’, because it is an unstable particle [20, 21]. In the previous section we presented the instanton with a winding and Chern–Simons number of 1. It turns out

that the instanton is less important than the sphaleron for our purposes because sphaleron rates become unsuppressed at high temperatures. As such we give it far closer attention. Physically, the instanton corresponds to tunneling through a barrier whereas a sphaleron corresponds to classically passing over the barrier. A sphaleron is an unstable particle corresponding to an instantaneous moment in time and is a solution to the classical equations of motion. It is due to its importance in the logical framework of this field that we give it such deep attention. It should be noted that we only focus on the lowest energy electroweak sphaleron before touching on the SU(3) sphaleron, since the lowest energy sphaleron will dominate. Of course we note that there is no formal proof that we are aware of that the sphaleron we present is indeed the lowest energy but it is widely believed to be so. To begin our bootstrap let us start with insisting that the Higgs field, which is an SU(2)<sub>L</sub> doublet, is well-behaved at infinity. Well-behaved in this case means the covariant derivative must vanish

$$D_\mu \phi \rightarrow 0 \text{ as } r \rightarrow \infty. \quad (3.69)$$

This gives the condition

$$\partial_\mu \phi \Big|_\infty = ig A_\mu^a \tau^a \Big|_\infty \phi \Big|_\infty. \quad (3.70)$$

In this case we keep the gauge coupling constant as we will eventually calculate the sphaleron rate. We want  $\partial\phi/\partial t = 0$  and we want a topologically non-trivial solution. So let us set  $A_0|_\infty$  to zero along with  $d\phi/dt|_\infty$  and map the space–time surface onto the internal space by setting  $A_i^\infty$  to be proportional to the right invariant one form—also called the Maurer–Cartan form

$$\phi^\infty = \Omega \begin{pmatrix} 0 \\ v/\sqrt{2} \end{pmatrix} \quad (3.71)$$

and

$$A_i^\infty = \frac{-i}{g} (\partial_i \Omega) \Omega^{-1}. \quad (3.72)$$

We will use  $\Omega$  instead of  $g$  here and throughout for an element of the gauge group to avoid confusion with the coupling constant. The Hermitian conjugate of the above is a solution. Both of these solutions can be verified by direct substitution.

This is the first requirement of a sphaleron: that it reduce to the Maurer–Cartan form at infinity in order to be a finite-energy solution. Fields with integer winding number are known to be (multi-)instantons. The only other topologically interesting cases that can potentially violate baryon number are the cases where we have a non-integer and non-zero Chern–Simons number. It will turn out that sphalerons have a Chern–Simons number of 1/2. However, the Chern–Simons number was shown in the previous section to be related to the winding number, which is forced to be an integer. So it is something of a surprise that a non-integer Chern–Simons number is possible given its close relationship to the winding number. Indeed the

Chern–Simons number of any *vacuum* state must be an integer so a non-integer Chern–Simons number means it must continuously deform from one vacuum state to another.

To complete our bootstrap we explicitly make use of the Pauli matrices and make our fields cover the internal group as we cover the spatial sphere at  $r = \infty$  while passing through zero somewhere in space via use of a radial function. Therefore a suitable ansatz is

$$\phi^\infty = h(r)\Omega \begin{pmatrix} 0 \\ v/\sqrt{2} \end{pmatrix} \quad (3.73)$$

and

$$A_i^\infty = \frac{-if(r)}{g}(\partial_i\Omega)\Omega^{-1} \quad (3.74)$$

with

$$\Omega = \bar{\sigma} \cdot \frac{\vec{x}}{r}. \quad (3.75)$$

Also  $f \equiv f(r)$  and  $h(r)$  are radial functions chosen to solve the equations of motion subject to the boundary conditions  $h(0) = f(0) = 0$  and  $h(\infty) = f(\infty) = 1$ . Let us now complete the motivation for studying closely this quasi-particle over the instanton, by demonstrating that these processes become unsuppressed when electroweak symmetry is restored at high temperature. We apologize to the reader for slightly skipping ahead in the flow of our logical argument by using a small amount of finite temperature field theory from the later parts of this primer. The reader should regard the form of the next few equations as divinely given and then return to this section after reading the later sections on finite temperature quantum field theory (QFT). The sphaleron rate can be found by substituting the above solution into the finite temperature version of the path integral. The high temperature sphaleron rate is given by

$$\Gamma_{\text{sph}} = \frac{\omega_-}{2\pi}(\mathcal{N}V)_{\text{rot}}(\mathcal{N}V)_{\text{tr}}\kappa e^{\Delta E_{\text{sph}}/T}, \quad (3.76)$$

where  $\Delta E_{\text{sph}}/T = S_3(\phi_{\text{sph}})$ , where

$$S_3[\phi_{\text{sph}}] = \frac{1}{T} \int d^3x |D_i\phi|^2 + \frac{1}{4}W_{ij}^a W_{ij}^a + V(\phi). \quad (3.77)$$

Here  $W_{ij}$  are the field strength tensors for  $A_i$ ,  $W_{ij} \equiv \partial_i A_j - \partial_j A_i$ . With some effort we can reduce this to

$$S_3[\phi_{\text{sph}}] \equiv \frac{\Delta E_{\text{sph}}}{T} = \frac{4\pi v(T)}{gT} B\left(\frac{\lambda}{g^2}\right) \quad (3.78)$$

with

$$B\left(\frac{\lambda}{g^2}\right) = \int_0^\infty dr \left[ 4\left(\frac{df}{dr}\right)^2 + \frac{8}{r^2}f^2(1-f)^2 + \frac{r^2}{2}\left(\frac{dh}{dr}\right)^2 h^2(1-f)^2 + \frac{1}{4}\frac{\lambda}{g^2}r^2(1-h^2)^2 \right], \quad (3.79)$$

where  $r \equiv gv(T)|x|^2$ . Note that when  $v(T) = 0$  the rate is no longer exponentially suppressed. We will show in later chapters that electroweak symmetry is indeed restored at very high temperatures, meaning that at some stage in our cosmic history sphalerons, and therefore baryon number violation, were unsuppressed! This is the key feature of sphalerons which makes them attractive as a source of baryon number violation at very high temperature when electroweak symmetry is restored. There is one remaining thing we have to show to conclude our discussion of sphalerons in terms of showing that we indeed have a non-zero Chern–Simons number. Recall that the Chern–Simons form is

$$\text{Tr} \left[ W \wedge dW + \frac{2}{3} W \wedge W \wedge W \right] \quad (3.80)$$

where for  $A_0 = 0$ , the above can be written

$$\begin{aligned} \text{Tr} [W \wedge dW] &= \epsilon_{ijk} W_i (\partial_j W_k - \partial_j W_i) = -\epsilon_{ijk} (\partial_i W_j - \partial_j W_i) W_k \\ \text{Tr} [W \wedge W \wedge W] &= -\epsilon_{ijk} \epsilon_{abc} W_i^a W_j^b W_k^c \end{aligned} \quad (3.81)$$

and the Chern–Simons number for the sphaleron is

$$Q(\text{Sphaleron}) = \frac{g^2}{32\pi^2} \int_{t=t_0} d^3x K^0, \quad (3.82)$$

where  $K^0$  is the Chern–Simons form. Recall our field configuration,

$$W_i^a \sigma^a = -\frac{2if}{g} \Omega^{-1} d\Omega \quad (3.83)$$

where  $\Omega$  is given above and  $d\Omega$  is the external derivative  $\frac{\partial \Omega}{\partial x_i} dx_i$ . Remarkably the form of  $f$  will not affect the Chern–Simons number as long as the boundary conditions given above are met. It is easy to see that the above equation reduces to

$$W_i^a dx_i = -\frac{2f}{g} \epsilon_{iab} x_b. \quad (3.84)$$

We cannot calculate the Chern–Simons number in this form as the derivation of the Chern–Simons number assumes that our field goes to zero faster than  $1/r$ . Let us therefore perform a gauge transformation  $U = \exp\left[\frac{i}{2}\Theta(r)\sigma \cdot \frac{x}{r}\right]$ , where  $\Theta(r)$  is a

radial function that goes to zero at the spatial origin. Recall that a gauge transformation for non-abelian fields has the form

$$gW_i^a \sigma_a \rightarrow U^\dagger \left( \frac{-2f}{r^2} \epsilon_{aik} x_k \sigma_a \right) U + i(\partial_i U^{-1})U. \quad (3.85)$$

It is straightforward to show that in this gauge the sphaleron solution looks like

$$gW_i^a = A\epsilon_{iab}x_b + B(\delta_{ia}r^2 - x_i x_a) + \Theta' \frac{x_i x_a}{r^2} \equiv \mathcal{A}_{ai} + \mathcal{B}_{ai} + \mathcal{C}_{ai}, \quad (3.86)$$

where the prime denotes a radial derivative and

$$\begin{aligned} A \equiv A(r) &= \frac{1}{r^2} \left[ (1 - 2f(r)) \cos(\Theta) - 1 \right] \text{ and} \\ B \equiv B(r) &= \frac{1}{r^3} \left[ (1 - 2f(r)) \sin(\Theta) \right]. \end{aligned} \quad (3.87)$$

Such abbreviations may be disorientating but we will continue to use them throughout because it becomes far too cumbersome to write out every term explicitly. The sphaleron now has the correct asymptotic behavior. Since  $W_i^a$  is spherically symmetric the integral over angular variables in the calculation is trivial allowing us to rewrite the Chern–Simons number of the sphaleron as

$$Q(\text{Sphaleron}) = \frac{g^2}{8\pi} \int_{t=t_0} r^2 dr K^0. \quad (3.88)$$

Using above equations and verifying this with equation (3.45) we can write

$$K^0 = - \left( \epsilon_{ijk} F_{ij}^a W_k^a + \frac{2g}{3} \epsilon_{ijk} \epsilon_{abc} W_i^a W_j^b W_k^c \right). \quad (3.89)$$

Let us first calculate the first term in the Chern–Simons density. Due to our gauge transformation it consists of three terms

$$\epsilon_{ijk} F_{ij}^a W_k^a \equiv (A_{ak} + B_{ak} + C_{ak}) W_k^a, \quad (3.90)$$

which in turn are defined by the three terms we defined before  $\mathcal{A}_{ia}$ ,  $\mathcal{B}_{ia}$  and  $\mathcal{C}_{ia}$  as follows

$$A_{ak} \equiv \epsilon_{ijk} \left[ \partial_i \mathcal{A}_{ja} - \partial_j \mathcal{A}_{ia} \right] \text{ etc.} \quad (3.91)$$

With a bit of effort one can simplify the expressions for  $(A_{ak}, B_{ak}, C_{ak})$ , reducing them down to the simple form

$$\begin{aligned} gA_{ak} &= \frac{2}{r} [r^2 \delta_{ka} - x_k x_a] A' + 4A \delta_{ka} \\ gB_{ak} &= 2\epsilon_{iak} x_i [B' r + 3B] \end{aligned} \quad (3.92)$$

$$gC_{ak} = -2\epsilon_{iak}x^i\Theta'. \quad (3.93)$$

We now contract the above with  $W^a_k$  which gives a sum of nine terms. It is easy to show that these terms are

$$\begin{aligned} g^2A_{ka}\mathcal{A}_{ka} &= 0 & g^2A_{ka}\mathcal{B}_{ka} &= 4BA'r^3 + 8ABr^2 & g^2A_{ka}\mathcal{C}_{ka} &= 4A\Theta' \\ g^2\mathcal{B}_{ka}\mathcal{A}_{ka} &= -4[B'r + 3B]Ar^2 & g^2\mathcal{B}_{ka}\mathcal{B}_{ka} &= 0 & g^2\mathcal{B}_{ka}\mathcal{C}_{ka} &= 0 \\ g^2\mathcal{C}_{ka}\mathcal{A}_{ka} &= 4A\Theta'r^2 & g^2\mathcal{C}_{ka}\mathcal{B}_{ka} &= 0 & g^2\mathcal{C}_{ka}\mathcal{C}_{ka} &= 0. \end{aligned} \quad (3.94)$$

So we have, in summary, the first term in the Chern–Simons density calculated as

$$\frac{g^2r^2}{8\pi}\epsilon_{ijk}F_{ij}^aW_k^a = \frac{1}{2\pi}BA'r^5 + \frac{1}{\pi}ABr^4 + \frac{1}{2\pi}r^4A[B'r + 3B] + \frac{1}{\pi}A\Theta'r^4. \quad (3.95)$$

Next we have the term  $g^2\epsilon_{ijk}\epsilon_{abc}W_i^aW_j^bW_k^c$ . Let us first calculate the product of two sphalerons contracted with the permutation symbols

$$\epsilon_{ijk}\epsilon_{abc}W_i^aW_j^b = \epsilon_{abc}\epsilon_{ijk}[\mathcal{A}_{ai} + \mathcal{B}_{ai} + \mathcal{C}_{ai}][\mathcal{A}_{bj} + \mathcal{B}_{bj} + \mathcal{C}_{bj}]. \quad (3.96)$$

It is useful to organize the terms into a matrix

$$\begin{aligned} &g^2\epsilon_{ijk}\epsilon_{abc} \begin{pmatrix} \mathcal{A}_{ai}\mathcal{A}_{bj} & \mathcal{A}_{ai}\mathcal{B}_{bj} & \mathcal{A}_{ai}\mathcal{C}_{bj} \\ \mathcal{B}_{ai}\mathcal{A}_{bj} & \mathcal{B}_{ai}\mathcal{B}_{bj} & \mathcal{B}_{ai}\mathcal{C}_{bj} \\ \mathcal{C}_{ai}\mathcal{A}_{bj} & \mathcal{C}_{ai}\mathcal{B}_{bj} & \mathcal{C}_{ai}\mathcal{C}_{bj} \end{pmatrix} \\ &= \begin{pmatrix} 2x_kx_cA^2 & 0 & -\Theta'A\epsilon_{kbc}x_b \\ 0 & 2x_kx_cB^2r^2 & B\Theta'(\delta_{kc}r^2 - x_kx_c) \\ -\Theta'A\epsilon_{kbc}x_b & B\Theta'(\delta_{kc}r^2 - x_kx_c) & 0 \end{pmatrix} \\ &\equiv M. \end{aligned} \quad (3.97)$$

Contracting the last sphaleron gives the following

$$\begin{aligned} g^2\epsilon_{ijk}\epsilon_{abc}W_i^aW_j^bW_k^c &= [(M_{11})_{kc} + (M_{22})_{kc} + 2(M_{23})_{kc} + 2(M_{13})_{kc}] \\ &\quad \times [\mathcal{A}_{kc} + \mathcal{B}_{kc} + \mathcal{C}_{kc}] \\ &= [\mu_{kc} + \nu_{kc} + \tau_{kc}][\mathcal{A}_{kc} + \mathcal{B}_{kc} + \mathcal{C}_{kc}], \end{aligned} \quad (3.98)$$

where we have again used the abbreviation

$$\mu_{kc} \equiv \{(M_{11})_{kc} + (M_{22})_{kc}\}, \quad \nu_{kc} \equiv 2(M_{23})_{kc}, \quad \tau_{kc} \equiv 2(M_{13})_{kc}. \quad (3.99)$$

We then have

$$\begin{pmatrix} \mu_{kc} \mathcal{A}_{kc} & \mu_{kc} \mathcal{B}_{kc} & \mu_{kc} \mathcal{C}_{kc} \\ \nu_{kc} \mathcal{A}_{kc} & \nu_{kc} \mathcal{C}_{kc} & \nu_{kc} \mathcal{C}_{kc} \\ \tau_{kc} \mathcal{A}_{kc} & \tau_{kc} \mathcal{B}_{kc} & \tau_{kc} \mathcal{C}_{kc} \end{pmatrix} = \begin{pmatrix} 0 & 0 & 2\Theta' r^2 [A^2 + r^2 B^2] \\ 0 & 4B^2 r^4 \Theta' & 0 \\ 4\Theta' A^2 r^2 & 0 & 0 \end{pmatrix}, \quad (3.100)$$

so we can therefore write

$$\frac{g^2 r^2}{24\pi} \epsilon_{ijk} \epsilon_{abc} W_i^a W_j^b W_k^c = \frac{1}{4\pi} \Theta' r^4 A^2 + \frac{1}{4\pi} r^6 B^2 \Theta'. \quad (3.101)$$

In total we have

$$Q = -\frac{1}{4\pi} \int_{t=t_0}^{} dr [2BA'r^5 + 4ABr^4 - 2r^4 A[B'r + 3B] + 4A\Theta'r^2 + 2\Theta'r^4 A^2 + 2r^6 B^2 \Theta']. \quad (3.102)$$

Simplifying the above equation we can then can the following solvable integral for the Chern–Simons number

$$\begin{aligned} Q(\text{sphaleron}) &= \frac{1}{2\pi} \int_{\Theta(0)}^{\Theta(\infty)} d\Theta [\Theta - \cos \Theta] \\ &= \frac{1}{2} \end{aligned} \quad (3.103)$$

as required.

So let us summarize. The sphaleron is an unstable quasi-particle due to localization in time and it must continuously go between vacuum states. It is a finite-energy solution so it is well-behaved at the spatial boundary. The simplest solution is then derived by mapping the external space onto the internal space and coupling to a radial function that gives the desired properties and is determined by insisting that the sphaleron be a solution to the classical equations of motion. Such a sphaleron would be a local extremum of the action for any gauge group with an SU(2) subgroup. It has the nice property that the sphaleron rate is unsuppressed when electroweak symmetry is restored. It also has the unusual property that the Chern–Simons number is fractional and shown to be to equal 1/2. That it is non-zero means it facilitates baryon number non-conservation.

## References

- [1] Coon S A and Holstein B R 2002 Anomalies in quantum mechanics: the  $1/r^2$  potential *Am. J. Phys.* **70** 513
- [2] Holstein B R 2014 Understanding an anomaly *Am. J. Phys.* **82** 591
- [3] Adler S 1969 Axial-vector vertex in spinor electrodynamics *Phys. Rev.* **177** 2426

- [4] Bell J S and Jackiw R 1969 A PCAC puzzle:  $\pi^0 \rightarrow \gamma\gamma$  in the omega-model *Nuovo Cimento A* **60** 47
- [5] Jegerlehner F 2000 Facts of life with gamma (5) arXiv: [0005255](https://arxiv.org/abs/0005255)(hep-th)
- [6] El-Menoufi B K and White G A 2015 The axial anomaly, dimensional regularization and Lorentz-violating QED arXiv: [1505.01754](https://arxiv.org/abs/1505.01754)(hep-th)
- [7] Ferrari R 2014 Managing  $\gamma_5$  in dimensional regularization and ABJ anomaly arXiv: [1403.4212](https://arxiv.org/abs/1403.4212)
- [8] Fujikawa K 1979 Path-integral measure for gauge-invariant fermion theories **42** 18
- [9] Donoghue J F, Golowich E and Holstein B R 2014 *Dynamics of the Standard Model* vol 35 (Cambridge: Cambridge University Press)
- [10] Rajaraman R 1982 *Solitons and Instantons: An Introduction to Solitons and Instantons in Quantum Field Theory* (North Holland: Amsterdam)
- [11] Coleman S 1988 *Aspects of Symmetry: selected Erice lectures* (Cambridge: Cambridge University Press)
- [12] Manton N and Sutcliffe P 2004 *Topological Solitons* (Cambridge: Cambridge University Press)
- [13] Chern S and Simons J 1974 Characteristic forms and geometric invariants *Ann. Math.* **99** 48–69
- [14] 't Hooft G 1976 Symmetry breaking through Bell-Jackiw anomalies *Phys. Rev. Lett.* **37** 8
- [15] Wilczek F 1976 Inequivalent embeddings of SU(2) and instanton interactions *Phys. Lett. B* **65** 160
- [16] Belavin A A, Polyakov A M, Schwartz A S and Tyupkin Y S 1975 Pseudoparticle solutions of the Yang–Mills equations *Phys. Lett. B* **59** 79
- [17] Jackiw R and Rebbi C 1976 Vacuum periodicity in a Yang–Mills quantum theory *Phys. Rev. Lett.* **37** 172
- [18] Callan C G, Dashen R F and Gross D J 1976 The structure of the gauge theory vacuum *Phys. Lett. B* **63** 334
- [19] Polyakov A M 1997 *Quark Confinement and Topology of Gauge Theories* **B 120** 429
- [20] Manton N S 1983 Topology in the Weinberg-Salam theory *Phys. Rev. D* **28** 8
- [21] Klinkhamer F R and Manton N S 1984 A saddle-point solution in the Weinberg-Salam theory *Phys. Rev. D* **30** 10

### 3.5 A brief review of thermal field theory

In this section I give a brief review of finite temperature quantum field theory referring the reader to my book for a more in depth discussion. It is inappropriate to use zero temperature quantum field theory in a far from equilibrium setting of cosmic phase transition. I begin by deriving the closed time path contour [76, 77, 78, 79, 80, 81]. Recall the equilibrium density matrix of a quantum system [82]

$$\rho(0) = \frac{e^{-\beta H}}{\text{Tr}e^{-\beta H}} . \quad (3.2)$$

Here the null argument of the density matrix refers to some time  $t$  after which the system departs from equilibrium. Time dependence can be introduced in the same way as ordinary quantum mechanics

$$\rho(t) = U(t, 0)\rho(0)U^\dagger(t, 0) \quad (3.3)$$

with the time evolution operator defined as

$$U(t, t') = T \left( e^{-i \int_{t'}^t dt'' H(t'')} \right) . \quad (3.4)$$

Note then that the density matrix itself can be written in terms of unitary operators

$$\rho(0) = \frac{U(T - i\beta, T)}{\text{Tr}U(T - i\beta, T)} . \quad (3.5)$$

The time dependent evolution of an operator is then

$$\langle A(t) \rangle = \frac{\text{Tr}U(t, 0)U(T - i\beta, T)U(0, t)A}{\text{Tr}U(T - i\beta, T)} \quad (3.6)$$

$$= \frac{\text{Tr}U(T - i\beta, T)U(T, T')U(T', t)AU(t, T)}{\text{Tr}U(T - i\beta, T)U(T, T')U(T', T)} \quad (3.7)$$

This suggests that for a finite temperature out of equilibrium system I should use the generating functional of the form

$$Z[\beta, \mathcal{J}_C] = \text{Tr}U_{\mathcal{J}_C}(T - i\beta, T)U_{\mathcal{J}_C}(T, T')U_{\mathcal{J}_C}(T', T) . \quad (3.8)$$

Let us take  $T \rightarrow \infty$ . The above equation then implies that I take a time contour from  $-\infty$  to the time  $t$  infinitesimally above the real axis, drop infinitesimally below the real axis and then travel back to  $-\infty$  before making a trip perpendicular to the real line by an amount  $i\beta$ . The result when calculating two point propagators is that there are now twice as many. One can have both fields on the top half of the time contour, both on the bottom, or one on each. Using causality, hermiticity and unitarity [83], one can constrain the form of these propagators. For example, scalar propagators take the form

$$\begin{pmatrix} \Delta^T(p) & \Delta^<(p) \\ \Delta^<(p) & \Delta^{\bar{T}}(p) \end{pmatrix} = \begin{pmatrix} \frac{1}{p^2 - M^2 + i\epsilon} & 0 \\ 0 & \frac{1}{p^2 - M^2 - i\epsilon} \end{pmatrix} - 2\pi i \left[ n_B(|p_0|) \begin{pmatrix} 1 & 1 \\ 1 & 1 \end{pmatrix} + \begin{pmatrix} 0 & \Theta(-p_0) \\ \Theta(p_0) & 0 \end{pmatrix} \right] \quad (3.9)$$

whereas the fermion propagators are

$$\begin{pmatrix} S^T(p) & S^<(p) \\ S^<(p) & S^T(p) \end{pmatrix} = \begin{pmatrix} \frac{\not{p}+m}{p^2-M^2+i\epsilon} & 0 \\ 0 & \frac{\not{p}+m}{p^2-M^2-i\epsilon} \end{pmatrix} - 2\pi i(\not{p}+m) \left[ n_F(|p_0|) \begin{pmatrix} 1 & 1 \\ 1 & 1 \end{pmatrix} + \begin{pmatrix} 0 & -\Theta(-p_0) \\ -\Theta(p_0) & 0 \end{pmatrix} \right]. \quad (3.10)$$

For our purposes it is enough to know just the form of these propagators.

### 3.6 The effective potential at finite temperature

The Higgs potential receives temperature corrections which eventually lead to the deepest minimum being one where electroweak symmetry is intact [84]. It is at this temperature where there is an electroweak phase transition. In this brief section I apply what I just derived for describing finite temperature field theory to derive the finite temperature corrections to a simple scalar theory

$$V = \frac{m^2}{2}\phi^2 + \frac{\lambda}{4!}\phi^4. \quad (3.11)$$

It is easiest to calculate the derivative of the effective potential at one loop with respect the mass [85, 86, 87]. This means calculating a single diagram and I can insert our finite temperature propagators. In fact there is only one propagator to consider since the external legs must be on the positive time contour

$$\frac{\partial \Delta V}{\partial m^2(\phi)} = \frac{1}{2} \int \frac{d^4 p}{(2\pi)^4} \left[ \frac{i}{p^2 - m^2(\phi) + i\epsilon} + 2\pi n_B(\omega_p) \delta(p^2 - m^2) \right]. \quad (3.12)$$

The key observation here is that the one loop correction to the effective potential is a sum of the usual zero temperature piece and the finite temperature piece. Integrating over the delta function I can write the finite temperature piece I have

$$\frac{\partial \Delta V_T}{\partial m^2(\phi)} = \int \frac{d^3 p}{(2\pi)^3} \frac{1}{2\omega} n_B(\omega). \quad (3.13)$$

The above equation can be integrated to give the thermal bosonic corrections to the effective potential in terms of the bosonic thermal function  $J_B$  (forthcoming). Similarly the thermal corrections to the effective potential due to fermions can be written in terms of the fermionic thermal function  $J_F$ . In total the thermal correction to the effective potential to one loop is

$$\Delta V_T = \sum_f \frac{T^4}{2\pi^2} J_F \left( \frac{m_f^2}{T^2} \right) + \sum_b \frac{T^4}{2\pi^2} J_B \left( \frac{m_b^2}{T^2} \right), \quad (3.14)$$

with

$$J_B(z^2) = \int_0^\infty dx x^2 \ln \left( 1 - e^{-\sqrt{x^2+z^2}} \right), \quad (3.15)$$

$$J_F(z^2) = \int_0^\infty dx x^2 \ln \left( 1 + e^{-\sqrt{x^2+z^2}} \right). \quad (3.16)$$

These thermal functions have a high temperature expansion

$$\begin{aligned} J_B(z^2) &\approx -\frac{\pi^4}{45} + \frac{\pi^2 z^2}{12} - \frac{\pi z^3}{6}, \\ J_F(z^2) &\approx \frac{7\pi^4}{360} - \frac{\pi^2 z^2}{24}. \end{aligned} \quad (3.17)$$

So finite temperature effectively give a temperature dependence to quadratic and cubic couplings in the effective potential. If the parameters are chosen right, the Higgs potential could evolve such that there remains a barrier between the true and false vacua as the Universe cools. In such a situation the phase transition would proceed through bubble nucleation [88, 89, 90, 91]. This is precisely the far from equilibrium setting one needs to catalyse baryon production in the EWBG mechanism.

### 3.6.1 Bubble nucleation

The phase transition occurs when a  $1/e$  fraction of the Hubble volume is in the new phase. This is known as the nucleation temperature. If I denote the tunneling probability as  $p(t)$  then via dimensional analysis I can write the relation

$$p(t)t^4 \sim 1. \quad (3.18)$$

I can also write the temperature dependent tunneling probability as follows

$$p(T) \approx T^4 e^{-S_E/T} \quad (3.19)$$

where  $S_E$  is the three dimensional Euclidean action which, assuming spherical symmetry, has the form

$$S_E = 4\pi \int_0^\infty r^2 dr \left[ \sum_i \frac{1}{2} \left( \frac{\partial \phi_i}{\partial r} \right)^2 + V(\{\phi_i\}) \right]. \quad (3.20)$$

Assuming the false vacuum is located at the origin in field space, the bounce satisfies the boundary conditions

$$\frac{d\phi_i}{dr} = 0, \quad \phi_i(\infty) = 0 \quad (3.21)$$

and of course is the solution to the classical equations of motion

$$\frac{\partial^2 \phi_i}{\partial r^2} + \frac{2}{r} \frac{\partial \phi_i}{\partial r} = \frac{\partial V}{\partial \phi_i}. \quad (3.22)$$

Using the relation between time and temperature

$$T^2 t = \sqrt{\frac{45}{16\pi^3}} \frac{M_p}{\sqrt{g^*}} \quad (3.23)$$

one can derive the condition for the nucleation temperature

$$\frac{S_E}{T_N} = 170 - 4 \ln \left[ \frac{T_N}{1\text{GeV}} \right] - 2 \ln g^* \quad (3.24)$$

which for the electroweak phase transition satisfies  $S_E/T_N \approx 140$ .

### 3.6.2 Transport equations

Within the closed time path formalism, divergences of particle number currents can be related to the same particles self energies through the manipulation of Dyson–Schwinger equations. Systematically doing so results in a network of coupled transport equations which have the general form [92, 93, 94]

$$\partial_\mu J_i^\mu = - \sum_j \Gamma^{ij} \mu_i + S_i^{CP} . \quad (3.25)$$

Let us begin with the Dyson-Schwinger equations

$$\begin{aligned} \tilde{G}(x, y) &= \tilde{G}^0(x, z) + \int d^4 w \int d^4 z \tilde{G}^0(x, w) \tilde{\Sigma}(w, z) \tilde{G}(z, y), \\ \tilde{G}(x, y) &= \tilde{G}^0(x, z) + \int d^4 w \int d^4 z \tilde{G}(x, w) \tilde{\Sigma}(w, z) \tilde{G}^0(z, y), \end{aligned} \quad (3.26)$$

where  $\tilde{\Sigma}(\cdot)$  is a matrix of self energies. To make use of these equations I hit both equations with the Klein Gordon operators  $\square_x$  and  $\square_y$  respectively. I then subtract each equation from the other taking the limit of  $x \rightarrow y$ . The left hand side gives  $\partial_\mu J^\mu$  whereas the right hand side gives a matrix where all the elements are equivalent. The result is

$$\begin{aligned} \partial_\mu J^\mu &= - \int_{-\infty}^{x_0} dz_0 \int d^3 z \text{Tr} [\Sigma^>(x, z) G^<(z, x) - G^<(x, z) \Sigma(z, x) \\ &\quad - \Sigma^>(x, z) G^<(z, x) + G^>(x, z) \Sigma^<(z, x)] . \end{aligned} \quad (3.27)$$

## Chapter 4

---

# Solving transport equations during a cosmic phase transitions

---

### 4.1 Introductory remarks

The behaviour of particle densities during a cosmic phase transition is described by a series of quantum transport equations which are a set of coupled non-linear inhomogeneous differential equations. These equations are generally either numerically solved or they are approximately solved using an assumption where certain interactions occur sufficiently fast that these interactions are in local equilibrium. However, it has been demonstrated that using this approximation can yield a baryon asymmetry two orders of magnitude different to the value acquired numerically [93]. As such there is ample motivation for a more reliable analytic approach. In this work I take the strategy of approximating the transport equations by a set of coupled linear differential equations solved in two regions. These linear differential equations are solved (semi-)analytically and then these solutions are matched at the phase boundary such that they satisfy continuity conditions. One can then take this solution and add a perturbation to give the true solution. Expanding everything in the transport equations to first order one can then derive a new set of coupled linear inhomogeneous differential equations which can also be solved. This sets up a perturbative series. I compare our results to a purely numeric calculation from [95].

### 4.2 Declaration for thesis chapter 4

#### Declaration by candidate

In the case of the paper present contained in chapter 4, the nature and extent of my contribution was as follows:

Publication	Nature of contribution	Extent of contribution
4	Single author	100%

The undersigned hereby certify that the above declaration correctly reflects the nature and extent of the candidate and co-authors' contributions to this work.

**Signatures:**

Graham White



**Date:** 3.04.2017

### **4.3 Published material for Chapter 4: General analytic methods for solving coupled transport equations: From cosmology to beyond**

# General analytic methods for solving coupled transport equations: From cosmology to beyond

G. A. White\*

*ARC Centre of Excellence for Particle Physics at the Tera-scale, School of Physics and Astronomy,  
Monash University, Victoria 3800, Australia*

(Received 23 November 2015; published 4 February 2016)

We propose a general method to analytically solve transport equations during a phase transition without making approximations based on the assumption that any transport coefficient is large. Using a cosmic phase transition in the minimal supersymmetric standard model as a pedagogical example, we derive the solutions to a set of 3 transport equations derived under the assumption of supergauge equilibrium and the diffusion approximation. The result is then rederived efficiently using a technique we present involving a parametrized ansatz which turns the process of deriving a solution into an almost elementary problem. We then show how both the derivation and the parametrized ansatz technique can be generalized to solve an arbitrary number of transport equations. Finally we derive a perturbative series that relaxes the usual approximation that inactivates vacuum-expectation-value dependent relaxation and  $CP$ -violating source terms at the bubble wall and through the symmetric phase. Our analytical methods are able to reproduce a numerical calculation in the literature.

DOI: 10.1103/PhysRevD.93.043504

## I. INTRODUCTION

The phase history of our Universe is unknown as it depends on the full content of the scalar potential [1]. The many possibilities have inspired a multitude of mechanisms to produce the observed asymmetry between particles and antiparticles during a phase transition [2–5]. The observed baryogenesis of the universe (BAU) is estimated to be [6]

$$Y_B = \frac{n_B}{s} = \begin{cases} (7.3 \pm 2.5) \times 10^{-11}, & \text{BBN} \\ (9.2 \pm 1.1) \times 10^{-11}, & \text{WMAP} \end{cases} \quad (1)$$

Although the methods derived in this work have general application, we will be working most closely with the electroweak-baryogenesis picture. In the electroweak baryogenesis picture, the BAU is produced during the electroweak phase transition [7]. To avoid electroweak sphalerons from washing out any produced electroweak baryogenesis one requires this phase transition to be strongly first order [8]. The particle dynamics become non-Markovian during the far-from-equilibrium conditions that occur during a cosmic phase transition, rendering equilibrium quantum field theory inadequate as a tool to analyze the behavior of particle number densities throughout. One instead is required to use the closed time path (CTP) formalism [9–14]. The usual treatment involves deriving a set of coupled quantum transport equations (QTE) involving  $CP$ -conserving relaxation terms and  $CP$ -violating sources derived from scattering amplitudes evaluated using the CTP formalism [15,16]. There are in general as many QTEs

as there are particle species in a given model so one may be left with a daunting number of coupled inhomogeneous differential equations to solve. Therefore one usually proceeds either by solving the system numerically or by using a set of approximations to reduce the number of QTEs to a single one which is then solved in two regions with the solutions matched at the phase boundary. The former method is very cumbersome and the latter method involves using a set of fast rate approximations to reduce the set of coupled transport equations down to one [see e.g., [16,17] and the references therein for this treatment in the minimal supersymmetric standard model (MSSM)]. However, recently it has been shown that in the case of the MSSM with  $R$ -parity conservation, the assumption of fast Yukawa and triscalar rates is infrequently justified [18]. Furthermore, the practice of solving the equations in two regions effectively approximates the VEV profile with a step function and ignores any effects of a thick bubble wall, an assumption we refer to in this paper as the “ultrathin wall approximation.” In this work we show how to analytically go beyond these approximations by deriving an exact solution to a general set of QTEs. We begin by considering the set of QTEs that govern the MSSM during an electroweak phase transition derived under the assumption of local supergauge equilibrium and null number densities for weak bosons. This is admittedly not an exact system to begin with but it is useful as an example before we generalizing our method to larger systems of coupled transport equations with multiple  $CP$ -violating source terms. We also show how to analytically derive an expansion that goes beyond the ultrathin wall approximation. Moreover, we show that once one knows the form of the solution—which has a general form—one can more

\*graham.white@monash.edu

quickly derive the solution using a parametrized ansatz whose parameters are determined by direct substitution. The layout of our paper is as follows. In Sec. II we use MSSM under supergauge equilibrium as an illustrative example of how to derive an analytic solution to a set of QTEs without using a fast rate approximation. In Sec. III we show how to rederive this solution quickly using a parametrized ansatz. We then generalize our methods to an, in principle, arbitrary set of transport equations with multiple  $CP$ -violating sources in Sec. IV, before showing how to go beyond the ultrathin wall approximation in Sec. V. Finally in Sec. VI we compare our analytic solution to what one might get using the fast rate approximation for one set of parameters as well as by numerically calculating the lowest-order correction to the ultrathin wall regime; our conclusions are then presented in Sec. VII.

## II. THE MSSM: AN ILLUSTRATIVE EXAMPLE

The transport equations for the MSSM under the assumption of supergauge equilibrium [19] as well the assumption that  $\mu_W^\pm \approx 0$  have been derived many times before (see for instance [16] and the references therein). Furthermore, under supergauge equilibrium, the transport equations have the same structure as a 2 Higgs doublet model up to wino-Higgsino-vacuum interactions. Thus, we just quote the result here. Under the assumption of supergauge equilibrium we only need to write coupled transport equation for the following number densities:

$$\begin{aligned} Q &= n_{t_L} + n_{b_L} + n_{\tilde{t}_L} + n_{\tilde{b}_L} \\ T &= n_{t_R} + n_{\tilde{t}_R} \\ H &= n_{H_u^+} + n_{H_u^0} - n_{H_d^-} - n_{H_d^0} \\ &\quad n_{\tilde{H}_u^+} + n_{\tilde{H}_u^0} - n_{\tilde{H}_d^-} - n_{\tilde{H}_d^0}. \end{aligned} \quad (2)$$

The set of coupled differential equations are

$$\begin{aligned} \partial_\mu T^\mu &= \Gamma_M^+ \left( \frac{T}{k_T} + \frac{Q}{k_Q} \right) - \Gamma_M^- \left( \frac{T}{k_T} - \frac{Q}{k_Q} \right) \\ &\quad - \Gamma_Y \left( \frac{T}{k_T} - \frac{H}{k_H} - \frac{Q}{k_Q} \right) \\ &\quad + \Gamma_{SS} \left( \frac{2Q}{k_Q} - \frac{T}{k_T} + \frac{9(Q+T)}{k_B} \right) + S_i^{C/P} \end{aligned} \quad (3)$$

$$\begin{aligned} \partial_\mu Q^\mu &= -\Gamma_M^+ \left( \frac{T}{k_T} + \frac{Q}{k_Q} \right) - \Gamma_M^- \left( \frac{T}{k_T} - \frac{Q}{k_Q} \right) \\ &\quad + \Gamma_Y \left( \frac{T}{k_T} - \frac{H}{k_H} - \frac{Q}{k_Q} \right) \\ &\quad - 2\Gamma_{SS} \left( \frac{2Q}{k_Q} - \frac{T}{k_T} + \frac{9(Q+T)}{k_B} \right) - S_i^{C/P} \end{aligned} \quad (4)$$

$$\partial_\mu H^\mu = -\Gamma_H \frac{H}{k_H} + \Gamma_Y \left( \frac{T}{k_T} - \frac{Q}{k_Q} - \frac{H}{k_H} \right) + S_{\tilde{H}}^{C/P}. \quad (5)$$

Our strategy will involve writing the above equation in what we call ‘‘cascading form’’ where the first equation is a function of just two number densities, the second a function of three and the third also a function of three number densities as well as the  $CP$ -violating source. In our example it is easy to write this set of equations in such a form, the only complication being the existence of two space-time-dependent source terms. To overcome this, notice that both sources have the same space-time dependence up to a overall constant of proportionality

$$S_i^{C/P} = \frac{1}{2a} S_{\tilde{H}}^{C/P}. \quad (6)$$

It is therefore straightforward to take a set of linear combinations that are in cascading form by taking the combinations (3) + (4),  $(1+a) \times (3) + (1-a) \times (4) + (5)$  and  $2 \times (3) + (4) + (5)$ . If we use the standard diffusion approximation

$$\partial_\mu J^\mu = v_W \dot{n} - D_n \nabla^2 n \quad (7)$$

and make an assumption about the geometry of the bubble wall, we can reduce the problem to a one-dimensional one. Shifting to the bubble wall rest frame using the variable  $z \equiv |v_W t - x|$ , we can write the set of coupled transport equations as a set of differential equations in  $z$ . A strategy for a solution becomes immediately apparent when the equations are written in cascade form. The first equation is a differential operator acting on  $T$  and  $Q$  which can be solved for  $T$  (or equivalently  $Q$ ) by treating  $Q$  and its derivatives as a inhomogeneous source. Thus we can write the second equation in terms of  $H$  and  $Q$  which can also be solved in a similar way so that  $H$  is a function of  $Q$ . The third and final equation is then an equation for  $Q$  and the  $CP$ -violating source which can be solved via the usual methods.

### A. Deriving the analytic solution

Let us rewrite our linear combinations of transport equations in terms of implicitly defined coefficients  $a_{Xj}^i$  where  $X \in \{Q, T, H\}$  is the field index,  $j \in \{1, 2, 3\}$  is the equation number and  $i \in \{0, 1, 2\}$  is the power of the derivative in  $z$ ,

$$a_{Q1}^i \partial^i Q + a_{T1}^i \partial^i T = 0 \quad (8)$$

$$a_{Q2}^i \partial^i Q + a_{T2}^i \partial^i T + a_{H2}^i \partial^i H = 0 \quad (9)$$

$$a_{Q3}^i \partial^i Q + a_{T3}^i \partial^i T + a_{H3}^i \partial^i H = \Delta(z). \quad (10)$$

In the above equation and throughout this paper we of course use Einstein's summation convention for repeated indices. The first equation can be used to solve for  $T$  in terms of  $Q$  if one uses the method of variable coefficients and treats the part of the equation involving  $Q$  and its derivatives as an inhomogeneous source for  $T$ . The result of this is

$$T = \frac{1}{a_{T1}^2} \sum_{\pm} \frac{1}{\kappa_{\mp} - \kappa_{\pm}} e^{\kappa_{\pm} z} \left[ \int^z e^{-\kappa_{\pm} y} \left( a_{Q1}^i \frac{\partial^i Q}{\partial y^i} \right) dy - \beta_i \right] \quad (11)$$

where the integration constants have to be zero as explained in Appendix B. We neglect them for the rest of the derivation as they clutter notation and detract from the main derivation. The above equation has the problem that if we used it to eliminate  $T$  in subsequent equations we would be left with a set of equations that are a mixture of an integral and differential equations. We wish to have a pure differential equation at the end. To achieve this we use a series of variable changes. The derivation is somewhat nontrivial so we give extra detail in Appendix A. Here we sketch out the main points of the calculation. We begin with the following change of variables:

$$h_{\pm} = \int^z e^{-\kappa_{\pm} y} Q dy \quad (12)$$

from which we can eliminate the integral and the exponent in Eq. (11) at the cost of having  $T$  now defined in terms of two functions. These functions are related via the identity

$$h'_+ = e^{(\kappa_- - \kappa_+)z} h'_-. \quad (13)$$

To remove the exponential outside of the former integral we use an additional change of variables

$$j_{\pm} = e^{\kappa_{\pm} z} h_{\pm}. \quad (14)$$

We are not quite done; we would like to now write everything in terms of a single variable. This can be achieved by either of the following variables:

$$k = e^{\kappa_{\mp} z} \int^z e^{-\kappa_{\mp} y} j_{\pm} dy, \quad (15)$$

from which we can relate both  $j_{\pm}$  to  $k$  through the equation

$$j_{\pm} = k' - \kappa_{\mp} k. \quad (16)$$

We now have a single variable  $k$  and it is straightforward to derive expressions relating  $T$  and  $Q$  to derivatives in  $k$ . For the sake of convenience let us rescale  $k$  to remove the denominator and write

$$T = -a_{Q1}^i \partial^i k \quad (17)$$

$$Q = a_{T1}^i \partial^i k. \quad (18)$$

It is a trivial check to verify that these solutions indeed solve the first transport equation. Substituting these equations into Eq. (8) we have a differential equation that is now a function of  $k$  and  $H$  only, which means we can use the same tricks,

$$0 = a_{Q2}^i \partial^i Q + a_{T2}^i \partial^i T + a_{H2}^i \partial^i H \quad (19)$$

$$= (a_{Q2}^i a_{T1}^j - a_{T2}^j a_{Q1}^i) \partial^{i+j} k + a_{H2}^i \partial^i H. \quad (20)$$

The solution for  $H$  is of course

$$H = \frac{1}{a_{H2}^2} \sum_{\pm} \frac{e^{\kappa_{\pm} z}}{\kappa_{\mp} - \kappa_{\pm}} \int^z e^{-\kappa_{\pm} y} \left( a_{Q2}^i a_{T1}^j - a_{T2}^j a_{Q1}^i \frac{\partial^{i+j} k}{\partial y^i} \right) dy. \quad (21)$$

We can make the exact same changes of variables as before to solve this in terms of  $l$  (which is analogous to  $k$  in the solution to the first equation),

$$H = - \sum_{n=0}^4 \delta_{i+j-n} (a_{Q2}^i a_{T1}^j - a_{T2}^j a_{Q1}^i) \partial^n l \quad (22)$$

$$k = a_{H2}^i \partial^i l \quad (23)$$

where the Kronecker delta was added to make the structure of the solution more transparent and we include the sum over  $n$  to make its limits obvious. Subbing our solution for  $k$  into the equations for  $Q$  and  $T$  gives

$$\begin{aligned} H &= - \sum_{n=0}^4 \delta_{i+j-n} (a_{Q2}^i a_{T1}^j - a_{T2}^j a_{Q1}^i) \partial^n l \\ T &= - \sum_{n=0}^4 \delta_{i+j-n} a_{Q1}^i a_{H2}^j \partial^n l \\ Q &= \sum_{n=0}^4 \delta_{i+j-n} a_{T1}^i a_{H2}^j \partial^n l. \end{aligned} \quad (24)$$

Equation (10) is now defined completely in terms of  $l$  and the source,

$$\begin{aligned}
\Delta(z) &= \sum_{n=0}^6 \delta_{i+j+k-n} (a_{T1}^i a_{H2}^j a_{Q3}^k - a_{Q1}^i a_{H2}^j a_{T3}^k \\
&\quad - a_{T1}^i a_{Q2}^j a_{H3}^k + a_{Q1}^i a_{T2}^j a_{H3}^k) \partial^n l \\
&= \sum_{n=0}^6 \delta_{i+j+k-n} \epsilon^{abc} a_{Ta}^i a_{Hb}^j a_{Qc}^k \partial^n l \\
&\equiv \sum_{n=0}^6 a_1^n \partial^n l. \tag{25}
\end{aligned}$$

The use of the permutation symbol arises from the fact that  $a_{H1}^i = 0$ . The above is a straightforward inhomogeneous differential equation which can be solved using the standard method of variable constants. The solution is

$$l = \sum_{i=1}^6 x_i e^{\alpha_i z} \left( \int^z e^{-\alpha_i y} \Delta(y) dy - \beta_i \right) \tag{26}$$

in the broken phase and

$$l = \sum_{i=1}^6 y_i e^{\gamma_i z} \tag{27}$$

in the symmetric phase. Here the exponents  $\alpha_i$  and  $\gamma_i$  are the roots of the equations

$$\begin{aligned}
\sum_{n=0}^6 a_1^n \alpha^n &= 0 \\
\sum_{n=0}^6 a_1^n \gamma^n &= 0, \tag{28}
\end{aligned}$$

for the broken and symmetric phase respectively; the values  $x_i$  can be derived from the equation

$$\vec{x} = M^{-1} \vec{d}. \tag{29}$$

The matrix  $M$  is given by  $M_{ij} \equiv \alpha_i^{j-1}$  where  $j$  doubles as an exponent and an index which both go from 1 to 6 and  $\vec{d} \equiv [0, \dots, 1/a_1^6]^T$ . Finally the integration constants  $\beta_i$  and  $y_i$  are determined by the boundary conditions as follows. Since we began with a set of three second-order differential equations for three densities we require that each of these number densities be continuous at the bubble wall along with their derivative. We also require the number densities to vanish at  $\pm\infty$ . All exponents therefore have to be positive definite in the symmetric phase. Therefore

$$y_i = 0 \quad \forall \gamma_i \leq 0. \tag{30}$$

To ensure number densities go to zero in the broken phase we have a condition on all positive definite exponents

$$x_i \beta_i = x_i \int_0^\infty dy e^{-\alpha_i y} \Delta(y) \equiv I_i \quad \forall \alpha_i \geq 0. \tag{31}$$

Finally our continuity conditions need to be met. The continuity conditions are not met by requiring  $l$  and its derivatives to be continuous at the phase boundary even though this will give the right number of conditions. Instead we require that  $H, T, Q, H', T'$  and  $Q'$  are continuous at  $z = 0$ . As an example consider the case when the last three  $\gamma_i$  exponents are greater than 0 as well as the first three  $\alpha_i$  exponents. The continuity conditions can be met when the following equation is satisfied:

$$\begin{aligned}
& \left( x_4 \beta_4 \quad x_5 \beta_5 \quad x_6 \beta_6 \quad x_1 \beta_1 \quad x_2 \beta_2 \quad x_3 \beta_3 \quad y_1 \quad y_2 \quad y_3 \right)^T \\
& = \begin{pmatrix} 1 & 0 & 0 & 0 & 0 & 0 & 0 & 0 & 0 \\ 0 & 1 & 0 & 0 & 0 & 0 & 0 & 0 & 0 \\ 0 & 0 & 1 & 0 & 0 & 0 & 0 & 0 & 0 \\ A_Q(\alpha_4) & A_Q(\alpha_5) & A_Q(\alpha_6) & A_Q(\alpha_1) & A_Q(\alpha_2) & A_Q(\alpha_3) & A_Q(\gamma_1) & A_Q(\gamma_2) & A_Q(\gamma_3) \\ \alpha_4 A_Q(\alpha_4) & \alpha_5 A_Q(\alpha_5) & \alpha_6 A_Q(\alpha_6) & \alpha_1 A_Q(\alpha_1) & \alpha_2 A_Q(\alpha_2) & \alpha_3 A_Q(\alpha_3) & \gamma_1 A_Q(\gamma_1) & \gamma_2 A_Q(\gamma_2) & \gamma_3 A_Q(\gamma_3) \\ A_T(\alpha_4) & A_T(\alpha_5) & A_T(\alpha_6) & A_T(\alpha_1) & A_T(\alpha_2) & A_T(\alpha_3) & A_T(\gamma_1) & A_T(\gamma_2) & A_T(\gamma_3) \\ \alpha_4 A_T(\alpha_4) & \alpha_5 A_T(\alpha_5) & \alpha_6 A_T(\alpha_6) & \alpha_1 A_T(\alpha_1) & \alpha_2 A_T(\alpha_2) & \alpha_3 A_T(\alpha_3) & \gamma_1 A_T(\gamma_1) & \gamma_2 A_T(\gamma_2) & \gamma_3 A_T(\gamma_3) \\ A_H(\alpha_4) & A_H(\alpha_5) & A_H(\alpha_6) & A_H(\alpha_1) & A_H(\alpha_2) & A_H(\alpha_3) & A_H(\gamma_1) & A_H(\gamma_2) & A_H(\gamma_3) \\ \alpha_4 A_H(\alpha_4) & \alpha_5 A_H(\alpha_5) & \alpha_6 A_H(\alpha_6) & \alpha_1 A_H(\alpha_1) & \alpha_2 A_H(\alpha_2) & \alpha_3 A_H(\alpha_3) & \gamma_1 A_H(\gamma_1) & \gamma_2 A_H(\gamma_2) & \gamma_3 A_H(\gamma_3) \end{pmatrix}^{-1} \begin{pmatrix} I_1 \\ I_2 \\ I_3 \\ 0 \\ 0 \\ 0 \\ 0 \\ 0 \\ 0 \end{pmatrix} \\
& \equiv \begin{pmatrix} \mathbf{1}_{3 \times 3} & 0 \\ \vec{A}_X(\alpha) & \vec{A}_X(\gamma) \\ (\vec{\alpha A})_X(\alpha) & (\vec{\alpha A})_X(\gamma) \end{pmatrix}^{-1} \begin{pmatrix} I_1 \\ I_2 \\ I_3 \\ 0 \end{pmatrix}. \tag{32}
\end{aligned}$$

It is now straightforward to derive the solutions to  $T$ ,  $H$  and  $Q$

$$\begin{aligned} H &= \sum_{i=1}^6 A_H(\alpha_i) x_i e^{\alpha_i z} \left( \int^z e^{-\alpha_i y} \Delta(y) dy - \beta_i \right) \\ T &= \sum_{i=1}^6 A_T(\alpha_i) x_i e^{\alpha_i z} \left( \int^z e^{-\alpha_i y} \Delta(y) dy - \beta_i \right) \\ Q &= \sum_{i=1}^6 A_Q(\alpha_i) x_i e^{\alpha_i z} \left( \int^z e^{-\alpha_i y} \Delta(y) dy - \beta_i \right) \end{aligned} \quad (33)$$

with known functions

$$\begin{aligned} A_H &= - \sum_{n=0}^4 \delta_{i+j-n} (a_{Q2}^i a_{T1}^j - a_{T2}^i a_{Q1}^j) \alpha^n \\ A_T &= - \sum_{n=0}^4 \delta_{i+j-n} a_{Q1}^i a_{H2}^j \alpha^n \\ A_Q &= \sum_{n=0}^4 \delta_{i+j-n} a_{T1}^i a_{H2}^j \alpha^n. \end{aligned} \quad (34)$$

### III. FAST REDERIVATION WITH A PARAMATERIZED ANSATZ

The above derivation was cumbersome even for the simple example we used and yet the solution was relatively simple. Now that we know the form of the solution, it is far more efficient to start with this form of the solution as a parametrized ansatz and use the differential equations to work out the parameters of the ansatz. This is achieved by the following simple steps. Let the ansatz for number density  $X$  that solves the homogeneous version of our differential equations be  $X = A_x(\alpha) e^{\alpha z}$ . To find these functions,  $A_x$ , as well as  $\alpha$  do the following:

- (i) To determine the functions  $A_x(\alpha)$  substitute our solutions into the first two equations to get relations between these functions. Doing so gives

$$\begin{aligned} A_T &= \frac{-a_{Q1}^i \alpha^i}{a_{T1}^j \alpha^j} A_Q \\ A_H &= \frac{-(a_{Q2}^i \alpha^i A_Q + a_{T2}^i \alpha^i A_T)}{a_{H2}^j \alpha^j}. \end{aligned} \quad (35)$$

This differs from our earlier expression. However this just amounts to a rescaling of  $x_i$  in our final expression. It is a trivial exercise to reverse this rescaling and verify that the expressions  $A_x$  are the same as before.

- (ii) Substitute our functions  $A_x(\alpha) e^{\alpha z}$  into the third equation with the  $CP$ -violating source switched off. The result is a rational polynomial which can

be turned into a polynomial by multiplying through with the denominators

$$\begin{aligned} 0 &= a_{Q3}^i \partial^i Q + A_T(\alpha) a_{T3}^j \partial^j T + A_H(\alpha) a_{H3}^k \partial^k H \\ &\mapsto \sum_{n=0}^6 \delta_{i+j+k-n} (a_{T1}^i a_{H2}^j a_{Q3}^k - a_{Q1}^i a_{H2}^j a_{T3}^k \\ &\quad - a_{T1}^i a_{Q2}^j a_{H3}^k + a_{Q1}^i a_{T2}^j a_{H3}^k) \partial^n e^{\alpha z} \\ &\equiv \sum_{n=0}^6 a_i^n \partial^n e^{\alpha z} \\ 0 &= a_i^n \alpha^n. \end{aligned} \quad (36)$$

Solving this gives the set of homogeneous solutions. Repeating the above steps in the symmetric phase with ansatz  $X = A_x(\gamma) e^{\gamma z}$  gives the solutions in that phase.

- (iii) Finally, solve the inhomogeneous equation

$$\begin{aligned} 0 &= \sum_{n=0}^6 \delta_{i+j+k-n} (a_{T1}^i a_{H2}^j a_{Q3}^k - a_{Q1}^i a_{H2}^j a_{T3}^k \\ &\quad - a_{T1}^i a_{Q2}^j a_{H3}^k + a_{Q1}^i a_{T2}^j a_{H3}^k) \partial^n l(z). \end{aligned} \quad (37)$$

The inhomogeneous solution is then trivially found to be

$$X = \sum_{i=1}^6 A_X(\alpha_i) x_i e^{\alpha_i z} \left( \int^z e^{-\alpha_i y} \Delta(y) dy - \beta_i \right) \quad (38)$$

in the broken phase and

$$X = \sum_{i=1}^6 A_X(\gamma_i) y_i e^{\gamma_i z} \quad (39)$$

in the symmetric phase as before. The values for  $x_i$  can be found by substituting Eq. (38) into the inhomogeneous equation and insisting that the coefficients of any derivatives of  $\Delta(z)$  are zero and the coefficient of  $\Delta(z)$  on the left-hand side is 1. This gives the familiar expression

$$\vec{x} = M^{-1} \vec{d} \quad (40)$$

with  $M_{ij} = \alpha_i^{j-1}$  and  $\vec{d}^T = [0, \dots, 0, 1/a_i^6]$  as before. The integration constants  $y_i$  and  $\beta_i$  can be found as above by insisting that  $Q$ ,  $T$  and  $H$  are well behaved at  $\pm\infty$  and all three functions as well as their derivatives are continuous at the bubble wall. The solutions for  $\beta_i$  and  $y_i$  are the same as in the previous section so we do not repeat it here. Remarkably, the above method of solving the set of differential equations analytically is at least as fast as using an approximation that assumes the strong sphaleron and Yukawa rates are fast in order to reduce our set of transport

equations to a single differential equation which one then solves.

#### IV. GENERALIZATIONS

In this section we discuss how far generalizations of the above procedure can go. The generalization of our procedure is trivial to any case where one has only one  $CP$ -violating source and one can manipulate the transport equations into the cascading form

$$\begin{aligned} D_1[X_1, X_2] &= 0 \\ D_2[X_1, X_2, X_3] &= 0 \\ &\vdots \\ D_{N-1}[X_1, X_2, X_3 \cdots X_N] &= 0 \\ D_N[X_1, X_2, X_3 \cdots X_N] &= \Delta(z). \end{aligned} \quad (41)$$

$$\begin{aligned} D_{N-1}[X_1, X_2, X_3 \cdots X_N] &= 0 \\ D_N[X_1, X_2, X_3 \cdots X_N] &= \Delta(z). \end{aligned} \quad (42)$$

One can just use the parametrized ansatz approach defined in the previous section to very quickly derive the solution. Much more daunting are the cases where one either has multiple  $CP$ -violating sources or one cannot manipulate the transport equations into the above form. Fortunately in this section we will show that in principle an analytical solution can always be found even in the presence of such complications and the parametrized ansatz approach generally reduces the difficulty of problems greatly.

##### A. Multiple $CP$ -violating sources

In the MSSM there are several  $CP$ -violating sources. Handling the extra  $CP$ -violating sources, however, was done by simply noting that they are all proportional to  $v(x)^2 \dot{\beta}(x)$ . This situation becomes far more nontrivial in the case where there are numerous  $CP$ -violating source terms proportional to different functions of  $z$ . For example the NMSSM has source terms that are a function of the singlet's VEV profile,  $v_S(z)$ , as well as the Higgs profiles  $v_u(z)$  and  $v_d(z)$ . Consider the set of transport equations from the previous section with an extra  $CP$ -violating term,

$$a_{Q1}^i \partial^i Q + a_{T1}^i \partial^i T = 0 \quad (43)$$

$$a_{Q2}^i \partial^i Q + a_{T2}^i \partial^i T + a_{H2}^i \partial^i H = \Delta_1(z) \quad (44)$$

$$a_{Q3}^i \partial^i Q + a_{T3}^i \partial^i T + a_{H3}^i \partial^i H = \Delta_2(z). \quad (45)$$

If we solve the first transport equation as before the second equation becomes

$$\begin{aligned} \Delta_1(z) &= (a_{Q2}^i a_{T1}^j - a_{Q1}^i a_{T2}^j) \partial^{i+j} l + a_{H2}^i \partial^i H \\ &= a_{H2}^i \partial^i l + a_{H2}^i \partial^i H. \end{aligned} \quad (46)$$

The solution to this equation is of course

$$\begin{aligned} H &= -a_{H2}^i \partial^i m + \frac{1}{a_{H2}^2} \sum_{\pm} \frac{1}{\kappa_{\mp} - \kappa_{\pm}} e^{\kappa_{\pm} z} \\ &\times \left( \int^z e^{-\kappa_{\pm} y} \Delta_1(y) dy - \beta_{\pm}^1 \right), \end{aligned} \quad (47)$$

with  $\beta_{\pm} = 0$  for reasons given in Appendix B. This solution feeds into the third equation which obtains a more complicated inhomogeneity as a result,

$$a_{m3}^i \partial^i m + f(\Delta_1) = \Delta_2, \quad (48)$$

with

$$\begin{aligned} f(\Delta_1) &= \sum_{\pm} \frac{(a_H^2)^{-1}}{\kappa_{\mp} - \kappa_{\pm}} \left[ a_{H3}^i \kappa_{\pm}^i e^{\kappa_{\pm} z} \left( \int^z e^{-\kappa_{\pm} y} \Delta_1(y) dy - \beta_{\pm}^1 \right) \right. \\ &\left. + a_{H3}^{i+1} \kappa_{\pm}^i \Delta_1(z) + a_{H3}^2 \Delta_1'(z) \right]. \end{aligned} \quad (49)$$

The solution now has a very similar structure to before,

$$m = \sum_i x_i e^{\alpha_i z} \left( \int^z e^{-\alpha_i y} [\Delta_2(y) - f(\Delta_1)] dy - \beta_i \right) \quad (50)$$

with  $x_i$ ,  $\alpha_i$ ,  $A_X(\alpha_i)$  and  $\beta_i$  determined as before. Thus in principle one can use the parametrized ansatz approach to simplify the problem here as well so long as one is careful in deriving what to replace  $\Delta(z)$  with.

##### B. Other equation structures

The equation structures that we encountered in the MSSM were not the only possible structures that could arise. In this brief subsection we would like to briefly consider other possible equation structures. Consider an equation where the linear terms are missing,

$$a_{1j}^1 \frac{\partial X_1}{\partial z} + a_{1j}^1 \frac{\partial^2 X_1}{\partial z^2} + a_{2j}^1 \frac{\partial X_2}{\partial z} + a_{2j}^1 \frac{\partial^2 X_2}{\partial z^2} = 0. \quad (51)$$

The procedure is subtly different from before. The first step is the same as before where we solve for  $X_1$  by treating the derivatives of  $X_2$  as inhomogeneous source,

$$X_1 = -\frac{e^{\frac{a_{1j}^1 z}{a_{1j}^1}}}{a_{1j}^2} \int^z e^{\frac{a_{1j}^1 y}{a_{1j}^1}} \left( a_{2j}^1 \frac{\partial X_2}{\partial z} + a_{2j}^1 \frac{\partial^2 X_2}{\partial z^2} \right). \quad (52)$$

Just as before we aim to remove the exponentials and the integral using a series of changes of variables. This time, though, our variables changes are

$$h(z) = \int^z e^{\frac{a_{1j}^1 y}{a_{1j}^2}} \frac{dX_2}{dy} dy \quad (53)$$

$$j(z) = \int^z e^{-\frac{a_{1j}^1 y}{a_{1j}^2}} h(y) \quad (54)$$

which leaves us with a very similar form for the solution (after a suitable rescaling),

$$X_1 = a_{2j}^1 j' + a_{2j}^1 j'' \quad (55)$$

$$X_2 = -a_{1j}^1 j' - a_{1j}^1 j'' \quad (56)$$

Another important extension is to consider the case where we cannot reduce the first equation to a differential equation involving only two number densities. In the simplest case our first equation is a differential operator acting on three number densities,

$$a_{1j}^i \partial^i X_1 + a_{2j}^i \partial^i X_2 + a_{3j}^i \partial^i X_3 = 0 \quad (57)$$

in which case we can reduce this to an equation involving only two number density by defining auxillary functions  $f(z)$  and  $g(z)$  as follows:

$$X_1(z) = g_{12} X_2(z) + g_{13}(z) X_3 + f(z) \quad (58)$$

$$X_2(z) = g_{23} X_3(z) + g(z) \quad (59)$$

if  $a_{kj}^0 \neq 0$  and

$$X_1(z) = g_{13}(z) X_3 + f(z) \quad (60)$$

$$X_2(z) = g_{23} X_3(z) + g(z) \quad (61)$$

otherwise. One can then choose  $g_{ij}$  such that they cancel the terms  $a_{3j}^i \partial^i X_3$  in the above transport equation. We therefore have two techniques to convert a set of transport equations to cascading form—taking linear combinations of equations and using the method as described immediately above.

### C. Arbitrary number of equations

Consider the case where we have  $N$  transport equations and a single  $CP$ -violating source. In general there are  $\frac{3}{2}(N-1)(N-2)$  conditions to satisfy to reorganize the equations into a cascading form. The most general extension of the use of auxiliary functions is to define the following:

$$X_1 = \sum_{j=2}^N g_{1j} X_j + f_1$$

$$\vdots = \vdots$$

$$X_i = \sum_{j=i+1}^N g_{ij} X_j + f_i$$

$$\vdots = \vdots$$

$$X_{N-1} = g_{N-1,N} X_N + f_{N-1}. \quad (62)$$

This gives us a total of  $\frac{1}{2}N(N-1)$  parameters to use. We can also take linear combinations of the  $N-1$  transport equations that do not contain the  $CP$ -violating source to meet another  $\frac{1}{2}N(N-1)$  condition. Unfortunately this brings us short of the required  $\frac{3}{2}(N-1)(N-2)$  conditions. In reality this analysis is probably unrealistically pessimistic for two reasons. First, while the initial set of transport equations indeed can have all  $N$  fields appearing in the relaxation terms of all equations, there are only two derivative terms initially in each transport equation. Thus it may be possible to make careful manipulations that evade the arguments given above. Second, the equations tend to have a lot more structure than our naive analysis lets on. For example a number of equations might have the same relaxation term on the right-hand side so the combination of two transport equations with this term might remove many coefficients,  $a_{ij}^0$ , for the price of one. Nevertheless it is useful to consider an unrealistically pessimistic scenario where all conditions need to be met. The lowest number of densities that are not guaranteed a path that converts our QTEs into a cascading form in this overly pessimistic scenario is 5. We then have the transport equations

$$a_{ji}^k \partial^k X_j = 0 \quad \forall i \leq 4 \quad (63)$$

$$a_{j5}^k \partial^k X_j = \Delta \quad (64)$$

with  $a_{ij}^k \neq 0 \forall i, j$  and  $k$ . We will now sketch out how a solution can be derived. Let us define

$$X_3(z) = g_{34} X_4(z) + g_{35}(z) X_5 + f_1^3(z) \quad (65)$$

$$X_4(z) = g_{45} X_5(z) + f_1^4(z) \quad (66)$$

in such a way as to remove  $X_5$  from the first equation. Throughout this argument the subscript on  $f$  will denote the number of times a variable has been changed and the superscript will denote the original field that was replaced. Repeating this process to remove  $f_1^4$  and then the resulting  $f_2^3$  allows us to write the first equation in terms of two linear combinations of number densities which can be denoted  $f_3^1$  and  $f_3^2$ . We can then solve this equation to write both in

terms of the variable  $k$  following the same steps as outlined in previous sections. The second through fifth equations now involve four variables only. One can again use the same trick to eliminate one number density from the second equation leaving us with something in the form (and we are only interested in a general form as we will use a parametrized ansatz approach shortly)

$$a_{21}^i \partial^i k + a_{2f(34)}^i \partial^i f_4^3 + a_{2f(44)}^i \partial^i f_4^4 = 0. \quad (67)$$

One can then define the following changes in variables:

$$f_4^3 = g_{34l}^0 k + g_{34l}^1 k l + g_{34l}^2 k l'' + f_5^3 \quad (68)$$

$$f_4^4 = g_{44l}^0 k + g_{44l}^1 k l + g_{44l}^2 k l'' + f_5^4 \quad (69)$$

to cancel the second equation's dependence on  $l$  (actually this gives us a couple too many parameters so we can set these to 1). This equation then can also be solved with the usual techniques to write  $f_5^3$  and  $f_5^4$  in terms of a new variable  $l$ . The remaining three equations are a function of  $k$ ,  $l$  and  $f_5^3$  only. We can use a similar trick to remove the dependency on  $l$  in the third equation with the variables

$$f_5^3 = g_{53l}^0 l + g_{53l}^1 l' + g_{53k}^0 l'' + f_5^4 \quad (70)$$

$$k = g_{kl} l + f_k^1. \quad (71)$$

The remaining equations are now in cascading form and can be solved using the methods described above. The derivation of the solution to this overly pessimistic case sketched above is very cumbersome. However, even in this case the solution is identical to what one would get if one used a parametrized ansatz from the start. Using the parametrized ansatz method we can write down the solutions immediately without setting pen to paper,

$$X_j = \sum_{i=0}^{10} x_i A_j(\alpha_i) e^{\alpha_i z} \left( \int^z e^{-\alpha_i y} \Delta(y) - \beta_i \right) \quad (72)$$

with  $\alpha_i$  being the 10 roots to the equation

$$\sum_{j=1}^5 A_j(\alpha) a_{j5}^k \alpha_i^k \quad (73)$$

with  $A_1(\alpha) = 1$  and

$$\begin{aligned} A_2 &= \frac{-1}{a_{21}^i \alpha^i} \sum_{j \neq 2} A_j(\alpha) a_{j1}^i \alpha^i \\ A_3 &= \frac{-1}{a_{32}^i \alpha^i} \sum_{j \neq 3} A_j(\alpha) a_{j2}^i \alpha^i \\ A_4 &= \frac{-1}{a_{43}^i \alpha^i} \sum_{j \neq 4} A_j(\alpha) a_{j3}^i \alpha^i \\ A_5 &= \frac{-1}{a_{54}^i \alpha^i} \sum_{j \neq 5} A_j(\alpha) a_{j4}^i \alpha^i, \end{aligned} \quad (74)$$

which can be rewritten as a matrix equation

$$\begin{pmatrix} A_2 \\ A_3 \\ A_4 \\ A_5 \end{pmatrix} = - \begin{pmatrix} a_{21}^i \alpha^i & a_{31}^i \alpha^i & a_{41}^i \alpha^i & a_{51}^i \alpha^i \\ a_{22}^i \alpha^i & a_{32}^i \alpha^i & a_{42}^i \alpha^i & a_{52}^i \alpha^i \\ a_{23}^i \alpha^i & a_{33}^i \alpha^i & a_{43}^i \alpha^i & a_{53}^i \alpha^i \\ a_{24}^i \alpha^i & a_{34}^i \alpha^i & a_{44}^i \alpha^i & a_{54}^i \alpha^i \end{pmatrix}^{-1} \begin{pmatrix} a_{11}^i \alpha^i \\ a_{12}^i \alpha^i \\ a_{13}^i \alpha^i \\ a_{14}^i \alpha^i \end{pmatrix}. \quad (75)$$

Inverting these equations and rescaling by multiplying through by the denominators gives the very simple structure

$$\begin{aligned} A_1(\alpha_i) &= \sum_{n=0}^8 e^{bcde} a_{2b}^i a_{3c}^j a_{4d}^k a_{5e}^l \delta_{i+j+k+l-n} \alpha_i^n \\ A_2(\alpha_i) &= - \sum_{n=0}^8 e^{bcde} a_{1b}^i a_{3c}^j a_{4d}^k a_{5e}^l \delta_{i+j+k+l-n} \alpha_i^n \\ A_3(\alpha_i) &= \sum_{n=0}^8 e^{bcde} a_{1b}^i a_{2c}^j a_{4d}^k a_{5e}^l \delta_{i+j+k+l-n} \alpha_i^n \\ A_4(\alpha_i) &= - \sum_{n=0}^8 e^{bcde} a_{1b}^i a_{2c}^j a_{3d}^k a_{5e}^l \delta_{i+j+k+l-n} \alpha_i^n \\ A_5(\alpha_i) &= \sum_{n=0}^8 e^{bcde} a_{1b}^i a_{2c}^j a_{3d}^k a_{4e}^l \delta_{i+j+k+l-n} \alpha_i^n. \end{aligned} \quad (76)$$

The analogous functions in the MSSM also have this form, although using a permutation symbol in that case is probably overkill since there would only be two terms contracted with it and one of those terms is zero two out of three times. Nevertheless this seems to be the standard form. The coefficients  $x_i$  are determined as before by the equation

$$\vec{x} = [\alpha_i^{j-1}]^{-1} \vec{d} \quad (77)$$

with  $\vec{d} = [0, \dots, 0, 1/(a_{5m}^{10})]^T$  with  $a_{5m}^{10}$  being the coefficient of  $\alpha^{10}$  in the fifth equation once  $A_j(\alpha_i)$  has been substituted in. The boundary conditions are determined by insisting each field is well behaved at  $\pm\infty$  and  $X_j$  as well as  $X'_j$  are

all continuous at the bubble wall, which means inverting the equations

$$\begin{aligned}
y_i &= \forall \gamma_i \leq 0 \\
\beta_i &= \int_0^\infty dy e^{-\alpha_i y} \Delta(y) \quad \forall \alpha_i \geq 0 \\
0 &= \sum_{i,j} A_j(\alpha_i) \beta_i + \sum_n y_n \\
0 &= \sum_{i,j} \alpha_i A_j(\alpha_i) \beta_i + \sum_n \gamma_n y_n. \quad (78)
\end{aligned}$$

That such a cumbersome problem was reduced to an elementary one shows the power of the parametrized ansatz method. If we had multiple  $CP$ -violating source terms we would then simply replace  $\Delta(z)$  for  $f[\Delta_1(z), \Delta_2(z) \dots]$  and solve as before.

## V. BEYOND AN ULTRATHIN WALL APPROXIMATION

Consider the earlier example given in Sec. II. There are VEV-dependent relaxation and source terms in the third transport equation that are assumed to switch off in the unbroken phase. For a thick-walled VEV profile this approximation might become a poor one. We would like to derive an analytical method to go beyond step-function VEVs. The second transport equation (9) has VEV-dependent relaxation terms proportional to  $a$ . For now let us simplify the situation by assuming that  $a$  is very small so we only need to seek corrections to the thin-wall approximation in Eq. (10). We will return to the more general case later. To do so we define a series of error functions,

$$\begin{aligned}
\Delta(z) &= \Theta(z)\Delta(z) + (1 - \Theta(z))\Delta(z) \equiv \Delta_0(z) + \epsilon(z) \\
a_{I_3}^0(z) &\equiv a_{I_3}^0(z)\Theta(z) + a_{I_3}^0(z)\Theta(-z) \\
&= a_{I_3}^0(z_{\max}) - [a_{I_3}^0(z_{\max}) - a_{I_3}^0(z)] + a_{I_3}^0(z)\Theta(-z) \\
&= a_{I_3}^0 + \delta a_{I_3}^0(z) \\
l(z) &= l_0(z) + \delta_1 l(z) + \delta_2 l(z) + \dots \quad (79)
\end{aligned}$$

Here  $l_0(z)$  solves the original transport equations in the ultrathin wall regime and  $\delta_i l$  is a correction of order  $i$ . We will take advantage of the fact that these error functions are finite for all  $z$ . This allows the possibility of a perturbative expansion. Our third transport equation can be written in terms of the error functions,

$$\begin{aligned}
a_{I_3}^i \partial^i l_0 + a_{I_3}^i \partial^i (\delta_1 l + \delta_2 l + \dots) \\
+ \delta a_{I_3}^0(z) (l_0 + \delta_1 l + \delta_2 l + \dots) = \Delta(z) + \epsilon(z). \quad (80)
\end{aligned}$$

The corrections to  $m$  can be found order by order,

$$\begin{aligned}
\delta_1 l &= \sum_{i=0}^6 e^{\alpha_i z} x_i \left( \int^z e^{-\alpha_i y} [\epsilon - l_0 \delta a_{I_3}^0(z)] - \delta_1 \beta_i \right) \\
\delta_2 l &= \sum_{i=0}^6 e^{\alpha_i z} x_i \left( \int^z e^{-\alpha_i y} [-\delta_1 l \delta a_{I_3}^0(z)] - \delta_2 \beta_i \right) \quad (81)
\end{aligned}$$

and so forth. Let us now turn our attention to the slightly more complicated case where we no longer assume  $a$  is small. The equation structure we will be left with is very similar to the case when there are multiple  $CP$ -violating source terms that are not proportional to each other that we considered in Sec. IV. Let us define a series of error functions as before. The corrections to the densities are

$$\begin{aligned}
H &= H_0 + \delta_1 H + \delta_2 H + \dots \\
T &= T_0 + \delta_1 T + \delta_2 T + \dots \\
Q &= Q_0 + \delta_1 Q + \delta_2 Q + \dots, \quad (82)
\end{aligned}$$

where  $H_0$ ,  $Q_0$  and  $T_0$  solve the QTEs in the ultrathin wall approximation. We can then look at terms that are first order only to set up a perturbative expansion. Using the fact that  $Q_0$ ,  $H_0$  and  $T_0$  solve the original set of QTEs we can write QTEs purely in terms of their error functions,

$$\begin{aligned}
a_{T_1}^i \partial^i \delta_1 T + a_{Q_1}^i \partial^i \delta_1 Q &= 0 \\
\delta a_{H_2}^0(z) H_0 + \delta a_{Q_2}^0(z) Q_0 + \delta a_{T_2}^0(z) T_0 \\
+ a_{H_2}^i \partial^i \delta_1 H + a_{Q_2}^i \partial^i \delta_1 Q + a_{T_2}^i \partial^i \delta_1 T &= 0 \\
\delta a_{H_3}^0(z) H_0 + \delta a_{Q_3}^0(z) Q_0 + \delta a_{T_3}^0(z) T_0 \\
+ a_{H_3}^i \partial^i \delta_1 H + a_{Q_3}^i \partial^i \delta_1 Q + a_{T_3}^i \partial^i \delta_1 T &= \epsilon(z). \quad (83)
\end{aligned}$$

This can be rewritten in the exact same form as the system we solved in Sec. IV with two  $CP$ -violating sources [i.e. Eqs. (45)],

$$\begin{aligned}
a_{T_1}^i \partial^i \delta_1 T + a_{Q_1}^i \partial^i \delta_1 Q &= 0 \\
a_{H_2}^i \partial^i \delta_1 H + a_{Q_2}^i \partial^i \delta_1 Q + a_{T_2}^i \partial^i \delta_1 T &= \Delta_1(z) \\
a_{H_3}^i \partial^i \delta_1 H + a_{Q_3}^i \partial^i \delta_1 Q + a_{T_3}^i \partial^i \delta_1 T &= \Delta_2(z). \quad (84)
\end{aligned}$$

## VI. A NUMERICAL COMPARISON

In this section we look at how large an error in the baryogenesis is caused by taking the fast rate approximation and the ultrathin wall approximation. We also look to reproduce a numerical result in the literature as a check of our method. Corrections of  $O(1/\Gamma_Y)$  were discussed in [18] which found that the corrections to the baryon asymmetry could be of  $O(1)$  in the case where  $\Gamma_Y$  and  $\Gamma_M^-$  were similar size in the broken phase. Since a numerical analysis on the effects of equilibrating top Yukawa and stop triscalar terms have already been studied in detail we mostly look at fast rate corrections as a check. We are more interested in

TABLE I. The base set of parameters used for our numerical study. The diffusion constants are taken from Ref. [27] and  $\Delta\beta$  is taken from Ref. [28].

$D_T$	$6/T$	$D_Q$	$6/100$	$D_H$	$110/T$
$a$	0.05	$\Gamma_M^-(x)$	$0.5v(x)^2/T^2$	$\Gamma_H(x)$	$2a\Gamma_M^-$
$\Gamma_Y$	1	$v_w$	0.05	$L_w$	$100/T$
$v = \sqrt{v_u^2 + v_d^2}$	100	$T$	100	$\Delta\beta$	0.015

determining whether corrections that go beyond the ultrathin wall approximation are large. In Table I we give the set of parameters we use for our numerical analysis. We also need to define an appropriate space-time-dependent VEV profile,

$$\begin{aligned} v(x) &= 0.5v \left( 1 - \tanh \left[ \frac{3x}{L_w} \right] \right) \\ \beta(x) &= 1 - 0.5\Delta\beta \left( 1 + \tanh \left[ \frac{3x}{L_w} \right] \right) \\ \Delta(x) &= 0.025\beta'(x)v(x)^2. \end{aligned} \quad (85)$$

We can then calculate numerical solutions to the densities  $Q$ ,  $T$  and  $H$  which allow us to calculate  $n_L = Q + Q_{1L} + Q_{2L} = 5Q + 4T$ . This density,  $n_L(z)$ , acts as a seed for the baryon density which satisfies the equation [20,21]

$$D_q \rho'' - v_w \rho'_B - \mathcal{R}(z) \rho_B = \Gamma_{ws}(z) \frac{n_F}{2} n_L(z) \quad (86)$$

with  $n_F$  the number of fermion families, where the relaxation term is given by

$$R(z) = \Gamma_{ws}(z) \left[ \frac{9}{4} \left( 1 + \frac{n_{sq}}{6} \right)^{-1} + \frac{3}{2} \right] \quad (87)$$

and  $n_{sq}$  is the number of squark flavors. Not much is lost treating the weak sphaleron rate profile as a step function—that is compared to treating the VEV profile as a step function when calculating source and relaxation terms—although in principle one could use the same techniques as in Sec. V to derive corrections to this equation as well. Our sphaleron rates then have the form [22–24]

$$\Gamma_{ws} = 120T\alpha_w^5 \Theta(-z) \quad (88)$$

and  $\Gamma_{ss} = (128/3)T\alpha_S^4$  [23] respectively. The baryon asymmetry is then

$$\rho_B = -\frac{n_F \Gamma_{ws}}{2v_w} \int_{-\infty}^0 n_L(x) e^{xR/v_w} dx. \quad (89)$$

As a point of comparison, we would like to compare our solutions with the analytic solution derived under the fast rate approximation in the ultrathin wall regime. The solution for  $n_L(z)$  and ultimately the baryon number is

TABLE II. Table of thick wall corrections to the baryon asymmetry.

$L_w$	$250/T$	$100/T$	$25/T$	$10/T$	$2.5/T$
$\delta\rho_B^E/\rho_B^E$	0.18	0.15	0.14	0.14	0.12

well known and can be found in Ref. [16], so we do not repeat it here. We find that our exact solution in the ultrathin wall approximation,  $\rho_B^E$ , differs from the approximate solution,  $\rho_B^A$  by a factor

$$\left| \frac{\rho_B^E - \rho_B^A}{\rho_B^E + \rho_B^A} \right| \approx 0.58 \quad (90)$$

which is consistent with the size of corrections found in [18]. The first-order corrections to the baryon asymmetry arising from deviations from the ultrathin wall regime are typically moderate to small.

In Fig. 1 we show the correction to the density  $n_L$  for several values for the bubble wall thickness. Even though the baryon asymmetry is weakly dependent on  $L_w$  in the ultrathin wall regime, for the very large values of  $L_w$  we consider this dependency becomes important. The typical correction for our set of parameters is typically small but nontrivial and grows monotonically with  $L_w$  as expected, which is shown in Table II. Indeed recent work has shown that bubble wall width for the electroweak phase transition in the NMSSM can have a large range of values [25]. As a check on our calculations we find that the correction indeed goes to zero as  $L_w \mapsto 0$  although the absolute minimum is numerically very difficult to take as it involves evaluating numerical integrals of very sharply peaked functions.

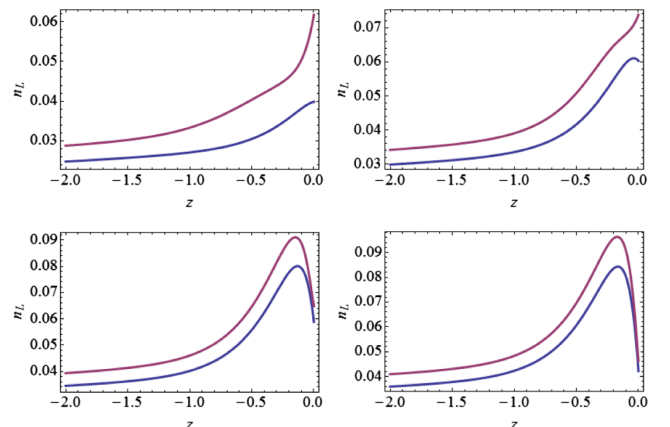


FIG. 1. The density  $n_L$  in the symmetric phase near the bubble wall as a function of  $z$ . The exact solution with first-order corrections to the ultrathin wall approximation is given by the magenta line and the solution without such corrections is given in blue. The parameters used to calculate  $n_L(z)$  are  $L_w = 250/T$  (top left),  $L_w = 100/T$  (top right),  $L_w = 25/T$  (bottom left) and  $L_w = 10/T$  (bottom right).

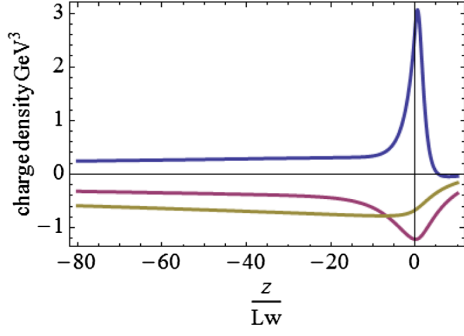


FIG. 2. Reproducing Winslow and Tulin's purely numerical calculation. Here the blue, magenta and golden lines correspond to the densities  $n_{Q_3}$ ,  $n_{u_3}$  and  $n_H$  respectively.

Finally for the sake of safety we would like a direct comparison to a numerical calculation. We use the parametrized ansatz approach to solve Eqs. (23) in Ref. [26] in order to produce their Fig. 3. This is shown in Fig. 2 where we are able to reproduce almost an almost identical plot (we remove the sum of densities to reduce clutter as little new information is given by this function). The small error can probably be attributed to our use of an ultrathin wall approximation.

## VII. CONCLUSION

In this work we have sketched out a method to derive exact solutions to quantum transport equations in a variety of cases including large sets of QTEs and situations where there are multiple  $CP$ -violating sources with nontrivially different space-time dependency. We have also produced a very quick and powerful method using a parametrized ansatz to derive the same solution. This method was found to turn cases which are cumbersome to the point of being almost intractable by standard methods to an elementary problem. Furthermore a general structure of the solution was made manifest when solving for large systems of equations. The third result of this paper was to sketch out a way of going beyond the ultrathin wall approximation. Our numerical analysis demonstrated that the correction to the baryon asymmetry coming from the smallest correction to the ultrathin wall regime can be small to moderate but nonetheless nontrivial even for moderately thick walls. It would interesting to see if other models have larger corrections from thick bubble walls. Our numerical results analyzing corrections to the fast rate approximation were consistent with those found in [18] which found that these corrections can be very large. Our method ensures that these corrections are taken into account while still keeping to a largely analytical framework.

## ACKNOWLEDGMENTS

I would like to acknowledge Csaba Balazs, Peter Winslow and Michael Ramsey Musolf for some useful

discussions relating to this work. This work was supported through the J.L. Williams Scholarship, Australian Postgraduate Award Scholarship. In addition, part of this work was made possible through the Keith Murdoch Scholarship via the American Australian Association as well as the Center of Excellence for Particle Physics.

## APPENDIX A: EXTRA DETAILS IN DERIVING THE SOLUTION

In this appendix we give extra details for how to solve the equation

$$a_{Q1}^i \partial^i Q + a_{T1}^i \partial^i T = 0. \quad (\text{A1})$$

We can write  $T$  as a function of  $Q$ , using the usual methods to write

$$T = \frac{1}{a_{T1}^2} \sum_{\pm} \frac{1}{\kappa_{\mp} - \kappa_{\pm}} e^{\kappa_{\pm} z} \left[ \int^z e^{-\kappa_{\pm} y} \left( a_{Q1}^i \frac{\partial^i Q}{\partial y^i} \right) dy - \beta_i \right]. \quad (\text{A2})$$

The first change of variables we use is of course

$$h'_{\pm} = e^{-\kappa_{\pm} Q} \quad (\text{A3})$$

which leads to the following identities:

$$\begin{aligned} Q &= e^{\kappa_{\pm} z} h'_{\pm} \\ Q' &= (\kappa_{\pm} h'_{\pm} + h''_{\pm}) e^{\kappa_{\pm} z} \\ Q'' &= (\kappa_{\pm}^2 h'_{\pm} + 2\kappa_{\pm} h''_{\pm} + h'''_{\pm}) e^{\kappa_{\pm} z}. \end{aligned} \quad (\text{A4})$$

This allows us to write the integrand for  $T$  in terms of  $h_{\pm}$  and remove the integral,

$$\begin{aligned} T &= \frac{1}{a_{T1}^2} \sum_{\pm} \frac{e^{\kappa_{\pm} z}}{\kappa_{\mp} - \kappa_{\pm}} \int^z e^{-\kappa_{\pm} y} \\ &\quad \times [(a_{Q1}^0 + \kappa_{\pm} a_{Q1}^1 + \kappa_{\pm}^2 a_{Q1}^2) h'_{\pm} \\ &\quad + (a_{Q1}^1 + 2a_{Q1}^2 \kappa_{\pm}) h''_{\pm} + a_{Q1}^2 h'''_{\pm}] \\ &= \frac{1}{a_{T1}^2} \sum_{\pm} \frac{e^{\kappa_{\pm} z}}{\kappa_{\mp} - \kappa_{\pm}} \\ &\quad \times [(a_{Q1}^0 + \kappa_{\pm} a_{Q1}^1 + \kappa_{\pm}^2 a_{Q1}^2) h_{\pm} \\ &\quad + (a_{Q1}^1 + 2a_{Q1}^2 \kappa_{\pm}) h'_{\pm} + a_{Q1}^2 h''_{\pm}]. \end{aligned} \quad (\text{A5})$$

To remove the exponents we use the change of variables

$$j_{\pm} = e^{\kappa_{\pm} z} h_{\pm} \quad (\text{A6})$$

from which we can derive the usual identities

$$\begin{aligned}
h_{\pm} &= e^{-\kappa_{\pm}z} j_{\pm} \\
h'_{\pm} &= (j'_{\pm} - \kappa_{\pm} j_{\pm}) e^{-\kappa_{\pm}z} \\
h''_{\pm} &= (j''_{\pm} - 2\kappa_{\pm} j'_{\pm} + \kappa_{\pm}^2 j_{\pm}) e^{-\kappa_{\pm}z}. \quad (\text{A7})
\end{aligned}$$

We can also use the second line in the above equation to derive an identity that relates  $Q$  to both new variables  $j_{\pm}$  and its derivative,

$$Q = j'_{\pm} - \kappa_{\pm} j_{\pm}. \quad (\text{A8})$$

Our expression for  $T$  is now free of any exponentials,

$$T = \frac{1}{a_{T1}^2} \sum_{\pm} \frac{1}{\kappa_{\mp} - \kappa_{\pm}} [a_{Q1}^0 j_{\pm} + a_{Q1}^1 j'_{\pm} + a_{Q1}^2 j''_{\pm}]. \quad (\text{A9})$$

We would like to write both  $T$  and  $Q$  in terms of a single variable. This task is achieved by the choice

$$k = e^{\kappa_{\mp}z} \int^z e^{-\kappa_{\mp}y} j_{\pm} dy \quad (\text{A10})$$

which can be inverted to write

$$j_{\pm} = k' - \kappa_{\mp} k. \quad (\text{A11})$$

Both expressions for  $Q$  are now satisfied,

$$\begin{aligned}
Q &= j'_+ - \kappa_+ j_+ \\
&= (k'' - \kappa_- k') - \kappa_+ (k' - \kappa_- k) \\
&= k'' - (\kappa_+ + \kappa_-) k' + \kappa_+ \kappa_- k \quad (\text{A12})
\end{aligned}$$

and

$$\begin{aligned}
Q &= j'_- - \kappa_- j_- \\
&= (k'' - \kappa_+ k') - \kappa_- (k' - \kappa_+ k) \\
&= k'' - (\kappa_+ + \kappa_-) k' + \kappa_+ \kappa_- k. \quad (\text{A13})
\end{aligned}$$

We would like to write  $\kappa_{\pm}$  in terms of the coefficients  $a_{X1,i}$

$$\kappa_{\pm} = \frac{-a_{T1}^1 \pm \sqrt{(a_{T1}^1)^2 - 4a_{T1}^0 a_{T1}^2}}{2a_{T1}^2} \quad (\text{A14})$$

which leads to the identities

$$\begin{aligned}
\kappa_+ + \kappa_- &= -\frac{a_{T1}^1}{a_{T1}^2} \\
\kappa_+ \kappa_- &= \frac{a_{T1}^0}{a_{T1}^2}. \quad (\text{A15})
\end{aligned}$$

Rescaling  $k$  we get

$$Q = a_{T1}^2 k'' + a_{T1}^1 k' + a_{T1}^0 k \quad (\text{A16})$$

as before. Finally, substituting in our rescaled expression for  $k$  we get

$$\begin{aligned}
T &= \sum_{\pm} \frac{1}{\kappa_{\mp} - \kappa_{\pm}} [a_{Q1}^2 k''' + (a_{Q1}^1 - \kappa_{\mp} a_{Q1}^2) k'' \\
&\quad \times (a_{Q1}^0 - \kappa_{\mp} a_{Q1}^1) k' - a_{Q1}^0 \kappa_{\mp} k] \\
&= -a_{Q1}^2 k''' - a_{Q1}^1 k'' - a_{Q1}^0 k' \quad (\text{A17})
\end{aligned}$$

as required.

## APPENDIX B: A NOTE ON EXTRA INTEGRATION CONSTANTS

Throughout this work we have ignored extra integration constants that are produced in the process of reducing a set of QTEs down to a single differential equation. The contexts in which we have ignored these constants vary but throughout we reference this appendix since the reason is the same. To demonstrate this let us consider the simplest nontrivial example. Let us have a system which can be described by the following set of QTEs:

$$\begin{aligned}
a_{11}^i \partial^i X_1 + a_{21}^i \partial^i X_2 &= 0 \\
a_{12}^i \partial^i X_1 + a_{22}^i \partial^i X_2 &= \Delta(z). \quad (\text{B1})
\end{aligned}$$

Solving the first equation for  $X_1$  after using the usual tricks we have

$$\begin{aligned}
X_1 &= -a_{21}^i \partial^i k + \frac{1}{a_{11}^2} \sum_{\pm} \frac{e^{\kappa_{\pm}z}}{\kappa_{\mp} - \kappa_{\pm}} e^{-\kappa_{\pm}z} \beta_{\pm} \\
&\mapsto -a_{21}^i \partial^i k + \sum_{\pm} e^{\kappa_{\pm}z} \beta_{\pm} \\
X_2 &= a_{11}^i \partial^i k. \quad (\text{B2})
\end{aligned}$$

The extra integration coefficients  $\beta_{\pm}$  should immediately rouse suspicion since the system we started with was a set of two coupled second-order differential equations and such a system is completely specified by four boundary conditions for every region it is solved in. Therefore solving the equations including the use of variable changes should not introduce the need for more initial conditions. As an analogy we could make a strange change of variables that shifts  $Q$  by a constant  $c$ . If we solve the system we should find that consistency demands that  $c = 0$  (rather than another condition being produced that specifies  $c$ ) or that  $c$  is redundant. These are the same requirements that will be imposed on  $\beta_{\pm}$ . Before we demonstrate that the  $\beta_{\pm} = 0$  let us first show that they can be removed by another variable change. Specifically one can take

$$k = k_2 + f \quad (\text{B3})$$

where  $f$  is any function that satisfies the equations

$$\begin{aligned} -a_{21}^i \partial_i f &= -\sum_{\pm} e^{\kappa_{\pm} z} \beta_{\pm} \\ a_{11}^i \partial^i f &= 0. \end{aligned} \quad (\text{B4})$$

The solution is then

$$f = \sum_{\pm} A_{\pm} e^{\kappa_{\pm} z} \quad (\text{B5})$$

with

$$A_{\pm} = \frac{\beta_{\pm}}{a_{21}^i \kappa_{\pm}^i}. \quad (\text{B6})$$

One can then just substitute the functions  $Q$  and  $T$  in terms of  $k_2$  into the second equation and derive the usual solution. For completeness we nonetheless consider the case where we keep  $\beta_{\pm}$  in the set of equations. Substituting these solutions into the second equation gives

$$\begin{aligned} (a_{22}^i a_{11}^j - a_{12}^i a_{21}^j) \partial^{i+j} k + \sum_{\pm} (a_{12}^i \kappa_{\pm}^i) e^{\kappa_{\pm} z} \beta_{\pm} &= \Delta(z) \\ \mapsto (a_{22}^i a_{11}^j - a_{12}^i a_{21}^j) \partial^{i+j} k + \sum_{\pm} B_{\pm} e^{\kappa_{\pm} z} \beta_{\pm} &= \Delta(z). \end{aligned} \quad (\text{B7})$$

Treating the term proportional to  $\exp \kappa_{\pm} z$  as an inhomogeneity one could naively write

$$k = \sum_{i=0}^4 x_i e^{\alpha_i z} \left( \int^z dy e^{-\alpha_i y} [\Delta(y) - B_{\pm} \beta_{\pm} e^{\kappa_{\pm} y}] - \beta_i \right). \quad (\text{B8})$$

We can immediately see that  $\kappa_{+(-)} = 0$  in the broken (symmetric) phase in order to have a well-behaved function at infinity. As for the  $\beta_-$  term let us try and derive the coefficients  $x_i$ ; we will find an inconsistency unless  $\beta_- = 0$  (we expect such an inconsistency due to the arguments given earlier). We demand that the coefficients of

$\Delta'(z), \Delta''(z)$  and  $\Delta''$  are null while the coefficient of  $\Delta(z)$  is unity. This gives

$$\begin{aligned} \sum_i x_i &= 0 \\ \sum_i \alpha_i x_i &= 0 \\ \sum_i \alpha_i^2 x_i &= 0 \\ \sum_i \alpha_i^3 x_i &= (a_{11}^2 a_{22}^2 - a_{12}^2 a_{21}^2)^{-1}, \end{aligned} \quad (\text{B9})$$

as in the usual case. However, we now have the additional condition that the coefficient of  $\exp \kappa_- z = \beta_- B_-$ ; this gives the extra condition

$$\sum_i \frac{x_i}{\kappa_- - \alpha_i} (a_{22}^k a_{11}^j - a_{12}^i a_{21}^k) \kappa_-^{i+j} = 1 \quad (\text{B10})$$

which gives an overdetermined set of equations unless  $\beta_- = 0$ . Alternatively we could make use of the last line in Eq. (B9) to write

$$k = \sum_{i=0}^4 x_i e^{\alpha_i z} \left( \int^z dy e^{-\alpha_i y} [\Delta(y) - A_i B_{\pm} \beta_{\pm} e^{\kappa_{\pm} y}] - \beta_i \right) \quad (\text{B11})$$

with

$$A_i = \alpha_i (\kappa_- - \alpha_i) a_{12}^i a_{21}^j \frac{\kappa_{i+j}}{a_{12}^2 a_{21}^2 - a_{11}^2 a_{22}^2}. \quad (\text{B12})$$

Upon substituting this solution back into Eq. (B7) we indeed get that the equation is satisfied. However,  $X_1$  and  $X_2$  are now independent of  $e^{\kappa_- z}$ . So, depending on the treatment of  $\beta_-$ , it is either zero for self-consistency or irrelevant in that it is a redundancy in the theory with now physical consequences. For our purposes it is most convenient to set it to zero.

- 
- [1] A. D. Linde, *Rep. Prog. Phys.* **42**, 389 (1979).  
[2] M. Trodden, *Rev. Mod. Phys.* **71**, 1463 (1999).  
[3] R. Allahverdi and A. Mazumdar, *New J. Phys.* **14**, 125013 (2012).  
[4] S. Inoue, G. Ovanesyan, and M. J. Ramsey-Musolf, arXiv:1508.05404 [*Phys. Rev. D* (to be published)].  
[5] T. Liu, M. J. Ramsey-Musolf, and J. Shu, *Phys. Rev. Lett.* **108**, 221301 (2012).

- [6] S. Eidelman *et al.* (Particle Data Group Collaboration), *Phys. Lett. B* **592**, 1 (2004); D. N. Spergel *et al.* (WMAP Collaboration), *Astrophys. J. Suppl. Ser.* **148**, 175 (2003).  
[7] A. G. Cohen, D. B. Kaplan, and A. E. Nelson, *Annu. Rev. Nucl. Part. Sci.* **43**, 1 (1993).  
[8] M. Quiros, arXiv:hep-ph/9901312.  
[9] J. Schwinger, *J. Math. Phys. (N.Y.)* **2**, 407 (1961).  
[10] K. T. Mahanthappa, *Phys. Rev.* **126**, 329 (1962).

- [11] P. M. Bakshi and K. T. Mahanthappa, *J. Math. Phys. (N.Y.)* **4**, 1 (1963).
- [12] L. V. Keldysh, *Zh. Eksp. Teor. Fiz.* **47**, 1515 (1964).
- [13] R. A. Craig, *J. Math. Phys. (N.Y.)* **9**, 605 (1968).
- [14] K. C. Chou, Z. B. Su, B. L. Hao, and L. Yu, *Phys. Rep.* **118**, 1 (1985).
- [15] A. Riotto, *Phys. Rev. D* **58**, 095009 (1998).
- [16] C. Lee, V. Cirigliano, and M. J. Ramsey-Musolf, *Phys. Rev. D* **71**, 075010 (2005).
- [17] P. Huet and A. E. Nelson, *Phys. Rev. D* **53**, 4578 (1996).
- [18] V. Cirigliano, M. J. Ramsey-Musolf, S. Tulin, and C. Lee, *Phys. Rev. D* **73**, 115009 (2006).
- [19] D. J. H. Chung, B. Garbrecht, M. J. Ramsey-Musolf, and S. Tulin, *J. High Energy Phys.* **12** (2009) 067.
- [20] M. Carena, M. Quiros, M. Seco, and C. E. M. Wagner, *Nucl. Phys.* **B650**, 24 (2003).
- [21] J. M. Cline, M. Joyce, and K. Kainulainen, *J. High Energy Phys.* **07** (2000) 018.
- [22] D. Bodeker, G. D. Moore, and K. Rummukainen, *Phys. Rev. D* **61**, 056003 (2000).
- [23] G. D. Moore, *Phys. Rev. D* **62**, 085011 (2000).
- [24] G. D. Moore and K. Rummukainen, *Phys. Rev. D* **61**, 105008 (2000).
- [25] J. Kozaczuk, S. Profumo, L. Haskins, and C. L. Wainwright, *J. High Energy Phys.* **01** (2015) 144.
- [26] P. Winslow and S. Tulin, *Phys. Rev. D* **84**, 034013 (2011).
- [27] M. Joyce, T. Prokopec, and N. Turok, *Phys. Rev. D* **53**, 2930 (1996).
- [28] J. M. Moreno, M. Quiros, and M. Seco, *Nucl. Phys.* **B526**, 489 (1998).



## Chapter 5

---

# Solving bubble wall profiles

---

### 5.1 Introductory remarks

To calculate the rate a false vacuum decays, one is required to calculate a solution to the classical equations of motion known as the bounce. The bounce is the solution where the field starts near the false vacuum and asymptotes to the true vacuum. Finding the bounce is necessary if one wishes to examine both phase transitions and vacuum stability [96, 97, 98, 99, 100, 101, 102, 103, 104]. Unfortunately, the bounce solution is notoriously difficult to calculate. Although solving a set of coupled non linear inhomogeneous equations numerically is typically a moderate but nonetheless tractable challenge, the situation is complicated by the fact that there is an easily found trivial solution where the field stays in one vacuum or the other. For a lot of numerical methods this means that the trivial solution is a powerful basin of attraction making the bounce solution difficult to find [105].

I provide a new method for performing such a calculation by first curve fitting the bounce solution in the entire parameter space of the most general renormalizable tree level potential of a single field. I then propose, similarly to another algorithm [106], that the bounce solution of a multifield problem can be approximated by the solution to a single field problem which I have in analytic form. Specifically the solution to the multifield problem is the one dimensional ansatz plus some arbitrary function which I refer to as a perturbation. The perturbation is then given by the solution to a set of linearized differential equations due to similar methods given in the previous chapter. This sets up a fast converging perturbative series. I test our method against a known result.

### 5.2 Declaration for thesis chapter 5

#### Declaration by candidate

In the case of the paper present contained in chapter 5, the nature and extent of my contribution was as follows:

<b>Publication</b>	<b>Nature of contribution</b>	<b>Extent of contribution</b>
6	Came up with the idea and derivation, wrote first draft of paper and implemented numerical treatment of multifield case. Involved in discussions throughout.	70%

The following coauthors contributed to the work. If the coauthor is a student at Monash, their percentage contribution is given:

<b>Author</b>	<b>Nature of contribution</b>	<b>Extent of contribution</b>
Csaba Balazs	Set up numeric code for single field case and involved in curve fitting. Involved in discussions throughout.	
Sujeet Akula	Edited draft and worked on figure presentation. Involved with initial discussion and ideas and worked heavily on making the ideas in the paper more transparent. Involved in discussions throughout.	

The undersigned hereby certify that the above declaration correctly reflects the nature and extent of the candidate and co-authors' contributions to this work.

**Signatures:**

Graham White

Sujeet Akula

Csaba Balazs

**Date:** 3.04.2017

### **5.3 Published material for chapter 5: Semi-analytic techniques for calculating bubble wall profiles**

# Semi-analytic techniques for calculating bubble wall profiles

Sujeet Akula<sup>1,2,a</sup>, Csaba Balázs<sup>1,2,3,b</sup>, Graham A. White<sup>1,2,3,c</sup>

<sup>1</sup> School of Physics and Astronomy, Monash University, Melbourne, VIC 3800, Australia

<sup>2</sup> ARC Centre of Excellence for Particle Physics at the Terascale, Monash University, Melbourne, VIC 3800, Australia

<sup>3</sup> Monash Centre for Astrophysics, Monash University, Melbourne, VIC 3800, Australia

Received: 22 September 2016 / Accepted: 15 November 2016 / Published online: 9 December 2016

© The Author(s) 2016. This article is published with open access at Springerlink.com

**Abstract** We present semi-analytic techniques for finding bubble wall profiles during first order phase transitions with multiple scalar fields. Our method involves reducing the problem to an equation with a single field, finding an approximate analytic solution and perturbing around it. The perturbations can be written in a semi-analytic form. We assert that our technique lacks convergence problems and demonstrate the speed of convergence on an example potential.

## 1 Introduction

The decay of a false vacuum is a complex problem with numerous applications in cosmology [1–6] and is particularly important in the study of baryogenesis [7–26] (although there are mechanisms for producing the baryon asymmetry that do not require calculating the decay of the false vacuum [27–33]). Calculating tunneling rates is also an important problem in the study of vacuum stability [34–40].

While the physics of the tunneling process is qualitatively well understood [41], quantitatively it is a complicated problem that involves solving a set of highly nonlinear coupled differential equations usually requiring a numerical solution. The two techniques that are most commonly used to solving the tunneling problem are path deformation [42, 43] and minimizing the integral of the squared equations of motion for a set of parametrized functions [44, 45], although other methods also exist [46]. Exact solutions only exist for specialized cases [47, 48].

In this paper we offer a new approach by solving the tunneling problem semi-analytically. First, we give an analytic

solution to an ansatz for an arbitrary potential. Since the ansatz is only an approximate solution, in the next step we derive a perturbative expansion that converges to the exact solution. For each term in the perturbative series we provide a semi-analytic solution. Since our starting potential is arbitrary, and because the convergence of the perturbative expansion is independent of the potential, our method is completely general.

To derive the ansatz we take advantage of the fact that the multi-field problem can be approximated by finding the solution to a single-field potential. The approximate tunneling solution can be found along the field direction that connects the true and false vacua. This single-field potential can be solved in terms of a single parameter. To improve the initial ansatz we compute correction functions to the ansatz in a manner analogous to Newton's method of finding roots. The result is a perturbative series of corrections that are expected to converge quadratically.

The differential equations that define these corrections can be solved analytically in terms of eigenvalues of the mass matrix and a function of the initial ansatz. In doing so we use techniques that were recently employed to analytically solve number densities across a bubble wall [49]. Although the technique has elements in common with Newton's method it does not share its trouble with null derivatives giving divergent corrections or oscillations around the solution. We also argue that the other problems with Newton's method are generically not relevant to our method.

The layout of this paper is as follows. In Sect. 2 we give a brief overview of the false vacuum problem. In Sect. 3 we develop an ansatz form that approximately solves a general variety of multi-field potentials with a false vacuum, where the potential is specified by a single parameter. In Sect. 4 we derive the perturbative corrections to the ansatz forms and discuss the convergence. In Sect. 5 we use this method to solve a problem which can be directly compared with the literature. Concluding remarks are given in Sect. 6.

<sup>a</sup> e-mail: [sujeet.akula@coepp.org.au](mailto:sujeet.akula@coepp.org.au)

<sup>b</sup> e-mail: [csaba.balazs@monash.edu](mailto:csaba.balazs@monash.edu)

<sup>c</sup> e-mail: [graham.white@monash.edu](mailto:graham.white@monash.edu)

## 2 Fate of the false vacuum

Consider a potential of multiple scalar fields  $V(\phi_i)$  with at least two minima. The trivial solution to the classical equations of motion is stationary extremizing the potential. This solution typically gives the field a non-zero vacuum expectation value and is responsible for giving standard model particles their mass via electroweak symmetry breaking. The other, less obvious solution is one where the fields continuously vary from one minimum to another. In this case, the false vacuum decays into the true vacuum via tunneling processes, and is termed the ‘bounce solution’ [41]. If this is achieved within a first order phase transition, regions of the new vacuum appear and expand as bubbles in space. In this paper we are interested in calculating the profile of the bubble, that is, the spacetime dependence of the bubble nucleation.

The spatial bubble profile is obtained by extremizing the Euclidean action

$$S_E = \int d^d x \left[ \frac{1}{2} (\partial_\mu \varphi_i)^2 + V(\varphi_i) \right] \quad (1)$$

where  $d = 4$  for zero temperature tunneling and  $d = 3$  for finite temperature tunneling relevant to cosmological phase transitions. The nucleation rate per unit volume is

$$\Gamma = A(T) e^{-\frac{S_E}{T}} \quad (2)$$

where  $A(T)$  is a temperature dependent prefactor proportional to the fluctuation determinant,  $T$  is the temperature and  $S_E$  is the euclidean action for the bounce solution which satisfies the classical equations of motion. In the case of a spherically symmetric bubble the classical equations of motion are

$$\frac{\partial^2 \varphi_i}{\partial \rho^2} + \frac{2}{\rho} \frac{\partial \varphi_i}{\partial \rho} - \frac{\partial V}{\partial \varphi_i} = 0 \quad (3)$$

and the bounce solution satisfies the conditions  $\varphi_i(0) \approx v_i^{\text{true}}$ ,  $\varphi_i(\infty) = v_i^{\text{false}}$  and  $\varphi_i'(0) = 0$ .<sup>1</sup> Here  $\rho$  is the ordinary 3D spherical coordinate, as we are considering finite temperature, and  $v_i^{\text{true}}$  and  $v_i^{\text{false}}$  are the vacuum expectation values of the field  $\varphi_i$  in the true and false vacua, respectively. The equations of motion resemble the classical solution of a ball rolling in a landscape of shape- $V$  with  $\rho$  playing the role of time, but including a  $\rho$ -dependent friction term.

<sup>1</sup> The first is not a boundary condition unlike the other two. It is instead the condition that differentiates the bounce from a trivial solution.

## 3 Approximate solution to the multi-field potential

### 3.1 Reducing to a single-field potential

The bounce solution can be approximated by the bounce solution of a single differential equation as follows [42, 43]. First make a shift of fields such that the false vacuum is at the origin in field space. The true vacuum is then at  $v\hat{\phi}_1$  where  $\hat{\phi}_1$  is a unit vector that points in the direction of the true vacuum. Then define a complete set of unit vectors orthogonal to  $\hat{\phi}_1$  and rewrite the potential in the rotated basis  $V(\varphi_1, \varphi_2, \dots) \mapsto V(\phi_1, \phi_2, \dots)$ . Then consider the potential only in the  $\hat{\phi}_1$  direction between the minima,  $V(\phi_1, 0, \dots)$ . One can then solve the single equation of motion

$$\frac{\partial^2 \phi_1}{\partial \rho^2} + \frac{(d-1)}{\rho} \frac{\partial \phi_1}{\partial \rho} - \frac{\partial V(\phi_1, 0, \dots)}{\partial \phi_1} = 0 \quad (4)$$

to derive an initial ansatz that approximately solves the full classical equations of motion. Let us therefore turn our attention to the most general renormalizable tree level potential with a single field,

$$V(\varphi) = M^2 \varphi^2 + b\varphi^3 + \lambda\varphi^4. \quad (5)$$

An approximate expression for the effective action of a similar potential was found in Ref. [50]. The above potential can be rescaled  $\phi = \varphi_{\min} \varphi$  where  $\varphi_{\min}$  is the global minimum of the above potential. Then the rescaled potential has a global minimum at  $\phi = 1$ . To ensure that the effective action is unaffected by this rescaling, we also make the replacement  $\rho \mapsto \varphi_{\min} \rho$ . We parametrize the rescaled potential as<sup>2</sup>

$$V(\phi) = \frac{(4\alpha - 3)}{2} E \phi^2 + E \phi^3 - \alpha E \phi^4. \quad (6)$$

Tunneling between two vacua requires the existence of a potential barrier or ‘‘bump’’ separating the two minima. As parametrized in Eq. (6), this type of barrier can only exist if  $E < 0$  and  $\alpha \in (0.5, 0.75)$ .<sup>3</sup> To illustrate this point, we present in Fig. 1 the potential in  $\phi$  given in Eq. (6) for both the edge choices of  $\alpha$  and the mean allowed choice, using several choices of  $E$ . One can see that, for  $\alpha = \frac{1}{2}$ , we have exactly the Mexican hat potential (albeit shifted to  $\phi = 0.5$ ) with degenerate minima, and for  $\alpha = \frac{3}{4}$ , there is no potential barrier between false and true minima.

<sup>2</sup> This definition of  $\alpha$  differs from that of [50] but the physical principles are the same.

<sup>3</sup> This is assuming the three turning points are in the positive  $\phi$  direction with the local minimum at the origin. The rest of potentials with three turning points are covered by this analysis simply by making combinations of the transformations  $\phi \mapsto \phi + a$  and  $\phi \mapsto -\phi$ .

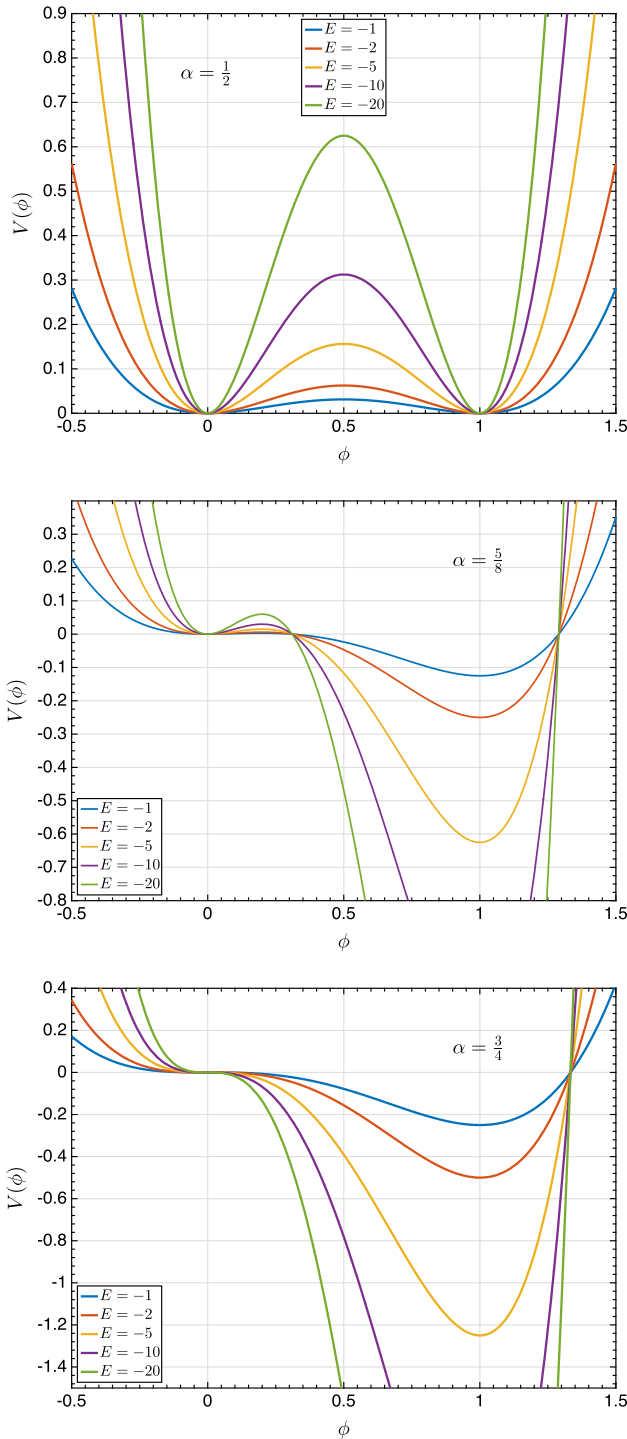


**Fig. 1** We present our rescaled scalar potential parametrized by  $E$  and  $\alpha$  given in Eq. (6). Each panel displays  $-E = 1, 2, 5, 10, 20$ . The *top* and *bottom* panels are the edge choices of  $\alpha$ , with  $\alpha = \frac{1}{2}$  on top and  $\alpha = \frac{3}{4}$  on the bottom. The *middle* panel has the mean value of  $\alpha = \frac{5}{8}$

### 3.2 Developing ansatz solutions

In deriving an approximate solution to the potential in Eq. (6), we first note that the effective potential is proportional to  $E$ .

Thus, one can factor  $|E|$  out of the equations of motion by further rescaling  $\rho \mapsto \rho/\sqrt{|E|}$ . Then the equations of motion only depend on  $\alpha$ .

Under the scaling we have introduced,

$$\begin{cases} \varphi \mapsto \phi = \varphi_{\min}\varphi \\ \rho \mapsto \frac{\varphi_{\min}}{\sqrt{|E|}}\rho \end{cases} \quad (7)$$

the Euclidean action becomes

$$S_E = 4\pi \frac{\phi_m^3}{\sqrt{|E|}} \int d\rho \rho^2 \left[ \left( \frac{\partial\phi}{\partial\rho} \right)^2 - \tilde{V}(\phi) \right] \quad (8)$$

where<sup>4</sup>  $\tilde{V} \equiv V/|E|$ , and we have integrated over the angular variables assuming isotropy. The integral in Eq. (8) must only depend on  $\alpha$ , as in

$$S_E = 4\pi \frac{\phi_m^3}{\sqrt{|E|}} f(\alpha). \quad (9)$$

Meanwhile, we will approximate the rescaled field itself with the well-known “kink” solution [44,45]

$$\phi \approx \frac{1}{2} \left( 1 - \tanh \left[ \frac{\rho - \delta(\alpha)}{L_w(\alpha)} \right] \right) \quad (10)$$

parametrized by the offset  $\delta$  and the bubble wall width  $L_w$ . Thus it remains to determine the  $\alpha$ -dependent functions  $\delta(\alpha)$ ,  $L_w(\alpha)$  from the kink solution, and  $f(\alpha)$  in the Euclidean action.

We first evenly sample values of  $\alpha$  within  $(0.5, 0.75)$ , then numerically solve the full bubble profile using conventional techniques. Next, for each value of  $\alpha$ , we fit the kink solution given in Eq. (10) to the full solution, extracting  $L_w$  and  $\delta$ . Lastly, we numerically integrate to find  $f$  in the Euclidean action. This results in a tabulation of values for  $L_w$ ,  $\delta$ , and  $f$ , for each value of  $\alpha$ . Using the apparent  $\alpha$  dependence and intuition from our parametrization of the potential, we find ansatz functional forms in terms of  $\alpha$  for each of these parameters.

The offset  $\delta$  should diverge at the boundaries  $\alpha = 0.5$  and  $\alpha = 0.75$ , and is found to be quite small otherwise. It also appears to have approximate odd parity about the mean allowed value of  $\alpha = 0.625$ . We modeled this with odd powers of non-removable poles at the boundaries of  $\alpha$ , along with an offset and a linear correction about the mean:

$$\delta(\alpha) \approx \delta_0 + k \left( \alpha - \frac{5}{8} \right) + \sum_{n=1}^2 a_n \left[ \frac{\alpha - \frac{5}{8}}{\left( \alpha - \frac{1}{2} \right) \left( \alpha - \frac{3}{4} \right)} \right]^{(2n-1)}. \quad (11)$$

We then fit these parameters using the tabulated values.

<sup>4</sup>  $\tilde{V}$  does not have any dependence on  $|E|$ .

**Table 1** The fitted values for the parameters that define the approximate ansatz functions for  $f$  which is used in the Euclidean action, the bubble wall width  $L_w$ , and the offset  $\delta$  from the kink solution

$f(\alpha)$		$L_w(\alpha)$		$\delta(\alpha)$	
Parameter	Value	Parameter	Value	Parameter	Value
$f_0$	0.0871	$\ell_0$	1.4833	$\delta_0$	2.2807
$p$	1.8335	$c$	0.4653	$k$	-4.6187
$q$	3.1416	$r$	18.0000	$a_1$	0.5211
		$s$	0.7035	$a_2 \times 10^5$	7.8756

The bubble wall width  $L_w$  is dominated by two asymptotes. It diverges at  $\alpha = \frac{3}{4}$ , and become small as  $\alpha \rightarrow \frac{1}{2}$ . We used this form to model the asymptotic behavior,

$$L_w(\alpha) \approx \ell_0 \left[ \left( \alpha - \frac{1}{2} \right)^r + \frac{c}{\left| \alpha - \frac{3}{4} \right|^s} \right]. \tag{12}$$

As before, the normalization  $\ell_0$ , the two exponents  $r$  and  $s$ , and the coefficient  $c$  are fit using the tabulated values from the full numerical calculation. Interestingly, we find almost exactly that  $r = 18$ . (The full fitted parameters are given in Table 1.)

The Euclidean action determined by  $f(\alpha)$  diverges at  $\alpha = \frac{1}{2}$  and is zero at  $\alpha = \frac{3}{4}$ . This is modeled by

$$f(\alpha) = f_0 \frac{\left| \alpha - \frac{3}{4} \right|^p}{\left| \alpha - \frac{1}{2} \right|^q} \tag{13}$$

where only a normalization parameter and exponents need to be fitted.

In Table 1 we present all the fitted values that go into these ansatz approximate forms. The numerical values computed for these functions as well as the resulting fits are given in Fig. 2. We did not estimate uncertainties in the full numerical calculations nor in the fitted parameters, though in principle this could be done. Thus we are not able to compute rigorous measures of the goodness of fits. As these fits are only used to form a base ansatz solution which then receives perturbative corrections, such an undertaking lies outside the scope of this work. We do, however, provide in Fig. 2 the residuals between the fitted curves and tabulated values.

We note that  $|E|$  scales as  $|b\phi^3|$  so  $S_E/T$  scales as  $\frac{\phi_m}{T} \sqrt{\frac{\phi_m}{b}}$ , where  $b$  is the cubic coupling of the unscaled field, as in Eq. (5). Also  $b$  controls the height of the barrier separating the two minima.

#### 4 Perturbative solution

In the previous section, we developed fitted curves to estimate the parameters of the well known kink solution. In this section, we will take advantage of rescaling to compute con-

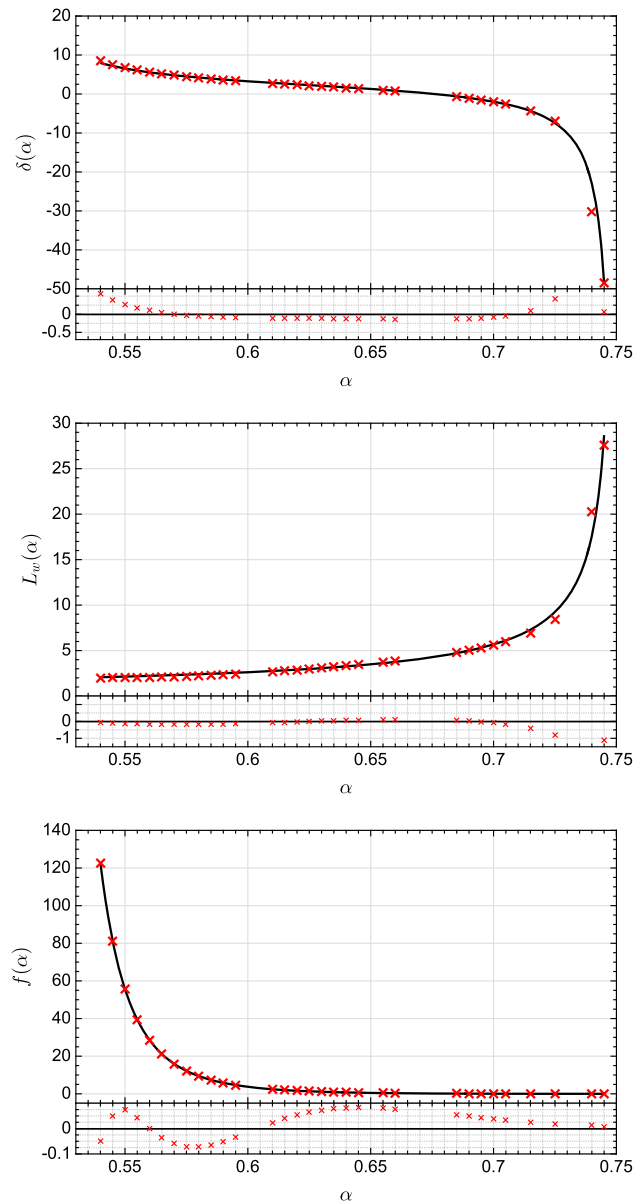


**Fig. 2** We present the fits to the offset  $\delta$  (top panel) and the bubble wall width  $L_w$  (middle panel) of the kink solution, and the integral  $f$  (bottom panel) appearing in the Euclidean action. The numerically computed values are presented along with the fitted curves, as well as the residuals

vergent perturbative corrections. The process is largely analogous to Newton’s method for finding roots of functions. Here, we iteratively determine functional corrections to the ansatz form.

##### 4.1 Perturbative corrections to the ansatz

We first note that along the trajectory in field space from the false vacuum to the true vacuum, the magnitude of any of the fields in  $\phi = \{\phi_i(\rho)\}$  generically does not exceed the distance between the two minima. That is,

$$|\phi_i(\rho)| \lesssim |v_{\text{true}} - v_{\text{false}}|. \tag{14}$$

If we rescale our fields as described in Sect. 3, the distance between the ansatz and the actual solution is bounded by 1, but is usually much smaller than 1. (This is illustrated with the concrete example presented in Sect. 5.) Let us call the ansatz to  $\phi_i$ ,  $A_i$  with correction  $\varepsilon_i$ , so that  $\phi_i = A_i + \varepsilon_i$ . Applying this to Eq. (3) yields

$$\begin{aligned} & \frac{\partial^2 A_i}{\partial \rho^2} + \frac{\partial^2 \varepsilon_i}{\partial \rho^2} + \frac{2}{\rho} \frac{\partial A_i}{\partial \rho} + \frac{2}{\rho} \frac{\partial \varepsilon_i}{\partial \rho} \\ &= \left. \frac{\partial V(\phi)}{\partial \phi_i} \right|_A + \sum_j \left. \frac{\partial^2 V(\phi)}{\partial \phi_i \partial \phi_j} \right|_A \varepsilon_j \end{aligned} \tag{15}$$

where  $A \equiv \{A_i\}$ . We can then rearrange the above to separate terms that depend only on the ansatz forms from those involving the unknown correction functions,  $\varepsilon_i$ . This leaves us with a set of coupled inhomogeneous differential equations for  $\varepsilon_i$ :

$$\frac{\partial^2 \varepsilon_i}{\partial \rho^2} + \frac{2}{\rho} \frac{\partial \varepsilon_i}{\partial \rho} - \left. \frac{\partial^2 V(\phi)}{\partial \phi_i \partial \phi_j} \right|_A \varepsilon_j = B_i(\rho). \tag{16}$$

Here the functions  $B_i(\rho)$  are the inhomogeneous part of the differential equations for  $\varepsilon_i$ , and they are given by

$$B_i(\rho) \equiv \left. \frac{\partial V(\phi)}{\partial \phi_i} \right|_A - \frac{\partial^2 A_i}{\partial \rho^2} - \frac{2}{\rho} \frac{\partial A_i}{\partial \rho}. \tag{17}$$

One can see that the value of the functions  $B_i$  represents how well the ansatz forms solve the equations of motion. This can be seen not only as the definition of  $B_i$  are the equations of motion where the fields are taken to be  $A_i$ , but also because if  $B_i$  were zero, then the differential equations for the corrections to the ansatz  $\varepsilon_i$  would become homogeneous.

We can linearize and approximately solve these differential equations analytically by approximating the mass matrix by a series of step functions with a correction which we will use to form the convergent series of perturbations. Considering only the homogeneous case ( $B_i = 0$ ), Eq. (16) is solved by introducing  $\varepsilon$  of the form

$$\varepsilon \sim \frac{z e^{\lambda \rho}}{\rho}. \tag{18}$$

This will reduce the equation to an eigenvalue problem in the mass matrix. It is therefore convenient to define the homogeneous solutions with the notation

$$\varepsilon_{ik}^h = \frac{z_{ik} e^{\lambda_k \rho}}{\rho} \tag{19}$$

where the index  $i$  refers to field  $\phi_i$ , and the index  $k$  will run over the  $n$  eigenvalues of the mass matrix, and  $k$  is not summed over. Substituting  $\varepsilon_{ik}^h$  for  $\varepsilon_i$  in Eq. (16) with  $B_i = 0$  yields

$$\sum_j M_{ij} z_{jk} = \lambda_k^2 z_{ik} \tag{20}$$

where  $M$  is the mass matrix

$$M_{ij} = \left. \frac{\partial^2 V(\phi)}{\partial \phi_i \partial \phi_j} \right|_A. \tag{21}$$

In this way,  $z_{ik}$  is the  $i$ th element of the eigenvector of  $M$  that has eigenvalue  $\lambda_k^2$ . It is necessary, however, to use both positive and negative roots,  $\pm \lambda_k$ . Thus we must further introduce  $\tilde{\lambda}_j$  and  $\tilde{z}_{ij}$  with

$$\tilde{\lambda}_1 = \lambda_1, \tilde{\lambda}_2 = -\lambda_1, \tilde{\lambda}_3 = \lambda_2, \dots \tag{22}$$

$$\tilde{z}_{i1} = z_{i1}, \tilde{z}_{i2} = z_{i1}, \tilde{z}_{i3} = z_{i2}, \tilde{z}_{i4} = z_{i2}, \dots \tag{23}$$

so that in  $\tilde{\lambda}_j$  and  $\tilde{z}_{ij}$ , the index  $j = 1, 2, \dots, 2n$ . Finally, we use the techniques described in [49] to arrive at the particular solution,

$$\varepsilon_i^{\leq} = \sum_{j=1}^{2n} \sum_{k=1}^n \tilde{z}_{ij} \frac{e^{\tilde{\lambda}_j \rho}}{\rho} \left( \int_0^\rho t e^{-\tilde{\lambda}_j t} h_{jk} B_k^{\leq}(t) dt - \beta_j^{\leq} \right). \tag{24}$$

In the above, the functions  $B_k$  are defined in Eq. (17), and the constants  $\beta_j^{\leq}$  are determined by boundary and matching conditions. The constants  $h_{jk}$  that appear in the integrand are determined by the  $2n^2$  constraint equations

$$\sum_{j=1}^{2n} \tilde{z}_{ij} h_{jk} \tilde{\lambda}_j = \delta_{ik}, \tag{25}$$

$$\sum_{j=1}^{2n} \tilde{z}_{ij} h_{ik} = 0. \tag{26}$$

Each of the above equations are  $n \times n$  matrix equations, giving  $2n^2$  total constraints.

To account for the corrections to the mass matrix we relabel the solution we found  $\varepsilon_i^0$ , substitute into the differential equations  $\varepsilon_i = \varepsilon_i^0 + \delta \varepsilon_i + \dots$  and restore  $\eta_{ij}(\rho)$  in the differential equations. Keeping only terms to first order we write

$$\begin{aligned} & \frac{\partial^2 \varepsilon_i}{\partial \rho^2} + \frac{2}{\rho} \frac{\partial \varepsilon_i}{\partial \rho} - \left. \frac{\partial^2 V(\phi)}{\partial \phi_i \partial \phi_j} \right|_A \varepsilon_j = B_i(\rho), \\ & \frac{\partial^2 \delta \varepsilon_i + \varepsilon_i^0}{\partial \rho^2} + \frac{2}{\rho} \frac{\partial \delta \varepsilon_i + \varepsilon_i^0}{\partial \rho} - (\delta \varepsilon_j + \varepsilon_j^0) (\bar{M}_{ij} + \eta_{ij}) = B_i(\rho). \end{aligned} \tag{27}$$

Since  $\varepsilon_i^0$  solve the initial differential equations in terms of  $\bar{M}_{ij}$  by definition we can make an immediate simplification. Keeping only terms up to first order in our expansion we then write

$$\begin{aligned} & \frac{\partial^2 \delta \varepsilon_i}{\partial \rho^2} + \frac{2}{\rho} \frac{\partial \delta \varepsilon_i}{\partial \rho} - \delta \varepsilon_j \bar{M}_{ij} - \eta_{ij} \varepsilon_j^0 = 0, \\ & \frac{\partial^2 \delta \varepsilon_i}{\partial \rho^2} + \frac{2}{\rho} \frac{\partial \delta \varepsilon_i}{\partial \rho} - \delta \varepsilon_j \bar{M}_{ij} = \eta_{ij} \varepsilon_j^0. \end{aligned} \tag{28}$$

This once again is a set of coupled linear differential equations which has the same form as the original set of differential equations. So the solution is the same as before with  $\eta_{ij}\varepsilon_j^0$  replacing  $B_i$ . One then finds the series of  $\delta\varepsilon_k$  up to a desired tolerance to find each value of  $\varepsilon_i$ . This process continues until the equations of motion are satisfied up to the desired tolerance.

### 4.2 Observations on convergence

Newton’s method is well known to have four major issues. In our analogous form, these issues would be:

1. If the initial ansatz function is too far from the true function, convergence will be slow.
2. Oscillating solutions where  $\varepsilon^{(n)}(\rho) \approx -\varepsilon^{(n+1)}(\rho)$ .
3. Divergent corrections that arise in Newton’s method if the function’s derivative becomes undefined or zero. The equivalent issue will be discussed in detail below.
4. Being in the wrong basin of attraction and converging to the wrong function.

We will demonstrate that our method as applied here does not suffer from these problems with the exception of issue 4, where in principle a local minimum could be closer to the initial ansatz than the closest bounce-like extrema. This, however, is a limitation of all other known algorithms for finding bubble wall profiles. Meanwhile, we have already demonstrated in Sect. 4.1, our that our algorithm is free from the first problem as the guess of the initial ansatz ensures that the error functions are generically bounded by 1 (but should be much less than 1). For the remaining two issues, a little more care is needed.

Let us examine the issue of oscillating solutions. Let the updated function be

$$A_i^{(n)} = A_i^{(0)} + \sum_{k=1}^{n-1} \varepsilon_i^{(k)}, \tag{29}$$

where  $A_i^{(0)}$  is the initial ansatz and  $\varepsilon_i^{(k)}$  are the correction functions. Suppose that, for field  $\phi_i$ , the successive correction functions begin oscillating at iteration  $n$ , so that  $\varepsilon_i^{(n)} = -\varepsilon_i^{(n+1)}$ . But this means that the equations of motion for  $A_i^{(n+2)} = A_i^{(n)} + \varepsilon_i^{(n)} + \varepsilon_i^{(n+1)}$  can be written before Taylor expanding as

$$\frac{\partial^2[A_i^{(n)} + \varepsilon_i^{(n)} + \varepsilon_i^{(n+1)}]}{\partial\rho^2} + \frac{2}{\rho} \frac{\partial[A_i^{(n)} + \varepsilon_i^{(n)} + \varepsilon_i^{(n+1)}]}{\partial\rho} + \frac{\partial V(\phi)}{\partial\phi_i} \Big|_{\{A_k^{(n)} + \varepsilon_k^{(n)} + \varepsilon_k^{(n+1)}\}}$$

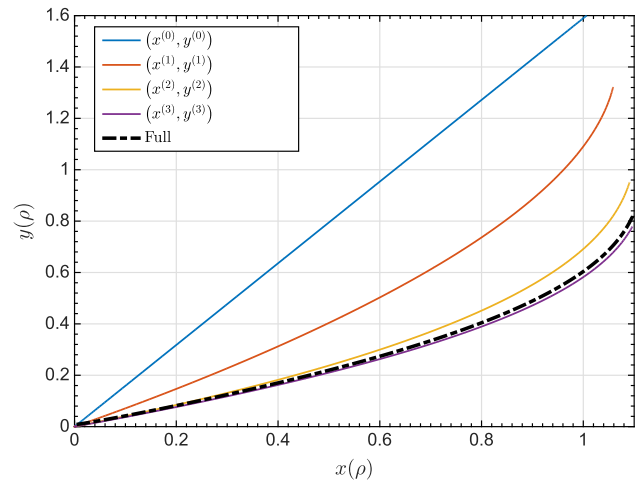


**Fig. 3** The tunneling trajectory in the space of the  $x$  and  $y$  fields at the level of the base ansatz (solid straight line), and including the first three iterative corrections (solid curved lines). Also included is the numerical result, independent of our semi-analytic method, from Ref. [43] (dashed curve)

$$= \frac{\partial^2 A_i^{(n)}}{\partial\rho^2} + \frac{2}{\rho} \frac{\partial A_i^{(n)}}{\partial\rho} + \frac{\partial V}{\partial\phi_i} \Big|_{\{A_1^{(n+2)}, \dots, A_i^{(n)}, A_{i_1}^{(n+2)}, \dots\}} = 0. \tag{30}$$

Thus, in the case of a single field, an oscillating solution means that corrected field at the order where oscillation begins has solved the equations of motion exactly. In the multi-field case, as the fields  $\phi_{j \neq i}$  converge without oscillating corrections, the changes to the derivative of the potential energy will diminish and thus will resemble the single-field case. In the case that more than one field has begun to receive oscillating corrections, this could prevent a rapid convergence but does not necessarily preclude it as the equations for the fields are still coupled.

In Newton’s method of finding roots, a major issue is when the derivative of the function becomes zero or undefined. The closest analogy to our method is the case where the mass matrix  $\frac{\partial^2 V(\phi)}{\partial\phi_i\phi_j} \Big|_{A^{(n)}}$  becomes zero or singular. In fact this is not an issue, as we can demonstrate. In the case that the mass matrix is zero, the differential equations become

$$\frac{\partial^2 \varepsilon_i}{\partial\rho^2} + \frac{2}{\rho} \frac{\partial \varepsilon_i}{\partial\rho} = B_i(\rho). \tag{31}$$

This is easily solved as

$$\varepsilon_i = \beta_0 + \frac{\beta_{-1}}{\rho} + \int_0^\rho \frac{dy}{y^2} \int_0^y x^2 B(x) dx \tag{32}$$

where  $\beta_0$  and  $\beta_{-1}$  are both zero if the mass is zero everywhere. The case to consider is when the mass matrix is singular. This in fact does arise quite typically at some spatial points, but this is not a problem because the matrix inverse is not needed, and zero eigenvalues can be treated easily by

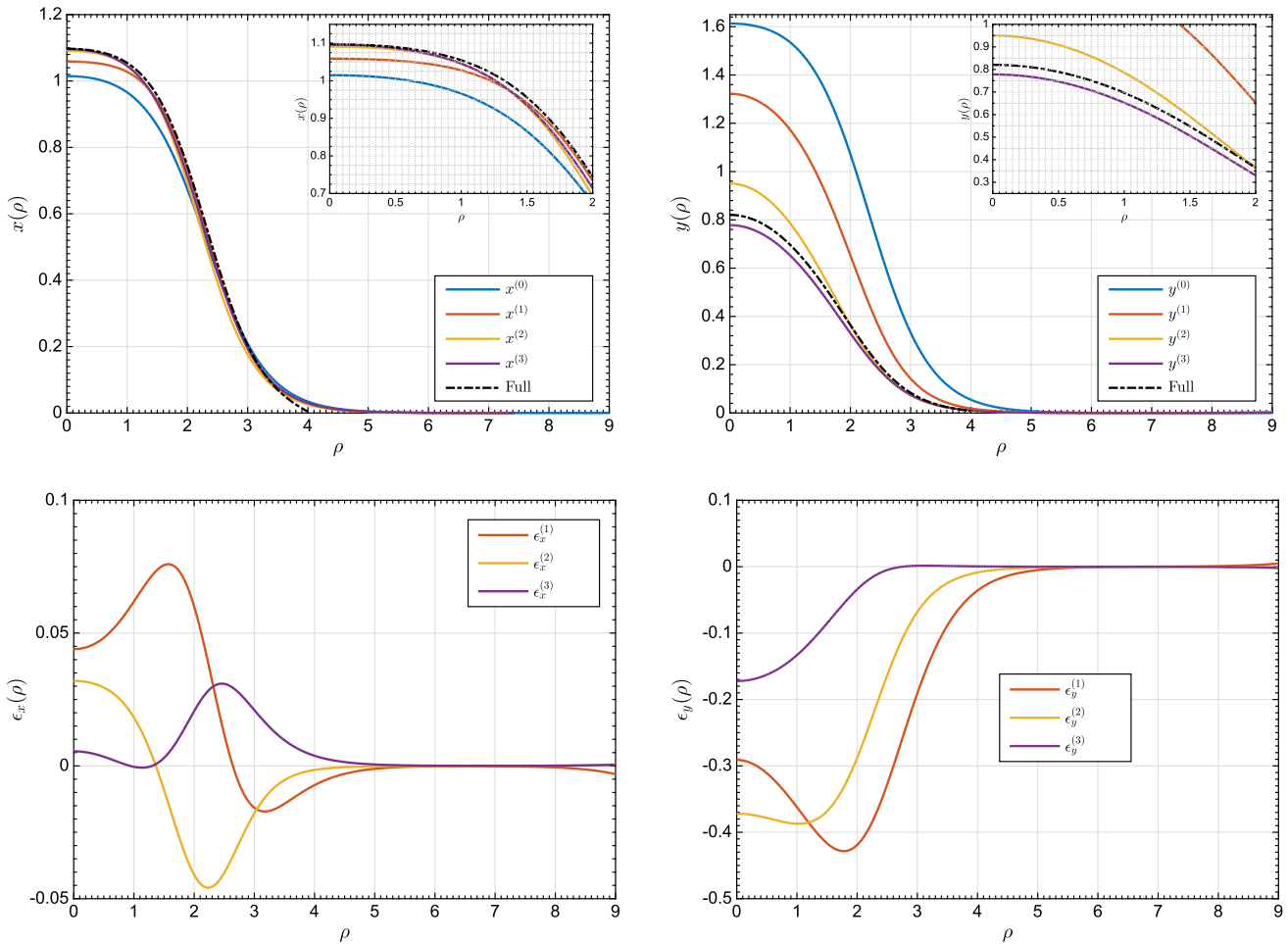


**Fig. 4** The base ansatz form, first three iterations of corrections and the full numerical result of the  $x$  and  $y$  fields are presented in the *top left* and *top right panels*, respectively. The first three iterative corrections

to the ansatz form of the  $x$  and  $y$  fields are given in the *bottom left* and *bottom right panels*, respectively

using singular value decomposition or strategic placement of the step functions. Also, this issue is avoided if the full inhomogeneous differential equation is directly solved numerically.

**5 Comparison with a solved example**

We apply our method with the sample potential given in [43]

$$V(x, y) = (x^2 + y^2) \left[ 1.8(x - 1)^2 + 0.2(y - 1)^2 - \delta \right]. \tag{33}$$

For  $\delta = 0.4$  the potential deforms quite dramatically from the initial Ansatz so the convergence will be slower than for a typical case. We make a rotation in field basis  $(x, y) \mapsto (u, v)$  such that  $u$  traces a straight line path from the origin to the global minimum and  $v$  is of course orthogonal to  $u$ . Our one dimensional potential is then given writing the potential in the rotated basis and setting  $v$  to zero. We then rescale such

that the minimum is at  $u = 1$  and then we divide by  $|E|$  to get

$$\frac{V(u, 0)}{|E|} = 0.36u^2 - u^3 + 0.57u^4. \tag{34}$$

We then use our analytic formulas to write the ansatz and make the appropriate rescalings to  $u(\rho)$  and  $\rho$  such that the ansatz is the solution to the original 1D potential. In the  $(x, y)$  basis the ansatz is

$$x(\rho) = 1.046 \left( 1 - \tanh \left[ \frac{\rho - 0.437}{1} \right] \right), \tag{35}$$

$$y(\rho) = 1.663 \left( 1 - \tanh \left[ \frac{\rho - 0.437}{1} \right] \right). \tag{36}$$

Note that the wall width is only equal to 1 due to the rescaling. We have to sanitize our initial ansatz to set the derivative to zero as  $\rho \mapsto 0$  or the correction diverges due to the  $\phi'/t$  term in the differential equations. To achieve this we subtract from our initial ansatz

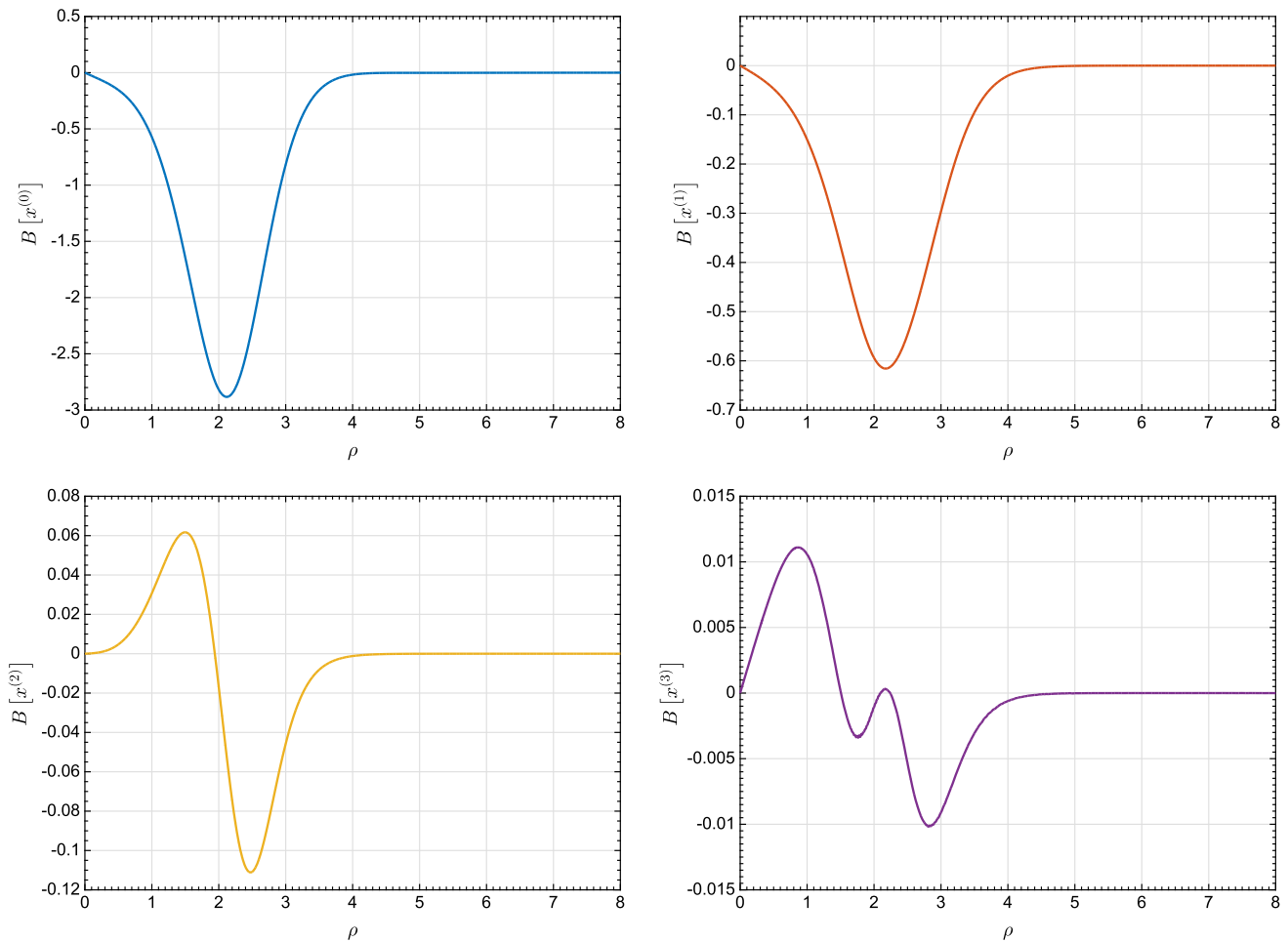


**Fig. 5** The error function,  $B$ , of the ansatz solution  $x^{(0)}$  when applied to the field equations, and the same for the ansatz solution including the first three perturbative corrections denoted by  $x^{(n)} = x^{(n-1)} + \varepsilon^{(n)}$

$$\delta x(\rho) = \left. \frac{\partial x}{\partial \rho} \right|_{\rho=0} \exp \left[ - \left. \frac{\partial x}{\partial \rho} \right|_{\rho=0} \rho \right], \tag{37}$$

$$\delta y(\rho) = \left. \frac{\partial y}{\partial \rho} \right|_{\rho=0} \exp \left[ - \left. \frac{\partial y}{\partial \rho} \right|_{\rho=0} \rho \right]. \tag{38}$$

If one uses a small amount of step functions to approximate the spacetime dependent mass matrix one can find that the corrections  $\delta \varepsilon_i$  are slowly converging. In particular it is useful to have step functions for regions where  $m_{12}(\rho) = 0$  and  $m_i^2 < 0$  as the functional form of the solutions changes in these regions. In the former the differential equations decouple for a region, for the latter, some of the exponents  $\alpha_i$  are imaginary (but the  $\varepsilon_i(\rho)$  remains real).

In Fig. 3 we show each iteration of the trajectory in the  $(x(\rho), y(\rho))$  field space, along with the numerical trajectory as derived in [43]. The algorithm essentially converges after 3 perturbations. In Fig. 4 we show the  $x$  and  $y$  fields starting with the base ansatz forms  $x^{(0)}$  and  $y^0$ , and then including the first three perturbative corrections, denoted by

$$\phi^{(n)}(\rho) = \phi^{(n-1)}(\rho) + \varepsilon_{\phi}^{(n)}(\rho), \quad \text{with } \phi = x, y. \tag{39}$$

Figure 4 also includes the error functions  $\varepsilon_{\phi}^{(n)}(\rho)$  to illustrate the overall and diminishing magnitude of corrections to the fields in successive perturbations.

In Fig. 5 we show the error function to the ansatz for the  $x$  field,  $B_x(\rho)$ , which arises from the inhomogeneous part of Eq. (16). The error function is given for the bare ansatz solution of  $x(\rho)$  and the first three perturbative corrections. We point out that the magnitude of the error is reduced by roughly a factor of 5–10 from each perturbative correction, and that the error function for  $x^{(3)}(\rho)$  has reduced in magnitude by a factor of 300 compared to that of  $x^{(0)}(\rho)$ .

### 6 Conclusion

In this work we presented a new method to calculate the bubble profile in a bounce solution for a multi-field potential with a false vacuum. The method uses fitted functions to estimate the parameters of the single-field kink solution

which is used as an ansatz form. It then applies this form to the full multi-field potential, which receive perturbative correction functions that are reduced to elementary numerical integrals. We have argued that the perturbative series of corrections should converge quadratically, and is immune to the issues of the analogous Newton's method. This method is shown to be effective in solving a toy model with two scalar fields.

**Acknowledgements** Funding was provided by Australian Research Council (Grant No. CE110001004).

**Open Access** This article is distributed under the terms of the Creative Commons Attribution 4.0 International License (<http://creativecommons.org/licenses/by/4.0/>), which permits unrestricted use, distribution, and reproduction in any medium, provided you give appropriate credit to the original author(s) and the source, provide a link to the Creative Commons license, and indicate if changes were made. Funded by SCOAP<sup>3</sup>.

## References

- B.A. Bassett, S. Tsujikawa, D. Wands, *Rev. Mod. Phys.* **78**, 537 (2006). doi:[10.1103/RevModPhys.78.537](https://doi.org/10.1103/RevModPhys.78.537)
- A. Aravind, D. Lorshbough, S. Paban, *Phys. Rev. D* **89**(10), 103535 (2014). doi:[10.1103/PhysRevD.89.103535](https://doi.org/10.1103/PhysRevD.89.103535)
- M. Dine, P. Draper, A. Monteux, *JHEP* **07**, 146 (2014). doi:[10.1007/JHEP07\(2014\)146](https://doi.org/10.1007/JHEP07(2014)146)
- R. Bouso, D. Harlow, L. Senatore, *Phys. Rev. D* **91**, 083527 (2015). doi:[10.1103/PhysRevD.91.083527](https://doi.org/10.1103/PhysRevD.91.083527)
- B. Garbrecht, P. Millington, *Phys. Rev. D* **91**, 105021 (2015). doi:[10.1103/PhysRevD.91.105021](https://doi.org/10.1103/PhysRevD.91.105021)
- A. Kasai, Y. Ookouchi, *Phys. Rev. D* **91**, 126002 (2015). doi:[10.1103/PhysRevD.91.126002](https://doi.org/10.1103/PhysRevD.91.126002)
- M. Trodden, *Rev. Mod. Phys.* **71**, 1463 (1999). doi:[10.1103/RevModPhys.71.1463](https://doi.org/10.1103/RevModPhys.71.1463)
- J.M. Cline, in *Les Houches Summer School-Session 86: Particle Physics and Cosmology: The Fabric of Spacetime Les Houches, France, July 31-August 25* (2006)
- C. Balázs, A. Mazumdar, E. Pukartas, G. White, *JHEP* **01**, 073 (2014). doi:[10.1007/JHEP01\(2014\)073](https://doi.org/10.1007/JHEP01(2014)073)
- C. Balázs, M. Carena, A. Menon, D.E. Morrissey, C.E.M. Wagner, *Phys. Rev. D* **71**, 075002 (2005). doi:[10.1103/PhysRevD.71.075002](https://doi.org/10.1103/PhysRevD.71.075002)
- J. Kozaczuk, S. Profumo, L.S. Haskins, C.L. Wainwright, *JHEP* **01**, 144 (2015). doi:[10.1007/JHEP01\(2015\)144](https://doi.org/10.1007/JHEP01(2015)144)
- A. Tommi, K. Kimmo, T. Kimmo, V. Ville J. Cosmol. Astropart. Phys. **2016**, 057 (2016). doi:[10.1088/1475-7516/2016/08/057](https://doi.org/10.1088/1475-7516/2016/08/057)
- C.W. Chiang, K. Fuyuto, E. Senaha (2016) *Phys. Lett. B* **762**, 315–320. doi:[10.1016/j.physletb.2016.09.052](https://doi.org/10.1016/j.physletb.2016.09.052)
- V.Q. Phong, N.C. Thao, H.N. Long (2015). [arXiv:1511.00579](https://arxiv.org/abs/1511.00579)
- T. Rindler-Daller, B. Li, P.R. Shapiro, M. Lewicki, J.D. Wells, in *Meeting of the APS Division of Particles and Fields (DPF 2015) Ann Arbor, Michigan, USA, August 4-8, 2015* (2015). <https://inspirehep.net/record/1401203/files/arXiv:1510.08369.pdf>
- G. Arcadi, L. Covi, M. Nardecchia, *Phys. Rev. D* **92**(11), 115006 (2015). doi:[10.1103/PhysRevD.92.115006](https://doi.org/10.1103/PhysRevD.92.115006)
- W. Chao, *JCAP* **1508**(08), 055 (2015). doi:[10.1088/1475-7516/2015/08/055](https://doi.org/10.1088/1475-7516/2015/08/055)
- G.C. Dorsch, S.J. Huber, K. Mimasu, J.M. No, *Phys. Rev. Lett.* **113**(21), 211802 (2014). doi:[10.1103/PhysRevLett.113.211802](https://doi.org/10.1103/PhysRevLett.113.211802)
- X. Chang, R. Huo, *Phys. Rev. D* **89**(3), 036005 (2014). doi:[10.1103/PhysRevD.89.036005](https://doi.org/10.1103/PhysRevD.89.036005)
- M. Lewicki, T. Rindler-Daller, J.D. Wells, *JHEP* **06**, 055 (2016). doi:[10.1007/JHEP06\(2016\)055](https://doi.org/10.1007/JHEP06(2016)055)
- M. Dhuria, C. Hati, U. Sarkar, *Phys. Lett. B* **756**, 376 (2016). doi:[10.1016/j.physletb.2016.03.018](https://doi.org/10.1016/j.physletb.2016.03.018)
- C. Lee, V. Cirigliano, M.J. Ramsey-Musolf, *Phys. Rev. D* **71**, 075010 (2005). doi:[10.1103/PhysRevD.71.075010](https://doi.org/10.1103/PhysRevD.71.075010)
- V. Cirigliano, M.J. Ramsey-Musolf, S. Tulin, C. Lee, *Phys. Rev. D* **73**, 115009 (2006). doi:[10.1103/PhysRevD.73.115009](https://doi.org/10.1103/PhysRevD.73.115009)
- D.J.H. Chung, B. Garbrecht, M.J. Ramsey-Musolf, S. Tulin, *JHEP* **2009**(12), 067 (2009). doi:[10.1088/1126-6708/2009/12/067](https://doi.org/10.1088/1126-6708/2009/12/067)
- D.J.H. Chung, B. Garbrecht, M.J. Ramsey-Musolf, S. Tulin, *Phys. Rev. D* **81**, 063506 (2010). doi:[10.1103/PhysRevD.81.063506](https://doi.org/10.1103/PhysRevD.81.063506)
- D.E. Morrissey, M.J. Ramsey-Musolf, *New J. Phys.* **14**, 125003 (2012). doi:[10.1088/1367-2630/14/12/125003](https://doi.org/10.1088/1367-2630/14/12/125003)
- G. Krnjaic (2016). [arXiv:1606.05344](https://arxiv.org/abs/1606.05344)
- S. Ipek, J. March-Russell, *Phys. Rev. D* **93**(12), 123528 (2016). doi:[10.1103/PhysRevD.93.123528](https://doi.org/10.1103/PhysRevD.93.123528)
- M. Fukushima, S. Mizuno, *Phys. Rev. D* **93**(10), 103513 (2016). doi:[10.1103/PhysRevD.93.103513](https://doi.org/10.1103/PhysRevD.93.103513)
- T. Fujita, K. Kamada, *Phys. Rev. D* **93**(8), 083520 (2016). doi:[10.1103/PhysRevD.93.083520](https://doi.org/10.1103/PhysRevD.93.083520)
- M. Yamada, *Phys. Rev. D* **93**(8), 083516 (2016). doi:[10.1103/PhysRevD.93.083516](https://doi.org/10.1103/PhysRevD.93.083516)
- F. Takahashi, M. Yamada, *Phys. Lett. B* **756**, 216 (2016). doi:[10.1016/j.physletb.2016.03.020](https://doi.org/10.1016/j.physletb.2016.03.020)
- P.S.B. Dev, R.N. Mohapatra, *Phys. Rev. D* **92**(1), 016007 (2015). doi:[10.1103/PhysRevD.92.016007](https://doi.org/10.1103/PhysRevD.92.016007)
- J.E. Camargo-Molina, B. O'Leary, W. Porod, F. Staub, *Eur. Phys. J. C* **73**(10), 2588 (2013). doi:[10.1140/epjc/s10052-013-2588-2](https://doi.org/10.1140/epjc/s10052-013-2588-2)
- J.E. Camargo-Molina, B. O'Leary, W. Porod, F. Staub, *JHEP* **12**, 103 (2013). doi:[10.1007/JHEP12\(2013\)103](https://doi.org/10.1007/JHEP12(2013)103)
- N. Blinov, D.E. Morrissey, *JHEP* **03**, 106 (2014). doi:[10.1007/JHEP03\(2014\)106](https://doi.org/10.1007/JHEP03(2014)106)
- P. Burda, R. Gregory, I.G. Moss, *Phys. Rev. Lett.* **115**, 071303 (2015). doi:[10.1103/PhysRevLett.115.071303](https://doi.org/10.1103/PhysRevLett.115.071303)
- X. Li, M.B. Voloshin, *Phys. Rev. D* **90**, 105028 (2014). doi:[10.1103/PhysRevD.90.105028](https://doi.org/10.1103/PhysRevD.90.105028)
- L.M. Krauss, A.J. Long, *Phys. Rev. D* **89**, 085023 (2014). doi:[10.1103/PhysRevD.89.085023](https://doi.org/10.1103/PhysRevD.89.085023)
- D. Chowdhury, R.M. Godbole, K.A. Mohan, et al. *J. High Energ. Phys.* **2014**, 110 (2014). doi:[10.1007/JHEP02\(2014\)110](https://doi.org/10.1007/JHEP02(2014)110)
- S.R. Coleman, *Phys. Rev. D* **15**, 2929 (1977). doi:[10.1103/PhysRevD.15.2929](https://doi.org/10.1103/PhysRevD.15.2929)(Erratum: *Phys. Rev. D* **16**, 1248(1977))
- S. Profumo, L. Ubaldi, C. Wainwright, *Phys. Rev. D* **82**, 123514 (2010). doi:[10.1103/PhysRevD.82.123514](https://doi.org/10.1103/PhysRevD.82.123514)
- C.L. Wainwright, *Comput. Phys. Commun.* **183**, 2006 (2012). doi:[10.1016/j.cpc.2012.04.004](https://doi.org/10.1016/j.cpc.2012.04.004)
- J.M. Moreno, M. Quirós, M. Seco, *Nucl. Phys. B* **526**, 489 (1998). doi:[10.1016/S0550-3213\(98\)00283-1](https://doi.org/10.1016/S0550-3213(98)00283-1)
- P. John, *Phys. Lett. B* **452**, 221 (1999). doi:[10.1016/S0370-2693\(99\)00272-5](https://doi.org/10.1016/S0370-2693(99)00272-5)
- T. Konstandin, S.J. Huber, *JCAP* **2006**(06), 021 (2006). <http://stacks.iop.org/1475-7516/2006/i=06/a=021>
- E. Nugaev, *Commun. Nonlinear Sci. Numer. Simul.* **20**(2), 443 (2015). doi:[10.1016/j.cnsns.2014.06.016](https://doi.org/10.1016/j.cnsns.2014.06.016)
- V.A. Gani, M.A. Lizunova, R.V. Radomskiy, *JHEP* **04**, 043 (2016). doi:[10.1007/JHEP04\(2016\)043](https://doi.org/10.1007/JHEP04(2016)043)
- G.A. White, *Phys. Rev. D* **93**(4), 043504 (2016). doi:[10.1103/PhysRevD.93.043504](https://doi.org/10.1103/PhysRevD.93.043504)
- M. Dine, R.G. Leigh, P.Y. Huet, A.D. Linde, D.A. Linde, *Phys. Rev. D* **46**, 550 (1992). doi:[10.1103/PhysRevD.46.550](https://doi.org/10.1103/PhysRevD.46.550)



## Chapter 6

---

# Particle cosmology in the NMSSM

---

## 6.1 Introductory remarks

The discovery of a Higgs boson of 125 GeV [107, 108] was the completion of the Standard Model and one of the most remarkable discoveries of the last century. It also makes electroweak baryogenesis difficult in the MSSM [47] and impossible in the Standard Model [109]. For the Standard Model the issue is that the electroweak phase transition is not strongly first order for a Higgs mass heavier than  $\sim 40$  GeV. Finally the Standard Model has no dark matter candidate and it is difficult for the Higgs to catalyze inflation.

For the MSSM such a heavy Higgs requires some amount of fine tuning – this is known as the little hierarchy problem [110]. Furthermore the MSSM requires light stops to catalyze a strongly first order electroweak phase transition which is virtually incompatible with collider searches. The NMSSM can catalyse a strongly first order phase transition through a weak scale singlet. Furthermore, the LSP provides a good dark matter candidate and there are many flat directions which can be exploited to catalyze inflation. In this work I explore the parameter space to verify the compatibility of the NMSSM these three pillars of particle cosmology – electroweak baryogenesis, dark matter and inflation.

## 6.2 Declaration for thesis chapter 6

### Declaration by candidate

In the case of the paper present contained in chapter 6, the nature and extent of my contribution was as follows:

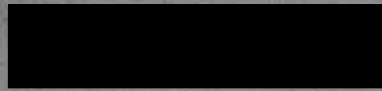
Publication	Nature of contribution	Extent of contribution
6	Worked on analytic derivations and numerical codes. Worked to understand the background needed and explained this to collaborators. Heavily involved in writeup. Contributed to discussions throughout	50%

The following coauthors contributed to the work. If the coauthor is a student at Monash, their percentage contribution is given:

<b>Author</b>	<b>Nature of contribution</b>	<b>Extent of contribution</b>
Csaba Balazs	Along with Anupam Mazumdar came up with the idea for the paper. Wrote a section and contributed to discussions throughout.	
Ernestas Pukartas	Heavily involved in implementation of numerical code. Co-wrote the paper with me apart from two sections written by Csaba Balazs and Anupam. Involved with discussions throughout	
Anupam Mazumdar	Along with Csaba Balazs came up with the concept. Wrote a section and contributed to ideas throughout.	

The undersigned hereby certify that the above declaration correctly reflects the nature and extent of the candidate and co-authors' contributions to this work.

Graham White



Csaba Balazs



Ernestas Pukartas



Anupam Mazumdar



Date:

3.04.2017

**6.3 Published material for chapter 6:  
Baryogenesis, dark matter and inflation in  
the Next-to-Minimal Supersymmetric  
Standard Model**

# Baryogenesis, dark matter and inflation in the next-to-minimal supersymmetric standard model

Csaba Balázs,<sup>a,b,c,d</sup> Anupam Mazumdar,<sup>e</sup> Ernestas Pukartas<sup>e</sup> and Graham White<sup>a,b,c</sup>

<sup>a</sup>*School of Physics, Monash University,  
Victoria 3800, Australia*

<sup>b</sup>*Monash Centre for Astrophysics, Monash University,  
Victoria 3800 Australia*

<sup>c</sup>*ARC Centre of Excellence for Particle Physics, Monash University,  
Victoria 3800 Australia*

<sup>d</sup>*Australian Collaboration for Accelerator Science, Monash University,  
Victoria 3800 Australia*

<sup>e</sup>*Consortium for Fundamental Physics, Lancaster University,  
Lancaster, LA1 4YB, U.K.*

*E-mail:* [csaba.balazs@monash.edu](mailto:csaba.balazs@monash.edu), [a.mazumdar@lancaster.ac.uk](mailto:a.mazumdar@lancaster.ac.uk),  
[e.pukartas@lancaster.ac.uk](mailto:e.pukartas@lancaster.ac.uk), [graham.white@monash.edu](mailto:graham.white@monash.edu)

**ABSTRACT:** Explaining baryon asymmetry, dark matter and inflation are important elements of a successful theory that extends beyond the Standard Model of particle physics. In this paper we explore these issues within Next-to-Minimal Supersymmetric Standard Model (NMSSM) by studying the conditions for a strongly first order electroweak phase transition, the abundance of the lightest supersymmetric particle (LSP), and inflation driven by a gauge invariant flat direction of MSSM - made up of right handed squarks. We present the regions of parameter space which can yield successful predictions for cosmic microwave background (CMB) radiation through inflation, the observed relic density for dark matter, and successful baryogenesis. Constraints by collider measurements (such as the recent Higgs mass bound), branching ratios of rare, flavour violating decays, and the invisible Z decay width are also imposed. We explore where dark matter interactions with xenon nuclei would fall within current bounds of XENON100 and the projected limits for the XENON1T and LUX experiments.

**KEYWORDS:** Beyond Standard Model, Supersymmetric Standard Model, CP violation, Renormalization Group

ARXIV EPRINT: [1309.5091](https://arxiv.org/abs/1309.5091)

---

**Contents**

<b>1</b>	<b>Introduction</b>	<b>1</b>
<b>2</b>	<b>The next-to-minimal supersymmetric standard model</b>	<b>3</b>
<b>3</b>	<b>Baryon asymmetry</b>	<b>4</b>
3.1	The scalar potential at high temperature	5
<b>4</b>	<b>Constraints applied</b>	<b>8</b>
4.1	Scanning the parameter space for dark matter and first order phase transition	10
<b>5</b>	<b>Gauge invariant inflaton</b>	<b>14</b>
5.1	Brief review of inflation	14
5.2	Parameter space for inflation, dark matter and baryogenesis	16
<b>6</b>	<b>Conclusions</b>	<b>18</b>
<b>A</b>	<b>Solving the toy model</b>	<b>18</b>

---

**1 Introduction**

Beyond the Standard Model (BSM) particle physics should aspire to include the following three cosmological cornerstones.

1. Inflation can explain the current temperature anisotropy in the cosmic microwave background (CMB) radiation measured by the Planck satellite [1]. Since inflation dilutes matter, the end of inflation must excite all the relevant Standard Model (SM) degrees of freedom without any excess of dark matter and dark radiation, along with the seed initial perturbations for the structure formation. This can be achieved minimally by embedding inflation within a visible sector of BSM, such as the Minimal Supersymmetric Standard Model (MSSM) [2–4]. For a review on inflation, see [5].
2. Dark matter is required to form the observed large scale structures of the Universe [6]. The lightest supersymmetric particle (LSP) is an ideal dark matter candidate since it is a weakly interacting massive particle (WIMP), and its interactions with the superpartners are sufficient to keep them in thermal bath until they decouple due to the expansion of the Universe and their abundance freezes out [7]. The thermal WIMP scenario is attractive due to its predictive power in estimating the abundance of the dark matter and potential link to the weak scale. Within the MSSM the neutralino plays this role of dark matter ideally. For reviews on dark matter, see [8, 9].

3. Baryon asymmetry, at the observed level of one part in about  $10^{10}$ , is necessary to realize Big Bang nucleosynthesis [10]. This asymmetry can be achieved by satisfying the three Sakharov conditions [11]: baryon number ( $B$ ) violation, charge ( $C$ ) and/or charge-parity ( $CP$ ) violation, and the out-of-equilibrium condition. These ingredients are present within the SM, but with a 126 GeV Higgs the model lacks sufficiently strong first order phase transition to keep the baryon asymmetry intact. For a review on baryon asymmetry, see [12].

The MSSM provides all three ingredients, however the electroweak baryogenesis in its context is becoming more and more constrained by the LHC data. In the simplest MSSM electroweak baryogenesis scenario (where the CP-violating phases catalyzing the asymmetry reside in the gaugino sector) it is getting hard, if not impossible, to generate enough asymmetry with a 126 GeV standard-like Higgs boson in a natural manner [13]. So we turn our attention to the electroweak baryogenesis in the Next to Minimal Supersymmetric Standard Model (NMSSM). (For a review on the NMSSM, see [14].) The NMSSM has more flexibility as it introduces a new Standard Model gauge singlet which helps achieving a strongly first order electroweak phase transition, since the order parameter is now determined by the singlet sector and becomes essentially independent of the Standard Model-like Higgs mass.

In this work, we present a highly efficient algorithm to delineate regions of the NMSSM with strongly first order phase transition. After finding these regions we reject model points where the neutralino relic abundance exceeds the upper limit imposed by Planck by more than  $3\sigma$ . Some of the dark matter particles, in particular those with high singlino fraction, tend to escape the most stringent bounds given by the XENON100 [15] and TEXONO [16] direct detection experiments, but they fall close to the regions where tantalizing positive signals from DAMA [17, 18], CoGeNT [19], CRESST-II [20] and CDMS [21] could be potentially explained by dedicated search of light DM. The NMSSM singlet sector can also affect other properties of dark matter. With a sizable singlino fraction the lightest neutralino can be very light even in the presence of heavy super-partners [22, 23].

The joint parameter space for satisfactory neutralino dark matter and first order electroweak phase transition has been studied in [24]. Here we supersede that study by a new algorithm for finding regions where electroweak baryogenesis can be successful, by considering the parameter space for neutralino dark matter and successful inflation driven by the MSSM squarks, and updating all experimental constraints, especially the vital Higgs limits from the LHC [25, 26].

In the next section we briefly summarize the relevant features of the NMSSM. In section 3 we examine the baryon washout condition and derive an algorithm to find regions of its parameter space satisfying a strongly first order electroweak phase transition. In section 4 we summarize the constraints applied to the theory, and in 4.1 we show model points jointly satisfying inflation, baryogenesis, and dark matter abundance. We discuss implications on inflation in 5 and finally conclude.

## 2 The next-to-minimal supersymmetric standard model

In this work we consider the  $Z_3$  conserving, scale invariant, version of the the Next-to-Minimal Supersymmetric Standard Model [27, 28] which is defined by the superpotential (see, for instance, ref. [14])

$$W = W^{\text{MSSM}}|_{\mu=0} + \lambda \widehat{S} \widehat{\mathbf{H}}_u \widehat{\mathbf{H}}_d + \frac{1}{3} \kappa \widehat{S}^3. \quad (2.1)$$

Above  $W^{\text{MSSM}}|_{\mu=0}$  is the MSSM superpotential without the  $\mu$  term (as defined in ref. [29]) and  $\widehat{\mathbf{H}}_{u,d}$  ( $\widehat{S}$ ) are SU(2) doublet (singlet) Higgs superfields:  $\widehat{\mathbf{H}}_u = (\widehat{H}_1^+, \widehat{H}_1^0)^T$ ,  $\widehat{\mathbf{H}}_d = (\widehat{H}_2^0, \widehat{H}_2^+)^T$ . The superscript in  $\widehat{H}_i^{\pm,0}$  denotes the electric charge of the component. The corresponding soft supersymmetry breaking scalar potential

$$V_{\text{soft}} = V_{\text{soft}}^{\text{MSSM}}|_{B=0} + V_{\text{soft}}^{\text{NMSSM}} \quad (2.2)$$

contains the MSSM soft terms with  $B$  set to zero [29] and

$$V_{\text{soft}}^{\text{NMSSM}} = m_s^2 |S|^2 - \lambda A_\lambda S \mathbf{H}_u \mathbf{H}_d + \frac{1}{3} \kappa A_\kappa S^3 + \text{h.c.} \quad (2.3)$$

Here  $\mathbf{H}_{u,d}$  and  $S$  denote the scalar components of the neutral Higgs superfields. During electroweak symmetry breaking the neutral components of these will acquire a non-zero vacuum expectation value.<sup>1</sup> The MSSM terms above are [29]

$$V_{\text{soft}}^{\text{MSSM}}|_{B=0} = V_{\text{softH}}^{\text{MSSM}} + V_{\text{scalar}} + V_{\text{gaugino}} + V_{\text{tri}}. \quad (2.4)$$

It is important for electroweak baryogenesis that the Higgs potential

$$V = V_D + V_{\text{softH}}^{\text{MSSM}} + V_{\text{soft}}^{\text{NMSSM}} + V_{\text{H}}^{\text{NMSSM}}, \quad (2.5)$$

receives contributions both from the MSSM

$$V_D = \frac{g_1^2 + g_2^2}{8} (\mathbf{H}_u^2 - \mathbf{H}_d^2)^2, \quad (2.6)$$

$$V_{\text{softH}}^{\text{MSSM}} = m_{H_u}^2 |\mathbf{H}_u|^2 + m_{H_d}^2 |\mathbf{H}_d|^2, \quad (2.7)$$

and the NMSSM

$$V_{\text{H}}^{\text{NMSSM}} = \lambda^2 |S|^2 (|\mathbf{H}_u|^2 + |\mathbf{H}_d|^2) + \lambda^2 |\mathbf{H}_u \mathbf{H}_d|^2 + \kappa^2 |S|^4 + \kappa \lambda S^2 \mathbf{H}_u^* \mathbf{H}_d^* + \text{h.c.} \quad (2.8)$$

While  $\lambda$  is a free parameter, perturbativity up to the Grand Unification Theory scale restricts it below 0.7. In this work we respect this limit and do not take  $\lambda$  higher. The cubic singlet coupling  $\kappa$  breaks the global U(1) Peccei-Quinn symmetry [34], and when  $\kappa$

---

<sup>1</sup>In this version of the NMSSM the formation of cosmological domain walls during electroweak symmetry breaking is a concern. The solution of the domain wall problem has been discussed, amongst others, in refs. [30–33]. It has been shown by Panagiotakopoulos and Tamvakis that the cosmological domain wall problem is eliminated after imposing a  $Z_2$  R-symmetry on the non-renormalizable sector of the NMSSM.

vanishes this symmetry is restored. For simplicity, in this work we consider the limit where  $\kappa$  is small, that is the Peccei-Quinn limit. This limit is also motivated by the desire to obtain a light dark matter candidate, as indicated in the next paragraph.

In this work we the lightest neutralino is the dark matter candidate. Neutralinos in the NMSSM are admixtures of the fermionic components of five superfields: the  $U(1)_Y$  gauge boson  $\widehat{B}$ , the neutral component of the  $SU(2)_L$  gauge boson  $\widehat{W}_3$ , the neutral components of each Higgs doublet  $\widehat{H}_u$  and  $\widehat{H}_d$ , and the singlet  $\widehat{S}$ . The mass of the lightest neutralino originates from soft supersymmetry breaking

$$V_{\text{gaugino}} = \frac{1}{2}(M_1\widetilde{B}\widetilde{B} + M_2\widetilde{W}_i\widetilde{W}_i + M_3\widetilde{G}_a\widetilde{G}_a), \quad (2.9)$$

where the fields above are the fermionic components of the vector superfields. The admixture of the lightest neutralino is controlled by the neutralino mass matrix which, in the  $(-i\widetilde{B}, -i\widetilde{W}_3, \widetilde{H}_d, \widetilde{H}_u, \widetilde{S})$  basis, is given by the symmetric matrix [14]

$$\mathcal{M}_{\widetilde{\chi}} = \begin{pmatrix} M_1 & 0 & -\frac{g_1\langle H_d \rangle}{\sqrt{2}} & \frac{g_1\langle H_u \rangle}{\sqrt{2}} & 0 \\ & M_2 & \frac{g_2\langle H_d \rangle}{\sqrt{2}} & -\frac{g_2\langle H_u \rangle}{\sqrt{2}} & 0 \\ & & 0 & -\lambda\langle S \rangle & -\lambda\langle H_u \rangle \\ & & & 0 & -\lambda\langle H_d \rangle \\ & & & & \kappa\langle S \rangle \end{pmatrix}. \quad (2.10)$$

Here  $g_{1,2}$  are the  $U(1)_Y$  and  $SU(2)_L$  gauge couplings, and  $\langle X \rangle$  denote vacuum expectation values. To obtain the mass eigenstates, we have to diagonalize the neutralino mass matrix. This can be done with the help of a unitary matrix  $N_{ij}$  whose entries provide the mixing amongst gauginos, higgsinos and the singlino. The lightest neutralino, for example, is given by:

$$\widetilde{\chi}_1^0 = N_{11}\widetilde{B} + N_{12}\widetilde{W}^0 + N_{13}\widetilde{H}_d^0 + N_{14}\widetilde{H}_u^0 + N_{15}\widetilde{S}, \quad (2.11)$$

where  $|N_{11}|^2$  gives the bino,  $|N_{12}|^2$  the wino,  $|N_{13}|^2 + |N_{14}|^2$  the higgsino and  $|N_{15}|^2$  the singlino fraction. When, for example,  $\kappa\langle S \rangle$  is the smallest entry of the mass matrix, the lightest neutralino tends to be singlino dominated. Alternatively, a small  $M_1$  entry can render the lightest neutralino to acquire mostly bino admixture.

### 3 Baryon asymmetry

As mentioned above, three conditions have to be met to generate baryon asymmetry:  $B$  violation,  $C$  and/or  $CP$  violation, and departure from thermal equilibrium. Remarkably, these conditions can be met in the Standard Model of particle physics. The difference of the baryon and lepton numbers,  $B - L$ , is an exactly conserved quantity in the SM (and within NMSSM). While at low temperatures  $B$  and  $L$  are individually conserved with a good approximation, at very high temperatures baryon number violation is unsuppressed through sphaleron processes [12, 35]. Unfortunately, there is not enough  $CP$  violation in the standard CKM matrix to generate the observed baryon asymmetry. In the NMSSM,

sufficient amount of  $CP$  violation can be added to the gaugino and singlino sectors. Provided that the third Sakharov condition is met, it is possible to generate the observed asymmetry in the NMSSM. In this paper we focus on the latter: where in the NMSSM parameter space a strong first order electroweak phase transition can be achieved?

At very high temperatures electroweak symmetry is restored [36]. As the Universe cools, the electroweak symmetry is broken during the phase transition. If the phase transition is first order, the electroweak symmetry is broken through tunneling processes. This occurs when the effective potential has degenerate minima  $\{0, \varphi_c\}$ , where  $\varphi$  denotes the Higgs vacuum expectation value (VEV). In such a case bubbles of broken phase grow in the otherwise symmetric vacuum, until the phase transition is complete and symmetry is broken everywhere in the Universe. Within the symmetric phase sphaleron processes, and therefore baryon violating processes are unsuppressed whereas they are exponentially dampened within the broken phase. The  $C$  and  $CP$  violating processes near the bubble walls can create a large baryon asymmetry. If the phase transition is strongly first order the baryon asymmetry will be preserved [12]. To this end we require [37–47]

$$\frac{T_c}{\varphi_c} \equiv \gamma \gtrsim 1, \quad (3.1)$$

where  $T_c$  is the temperature at which the effective potential obtains degenerate minima. This is known as the baryon washout condition. Equation (3.1) only approximately quantifies the baryon washout. A more precise condition can be obtained in the gauge invariant formalism of electroweak baryogenesis [48, 49]. The Standard Model cannot satisfy the baryon washout condition for a Higgs like particle of mass about 125 GeV [50–52]. This experimental constraint also all but rules out electroweak baryogenesis in the MSSM [53]. Recent work however has suggested that the NMSSM is compatible with a strongly first order phase transition and the observed Higgs mass [54]. As noted before the baryon washout condition is not the only hurdle that prevents the Standard Model from being consistent with electroweak baryogenesis, there is also the issue of insufficient  $CP$  violation. Here we focus on the baryon washout condition and postpone the detailed investigation of the relevant  $CP$  violating phases in the NMSSM to a later work.

### 3.1 The scalar potential at high temperature

Previous analysis of the electroweak phase transition within the NMSSM near the Peccei-Quinn limit found that the parameter space that satisfies the baryon washout condition is heavily constrained [54]. Seeing as we also wish to satisfy other, in some cases rather strict, experimental and cosmological constraints, we are motivated to find a numerically efficient way of finding regions of parameter space that allow for a strongly first order phase transition. In a prior analysis, Wagner *et al.* considered a toy model which included the tree level effective potential of the NMSSM at the Peccei-Quinn limit with the largest temperature corrections. Our strategy will be to derive a semi-analytic solution to the toy model from ref. [54] and consider higher order temperature corrections, loop corrections and small deviations from the so called Peccei-Quinn limit as perturbations to the toy model solution. If we only scan regions of parameter space where our approximations hold,

it is numerically efficient to produce a very large volume of points that easily satisfy all of our cosmological and experimental constraints.

The one loop temperature corrections to the effective potential are:

$$V(T, m \pm 1) = g_{\pm} \mp \frac{T^4}{2\pi^2} \int_0^{\infty} dx x^2 \log \left( 1 \pm e^{-\sqrt{x^2 + \frac{m(\phi)^2}{T^2}}} \right), \quad (3.2)$$

where  $g_{\pm}$  is the number of fermionic or bosonic degrees of freedom respectively. Similarly the argument is + for fermions and - for bosons. The high temperature expansion is up to an overall temperature dependent constant [55]

$$\begin{aligned} V(T, m, +1) &\sim \frac{g_+ m^2(\phi) T^2}{24} - \frac{g_+ [m(\phi)^2]^{3/2}(\phi) T}{12\pi} - \frac{g_+ m(\phi)^4}{64\pi^2} \log \left( \frac{m(\phi)^2}{a_b T^2} \right) \\ &\equiv \frac{g_+ m^2(\phi) T^2}{24} - \frac{g_+ [m(\phi)^2]^{3/2}(\phi) T}{12\pi} + \Delta V_T, \end{aligned} \quad (3.3)$$

for bosons, and

$$\begin{aligned} V(T, m, -1) &\sim \frac{g_- m^2(\phi) T^2}{48} + \frac{g_- m(\phi)^4}{64\pi^2} \log \left( \frac{m(\phi)^2}{a_f T^2} \right) \\ &\equiv \frac{g_- m^2(\phi) T^2}{48} + \Delta V_T, \end{aligned} \quad (3.4)$$

for fermions. Here  $a_b = (4\pi e^{-\gamma_E})^2$  and  $a_f = (\pi e^{-\gamma_E})^2$ . We have also identified the log term as  $\Delta V_T$  to highlight that these terms will be treated as a perturbation. To keep notation compact, all small temperature corrections that are not included in our toy model (i.e. the ones that we treat as a perturbation) and their sum we denote as  $\Delta V_T$ . It should be noted that the high temperature approximation for the one loop temperature corrections cannot be assumed to be valid. Indeed it is only valid when  $m(\phi)/T \lesssim 2.2$  and  $1.9$  for bosons and fermions respectively. Our numerical scans stay away from this limit, we generally have  $m(\phi)/T \lesssim 1.5$ . The temperature dependent effective potential is a function of the Higgs field and the singlet field which we denote  $\varphi_S$ . (We also use the short hand that  $\varphi \equiv \sqrt{H_u^2 + H_d^2}$ .) Within one loop accuracy under the high temperature expansion, it is given by

$$V(\varphi, \varphi_s, T) = V^T + \Delta V_S + \Delta V_{\text{loop}} + \Delta V_T. \quad (3.5)$$

Here we have defined  $\Delta V_{\text{loop}}$  as the loop corrections,  $\Delta V_S$  as the terms that violate the Peccei-Quinn limit (which is approximately  $\kappa A_{\kappa} \varphi_s^3/3$ ). The term  $V^T$  is the toy model effective potential from ref. [24], which is given by

$$V^T = M^2 \varphi^2 + c T^2 \varphi^2 - E T \varphi^3 + m_s^2 \varphi_s^2 + \lambda^2 \varphi_s^2 \varphi^2 - 2\tilde{a} \varphi^2 \varphi_s + \frac{\tilde{\lambda}}{2} \varphi^4, \quad (3.6)$$

where

$$\begin{aligned}
 M^2 &= m_{H_u}^2 \cos^2 \beta + m_{H_d}^2 \sin^2 \beta, \\
 \tilde{a} &= \lambda A_\lambda \sin \beta \cos \beta, \\
 \frac{\tilde{\lambda}}{2} &= \frac{g_1^2 + g_2^2}{8} (\cos^2 \beta - \sin^2 \beta)^2 + \lambda^2 \sin^2 \beta \cos^2 \beta + \frac{\delta \tilde{\lambda}}{2}.
 \end{aligned} \tag{3.7}$$

In the last equation the parameter  $\delta \tilde{\lambda}$  acquires large loop corrections from the stop mass. Note that we have not included any temperature corrections to the bare mass of the singlet. Therefore our scheme is valid in the region where

$$\frac{\lambda \varphi_s}{\gamma \varphi_c} \gtrsim 1.9. \tag{3.8}$$

In the region where temperature corrections to the bare singlet mass become important it is possible for a first order phase transition to occur when  $m_s^2 < 0$ . These points however are relatively rare and we lose little in ignoring them.

We recall that at the critical temperature the effective potential obtains degenerate minima with one minima at  $\varphi = 0$ . It is easy to see that  $V(0, 0, T) = V^T(0, 0, T) = 0$ . Let the critical temperature and the non zero VEV at this temperature for our toy model be denoted by  $T_c$  and  $\varphi_c$ , respectively. It is also useful to define  $\tilde{\gamma} = T/\varphi$  for  $T \neq T_c$ . Note that  $V$  can be written as a function of  $\varphi$ ,  $\varphi_s$  and  $\tilde{\gamma}$ . We will denote the fields,  $\varphi_x$ , away from the respective minima as  $\tilde{\varphi}_x$ . Let us assume that  $V$  is continuous in its three arguments near the critical temperature. It is then apparent that  $V(\varphi_c + \delta\varphi_c, \tilde{\varphi}_s + \delta\varphi_s, \gamma + \delta\gamma) = 0$ , where the non trivial VEV of the full temperature dependent potential at the critical temperature is a small perturbation to the tree level critical VEV,  $\varphi_c + \delta\varphi_c$ . Similarly, the singlet VEV at the critical and the inverse order parameter both obtain small corrections,  $\delta\varphi_s, \delta\gamma$ , respectively. From the small change formula in three variables, we can write:

$$\begin{aligned}
 &V(\varphi_c + \delta\varphi_c, \tilde{\varphi}_s + \delta\tilde{\varphi}_s, \gamma + \delta\gamma) \\
 &\approx V^T(\varphi_c, \tilde{\varphi}_s, \gamma) + (\Delta V_T + \Delta V_{\text{loop}} + \Delta V_S)|_{\varphi_c, \tilde{\varphi}_s, \gamma} \\
 &\quad + \left. \frac{\partial V^T}{\partial \varphi} \right|_{\varphi_c, \varphi_s, \gamma} \delta\varphi_c + \left. \frac{\partial V^T}{\partial \tilde{\varphi}_s} \right|_{\varphi_c, \varphi_s, \gamma} \delta\varphi_s + \left. \frac{\partial V^T}{\partial \tilde{\gamma}} \right|_{\varphi_c, \varphi_s, \gamma} \delta\gamma.
 \end{aligned} \tag{3.9}$$

The first term on the right hand side of the above equation is identical to zero for the reasons discussed above. Furthermore, the derivative of our toy model effective Lagrangian with respect to either  $\varphi$  or  $\varphi_c$  is also zero by definition when the derivative is evaluated at its minimum. Setting the left hand side of the above equation to zero and defining  $\Delta V \equiv \Delta T + \Delta_S + \Delta_{\text{loop}}$ , we can then write:

$$\delta\gamma = -\Delta V \left/ \frac{\partial V^T}{\partial \tilde{\gamma}} \right|_{\varphi_c, \varphi_s, \gamma}. \tag{3.10}$$

Noting that  $\partial\varphi/\partial\tilde{\gamma} = -\varphi/\tilde{\gamma}$ , we can write

$$\frac{\partial V}{\partial \tilde{\gamma}} = \frac{2G\varphi^2}{\tilde{\gamma}} - 2c\tilde{\gamma}\varphi^4 - \frac{2\tilde{\lambda}\varphi^4}{\tilde{\gamma}} + 3E\varphi^4 + \frac{\tilde{a}^2\varphi^4(4m_s^2 + 2\lambda^2\varphi^2)}{\tilde{\gamma}(m_s^2 + \lambda^2\varphi^2)^2}. \tag{3.11}$$

Finally we solve our toy model. We begin this calculation by insisting that the zero temperature VEV is  $v = 174$  GeV. This gives us the relation:

$$-M^2 = v^2 \left( \tilde{\lambda} - \frac{\tilde{a}^2(2m_s^2 + \lambda^2 v^2)}{(m_s^2 + \lambda^2 v^2)^2} \right) \equiv G. \quad (3.12)$$

Using the condition of degenerate minima occurring at a critical temperature, it is easy to derive the following equation

$$0 = -\frac{\tilde{\lambda}}{2} + \gamma E - c\gamma^2 + \frac{\sqrt{\tilde{a}^2(\tilde{\lambda} - \gamma E)}}{\sqrt{2}m_s} + \frac{\lambda^2 G}{-m_s^2 + \sqrt{\frac{2\tilde{a}^2 m_s^2}{\tilde{\lambda} - \gamma E}}} \equiv F(\gamma). \quad (3.13)$$

The details of this calculation are given in the appendix. Note that, apart from  $\gamma$ , this equation is a function of only four parameters:  $\{m_s, \lambda, A_\lambda, \tan \beta\}$ . We therefore calculate  $\delta\gamma$  for values of  $\{m_s, \lambda, A_\lambda, \tan \beta\}$  such that  $F(\gamma + \delta\gamma)$  is significantly smaller than any of its five components. We ensure that all components of  $\Delta V$  are small compared to the derivative of  $V^T$  with respect to gamma evaluated at the vev at the critical temperature. Finally we insist that  $\delta\gamma \lesssim 0.4$ . The baryon washout condition is satisfied for  $\gamma + \delta\gamma \lesssim 1$ .

## 4 Constraints applied

To find regions consistent with experiment we used `micrOMEGAs2.4` [56–58] coupled to `NMSSMTools` [59] to calculate observables and performed a scan over NMSSM parameter ranges shown in table 2. Most importantly, we require the dark matter relic abundance to be consistent with Planck along with the constraint of strongly first order electroweak phase transition of eq. (3.13). Additionally, we impose current limits from various experiments, as we enumerate them below.

- *Relic abundance*: we require that model points satisfy an upper limit on dark matter relic abundance observed by the Planck satellite, i.e.  $\Omega_{\tilde{\chi}_1^0} h^2 < 0.128$  [1]. We find that in large part of the parameter space the lightest neutralino is not enough to account for the total Planck measured value, and multi-component dark matter should be considered. The points which pass the Planck constraint within  $3\sigma$  CL i.e.  $0.1118 < \Omega_{\tilde{\chi}_1^0} h^2 < 0.128$  [1] are highlighted.
- *Higgs mass*: we impose the LHC bound on the Higgs boson mass by taking the combined theoretical and experimental uncertainties within the following range, i.e.  $121.5 < m_h < 129.5$  GeV.
- *Direct dark matter detection*: we illustrate the bounds on a neutralino-nucleon interaction cross-section as measured by the XENON100 experiment [15] and CRESST-II [20]. We also consider the projected bounds of XENON1T [60] and LUX [61]. These bounds are derived using standard assumptions, i.e. dark matter density in the Galactic halo  $\rho_{\tilde{\chi}_1^0} = 0.3$  GeV/cm<sup>3</sup>, the circular velocity  $v = 220$  km/s and the Galactic escape velocity  $v_{esc} = 544$  km/s [62].

Quantity	Value	Source
$\Omega_{\tilde{\chi}_1^0} h^2$	$< 0.128$	[1]
$m_h$	$125.5 \pm 4 \text{ GeV}$	[25, 26]
$(m_{\tilde{\chi}_1^0} + m_{\tilde{\chi}_2^0})$	$> 209 \text{ GeV}$	[14, 68]
$\mathcal{B}(B_s \rightarrow \mu^+ \mu^-)$	$(3.2_{-1.2}^{+1.5}) \times 10^{-9}$	[63]
$\mathcal{B}(b \rightarrow s \gamma)$	$(3.43 \pm 0.22) \times 10^{-4}$	[64]
$\delta a_\mu$	$(-2.4 : 4.5) \times 10^{-9}$	[65]
$\Gamma_{Z \rightarrow \tilde{\chi}_1^0 \tilde{\chi}_1^0}$	$< 3 \text{ MeV}$	[69]
$m_{\tilde{\chi}_1^+}$	$> 103.5 \text{ GeV}$	[66]

**Table 1.** List of the experimental constraints which we imposed in our NMSSM scan.

- *Flavour physics:* we enforce limits on the branching ratios of flavour violating decays,  $\mathcal{B}(B_s \rightarrow \mu^+ \mu^-) = (3.2_{-1.2}^{+1.5}) \times 10^{-9}$  [63] and  $\mathcal{B}(b \rightarrow s \gamma) = (3.55 \pm 0.26) \times 10^{-4}$  [64]. Baryogenesis does not conflict with these constraints, since these processes are enhanced for large values of  $\tan \beta$  while electroweak baryogenesis in the NMSSM has a preference for moderate  $\tan \beta$  values [24].
- *Muon anomalous magnetic moment:* we require the supersymmetric contribution to  $g_\mu - 2$  to be in the range:  $-2.4 \times 10^{-9} < \delta a_\mu^{SUSY} < 4.5 \times 10^{-9}$  [65].
- *Chargino mass:* we take the lower LEP bound on a mass of chargino to be  $m_{\tilde{\chi}_1^+} > 103.5 \text{ GeV}$  [66].<sup>2</sup> A null result in LEP searches on a process  $e^+ e^- \rightarrow \tilde{\chi}_1 \tilde{\chi}_j$  with  $j > 1$ , sets an upper bound on the neutralino production cross-section  $\sigma(e^+ e^- \rightarrow \tilde{\chi}_1 \tilde{\chi}_j) \lesssim 10^{-2} \text{ pb}$  [14], which can be translated into  $(m_{\tilde{\chi}_1^0} + m_{\tilde{\chi}_2^0}) > 209 \text{ GeV}$  [68]. This limits the mass of the lightest neutralino from below.
- *Invisible Z boson decay width:* in the light neutralino regions where  $m_{\tilde{\chi}_1^0} < M_Z/2$ , one has to take into account of the invisible decay width of Z boson into neutralinos. Analytical expression for this process is given by [14]:

$$\Gamma_{Z \rightarrow \tilde{\chi}_1^0 \tilde{\chi}_1^0} = \frac{M_Z^3 G_F}{12\sqrt{2}\pi} (N_{13}^2 + N_{14}^2)^2 \left(1 - \frac{4m_{\tilde{\chi}_1^0}^2}{M_Z^2}\right)^{3/2}, \quad (4.1)$$

where  $N_{13}^2$  and  $N_{14}^2$  are Higgsino fractions coming from eq. (2.11). This relationship is derived assuming three massless neutrinos. In order to satisfy this constraint the lightest neutralino must mostly be either a bino, a wino, or a singlino with minimal or no admixture from higgsinos.

Our constrains are summarized in table 1.

---

<sup>2</sup>We used a general limit on the chargino mass, however for possible caveats, see ref. [67].

Parameter	Range
$\lambda$	[0 : 0.7]
$A_\lambda$	[0:10000] GeV
$\tan \beta$	[1:65]
$\mu$	[0 : $A_\lambda \cos \beta \sin \beta$ ] GeV
$A_\kappa \cdot \kappa$	[0 : 0.01] GeV
$M_1$	[10:3000] GeV
$M_2$	[10:4000] GeV
$M_3$	[800:6000] GeV
$m_{\tilde{e}_L} = m_{\tilde{\mu}_L} = m_{\tilde{\tau}_L}$	6000 GeV
$m_{\tilde{e}_R} = m_{\tilde{\mu}_R} = m_{\tilde{\tau}_R}$	6000 GeV
$m_{\tilde{Q}_{1L}} = m_{\tilde{Q}_{2L}}$	6000 GeV
$m_{\tilde{Q}_{3L}}$	3300 GeV
$m_{\tilde{u}_R} = m_{\tilde{c}_R}$	6000 GeV
$m_{\tilde{t}_R}$	4000 GeV
$m_{\tilde{d}_R} = m_{\tilde{s}_R} = m_{\tilde{b}_R}$	6000 GeV
$A_t$	-5000 GeV
$A_\tau$	-2500 GeV
$A_b$	-2500 GeV

**Table 2.** Scan ranges and fixed values of the NMSSM parameters. The upper bound on  $\mu$  comes from our requirement for  $m_s^2$  to be positive. The first four parameters are constrained by the strongly first order phase transition. We vary the gaugino masses in order to explore the dark matter phenomenology and inflation, which we shall discuss below.

#### 4.1 Scanning the parameter space for dark matter and first order phase transition

Table 2 shows the parameter ranges of our scan. We fixed the first and second generation sfermionic masses to high values in order to avoid large potential supersymmetric contributions to electron and nuclear electric dipole moments [70]. The masses of left and right handed stops are adjusted to yield the measured value of the Higgs boson mass. We varied the electroweak gaugino masses in a wide range to explore dark matter phenomenology. Varying the gluino mass is important to determine the running of the  $\tilde{u}\tilde{d}\tilde{d}$  inflaton. The selected ranges also guarantee that our spectrum does not conflict with the LEP [71], ATLAS [72] and CMS [73] bounds on squarks and sleptons.

Figure 1 shows the bino (green dots), wino (red stars), higgsino (blue squares), and singlino (pink diamonds) fractions of the lightest neutralino. We restrict the relic density of the lightest neutralino below  $\Omega_{CDM}h^2 < 0.128$  which is the upper value on the dark matter abundance set by Planck at  $3\sigma$  confidence level. As mentioned above, neutralinos

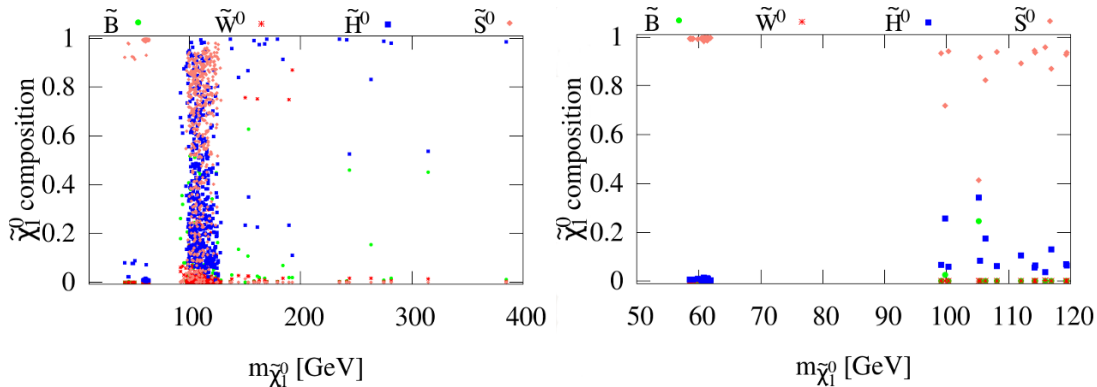


**Figure 1.** Bino (green dots), wino (red stars), higgsino (blue squares), and singlino (pink diamonds) components of the lightest neutralino for scanned model points. All points shown satisfy the condition of the strongly first order electroweak phase transition and pass all constraints listed in section 4. On the right hand panel we only show the points that fall within  $3\sigma$  of the Planck central value for the relic abundance of dark matter:  $0.1118 < \Omega_{\tilde{\chi}_1^0} h^2 < 0.128$  [1].

with masses  $m_{\tilde{\chi}_1^0} < m_Z/2$  have to have small higgsino fraction due to strict limits on the invisible Z boson decay (from eq. (4.1)) and the mass of the lightest chargino. Also, light dark matter regions are very fine tuned and require separate detailed analysis and more sophisticated scanning techniques, see for instance, ref. [23].

The heavier neutralino can have a larger higgsino fraction. This is also connected to the fact that the positivity of  $m_s^2$  sets an upper bound on the parameter  $\mu < A_\lambda \cos \beta \sin \beta$ , which allows larger higgsino fraction in the lightest neutralino. As we shall argue in the next paragraph this opens up more annihilation channels to satisfy the relic density constraint.

In figure 2, we show the dark matter relic density dependence on  $m_{\tilde{\chi}_1^0}$ . We only show points for which the dark matter relic density to falls below the upper limit from Planck, that is to satisfy  $\Omega_{\tilde{\chi}_1^0} h^2 < 0.128$  at  $3\sigma$  confidence level [1]. The peculiar clustering of the points in this plot is understood as follows. The first, smaller group around  $m_{\tilde{\chi}_1^0} \approx 63$  GeV is due to neutralino annihilation through the 126 GeV Higgs. This resonant annihilation depletes the neutralino abundance making it possible to satisfy the Planck bound. The second, larger group of points originate from the lightest neutralinos with an enhanced higgsino component coupling to Z boson. As this, and the previous, figure shows our model points also have the potential to explain the origin of the 130 GeV  $\gamma$ -ray line observed from the Galactic Centre in terms of the annihilation of a 130 GeV neutralino [74].

In figure 3, we show how spin independent dark matter-nucleon scattering experiments probe the scenarios with the constraints listed in table 1 and  $F(\gamma) = 0$ , see eq. (3.13). The points that are circled in black fall within the range  $0.1118 < \Omega_{\tilde{\chi}_1^0} h^2 < 0.128$  set by Planck. It is interesting to note that quite a few points lie in the regions where LSP is relatively light and dedicated searches for light neutralino DM potentially could explain excess interactions in background detected by DAMA/LIBRA [17, 18], CRESST-II [20], CoGeNT [19] and CDMS [21]. All the points with the smallest  $m_{\tilde{\chi}_1^0}$  have a large singlino fraction, and are ruled out by XENON100 experiment. We also show the projected bounds from the XENON1T and LUX experiments. These bounds are based on the assumptions already mentioned in the 4 section.

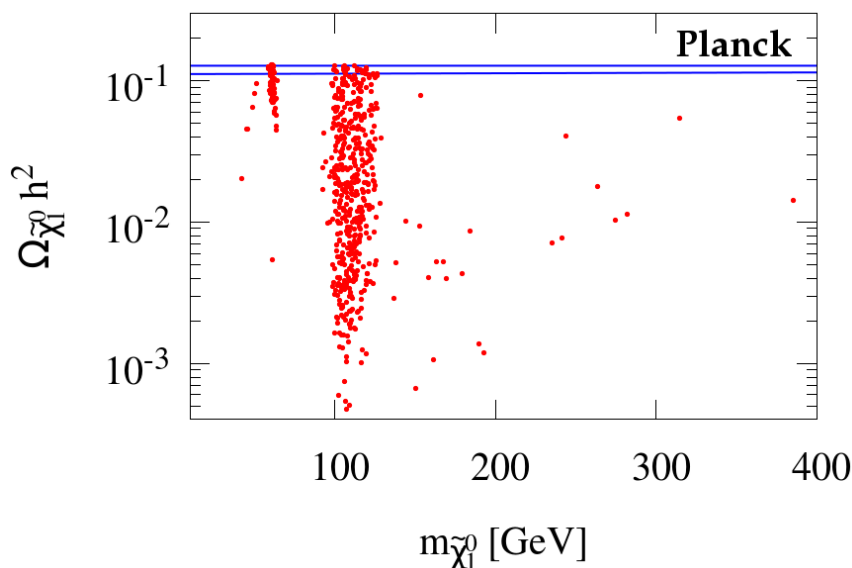


**Figure 2.** Relic abundance versus the mass of the dark matter particle for our scan. The blue lines indicate the bounds on dark matter density implied by the Planck satellite:  $0.1118 < \Omega_{\tilde{\chi}_1^0} h^2 < 0.128$ . All the points satisfy the condition for a first order electroweak phase transition, as indicated by eq. (3.13). They also pass all the constraints listed in section 4.

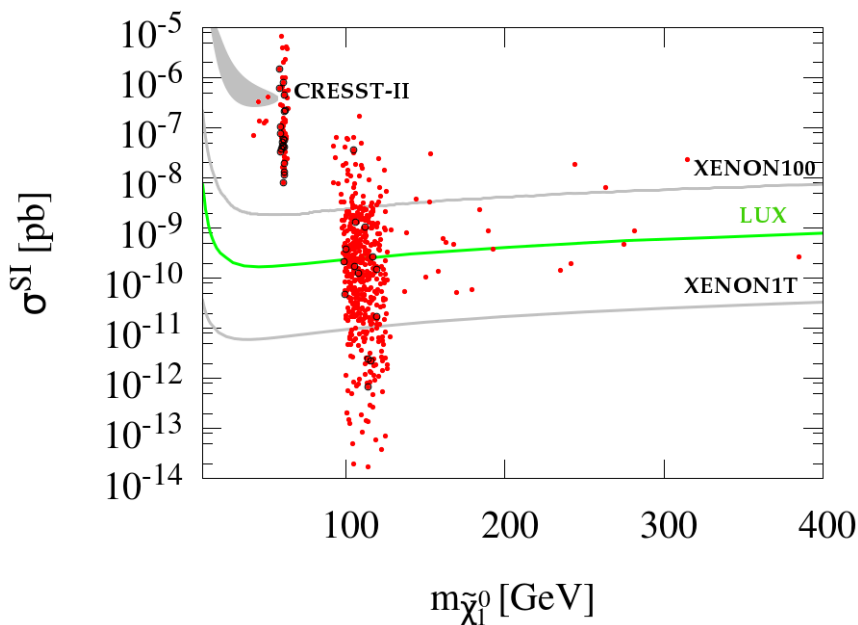


**Figure 3.** Spin independent direct detection cross section vs. mass of the neutralino in our scan. The current bounds from XENON100 and the  $2\sigma$  signal region from CRESST-II are shown. We also show projected bounds for XENON1T and LUX experiments. The points where neutralino relic abundance accounts for the full dark matter content of the Universe measured by Planck within  $3\sigma$ , i.e.  $0.1118 < \Omega_{\tilde{\chi}_1^0} h^2 < 0.128$ , are highlighted in black circles.

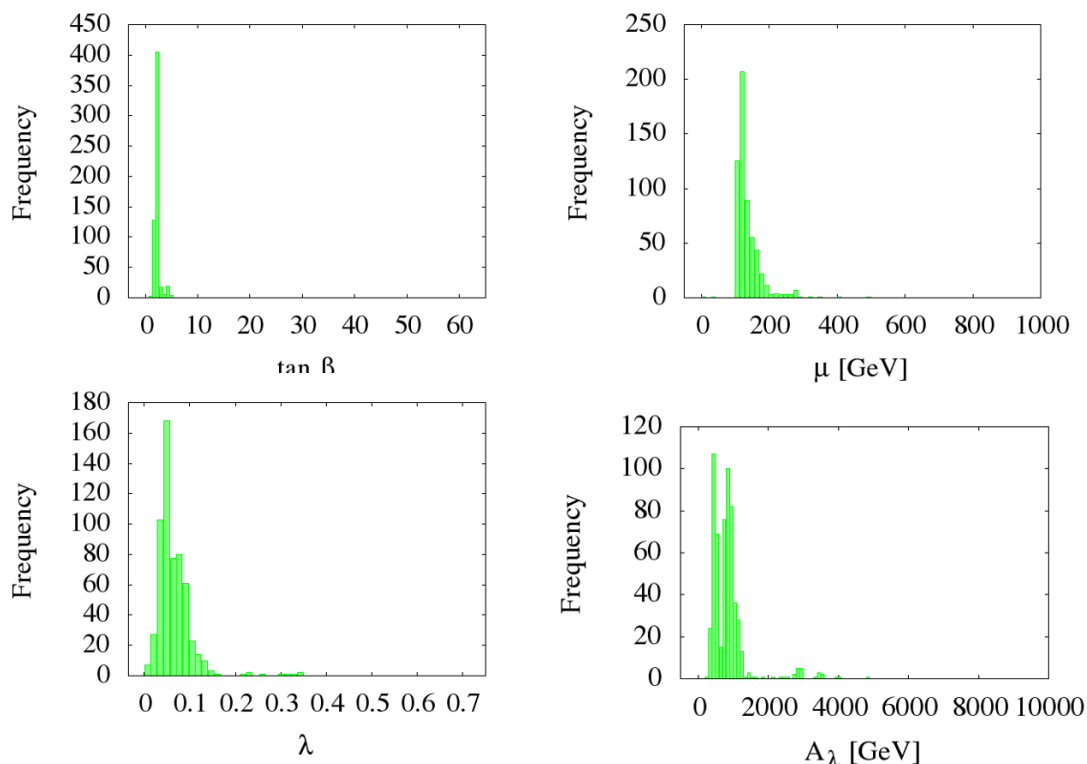


**Figure 4.** Distribution of the parameters which are relevant for baryogenesis in our scan.

Since in most of the cases that we have found the relic abundance is significantly lower than the set limits by the direct detection experiments, we need to lower the cross section  $\sigma^{SI}$  by a factor ( $\Omega_{\tilde{\chi}_1^0}/\Omega_{observed}$ ). Here we take the Planck central value  $\Omega_{observed} = 0.1199$ . As we see, most of the points that fall below XENON100 will be tested very soon by LUX and XENON1T experiments.

In figure 4, we show how the relevant parameters that enter eq. (3.13) are distributed in the scans. In the top left panel we can see that  $\tan \beta$  tend to cluster around lower values. This is not because a higher  $\tan \beta$  is inconsistent with the baryon washout condition, just that our approximations break down for the large  $\tan \beta$  so we avoided scanning those. The breakdown is due to terms in  $\Delta V$  that are  $\tan \beta$  dependent and for large  $\tan \beta$  can make  $\Delta V$  too large so that our assumption of  $\Delta V$  being small is violated. Similarly the upper bound on  $A_\lambda$  and  $\lambda$  is a relic of our approximations rather than any real difficulty in satisfying the baryon washout condition in that parameter range. The lower bound on  $\lambda$ , however, originates from baryogenesis since the low  $\kappa$  and low  $\lambda$  region is the MSSM limit and it is difficult to satisfy the baryon washout condition in the MSSM for a Higgs mass of 125 GeV [13]. We kept  $A_t = -5000$  GeV fixed to be able to satisfy the Higgs mass bound more easily. Values of  $\mu$  are mainly within a 100-200 GeV range because, as mentioned above, large values are constrained by the requirement of  $m_s^2$  being positive. This translates into upper bound, lower than  $A_\lambda \cos \beta \sin \beta$ , for a particular  $\tan \beta$ . Lower  $\mu$  values are constrained because of the invisible Z decay and the chargino mass, which

set bounds on the higgsino component of the neutralino which is directly related to low  $\mu$ . Since  $A_\lambda$  enters eq. (A.8) through  $\tilde{a}$ , in order to satisfy condition  $F(\gamma) = 0$  there needs to be some tuning between fourth and fifth terms. This fine tuning increases with increasing  $A_\lambda$ , and so condition A.8 is much easier met at low values.

## 5 Gauge invariant inflaton

Within the MSSM there are nearly 300 gauge-invariant  $F$ - and  $D$ -flat directions, for a review see [75]. Out of these flat directions, we will be interested in studying  $\tilde{u}\tilde{d}\tilde{d}$  as an inflaton [2–4], where  $\tilde{u}$ ,  $\tilde{d}$  correspond to the right handed squarks. In fact within the MSSM,  $\tilde{L}\tilde{L}\tilde{e}$  [2, 3] and  $H_u H_d$  [76] could also be good inflaton candidates. All the inflaton candidates provide *inflection point* in their respective potentials [77, 78], where inflation can be driven for sufficiently large e-foldings of inflation to explain the current Universe and explain the seed perturbations for the temperature anisotropy in the CMB, which has been confirmed by the recent Planck data [79, 80].

Within the NMSSM with the introduction of a singlet it becomes necessary to include the dynamics of a singlet field. Since the singlet here is not gauged there will be contributions to the  $S H_u H_d$  potential which would potentially ruin the flatness and therefore the success of inflation driven solely by the gauge invariant inflaton [5]. While  $\tilde{L}\tilde{L}\tilde{e}$  could still be a good inflaton candidate in our current scenario, but in our analysis slepton masses are not constrained by the dark matter and the baryogenesis constraints, therefore we only concentrate on  $\tilde{u}\tilde{d}\tilde{d}$  as an inflaton for this study.

Previous studies on MSSM inflation only considered the overlap between the parameter space for a successful inflation and the neutralino as the dark matter, which satisfies the relic abundance [81–83]. In this paper, we will consider one further step and we wish to constrain primordial inflation along with neutralino dark matter and condition for sufficient baryogenesis.

### 5.1 Brief review of inflation

The  $\tilde{u}\tilde{d}\tilde{d}$  flat direction is lifted by a higher order superpotential term of the following form [75],

$$W \supset \frac{y}{6} \frac{\Phi^6}{M_p^3}, \tag{5.1}$$

where  $y \sim \mathcal{O}(1)$ , and the scalar component of the superfield  $\Phi$  is given by:

$$\phi = \frac{\tilde{u} + \tilde{d} + \tilde{d}}{\sqrt{3}}. \tag{5.2}$$

After minimizing the potential along the angular direction  $\theta$  ( $\Phi = \phi e^{i\theta}$ ), we can consider the real part of  $\phi$ , for which the scalar potential is then given by [2, 4]

$$V(\phi) = \frac{1}{2} m_\phi^2 \phi^2 - A_y \frac{\phi^6}{6 M_p^6} + \frac{\phi^{10}}{M_p^6}, \tag{5.3}$$

where  $m_\phi$  and  $A$  are the soft breaking mass and the  $A_y$ -term respectively ( $A_y$  is a positive quantity since its phase is absorbed by a redefinition of  $\theta$  during the process). The mass for  $\tilde{u}\tilde{d}\tilde{d}$  is given by:

$$m_\phi^2 = \frac{m_u^2 + m_{\tilde{d}}^2 + m_{\tilde{d}}^2}{3}. \quad (5.4)$$

Note that the masses are now VEV dependent, i.e.  $m^2(\phi)$ . The inflationary perturbations will be able to constrain the inflaton mass only at the scale of inflation, i.e.  $\phi_0$ , while LHC will be able to constrain the masses at the LHC scale. However both the physical quantities are related to each other via renormalization group equations (RGEs), as we shall discuss below.

For [4]

$$\frac{A_y^2}{40m_\phi^2} \equiv 1 + 4\alpha^2, \quad (5.5)$$

where  $\alpha^2 \ll 1$ , there exists a point of inflection ( $\phi_0$ ) in  $V(\phi)$ , where

$$\phi_0 = \left( \frac{m_\phi M_p^3}{\lambda\sqrt{10}} \right)^{1/4} + \mathcal{O}(\alpha^2), \quad (5.6)$$

$$V''(\phi_0) = 0, \quad (5.7)$$

at which

$$V(\phi_0) = \frac{4}{15} m_\phi^2 \phi_0^2 + \mathcal{O}(\alpha^2), \quad (5.8)$$

$$V'(\phi_0) = 4\alpha^2 m_\phi^2 \phi_0 + \mathcal{O}(\alpha^4), \quad (5.9)$$

$$V'''(\phi_0) = 32 \frac{m_\phi^2}{\phi_0} + \mathcal{O}(\alpha^2). \quad (5.10)$$

The Hubble expansion rate during inflation is given by [2, 4]

$$H_{inf} \simeq \frac{1}{\sqrt{45}} \frac{m_\phi \phi_0}{M_p}. \quad (5.11)$$

The amplitude of the initial perturbations and the spectral tilt are given by:

$$\delta_H = \frac{8}{\sqrt{5}\pi} \frac{m_\phi M_p}{\phi_0^2} \frac{1}{\Delta^2} \sin^2[\mathcal{N}_{\text{COBE}} \sqrt{\Delta^2}], \quad (5.12)$$

and

$$n_s = 1 - 4\sqrt{\Delta^2} \cot[\mathcal{N}_{\text{COBE}} \sqrt{\Delta^2}], \quad (5.13)$$

respectively, where

$$\Delta^2 \equiv 900\alpha^2 \mathcal{N}_{\text{COBE}}^{-2} \left( \frac{M_p}{\phi_0} \right)^4. \quad (5.14)$$

In the above,  $\mathcal{N}_{\text{COBE}}$  is the number of e-foldings between the time when the observationally relevant perturbations are generated till the end of inflation and follows:  $\mathcal{N}_{\text{COBE}} \simeq$

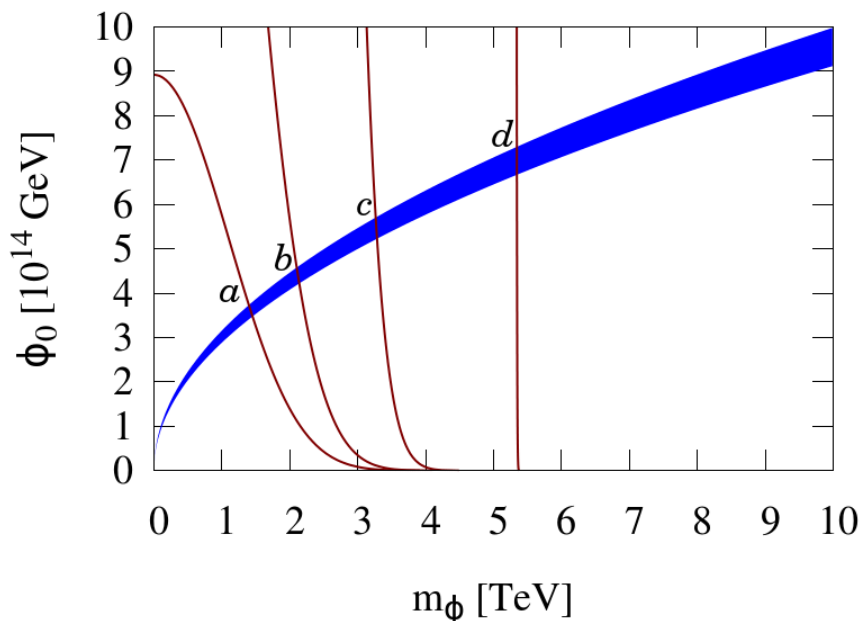


**Figure 5.** Blue region depicts the parameter space for inflation where it yields the right amplitude of density perturbations in the CMB, i.e.  $P_\zeta = 2.196 \times 10^{-9}$  and the  $\pm 1\sigma$  variance of the spectral tilt,  $n_s = 0.9606 \pm 0.0073$ . The brown lines show the running of the inflaton mass, where they intersect with the blue region depict the correct relic abundance,  $0.1118 < \Omega_{\tilde{\chi}_1^0} h^2 < 0.128$  [1], and strongly first order phase transition. From these intersections,  $a, b, c, d$  we can determine the masses of the inflaton at the inflationary scale  $\phi_0$ . The running of the inflaton mass is mainly determined by the bino and gluino masses, see table 2.

$66.9 + (1/4)\ln(V(\phi_0)/M_p^4) \sim 50$ . Since inflaton is made up of squarks, reheating and thermalisation happens instantly as showed in ref. [84]. The reheat temperature at which all the degrees of freedom are in thermal equilibrium (kinetic and chemical equilibrium) is given by  $T_{rh} = (120/15\pi^2 g_*)^{1/4} \sqrt{m_\phi \phi_0}$ , where  $g_* = 231.5$  is the relativistic degrees of freedom present within NMSSM. Since all the physical parameters are fixed in this model once we determine the soft SUSY breaking mass,  $m_\phi$ , the estimation of the reheat temperature can be made rather accurately.

## 5.2 Parameter space for inflation, dark matter and baryogenesis

Since the requirement for a successful baryogenesis implicitly constraints the right handed squark, i.e.  $\tilde{u}_3$ , we can assign the flat direction combination to be:  $\tilde{u}_i \tilde{d}_j \tilde{d}_k$ , where  $i = 3$  and  $i \neq j \neq k$ .

We can then use the RGEs for the  $\tilde{u}\tilde{d}\tilde{d}$  flat direction, in order to relate the low energy physics that we can probe at the LHC with the high energy inflation, which is constrained by the Planck data. The RGEs for the inflaton mass and the  $A_y$ -term are given by [4]:

$$\begin{aligned} \hat{\mu} \frac{dm_\phi^2}{d\hat{\mu}} &= -\frac{1}{6\pi^2} \left( 4M_3^2 g_3^2 + \frac{2}{5} M_1^2 g_1^2 \right), \\ \hat{\mu} \frac{dA_y}{d\hat{\mu}} &= -\frac{1}{4\pi^2} \left( \frac{16}{3} M_3 g_3^2 + \frac{8}{5} M_1 g_1^2 \right), \end{aligned} \tag{5.15}$$

Parameter	a	b	c	d	Constrained by
$\lambda$	0.06405	0.06520	0.10418	0.02906	1 <sup>st</sup> order phase transition
$A_\lambda(\text{GeV})$	1127	524	772	796	1 <sup>st</sup> order phase transition
$\tan\beta$	2.659	2.042	2.276	2.123	1 <sup>st</sup> order phase transition
$\mu_{\text{eff}}(\text{GeV})$	165.214	142.985	176.515	137.963	1 <sup>st</sup> order phase transition
$\Omega_{\tilde{\chi}_1^0} h^2$	0.119	0.112	0.124	0.112	Dark Matter abundance
$m_{\tilde{\chi}_1^0}(\text{GeV})$	61.17	119.2	59.8	126.3	Dark Matter abundance
$M_1(\text{GeV})$	2151	2006	1375	1084	Inflaton RGE
$M_3(\text{GeV})$	5269	4986	4281	861	Inflaton RGE
$\phi_0[\times 10^{14}](\text{GeV})$	3.5 – 3.8	4.2 – 4.6	5.3 – 5.7	6.6 – 7.3	CMB temperature anisotropy
$m_\phi(\text{GeV})$	1425	2120	3279	5349	CMB temperature anisotropy

**Table 3.** We show the benchmark points that are depicted in figure 5. The gaugino masses which enter in the RG equations are mainly sensitive due to different  $M_1$  and  $M_3$ . The parameters  $\lambda, A_\lambda, \tan\beta, \mu_{\text{eff}}$  are constrained from baryogenesis point of view, and this in turn uniquely determine the mass of the lightest stop which sets the mass for  $\tilde{u}_3\tilde{d}_i\tilde{d}_j$  inflaton candidate ( $3 \neq i \neq j$ ). Once again we reiterate that without our approximation scheme, the constraints on baryogenesis would be significantly less strict. The mass of the inflaton is given at the inflationary scale  $\phi_0$ .

where  $\hat{\mu} = \hat{\mu}_0 = \phi_0$  is the VEV at which inflation occurs,  $M_1$  and  $M_3$  are U(1) and SU(3) gaugino masses, and  $g_1$  and  $g_3$  are the associated couplings.

To solve these equations, we need to take into account of the running of the gaugino masses and coupling constants which are given by, see [4]:

$$\beta(g_i) = \alpha_i g_i^3 \quad \beta\left(\frac{M_i}{g_i^2}\right) = 0, \quad (5.16)$$

with  $\alpha_1 = 11/16\pi^2$  and  $\alpha_3 = -3/16\pi^2$ . Since from eq. (5.4), we know the mass of the inflaton at the electroweak scale, by using the RGEs we are able to evolve it to the high scale  $\phi_0$ , where inflation can happen. This can be seen in figure 5. The blue region shows the parameter of  $\tilde{u}_3\tilde{d}_j\tilde{d}_k$  as an inflaton for  $j \neq k \neq 3$ . It includes central value of density perturbations together with  $\pm 1\sigma$  variation in spectral tilt  $n_s$ . The brown lines show the mass of the inflaton at a particular scale and its running from high scale to low scale is determined by the RGEs, and it is mostly sensitive to bino and gluino masses.

In figure 5, we show the four benchmark points,  $a, b, c, d$ , which satisfy the condition for a successful baryogenesis, eq. (3.13), and also accommodate neutralino as a dark matter which satisfies the relic abundance constraint  $0.1118 < \Omega_{\tilde{\chi}_1^0} h^2 < 0.128$ . In table 3, we summarise the relevant parameters for NMSSM required to explain the Universe beyond the Standard Model.

## 6 Conclusions

In this work we examined inflation, baryogenesis and dark matter in the context of Next-to-Minimal Supersymmetric Standard Model. We have found that these three important cosmological requirements can be simultaneously accommodated by the theory. In particular, we have shown that a strongly first order phase transition can be easily achieved even with recent LHC constrains applied. Then we demonstrated that an abundance of lightest neutralinos can be generated thermally which satisfies the present dark matter density limits. Part of these model points also pass the most stringent dark matter direct detection constraints. Finally, we have shown that the presented scenario is fully consistent with inflation, where the inflaton is a  $D$ -flat direction and it is made up of right handed squarks. The visible sector inflation would explain not only the temperature anisotropy of the CMB, but also all the relevant matter required for baryogenesis and dark matter.

## Acknowledgments

We thank Michael Morgan for invaluable help, continuous discussions, feedback and support throughout this project. EP also would like to thank Sofiane Boucenna, Jonathan Da Silva and Lingfei Wang for valuable discussions. This work was supported in part by the *ARC Centre of Excellence for Particle Physics at the Tera-scale*. EP is supported by STFC ST/J501074. AM is supported by the Lancaster-Manchester-Sheffield Consortium for Fundamental Physics under STFC grant ST/J000418/1. CB thanks the Kavli Institute of Theoretical Physics, China for providing partial financial support and an excellent research environment during part of this project.

## A Solving the toy model

The first derivative with respect to  $\varphi_c^2$  is

$$\begin{aligned} \varphi_c^2 \frac{\partial V}{\partial \varphi_c^2} \Big|_{\varphi_c, T_c} &= M^2(T) \varphi_c^2 - \frac{3T_c E}{2} \varphi_c^3 + \tilde{\lambda} \varphi_c^4 \\ &\quad - \frac{\tilde{a}^2 \varphi_c^4 (2m_s^2 + \lambda^2 \varphi_c^2)}{(m_s^2 + \lambda^2 \varphi_c^2)^2} . \end{aligned} \tag{A.1}$$

Using the condition that the potential at the critical VEV is equal to the potential at  $\varphi = 0$  we have a second equation

$$M^2(T_c) \varphi_c^2 - T_c E \varphi_c^3 + \frac{\tilde{\lambda}}{2} \varphi_c^4 - \frac{\tilde{a}^2 \varphi_c^4}{m_s^2 + \lambda \varphi_c^2} = 0 . \tag{A.2}$$

We can then use eq. (A.1) and set it to 3/2 times eq. (A.2) to get

$$cT_c^2 + M^2 = \frac{\varphi_c^2}{2} \left( \tilde{\lambda} - \frac{2\tilde{a}^2 m_s^2}{(m_s^2 + \lambda^2 \varphi_c^2)^2} \right) + \frac{\lambda^2 \tilde{a}^2 \varphi_c^4}{(m_s^2 + \lambda^2 \varphi_c^2)^2} \tag{A.3}$$

Finally we can set eq. (A.1) equal to eq. (A.2) to get a second equation

$$ET_c \varphi_c^3 = \tilde{\lambda} \varphi_c^4 - \frac{2\tilde{a}^2 m_s^2 \varphi_c^4}{(m_s^2 + \lambda^2 \varphi_c^2)^2} . \tag{A.4}$$

We can then divide both sides of the above equation to obtain

$$E\gamma = \tilde{\lambda} - \frac{2\tilde{a}^2 m_s^2}{(m_s^2 + \lambda^2 \varphi_c^2)^2} . \quad (\text{A.5})$$

To solve this we use the ansatz  $\varphi_c^2 = \frac{1}{\lambda^2}(-m_s^2 + \delta)$  and it is straight forward to show that

$$\varphi_c^2 = \frac{1}{\lambda^2} \left( -m_s^2 + \sqrt{2\frac{\tilde{a}^2 m_s^2}{\tilde{\lambda} - \gamma E}} \right) . \quad (\text{A.6})$$

Consider the first term on the right hand side of eq. (A.3). It is proportional to  $\gamma$ . Using this and dividing both sides by  $\varphi_c^2$  we have

$$c\gamma^2 = \frac{G}{\varphi_c^2} + \frac{\gamma E}{2} + \frac{\lambda^2 \tilde{a}^2 \varphi_c^2}{(m_s^2 + \lambda^2 \varphi_c^2)^2} . \quad (\text{A.7})$$

We then use eq. (A.6) to get the following equation

$$\begin{aligned} 0 &= -\frac{\tilde{\lambda}}{2} + \gamma E - c\gamma^2 + \frac{\sqrt{\tilde{a}^2(\tilde{\lambda} - \gamma E)}}{\sqrt{2}m_s} + \frac{\lambda^2 G}{-m_s^2 + \sqrt{\frac{2\tilde{a}^2 m_s^2}{\tilde{\lambda} - \gamma E}}} \\ &\equiv F(\gamma) \end{aligned} \quad (\text{A.8})$$

as required.

**Open Access.** This article is distributed under the terms of the Creative Commons Attribution License ([CC-BY 4.0](https://creativecommons.org/licenses/by/4.0/)), which permits any use, distribution and reproduction in any medium, provided the original author(s) and source are credited.

## References

- [1] PLANCK collaboration, P. Ade et al., *Planck 2013 results. XVI. Cosmological parameters*, [arXiv:1303.5076](https://arxiv.org/abs/1303.5076) [[INSPIRE](#)].
- [2] R. Allahverdi, K. Enqvist, J. García-Bellido and A. Mazumdar, *Gauge invariant MSSM inflaton*, *Phys. Rev. Lett.* **97** (2006) 191304 [[hep-ph/0605035](#)] [[INSPIRE](#)].
- [3] R. Allahverdi, A. Kusenko and A. Mazumdar, *A-term inflation and the smallness of neutrino masses*, *JCAP* **07** (2007) 018 [[hep-ph/0608138](#)] [[INSPIRE](#)].
- [4] R. Allahverdi, K. Enqvist, J. García-Bellido, A. Jokinen and A. Mazumdar, *MSSM flat direction inflation: Slow roll, stability, fine tuning and reheating*, *JCAP* **06** (2007) 019 [[hep-ph/0610134](#)] [[INSPIRE](#)].
- [5] A. Mazumdar and J. Rocher, *Particle physics models of inflation and curvaton scenarios*, *Phys. Rept.* **497** (2011) 85 [[arXiv:1001.0993](#)] [[INSPIRE](#)].
- [6] P.J.E. Peebles, *Principles of physical cosmology*, Princeton University Press, Princeton U.S.A. (1993).
- [7] P. Gondolo and G. Gelmini, *Cosmic abundances of stable particles: Improved analysis*, *Nucl. Phys. B* **360** (1991) 145 [[INSPIRE](#)].

- [8] G. Jungman, M. Kamionkowski and K. Griest, *Supersymmetric dark matter*, *Phys. Rept.* **267** (1996) 195 [[hep-ph/9506380](#)] [[INSPIRE](#)].
- [9] G. Bertone, D. Hooper and J. Silk, *Particle dark matter: evidence, candidates and constraints*, *Phys. Rept.* **405** (2005) 279 [[hep-ph/0404175](#)] [[INSPIRE](#)].
- [10] B. Fields and S. Sarkar, *Big-bang nucleosynthesis (2006 particle data group mini-review)*, [astro-ph/0601514](#) [[INSPIRE](#)].
- [11] A. Sakharov, *Violation of CP Invariance, c Asymmetry and Baryon Asymmetry of the Universe*, *Pisma Zh. Eksp. Teor. Fiz.* **5** (1967) 32 [*JETP Lett.* **5** (1967) 24] [*Sov. Phys. Usp.* **34** (1991) 392] [*Usp. Fiz. Nauk* **161** (1991) 61] [[INSPIRE](#)].
- [12] V. Rubakov and M. Shaposhnikov, *Electroweak baryon number nonconservation in the early universe and in high-energy collisions*, *Usp. Fiz. Nauk* **166** (1996) 493 [*Phys. Usp.* **39** (1996) 461] [[hep-ph/9603208](#)] [[INSPIRE](#)].
- [13] M. Carena, G. Nardini, M. Quirós and C.E. Wagner, *MSSM electroweak baryogenesis and LHC data*, *JHEP* **02** (2013) 001 [[arXiv:1207.6330](#)] [[INSPIRE](#)].
- [14] U. Ellwanger, C. Hugonie and A.M. Teixeira, *The next-to-minimal supersymmetric standard model*, *Phys. Rept.* **496** (2010) 1 [[arXiv:0910.1785](#)] [[INSPIRE](#)].
- [15] XENON100 collaboration, E. Aprile et al., *Dark matter results from 225 live days of XENON100 data*, *Phys. Rev. Lett.* **109** (2012) 181301 [[arXiv:1207.5988](#)] [[INSPIRE](#)].
- [16] TEXONO collaboration, H. Li et al., *Limits on spin-independent couplings of WIMP dark matter with a p-type point-contact germanium detector*, *Phys. Rev. Lett.* **110** (2013) 261301 [[arXiv:1303.0925](#)] [[INSPIRE](#)].
- [17] DAMA collaboration, R. Bernabei et al., *First results from DAMA/LIBRA and the combined results with DAMA/NaI*, *Eur. Phys. J. C* **56** (2008) 333 [[arXiv:0804.2741](#)] [[INSPIRE](#)].
- [18] DAMA AND LIBRA collaborations, R. Bernabei et al., *New results from DAMA/LIBRA*, *Eur. Phys. J. C* **67** (2010) 39 [[arXiv:1002.1028](#)] [[INSPIRE](#)].
- [19] COGENT collaboration, C. Aalseth et al., *Results from a search for light-mass dark matter with a p-type point contact germanium detector*, *Phys. Rev. Lett.* **106** (2011) 131301 [[arXiv:1002.4703](#)] [[INSPIRE](#)].
- [20] G. Angloher et al., *Results from 730 kg days of the CRESST-II dark matter search*, *Eur. Phys. J. C* **72** (2012) 1971 [[arXiv:1109.0702](#)] [[INSPIRE](#)].
- [21] CDMS collaboration, R. Agnese et al., *Silicon detector results from the first five-tower run of CDMS II*, *Phys. Rev. D* **88** (2013) 031104 [[arXiv:1304.3706](#)] [[INSPIRE](#)].
- [22] D.A. Vasquez, G. Bélanger, C. Boehm, A. Pukhov and J. Silk, *Can neutralinos in the MSSM and NMSSM scenarios still be light?*, *Phys. Rev. D* **82** (2010) 115027 [[arXiv:1009.4380](#)] [[INSPIRE](#)].
- [23] C. Boehm, P.S.B. Dev, A. Mazumdar and E. Pukartas, *Naturalness of light neutralino dark matter in pMSSM after LHC, XENON100 and Planck data*, *JHEP* **06** (2013) 113 [[arXiv:1303.5386](#)] [[INSPIRE](#)].
- [24] M. Carena, N.R. Shah and C.E. Wagner, *Light dark matter and the electroweak phase transition in the NMSSM*, *Phys. Rev. D* **85** (2012) 036003 [[arXiv:1110.4378](#)] [[INSPIRE](#)].

- [25] ATLAS collaboration, *An update of combined measurements of the new Higgs-like boson with high mass resolution channels*, [ATLAS-CONF-2012-170](#) (2012).
- [26] CMS collaboration, *Combination of standard model Higgs boson searches and measurements of the properties of the new boson with a mass near 125 GeV*, [CMS-PAS-HIG-12-045](#) (2012).
- [27] P. Fayet, *Supergauge invariant extension of the Higgs mechanism and a model for the electron and its neutrino*, *Nucl. Phys. B* **90** (1975) 104 [[INSPIRE](#)].
- [28] H.P. Nilles, M. Srednicki and D. Wyler, *Weak interaction breakdown induced by supergravity*, *Phys. Lett. B* **120** (1983) 346 [[INSPIRE](#)].
- [29] C. Balázs and D. Carter, *Likelihood analysis of the next-to-minimal supergravity motivated model*, *JHEP* **03** (2010) 016 [[arXiv:0906.5012](#)] [[INSPIRE](#)].
- [30] S.A. Abel and P.L. White, *Baryogenesis from domain walls in the next-to-minimal supersymmetric standard model*, *Phys. Rev. D* **52** (1995) 4371 [[hep-ph/9505241](#)] [[INSPIRE](#)].
- [31] S.A. Abel, S. Sarkar and P.L. White, *On the cosmological domain wall problem for the minimally extended supersymmetric standard model*, *Nucl. Phys. B* **454** (1995) 663 [[hep-ph/9506359](#)] [[INSPIRE](#)].
- [32] C. Panagiotakopoulos and K. Tamvakis, *Stabilized NMSSM without domain walls*, *Phys. Lett. B* **446** (1999) 224 [[hep-ph/9809475](#)] [[INSPIRE](#)].
- [33] K. Tamvakis, *Stabilized NMSSM without domain walls*, talk given at the *Trieste Meeting of the TMR Network on Physics beyond the SM 1999*, February 24–27, Trieste, Italy (1999).
- [34] K.S. Jeong, Y. Shoji and M. Yamaguchi, *Peccei-Quinn invariant extension of the NMSSM*, *JHEP* **04** (2012) 022 [[arXiv:1112.1014](#)] [[INSPIRE](#)].
- [35] V.A. Kuzmin, V.A. Rubakov and M.E. Shaposhnikov, *Nuclear optical potential in first born approximation*, *Phys. Lett. B* **155** (1985) 1 [[INSPIRE](#)].
- [36] L. Dolan and R. Jackiw, *Symmetry behaviour at finite temperature*, *Phys. Rev. D* **9** (1974) 3320 [[INSPIRE](#)].
- [37] V.A. Kuzmin, V.A. Rubakov and M.E. Shaposhnikov, *On the anomalous electroweak baryon number nonconservation in the early universe*, *Phys. Lett. B* **155** (1985) 36 [[INSPIRE](#)].
- [38] A.G. Cohen, D.B. Kaplan and A.E. Nelson, *Baryogenesis at the weak phase transition*, *Nucl. Phys. B* **349** (1991) 727 [[INSPIRE](#)].
- [39] M. Joyce, T. Prokopec and N. Turok, *Constraints and transport in electroweak baryogenesis*, *Phys. Lett. B* **339** (1994) 312 [[INSPIRE](#)].
- [40] P. Huet and A.E. Nelson, *Electroweak baryogenesis in supersymmetric models*, *Phys. Rev. D* **53** (1996) 4578 [[hep-ph/9506477](#)] [[INSPIRE](#)].
- [41] V. Rubakov and M. Shaposhnikov, *Electroweak baryon number nonconservation in the early universe and in high-energy collisions*, *Usp. Fiz. Nauk* **166** (1996) 493 [*Phys. Usp.* **39** (1996) 461] [[hep-ph/9603208](#)] [[INSPIRE](#)].
- [42] M.S. Carena and C.E.M. Wagner, *Electroweak baryogenesis and Higgs physics*, [hep-ph/9704347](#) [[INSPIRE](#)].
- [43] A. Riotto and M. Trodden, *Recent progress in baryogenesis*, *Annu. Rev. Nucl. Part. Sci.* **49** (1999) 35.

- [44] J.M. Cline, M. Joyce and K. Kainulainen, *Supersymmetric electroweak baryogenesis in the WKB approximation*, *Phys. Lett. B* **417** (1998) 79 [Erratum *ibid.* **B 448** (1999) 321] [[hep-ph/9708393](#)] [[INSPIRE](#)].
- [45] J.M. Cline, M. Joyce and K. Kainulainen, *Supersymmetric electroweak baryogenesis*, *JHEP* **07** (2000) 018 [[hep-ph/0006119](#)] [[INSPIRE](#)].
- [46] M. Quirós, *Field theory at finite temperature and phase transitions*, *Acta Phys. Polon.* **B 38** (2007) 3661 [[INSPIRE](#)].
- [47] K. Kajantie, M. Laine, K. Rummukainen and M.E. Shaposhnikov, *The electroweak phase transition: a nonperturbative analysis*, *Nucl. Phys. B* **466** (1996) 189 [[hep-lat/9510020](#)] [[INSPIRE](#)].
- [48] H.H. Patel and M.J. Ramsey-Musolf, *Baryon washout, electroweak phase transition and perturbation theory*, *JHEP* **07** (2011) 029 [[arXiv:1101.4665](#)] [[INSPIRE](#)].
- [49] M. Garny and T. Konstandin, *On the gauge dependence of vacuum transitions at finite temperature*, *JHEP* **07** (2012) 189 [[arXiv:1205.3392](#)] [[INSPIRE](#)].
- [50] K. Jansen, *Status of the finite temperature electroweak phase transition on the lattice*, *Nucl. Phys. Proc. Suppl.* **47** (1996) 196 [[hep-lat/9509018](#)] [[INSPIRE](#)].
- [51] K. Rummukainen, M. Tsypin, K. Kajantie, M. Laine and M. Shaposhnikov, *The universality class of the electroweak theory*, *Nucl. Phys. B* **532** (1998) 283 [[hep-lat/9805013](#)] [[INSPIRE](#)].
- [52] K. Rummukainen, K. Kajantie, M. Laine, M.E. Shaposhnikov and M. Tsypin, *The universal properties of the electroweak phase transition*, [hep-ph/9809435](#) [[INSPIRE](#)].
- [53] C. Balazs, M. Carena, A. Menon, D.E. Morrissey and C.E.M. Wagner, *The supersymmetric origin of matter*, *Phys. Rev. D* **71** (2005) 075002 [[hep-ph/0412264](#)] [[INSPIRE](#)].
- [54] M. Carena, N.R. Shah and C.E. Wagner, *Light dark matter and the electroweak phase transition in the NMSSM*, *Phys. Rev. D* **85** (2012) 036003 [[arXiv:1110.4378](#)] [[INSPIRE](#)].
- [55] L. Dolan and R. Jackiw, *Symmetry behavior at finite temperature*, *Phys. Rev. D* **9** (1974) 3320 [[INSPIRE](#)].
- [56] G. Bélanger, F. Boudjema, A. Pukhov and A. Semenov, *MicrOMEGAs 2.0: a program to calculate the relic density of dark matter in a generic model*, *Comput. Phys. Commun.* **176** (2007) 367 [[hep-ph/0607059](#)] [[INSPIRE](#)].
- [57] G. Bélanger, F. Boudjema, A. Pukhov and A. Semenov, *MicrOMEGAs: a tool for dark matter studies*, *Nuovo Cim. C* **033N2** (2010) 111 [[arXiv:1005.4133](#)] [[INSPIRE](#)].
- [58] G. Bélanger et al., *Indirect search for dark matter with MicrOMEGAs2.4*, *Comput. Phys. Commun.* **182** (2011) 842 [[arXiv:1004.1092](#)] [[INSPIRE](#)].
- [59] U. Ellwanger and C. Hugonie, *NMHDECAY 2.0: an updated program for sparticle masses, Higgs masses, couplings and decay widths in the NMSSM*, *Comput. Phys. Commun.* **175** (2006) 290 [[hep-ph/0508022](#)] [[INSPIRE](#)].
- [60] XENON1T collaboration, E. Aprile, *The XENON1T dark matter search experiment*, [arXiv:1206.6288](#) [[INSPIRE](#)].
- [61] LUX collaboration, D. Akerib et al., *The Large Underground Xenon (LUX) experiment*, *Nucl. Instrum. Meth. A* **704** (2013) 111 [[arXiv:1211.3788](#)] [[INSPIRE](#)].
- [62] M.C. Smith et al., *The RAVE survey: constraining the local galactic escape speed*, *Mon. Not. Roy. Astron. Soc.* **379** (2007) 755 [[astro-ph/0611671](#)] [[INSPIRE](#)].

- [63] LHCb collaboration, *First evidence for the decay  $B_s^0 \rightarrow \mu^+ \mu^-$* , *Phys. Rev. Lett.* **110** (2013) 021801 [[arXiv:1211.2674](#)] [[INSPIRE](#)].
- [64] HEAVY FLAVOR AVERAGING GROUP collaboration, Y. Amhis et al., *Averages of B-hadron, C-hadron and tau-lepton properties as of early 2012*, [arXiv:1207.1158](#) [[INSPIRE](#)].
- [65] A. Arbey, M. Battaglia and F. Mahmoudi, *Implications of LHC searches on SUSY particle spectra: the pMSSM parameter space with neutralino dark matter*, *Eur. Phys. J. C* **72** (2012) 1847 [[arXiv:1110.3726](#)] [[INSPIRE](#)].
- [66] [http://lepsusy.web.cern.ch/lepsusy/www/inos\\_moriond01/charginos\\_pub.html](http://lepsusy.web.cern.ch/lepsusy/www/inos_moriond01/charginos_pub.html).
- [67] DELPHI collaboration, J. Abdallah et al., *Searches for supersymmetric particles in  $e^+e^-$  collisions up to 208 GeV and interpretation of the results within the MSSM*, *Eur. Phys. J. C* **31** (2003) 421 [[hep-ex/0311019](#)] [[INSPIRE](#)].
- [68] A. Menon, D. Morrissey and C. Wagner, *Electroweak baryogenesis and dark matter in the NMSSM*, *Phys. Rev. D* **70** (2004) 035005 [[hep-ph/0404184](#)] [[INSPIRE](#)].
- [69] *The LEP Electroweak Working Group*, <http://lepewwg.web.cern.ch/LEPEWWG/>.
- [70] S. Abel, S. Khalil and O. Lebedev, *EDM constraints in supersymmetric theories*, *Nucl. Phys. B* **606** (2001) 151 [[hep-ph/0103320](#)] [[INSPIRE](#)].
- [71] DELPHI collaboration, J. Abdallah et al., *Photon events with missing energy in  $e^+e^-$  collisions at  $\sqrt{s} = 130$  GeV to 209-GeV*, *Eur. Phys. J. C* **38** (2005) 395 [[hep-ex/0406019](#)] [[INSPIRE](#)].
- [72] <https://twiki.cern.ch/twiki/bin/view/AtlasPublic/SupersymmetryPublicResults>.
- [73] <https://twiki.cern.ch/twiki/bin/view/CMSPublic/PhysicsResultsSUS>.
- [74] G. Tomar, S. Mohanty and S. Rao, *130 GeV gamma ray signal in NMSSM by internal bremsstrahlung*, [arXiv:1306.3646](#) [[INSPIRE](#)].
- [75] K. Enqvist and A. Mazumdar, *Cosmological consequences of MSSM flat directions*, *Phys. Rept.* **380** (2003) 99 [[hep-ph/0209244](#)] [[INSPIRE](#)].
- [76] A. Chatterjee and A. Mazumdar, *Tuned MSSM Higgses as an inflaton*, *JCAP* **09** (2011) 009 [[arXiv:1103.5758](#)] [[INSPIRE](#)].
- [77] K. Enqvist, A. Mazumdar and P. Stephens, *Inflection point inflation within supersymmetry*, *JCAP* **06** (2010) 020 [[arXiv:1004.3724](#)] [[INSPIRE](#)].
- [78] S. Hotchkiss, A. Mazumdar and S. Nadathur, *Inflection point inflation: WMAP constraints and a solution to the fine-tuning problem*, *JCAP* **06** (2011) 002 [[arXiv:1101.6046](#)] [[INSPIRE](#)].
- [79] L. Wang, E. Pukartas and A. Mazumdar, *Visible sector inflation and the right thermal history in light of Planck data*, *JCAP* **07** (2013) 019 [[arXiv:1303.5351](#)] [[INSPIRE](#)].
- [80] S. Choudhury, A. Mazumdar and S. Pal, *Low  $\mathcal{E}$  high scale MSSM inflation, gravitational waves and constraints from Planck*, *JCAP* **07** (2013) 041 [[arXiv:1305.6398](#)] [[INSPIRE](#)].
- [81] R. Allahverdi, B. Dutta and A. Mazumdar, *Probing the parameter space for an MSSM inflation and the neutralino dark matter*, *Phys. Rev. D* **75** (2007) 075018 [[hep-ph/0702112](#)] [[INSPIRE](#)].
- [82] R. Allahverdi, B. Dutta and Y. Santoso, *MSSM inflation, dark matter and the LHC*, *Phys. Rev. D* **82** (2010) 035012 [[arXiv:1004.2741](#)] [[INSPIRE](#)].

- [83] C. Boehm, J. Da Silva, A. Mazumdar and E. Pukartas, *Probing the supersymmetric inflaton and dark matter link via the CMB, LHC and XENON1T experiments*, *Phys. Rev. D* **87** (2013) 023529 [[arXiv:1205.2815](#)] [[INSPIRE](#)].
- [84] R. Allahverdi, A. Ferrantelli, J. García-Bellido and A. Mazumdar, *Non-perturbative production of matter and rapid thermalization after MSSM inflation*, *Phys. Rev. D* **83** (2011) 123507 [[arXiv:1103.2123](#)] [[INSPIRE](#)].
- [85] J.L. Feng, J. Kumar and D. Sanford, *Xenophobic dark matter*, *Phys. Rev. D* **88** (2013) 015021 [[arXiv:1306.2315](#)] [[INSPIRE](#)].



# Gravitational waves as a probe of vacuum stability via high scale phase transitions

---

## 7.1 Introductory remarks

The recent discovery of gravitational waves [111] has led to a surge in interest in this new way of gaining information about the Universe [112, 113, 114, 115, 116, 117, 118, 119]. Of particular relevance to particle cosmology are gravitational wave signatures left by cosmic phase transitions [120, 121, 122]. There are proposed gravitational wave detectors that are sensitive to cosmic phase transitions, LISA and aLIGO. If the electroweak phase transition was strongly first order this will leave a stochastic gravitational background at a frequency and amplitude that can be detected by LISA. In contrast, aLIGO is insensitive to phase transitions at the weakscale and is instead sensitive to phase transitions occurring at a much higher scale,  $T$  between about  $10^6$  and  $10^8$  GeV [12]. Unfortunately the time-frame of LISA is several decades in the future in contrast to aLIGO. It is therefore of more pressing interest whether there are physical motivations for their to be a phase transition occurring at a temperature that could leave relic gravitational wave backgrounds visible to aLIGO.

In this paper I consider the problem of vacuum stability in the Standard Model and note the coincidence of scales between the sensitivity of aLIGO and the instability scale in the Standard Model. Adding a gauge singlet to the Standard Model is arguably the simplest method to improve its stability. This can occur through improved running or through a threshold correction to the Higgs self coupling. Such a gauge singlet can also acquire a vacuum expectation value at some time during the history of the Universe. If it does so through a strongly first order phase transition then it will contribute to the relic gravitational wave background.

I present three bench mark points where the Higgs self coupling remains positive up to the GUT scale,  $\mathcal{O}(10^{16})$  GeV, as well as having a strongly first order phase transition, fast enough bubble nucleation for the phase transition to proceed, peak frequency and amplitude that is potentially visible to aLIGO and acceptable zero temperature phenomenology. I also present a scan with slightly weaker criteria where there is a moderate to large threshold correction to the Higgs self coupling

and a strongly first order singlet phase transition occurs at the right temperature. To our knowledge this is the first paper that gives a physical motivation for a phase transition that leaves a relic visible to aLIGO.

## 7.2 Declaration for thesis chapter 7

### Declaration by candidate

In the case of the paper present contained in chapter 7, the nature and extent of my contribution was as follows:

Publication	Nature of contribution	Extent of contribution
6	Found the hole in the literature about physical motivations for phase transitions potentially visible to aLIGO and suggested this direction. Calculated the high scale phase transition and its thermal properties. Analysed bench marks in detail calculating the gravitational wave amplitude and frequency, the nucleation temperature. Calculated the running of each of the bench marks. Worked on producing multiple plots. Worked substantially on the draft writing many sections and editing all others. Contributed to discussions throughout.	60%

The following coauthors contributed to the work. If the coauthor is a student at Monash, their percentage contribution is given:

Author	Nature of contribution	Extent of contribution
Csaba Balazs	Digitized the plot for aLIGO sensitivity and superimposed our data on top. Wrote the introduction and was heavily involved in editing. Contributed to discussions throughout.	
Andrew Fowlie	Set up scan to verify zero temperature phenomenology is correct and implemented the communication with my code. Wrote several sections and edited all others. Substantially expanded understanding of vacuum stability. Contributed to discussions throughout.	
Anupam Mazumdar	Wrote a section. Contributed to discussions throughout.	

The undersigned hereby certify that the above declaration correctly reflects the nature and extent of the candidate and co-authors' contributions to this work.

**Signatures:**

Graham White



Csaba Balazs



Andrew Fowlie



Anupam Mazumdar



**Date:**

3.04.2017

### **7.3 Published material for chapter 7: Gravitational waves at aLIGO and vacuum stability with a scalar singlet extension of the Standard Model**

Begins overleaf

## Gravitational waves at aLIGO and vacuum stability with a scalar singlet extension of the standard model

Csaba Balázs,<sup>1,2,\*</sup> Andrew Fowlie,<sup>1,†</sup> Anupam Mazumdar,<sup>3,4,‡</sup> and Graham A. White<sup>1,§</sup><sup>1</sup>*ARC Centre of Excellence for Particle Physics at the Tera-Scale,**School of Physics and Astronomy, Monash University, Melbourne, Victoria 3800, Australia*<sup>2</sup>*Monash Centre for Astrophysics, School of Physics and Astronomy,  
Monash University, Melbourne, Victoria 3800, Australia*<sup>3</sup>*Consortium for Fundamental Physics, Physics Department,  
Lancaster University, LA1 4YB Lancaster, United Kingdom*<sup>4</sup>*Kapteyn Astronomical Institute, University of Groningen, 9700 AV Groningen, The Netherlands*

(Received 30 November 2016; published 8 February 2017)

A new gauge singlet scalar field can undergo a strongly first-order phase transition (PT) leading to gravitational waves (GW) potentially observable at aLIGO and stabilizes the electroweak vacuum at the same time by ensuring that the Higgs quartic coupling remains positive up to at least the grand unification (GUT) scale. aLIGO (O5) is potentially sensitive to cosmological PTs at  $10^7$ – $10^8$  GeV, which coincides with the requirement that the singlet scale is less than the standard model (SM) vacuum instability scale, which is between  $10^8$  GeV and  $10^{14}$  GeV. After sampling its parameter space, we identify three benchmark points with a PT at about  $T \approx 10^7$  GeV in a gauge singlet extension of the SM. We calculate the nucleation temperature, order parameter, characteristic time scale, and peak amplitude and frequency of GW from bubble collisions during the PT for the benchmarks and find that, in an optimistic scenario, GW from such a PT may be in reach of aLIGO (O5). We confirm that the singlet stabilizes the electroweak vacuum while remaining consistent with zero-temperature phenomenology as well. Thus, this scenario presents an intriguing possibility that aLIGO may detect traces of fundamental physics motivated by vacuum stability at an energy scale that is well above the reach of any other experiment.

DOI: 10.1103/PhysRevD.95.043505

### I. INTRODUCTION

The recent detection of gravitational waves (GW) by the LIGO Collaboration opened a new observational window for the early Universe [1]. Among the most exciting prospects is the observation of GW from cosmological events that happened well before the first observable photons were created [2]. Not limited by recombination, GW can be used to directly probe fundamental physics, reaching to considerably higher energies than any other existing experiments. There are potentially several known sources of observable GW, which can be split into three categories [3]: (i) binary black hole mergers, mergers of binary neutron stars or a neutron star and a black hole, or supernova core collapse, with a duration between a millisecond and several hours; (ii) long duration signals, i.e., from spinning neutron stars; and (iii) stochastic background arising from the superposition of unresolved astrophysical sources. The latter can be a stochastic background of GW which can also arise from cosmological events, such as during primordial inflation [4–6], resonant preheating

[7–11], fragmentation of the inflaton or any scalar condensate [12–14], cosmic strings [15,16], or a cosmological phase transition (PT) accompanying either the breakdown of a fundamental symmetry or a scalar field acquiring a vacuum expectation value (VEV). If this PT is first order, then GW are created by violent collisions between expanding bubble walls of the new vacuum (see, e.g., Refs. [3,17–46]), which can be potentially constrained by the current and future GW observatories, such as the future space mission eLISA [47,48], and also possibly by aLIGO within the next 5 years [49]. Recently, it has been shown that these GW are detectable by BBO or DECIGO [50–54].

In the present work, we explore the detectability of GW originating from fundamental physics at the upgraded LIGO detector, aLIGO, in the near future (2020–2022) [55–58]. It is known that the frequency of GW from the electroweak PT is too low to be detected at aLIGO [21,22]. Therefore, our main emphasis here is to seek GW accompanying an earlier PT with physics beyond the Standard Model (BSM). In search of detectable primordial GW at aLIGO (LIGO run phase O5), we provide a simple but concrete particle physics model which can yield the observed amplitude and peak frequency for GW which have been recently proposed in Ref. [49]. In the current paper we analyze a framework which is an extension of the standard model (SM) of elementary particles with a gauge

\*csaba.balazs@monash.edu

†andrew.fowlie@monash.edu

‡a.mazumdar@lancaster.ac.uk

§graham.white@monash.edu

singlet scalar (SSM) (see, e.g., Refs. [59,60]). Indeed, this is the simplest example of BSM physics that could enhance electroweak vacuum stability [61–63]. Besides this, such a simple choice for physics beyond the SM could also help us understand primordial inflation [64–66] (for a review see Ref. [67]).

As noticed before in Ref. [49], aLIGO is potentially sensitive to cosmological PTs occurring at scales  $10^7$  GeV to  $10^8$  GeV, which raises the question of whether such a new scale emerges in BSM physics. It is a well-established result that the observed values of the top-quark mass, Higgs mass and strong coupling drive the SM Higgs quartic coupling, via renormalization evolution, to negative values at about  $\Lambda_1 \sim 10^{10}$  GeV. The latter is known as the Higgs or vacuum instability scale [68–72]. The SM scalar potential is believed to be metastable; although we live in a false vacuum, the probability of tunneling to the true vacuum is negligible, and for a heavy Higgs boson,  $m_h \gtrsim 130$  GeV, the Higgs potential would be stable [70].

In this paper we show two important results, which we can summarize below:

- (i) It is possible to realize a successful strong first-order PT in the singlet direction with the nucleation temperature within the range of  $10^7$ – $10^8$  GeV, which would give rise to a GW signal within the frequency range of aLIGO, i.e., 10–100 Hz. We will establish this by taking into account finite-temperature corrections, first incorporated in Ref. [73] in the context of the next-to-minimal supersymmetric SM.
- (ii) We carefully compute the running of the couplings in the SSM at two loops, and conclude that for the range of parameters we have scanned, parameters that yield a strong first-order PT could also ameliorate the SM Higgs metastability. In this paper we shall provide three benchmark points, where the scale of BSM physics would leave an undeniable footprint in the GW signal, potentially within the range of aLIGO (O5).

Our paper is organized as follows. In Sec. II, we first explain the SSM model. In Sec. III, we discuss what range of parameters of the singlet can yield strong first-order PT, and what are the conditions to be fulfilled. In Sec. IV, we briefly discuss GW amplitude and frequency from the first-order PT. In Sec. V, we discuss the Higgs vacuum stability in the presence of a singlet-Higgs interaction, and in Sec. VI we discuss our numerical results. In Sec. VII, we conclude with our results and discuss briefly future directions.

## II. SINGLET EXTENSION OF THE STANDARD MODEL

We consider the SM plus a real scalar (see, e.g., Refs. [59,60]) that is a singlet under the SM gauge groups and carries no, e.g., discrete charges. Thus, our model is described by the tree-level scalar potential

$$V_0(H, S) = \mu^2 |H|^2 + \frac{1}{2} \lambda |H|^4 + \frac{1}{2} M_S^2 S^2 + \frac{1}{3} \kappa S^3 + \frac{1}{2} \lambda_S S^4 + \kappa_1 S |H|^2 + \frac{1}{2} \kappa_2 S^2 |H|^2, \quad (1)$$

where  $M_S$  is the mass parameter of the singlet,  $\kappa$  is a dimensionful coupling,  $\lambda_S$  is the singlet quartic coupling, and  $\kappa_{1,2}$  are singlet-Higgs couplings. The above potential is the most general gauge invariant, renormalizable scalar potential with the considered particle content. The linear operator  $m^3 S$  is removed by a shift in the singlet field without loss of generality.

To account for changing field properties during cosmological PTs, we consider a one-loop effective potential with finite-temperature corrections (i.e., a free energy). As the Universe cools the free energy develops a deeper minimum in the singlet direction, there is a PT to a new ground state and the singlet acquires a VEV, although no symmetries are broken. If there is a discontinuity in the order parameter

$$\gamma \equiv \langle S \rangle / T,$$

i.e., the PT is first order, bubbles spontaneously emerge in the Universe in which the singlet VEV is nonvanishing  $\langle S \rangle \neq 0$ . We will scan over the Lagrangian parameters at the high scale; guarantee that a strongly first-order PT occurs at a critical temperature in the range  $(10^7, 10^8)$  GeV by solving for Lagrangian parameters; and impose the constraints on weak-scale parameters by requiring that the Higgs mass be  $125 \pm 1$  GeV and that the VEV be 246 GeV. This typically requires dimensionful parameters to be  $\mathcal{O}(T_C)$  and dimensionless parameters to be  $\mathcal{O}(1)$  at the high scale. GW from high-energy PTs were considered in Ref. [74].

A fraction of the latent heat from the PT could ultimately be released in collisions between bubbles, which result in striking GW signatures. This occurs at the bubble nucleation temperature,  $T_N$ , which is typically similar to the critical temperature,  $T_N \lesssim T_C$ , i.e., the temperature at which the original ground state and emerging ground state are degenerate. We will calculate the nucleation temperature in order to calculate the peak frequency and the amplitude of the GW resulting from the singlet PT.

## III. PHASE TRANSITIONS IN A TEMPERATURE IMPROVED POTENTIAL

In this section we investigate whether the SM extended with a singlet can produce GW at a strongly first-order PT which could be detected by aLIGO. Acceptable low-energy phenomenology, including standard Higgs properties and vacuum stability, is imposed. To achieve such a scenario we require the following cosmological history.

- (1) Higgs and singlet fields are in true, stable vacuum at the origin at high temperature.
- (2) At  $T \approx T_N \approx T_C \in (10^7, 10^8)$  GeV, the singlet acquires a VEV in a strongly first-order PT generating GW, potentially in reach of aLIGO. [The

temperature was chosen to coincide with the peak frequency sensitivity in aLIGO (O5).]

- (3) At low temperature, the Higgs acquires a VEV,  $\langle H \rangle \approx 246$  GeV, resulting in the correct weak scale, Higgs mass, and satisfying constraints on Higgs-singlet mixing.

We will calculate the critical and nucleation temperatures numerically as functions of the Lagrangian parameters. This is needed to calculate the frequency and amplitude of GW originating from bubble collisions. The first step is to include finite-temperature corrections to the effective potential. The one-loop finite-temperature corrections to the scalar potential have the form [75,76]

$$\Delta V_T = \frac{T^4}{2\pi^2} \left[ \sum_b J_B \left( \frac{m_b^2}{T^2} \right) + \sum_f J_F \left( \frac{m_f^2}{T^2} \right) \right], \quad (2)$$

where  $J_B$  and  $J_F$  are thermal bosonic and fermionic functions, respectively, and the sums are over field-dependent boson and fermion mass eigenvalues. We also add zero-temperature one-loop Coleman-Weinberg corrections [75,76],

$$\Delta V_{\text{CW}} = \sum_i \frac{g_i m_i^2}{64\pi^2} \left[ \log \left( \frac{m_i^2}{\mu^2} \right) - n_i \right], \quad (3)$$

summed over massive particles, where  $\mu$  is the renormalization scale, chosen to minimize large logarithms;  $m_i$  is a field-dependent mass eigenvalue;  $g_i$  is the number of degrees of freedom associated with the massive particle; and  $n_i = 3/2$  for scalars and fermions and  $5/6$  for massive gauge bosons (up to an overall sign for fermions).

Note that when one considers a PT in the singlet direction the only relevant masses are field-dependent mass eigenvalues of both the  $CP$  even and  $CP$  odd scalar mass matrices as well as the charged Higgs. Also, there are no issues with gauge dependence. The final corrections to the finite-temperature effective potential are the Debye masses  $\Delta V_D$  which result in the Lagrangian bare mass terms obtaining corrections of the form  $\Delta m_T^2 \propto T^2$  [77]. Thus, we consider the one-loop finite-temperature potential

$$V = V_0 + \Delta V_D + \Delta V_T + \Delta V_{\text{CW}}. \quad (4)$$

The conditions for a strongly first-order PT generating GW are that

- (1) There are at least two minima,

$$\left. \frac{\partial V}{\partial S} \right|_{\mathcal{F}} = \left. \frac{\partial V}{\partial S} \right|_{\mathcal{T}} = 0. \quad (5)$$

The calligraphic subscripts indicate the expression should be evaluated in the true ( $\mathcal{T}$ ) and false ( $\mathcal{F}$ ) vacua.<sup>1</sup>

<sup>1</sup>The vacua are degenerate at the critical temperature. We, however, always refer to the deepest minimum at zero temperature as the true minimum.

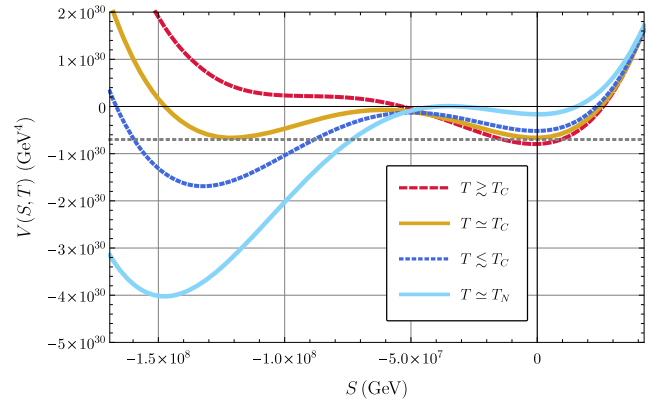


FIG. 1. The effective potential (i.e., free energy) for benchmark SSM II, shown above, below and at the critical temperature,  $T_C$ , at which the minima are degenerate, and at the nucleation temperature,  $T_N$ .

- (2) There exists a critical temperature,  $T_C$ , at which the two minima are degenerate,

$$V|_{\mathcal{F}} = V|_{\mathcal{T}}. \quad (6)$$

This is illustrated in Fig. 1 for a benchmark point tabulated in Table I by SSM I.

- (3) The order parameter at the critical temperature

$$\gamma \equiv \frac{\langle S \rangle}{T_C}, \quad (7)$$

must be substantial [i.e.,  $\mathcal{O}(1)$ ] in order to yield a strong first-order PT. The fact that  $S$  is a gauge singlet means that we do not need to concern ourselves with subtleties involving gauge invariance [75].

- (4) Bubbles form, expand, dominate the Universe and violently collide.

For the first-order PT generating GW, we fix the critical temperature and order parameter, and solve for Lagrangian parameters at the high scale such that the conditions hold.

The peak frequency and peak amplitude of the resulting GW are controlled by the nucleation temperature,  $T_N$ , which is the temperature at which a  $1/e$  volume fraction (given by the Guth-Tye formula [78]) of the Universe is in the true vacua. By dimensional analysis, this approximately occurs once

$$p(t)t^4 \approx 1, \quad (8)$$

where  $p(t)$  is the probability per unit time per unit volume that a critical bubble forms. As a function of temperature,

$$p(T) \approx T^4 e^{-\frac{\mathcal{S}_E(T; S_b(r; T))}{T}}, \quad (9)$$

where  $\mathcal{S}_E(T; S_b(r; T))$  is the Euclidean action evaluated along a so-called bounce solution. The Euclidean action is defined as

TABLE I. Benchmark points, at the scale  $Q = 250$  GeV, that exhibit GW potentially in reach of aLIGO (O5), vacuum stability, and acceptable low-energy phenomenology. The peak amplitudes were calculated numerically for  $\beta/H_N$  from Eq. (14).

Point	$M_S^2(\text{GeV}^2)$	$\lambda_S$	$\kappa(\text{GeV})$	$\kappa_1(\text{GeV})$	$\kappa_2$	$\lambda$	$m_S(\text{GeV})$	$\gamma$	$T_C(\text{GeV})$	$T_N/T_C$	$\beta/H_N$	$\Omega_{\text{GW}}$
SSM I	$4.2 \times 10^{14}$	0.064	$2.1 \times 10^7$	$-4.9 \times 10^5$	0.14	0.53	$4.5 \times 10^7$	2.8	$3.7 \times 10^7$	0.44	118	$1.3 \times 10^{-9}$
SSM II	$6.9 \times 10^{14}$	0.073	$2.8 \times 10^7$	$-7.3 \times 10^5$	0.15	0.51	$5.5 \times 10^7$	2.9	$4.2 \times 10^7$	0.45	110	$1.3 \times 10^{-9}$
SSM III	$1.3 \times 10^{15}$	0.13	$7.4 \times 10^7$	$-1.4 \times 10^6$	0.09	0.40	$1.3 \times 10^8$	2.3	$8.2 \times 10^7$	0.35	45	$6 \times 10^{-9}$

$$\mathcal{S}_E = 4\pi \int_0^\infty r^2 dr \left[ \left( \frac{dS(r)}{dr} \right)^2 + V(S, T) \right], \quad (10) \quad \frac{\beta}{H_N} \approx \frac{\mathcal{S}_E(T_N)}{T_N}, \quad (15)$$

and is a functional of the singlet field,  $S(r)$ . A bounce solution is a solution to the classical equation of motion for the singlet [79]. That is, we must solve

$$\frac{\partial^2 S}{\partial r^2} + \frac{2}{r} \frac{\partial S}{\partial r} = \frac{\partial V(S, T)}{\partial S}, \quad S'(0) = 0, \quad S(\infty) = 0, \quad (11)$$

for  $S_b(r; T)$ , where the effective potential is defined in Eq. (4). In a radiation dominated Universe, temperature and time are related by

$$T^2 t = \sqrt{\frac{45}{16\pi^3}} \frac{M_P}{\sqrt{g_\star}}, \quad (12)$$

where  $g_\star \approx 100$  is the number of relativistic degrees of freedom and  $M_P$  is the Planck mass. Combining Eqs. (8), (9) and (12) results in the condition that the Euclidean action satisfies

$$\frac{\mathcal{S}_E(T_N; S_b(r; T_N))}{T_N} \approx 170 - 4 \ln \left( \frac{T_N}{1 \text{ GeV}} \right) - 2 \ln g_\star. \quad (13)$$

We solve for the nucleation temperature  $T_N$  in Eq. (13) by bisection, finding the bounce solution and the resulting Euclidean action for every trial temperature. To find a bounce solution, we approximate the bounce solution by perturbing about an approximate kink solution [80].

#### IV. GRAVITATIONAL WAVES

The amplitude of GW from a first-order PT depends on the wall velocity of a bubble,  $v_w$ ; the latent heat released in the transition between the true and false vacuum,  $\Delta\rho$ ; the efficiency of the conversion of latent heat to GW; and the duration of the transition. The latter is parametrized by

$$\beta \equiv - \left. \frac{d\mathcal{S}_4}{dt} \right|_{t_N} = H_N \left[ \frac{d \ln \mathcal{S}_E/T}{d \ln T} \right] \left. \frac{\mathcal{S}_E}{T} \right|_{T_N} \quad (14)$$

where  $\mathcal{S}_4 = \mathcal{S}_E/T$  is the four-dimensional Euclidean action for a bounce solution to the equations of motion,  $t_N$  is the nucleation time and  $H = -\dot{T}/T$ . The characteristic time scale of the PT is  $1/\beta$ . We can approximate the time scale by [81,82]

up to an  $\mathcal{O}(1)$  factor. We solved the right-hand side in Eq. (13). We attempt to calculate  $\beta$  by numerical differentiation of the action with respect to temperature in Eq. (14); however, to reflect uncertainties in our calculation, we furthermore present results from varying the time scale of the PT in the range  $1 \leq \beta/H_N \leq 200$ . The lower bound is from causality [83]—the characteristic size of a bubble cannot exceed a horizon—and the upper bound is slightly greater than the approximation in Eq. (15).

The latent heat is parametrized by

$$\alpha \equiv \frac{\Delta\rho}{\rho_N} \quad \text{where } \rho_N \equiv \frac{\pi^2 g_\star T_N^4}{30}. \quad (16)$$

The denominator  $\rho_N$  is the energy density of the false vacuum and  $g_\star = 107.75$  is the number of relativistic degrees of freedom at the nucleation temperature  $T_N$ . The numerator,  $\Delta\rho$ , is the latent heat in the transition between the true and false vacuum,

$$\Delta\rho = \left[ V - \frac{dV}{dT} T_N \right]_{\mathcal{F}} - \left[ V - \frac{dV}{dT} T_N \right]_{\mathcal{T}}, \quad (17)$$

evaluated at the nucleation temperature, where  $V$  is the temperature improved scalar potential (i.e., free energy) and subscripts indicate true ( $\mathcal{T}$ ) and false ( $\mathcal{F}$ ) vacua.

The bubble wall velocity—a factor that influences the amplitude of GW—is slowed by friction terms arising from interactions with particles in the plasma. In the high-scale PT that we are considering, because there are fewer friction terms than in the electroweak phase transition (EWPT) in the SM, we expect that  $v_w \approx 1$  in general.<sup>2</sup> The efficiency of converting latent heat into GW—the final factor affecting GW—is denoted by  $\epsilon$ . Because in our scenario  $\gamma \gtrsim 1.75$  (i.e., we consider a very strongly first-order PT), one finds that  $\epsilon \approx 1$ . We take  $\epsilon = 1$  throughout.

Combining all the factors, from numerical simulations using the so-called envelope approximation (see, e.g.,

<sup>2</sup>In supersymmetric models, the wall velocity of bubbles in an EWPT tends to be heavily suppressed by strongly interacting scalars [84]. In the SM, the wall velocity in an EWPT is significantly higher without these friction terms. Thus, for a high-scale PT in the SSM, with even fewer friction terms, we expect  $v_w \approx 1$ .

Ref. [85] for an analytic calculation), the peak amplitude of the GW strength, defined as the energy density per logarithmic frequency interval in units of the critical energy density of the Universe, due to bubble collisions measured today, is given by

$$\Omega_{\text{GW}} \approx 10^{-9} \times \left( \frac{31.6 H_N}{\beta} \right)^2 \left( \frac{\alpha}{\alpha + 1} \right)^2 \epsilon^2 \left( \frac{4v_w^3}{0.43 + v_w^2} \right) \times \left( \frac{100}{g_\star} \right)^{\frac{1}{3}}, \quad (18)$$

where  $g_\star = 107.75$  in our model. The factors are  $\mathcal{O}(1)$  for a PT at a nucleation temperature  $10^7 \text{ GeV} \lesssim T_N \lesssim 10^8 \text{ GeV}$ . The peak amplitude is  $\mathcal{O}(10^{-9})$  for  $\alpha \approx 1$  and  $\gamma \approx 2$ . The aLIGO experiment, LIGO running phase O5, should be sensitive to amplitudes greater than about  $\Omega_{\text{GW}} \gtrsim 5 \times 10^{-10}$  at about  $\mathcal{O}(10)$ – $\mathcal{O}(100)$  Hz [58,86].

The peak amplitude observable today occurs at the peak frequency

$$f_0 \approx 16.5 \text{ Hz} \times \left( \frac{f_N}{H_N} \right) \left( \frac{T_N}{10^8 \text{ GeV}} \right) \left( \frac{g_\star}{100} \right)^{1/6} \quad (19)$$

where  $f_N$  is the peak frequency at the nucleation time,

$$f_N = \frac{0.62\beta}{1.8 - 0.1v_w + v_w^2}. \quad (20)$$

The peak frequency of GW from a PT coincides with aLIGO's maximum sensitivity at about 20 Hz if the nucleation temperature is about  $10^7 \text{ GeV} \lesssim T_N \lesssim 10^8 \text{ GeV}$  [49].

## V. VACUUM STABILITY

After the discovery of the Higgs boson, and subsequent determinations of its mass, the stability of the SM vacuum was reexamined [68–72]. At large-field values, the SM effective potential is approximately

$$V_{\text{eff}}(h) = \frac{1}{2} \lambda(\mu \approx h) h^4, \quad (21)$$

and for stability it is sufficient to ensure that, given an initial value of the quartic coupling at low energy, the renormalization group (RG) evolution is such that the quartic coupling is positive at least until the Planck scale.

The result is sensitive to low-energy data—notably the top-quark mass, Higgs mass and strong coupling—in the quartic coupling's renormalization group equation (RGE). With present experimental data, however, it is believed that the quartic coupling turns negative at about  $\Lambda_1 \approx 10^{10} \text{ GeV}$ , referred to as the SM Higgs instability scale. The SM Higgs potential is believed to be metastable; although we live in a false vacuum, the probability of tunneling to the true vacuum is negligible [70].

This instability can be remedied in simple extensions of the SM, including the SSM, which could alleviate it by

modifying the beta function for the quartic coupling (at one loop by a fish diagram) or by negative corrections to the Higgs mass. The latter implies that a Higgs mass of about 125 GeV, as required by experiments, could be achieved with a quartic coupling larger than that in the SM, and could be realized by tree-level mixing which should result in a negative correction, as eigenvalues are repelled by mixing [62,63]. A quartic coupling sufficiently greater than that in the SM could ensure that the quartic coupling remains positive until the Planck scale, though it should remain perturbative until that scale.

There are, however, additional stability conditions in the SSM, such as

$$\lambda \geq 0, \quad \lambda_S \geq 0, \quad \text{and} \quad \kappa_2 \geq -2\sqrt{\lambda_S \lambda}, \quad (22)$$

that result from considering large-field behavior in the  $H = 0$ ,  $S = 0$  and  $\lambda H^4 = \lambda_S S^4$  directions in field space. Note that if  $\kappa_2$  is negative, the latter condition is equivalent to  $\lambda_{\text{SM}} \geq 0$ , that is, the SM vacuum stability condition. In this case, stability cannot be improved by a threshold correction, though it could be improved by modified RGEs (see the Appendix). Thus, we consider  $\kappa_2 > 0$ . To ensure perturbative unitarity, we followed Ref. [87]. Because in our solutions the Higgs and singlet are approximately decoupled, it resulted in a constraint that  $\lambda_S \lesssim 4.2$  below the GUT scale.

We ensure that the mixing angle between the doublet and singlet is negligible, such that our model agrees with experimental measurements indicating that the Higgs is SM-like. There is, however, a residual threshold correction to the SM quartic. After eliminating the mass squared terms by tadpole conditions, the tree-level mass-squared matrix in the basis  $(h, s)$  reads

$$M^2 = \begin{pmatrix} \lambda v^2 & \kappa_1 + \kappa_2 v_S \\ \kappa_1 v + \kappa_2 v_S v & (4\lambda_S v_S + \kappa) v_S - \frac{1}{2} \frac{v}{v_S} \kappa_1 v \end{pmatrix}. \quad (23)$$

The off-diagonal elements lead to mixing between mass and interaction eigenstates, described by a mixing angle

$$\tan \theta \approx -\frac{\kappa_1 + \kappa_2 v_S}{4\lambda_S v_S + \kappa} \frac{v}{v_S} + \mathcal{O}\left(\frac{v^3}{v_S^3}\right). \quad (24)$$

As the mixing is small, we use the same notation for mass and interaction eigenstates. The mass eigenvalues are approximately

$$m_h^2 \approx \left( \lambda - \frac{(\kappa_1 + \kappa_2 v_S)^2}{v_S (4\lambda_S v_S + \kappa)} \right) v^2, \quad (25)$$

$$m_S^2 \approx v_S (4\lambda_S v_S + \kappa) - \frac{1}{2} \frac{v^2}{v_S} \left( \kappa_1 - \frac{2(\kappa_1 + \kappa_2 v_S)^2}{\kappa + 4\lambda_S v_S} \right), \quad (26)$$

neglecting terms  $\mathcal{O}(v^4/v_S^2)$ . As stressed in Refs. [62,63], in the limit  $v/v_S \rightarrow 0$ , the singlet only partially decouples. While the mixing vanishes ( $\tan \theta \rightarrow 0$ ), a negative tree-level contribution to the Higgs mass survives:

$$m_h^2 = \left( \lambda - \frac{(\kappa_1 + \kappa_2 v_S)^2}{v_S(4\lambda_S v_S + \kappa)} \right) v^2 \leq \lambda v^2. \quad (27)$$

Thus, the quartic coupling in the SM plus a singlet that achieves  $m_h \approx 125$  GeV is greater than that in the SM (or equivalently, there is a threshold correction to the quartic coupling in an effective theory in which the singlet is integrated out from the SM plus singlet), which improves the stability of the Higgs potential. That is,

$$\Delta\lambda = \frac{(\kappa_1 + \kappa_2 v_S)^2}{v_S(4\lambda_S v_S + \kappa)} \geq 0. \quad (28)$$

If  $\kappa \rightarrow 0$  and  $\kappa_1 \rightarrow 0$ ,  $\Delta\lambda \rightarrow \kappa_2^2/4\lambda_S$ , reproducing the expression in Refs. [62,63]. Substantial  $\kappa_1$  in the numerator or cancellations involving  $\kappa$  in the denominator could, however, help generate a sizable threshold correction.

There are, however, subtleties: the conditions in Eq. (22) were necessary, but insufficient for stability. For example, in Ref. [62] it was shown that for a  $\mathbb{Z}_2$  symmetric potential and renormalization scales  $\mu \lesssim M_S$ , if  $\kappa_2 > 0$ , the SM vacuum stability condition,

$$\lambda_{\text{SM}} \equiv \lambda - \Delta\lambda \geq 0, \quad (29)$$

is required to avoid deeper minima in the  $S = 0$  direction. We thus require  $\mu \lesssim M_S \lesssim \Lambda_I$ , that is, that the singlet scale is less than the SM instability scale. This ensures that although there is an instability scale at which the SM vacuum stability condition is broken,

$$\lambda_{\text{SM}}(\mu = \Lambda_I \gtrsim M_S) < 0, \quad (30)$$

the vacuum may in fact be stable, as we may violate the SM vacuum stability condition at scales  $\mu \gtrsim M_S$ . We trust that lessons from the  $\mathbb{Z}_2$  symmetric case are applicable to our general potential in Eq. (1). Thus, in this paper, we describe our model as stable if the couplings satisfy the large-field conditions on vacuum stability in Eq. (22) and the SM vacuum stability condition in Eq. (29) for  $\mu \lesssim M_S \lesssim \Lambda_I$ . We leave a detailed analysis to a future work.

## VI. NUMERICAL RESULTS

As well as generating GW potentially within reach of aLIGO and improving vacuum stability, our models must satisfy low-energy experimental constraints on the weak scale (i.e., the  $Z$ -boson mass), the Higgs mass and Higgs-singlet mixing, and be free from Landau poles below the GUT scale. We fixed an order parameter,  $1.75 \lesssim \gamma \lesssim 5$ , and a critical temperature of  $10^7 \text{ GeV} \lesssim T_C \lesssim 10^8 \text{ GeV}$ .

We included low-energy constraints by building two-loop RGEs in SARAH-4.8.2 [88] by modifying the SSM model and constructing a tree-level spectrum generator by finding consistent solutions to the tree-level tadpole equations and diagonalizing the weak-scale mass matrix. Our spectrum generator guaranteed the correct weak scale by tuning the

Higgs mass parameter in the tree-level tadpole equations. To approximately satisfy limits on Higgs-singlet mixing from hadron colliders (see, e.g., Ref. [89]), we required a tiny mixing angle between Higgs and singlet scalars,  $\tan\theta \leq 10^{-6}$ . We tuned the Higgs mass by bisection in the Higgs quartic such that  $m_h = 125 \pm 1$  GeV. We found simultaneous solutions to the low-energy constraints and GW requirements by iterating between the weak scale and the critical temperature.

In Table I we present three benchmark points with GW amplitudes potentially within the reach of aLIGO (O5), acceptable zero-temperature phenomenology and a substantial threshold correction to the tree-level Higgs quartic for improved vacuum stability. The running of the Higgs

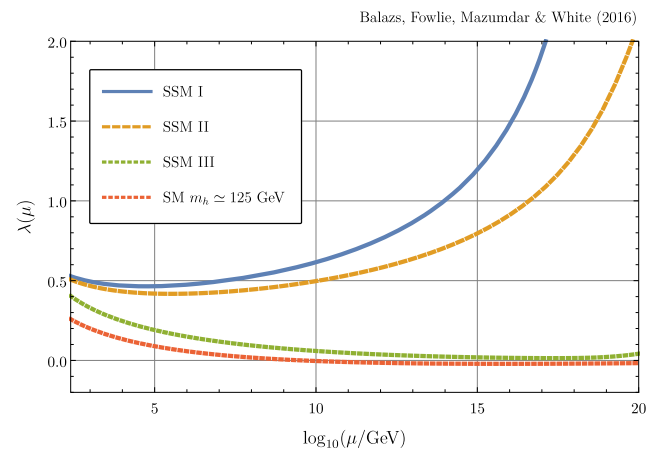


FIG. 2. Running of the Higgs quartic  $\lambda$  in the SM and for our solutions in the SSM. All lines correspond to  $m_h \approx 125$  GeV.

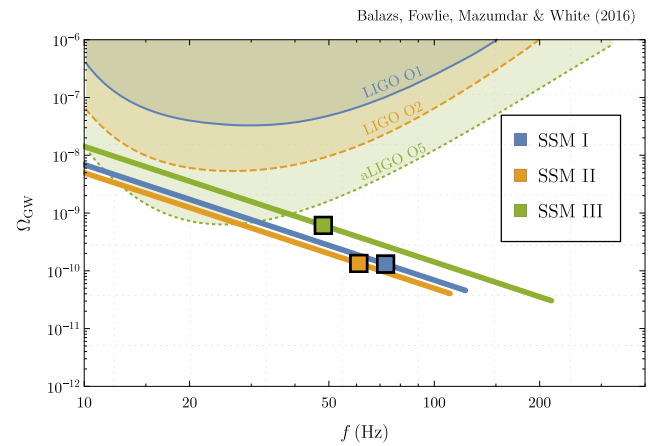


FIG. 3. Peak amplitudes and frequencies of GW for our SSM benchmark points from our approximate numerical calculation of  $\beta/H_N$  (squares), with uncertainty represented by varying between  $\beta/H_N = 1$  and  $\beta/H_N = 200$  (lines). The shaded regions indicate LIGO sensitivities during various phases of running [58,86]. All lines intersect the sensitivity of aLIGO (LIGO running phase O5).

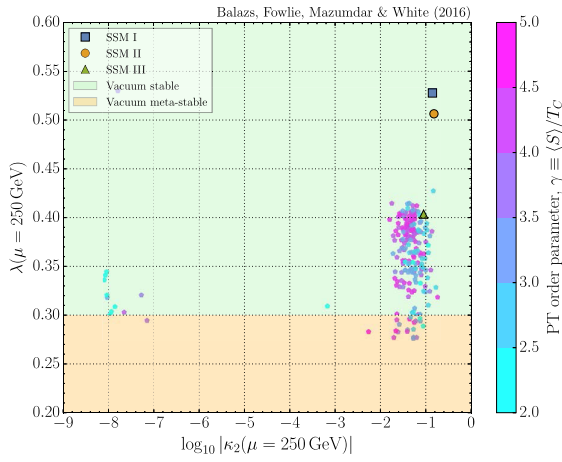
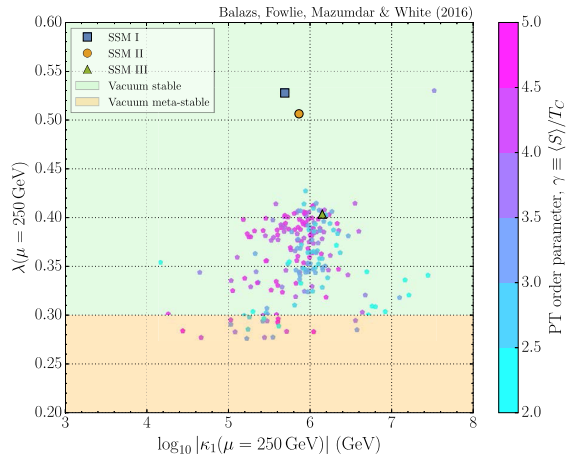
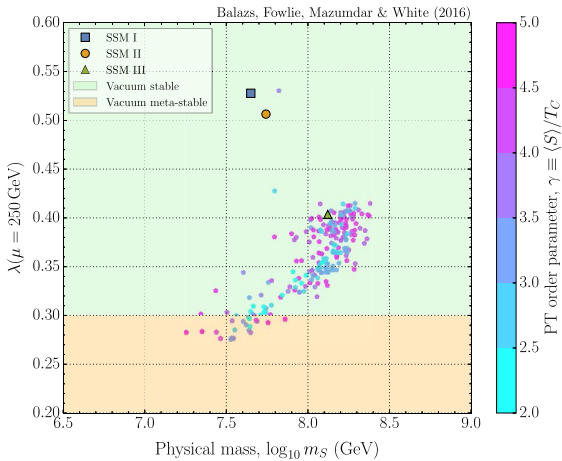
quartic for our three benchmarks and in the SM is shown in Fig. 2, demonstrating that for our benchmarks, the quartic coupling remains positive below the Planck scale, unlike in the SM. Note that the running of the Higgs quartic coupling is sensitive to the precise values of the top Yukawa,  $y_t$ , and the strong coupling,  $g_3$ . The experimental measurements for  $y_t$  and  $g_3$  were boundary conditions at  $Q \approx 10^7$  GeV; this introduced an error of up to about 3% in their weak-scale values for our benchmarks. As such the running for SSM III is pessimistic; its quartic running is probably steeper. For benchmark SSM I, the quartic coupling hits a Landau pole above the GUT scale. We illustrate that our benchmark points result in peak amplitudes and frequencies of GW potentially within reach of aLIGO (O5) in Fig. 3. However, note that here we have varied  $1 \leq \beta/H_N \leq 200$ .

We selected our benchmarks from thousands of solutions found by Monte Carlo (MC) sampling SSM parameters at the GW scale,  $Q = T_C$ , from the intervals

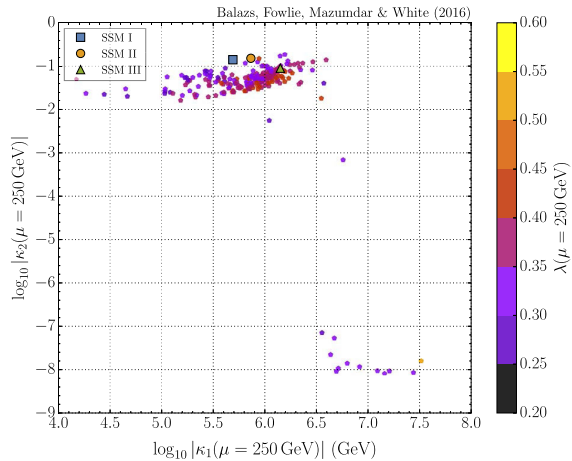
$$\begin{aligned} 10^{-8} \text{ GeV} &\leq |\kappa_1| \leq 10^8 \text{ GeV} \\ 10^{-8} &\leq \kappa_2 \leq 2 \\ 10^{12} \text{ GeV}^2 &\leq M_S^2 \leq 10^{18} \text{ GeV}^2 \\ 10^7 \text{ GeV} &\leq T_C \leq 10^8 \text{ GeV} \\ 2.3 &\leq \gamma \leq 3. \end{aligned} \quad (31)$$

We traded the Lagrangian parameters  $\kappa$  and  $\lambda_S$  for  $T_C$  and  $\gamma$  by solving Eqs. (5) and (6), and  $\lambda$  and  $\mu^2$  by requiring correct Higgs and  $Z$ -boson masses. A substantial fraction of our MC solutions could exhibit GW in reach of aLIGO; however, calculating the amplitude of GW accurately requires a thorough lattice simulation.

When selecting our benchmarks, however, we found that if  $\gamma \gtrsim 3$ , the rate of tunneling is sometimes too slow for a PT to dominate the Universe, with this being the case more often as  $\gamma$  approaches 5. That is, it is impossible to satisfy

(a) Higgs quartic and dimensionless  $S^2H^2$  coupling.(b) Higgs quartic and dimensionful  $SH^2$  coupling.

(c) Higgs quartic and physical singlet mass.



(d) The singlet-Higgs couplings

FIG. 4. Scatter plots of solutions in the SSM that exhibit strongly first-order PT at  $T_C \in (10^7, 10^8)$  GeV, acceptable weak-scale phenomenology, and no Landau poles below the GUT scale. For the benchmark points shown, in addition, we checked that the PT results in GW signatures are potentially within reach of aLIGO (O5).

condition Eq. (13) for any temperature. This is consistent with Ref. [90], in which no solutions with  $\gamma > 5$  were found. Since we desire a completed PT, we discarded solutions with an order parameter  $\gamma \gtrsim 5$ . This may, in fact, be optimistic, as Ref. [90] indicates that completed PTs with  $\gamma \approx 5$  are rare and as we require a lower value of  $\mathcal{S}_E/T$  since the nucleation temperature is 5 orders of magnitude higher than the EW scale [see Eq. (13)]. On the other hand, if the order parameter  $\gamma \lesssim 2.3$ , the amplitude of GW may be too far below aLIGO (O5) sensitivity for all but the most optimistic estimate of the peak amplitude. There is therefore a “Goldilocks region” for the strength of the PT,  $2.3 \lesssim \gamma \lesssim 3$ , for which GW could be observed at aLIGO. Thus, to roughly select GW amplitudes in reach of aLIGO, we sampled from  $2.3 \lesssim \gamma \lesssim 3$ .

We scatter our MC solutions in Fig. 4. We find that moderate Higgs quartics of  $\lambda \sim 0.35$  are common, although there are outliers at  $\lambda \gtrsim 0.4$ . We see in Fig. 4(a) that the dimensionless singlet-Higgs coupling is moderate,  $\kappa_2 \lesssim 0.1$ . We find, unsurprisingly, in Figs. 4(b) and 4(c) that dimensionful parameters are similar to the critical temperature,  $m_S \sim \kappa_1 \sim T_C \sim 10^7$  GeV. The Higgs-singlet couplings appear correlated in Fig. 4(d). This is likely due to the fact that the Higgs-singlet mixing angle is reduced for  $\kappa_1 \sim -2\kappa_2 v_s$ . The sizes of the Higgs-singlet couplings are related to the threshold correction in Eq. (28), which we require to be moderate. There exist points with a Higgs quartic larger than in the benchmark SSM I that may suffer from Landau poles in the Higgs quartic below the GUT scale.

## VII. DISCUSSION AND CONCLUSIONS

GW detectors, such as LIGO, are a novel way of probing new physics. In this work, we studied the detectability of primordial GW in the context of the SM augmented with a single real scalar field that is a singlet under all SM gauge groups. The scale of the scalar singlet (its mass and VEV) was motivated by vacuum stability to be  $10^7$ – $10^8$  GeV. We have shown that, with this scale, the singlet dynamics leads to a strongly first-order PT that generates GW potentially within reach of aLIGO (LIGO run phase O5). Selected from a wide sample over the parameter space, we presented three benchmark points with detailed calculations of the peak GW frequency and amplitude, demonstrating that for an optimistic estimate of the peak frequency and amplitude, they lie within aLIGO sensitivity. The most optimistic scenario, of course, arises for  $\beta/H_N \sim \mathcal{O}(1)$ .

While it is known that eLISA is able to probe PTs at or near the EW scale, to our knowledge this work is the first to discuss a physical motivation for a PT to leave a relic background potentially detectable by aLIGO. Our result is due to the coincidence of aLIGO sensitivity with the EW

instability scale. Indeed, the original analysis that proposed the existence of a heavy singlet leading to a tree-level boost in the Higgs quartic coupling promoted the case where the mass of the singlet was  $10^7$ – $10^8$  GeV [62]. This is precisely in the region where the stochastic background is visible at aLIGO. It should be stressed, though, that it is also possible to boost the stability of the vacuum with a lighter singlet.

With planned LIGO running phases sensitive to GW amplitudes below  $10^{-9}$ , it is interesting to consider motivations for a PT at  $10^7$ – $10^8$  GeV, which, on a logarithmic scale, lies about halfway between the EW and the grand unification scales. One exotic possibility is EW baryogenesis through a multistep PT with the first transition at around  $10^7$ – $10^8$  GeV as proposed in Ref. [91]. This presents another intriguing possibility about physically motivated PTs occurring at such a high scale. This and other scenarios we leave to future work.

## ACKNOWLEDGMENTS

We thank Bhupal Dev, Eric Thrane and Peter Athron for helpful discussions. This work in part was supported by the Australian Research Council Centre of Excellence for Particle Physics at the Terascale. A. M. is supported by Science and Technology Facilities Council Grant No. ST/J000418/1.

## APPENDIX: SSM $\beta$ FUNCTIONS

We generated beta functions from our modified SSM model in SARAH-4.8.2 [88]. The beta functions for  $\lambda_S$  and  $\kappa_2$  were such that the quartics remained positive. The former is positive at one loop,

$$16\pi^2 \beta_{\lambda_S}^{1L} = \kappa_2^2 + 36\lambda_S^2, \quad (\text{A1})$$

though there are negative terms at two loops, and the latter is proportional to  $\kappa_2$  at one loop,

$$16\pi^2 \beta_{\kappa_2}^{1L} = \frac{1}{10} \kappa_2 (-9g_1^2 - 45g_2^2 + 60\lambda + 60y_t^2 + 40\kappa_2 + 120\lambda_S), \quad (\text{A2})$$

and at two loops. Thus at two loops it cannot change sign. There is, furthermore, an additional contribution to the beta function of the SM quartic,

$$16\pi^2 \beta_{\lambda}^{1L} = \frac{27}{100} g_1^4 + \frac{9}{10} g_1^2 g_2^2 + \frac{9}{4} g_2^4 - \frac{9}{5} g_1^2 \lambda - 9g_2^2 \lambda + 12\lambda^2 + 12\lambda y_t^2 - 12y_t^4 + \kappa_2^2, \quad (\text{A3})$$

which could improve vacuum stability.

- [1] B. P. Abbott *et al.* (VIRGO, LIGO Scientific Collaborations), *Phys. Rev. Lett.* **116**, 061102 (2016).
- [2] P. D. Lasky *et al.*, *Phys. Rev. X* **6**, 011035 (2016).
- [3] M. Maggiore, *Phys. Rep.* **331**, 283 (2000).
- [4] L. P. Grishchuk, *Zh. Eksp. Teor. Fiz.* **67**, 825 (1974) [*Sov. Phys. JETP* **40**, 409 (1975)].
- [5] A. A. Starobinsky, *Pis'ma Zh. Eksp. Teor. Fiz.* **30**, 719 (1979) [*JETP Lett.* **30**, 682 (1979)].
- [6] V. A. Rubakov, M. V. Sazhin, and A. V. Veryaskin, *Phys. Lett.* **115B**, 189 (1982).
- [7] S. Y. Khlebnikov and I. I. Tkachev, *Phys. Rev. D* **56**, 653 (1997).
- [8] R. Easther and E. A. Lim, *J. Cosmol. Astropart. Phys.* **04** (2006) 010.
- [9] J. F. Dufaux, A. Bergman, G. N. Felder, L. Kofman, and J.-P. Uzan, *Phys. Rev. D* **76**, 123517 (2007).
- [10] J. Garcia-Bellido, D. G. Figueroa, and A. Sastre, *Phys. Rev. D* **77**, 043517 (2008).
- [11] A. Mazumdar and H. Stoica, *Phys. Rev. Lett.* **102**, 091601 (2009).
- [12] A. Kusenko and A. Mazumdar, *Phys. Rev. Lett.* **101**, 211301 (2008).
- [13] A. Kusenko, A. Mazumdar, and T. Multamaki, *Phys. Rev. D* **79**, 124034 (2009).
- [14] A. Mazumdar and I. M. Shoemaker, [arXiv:1010.1546](https://arxiv.org/abs/1010.1546).
- [15] T. Damour and A. Vilenkin, *Phys. Rev. Lett.* **85**, 3761 (2000).
- [16] S. Olmez, V. Mandic, and X. Siemens, *Phys. Rev. D* **81**, 104028 (2010).
- [17] A. Kosowsky, M. S. Turner, and R. Watkins, *Phys. Rev. Lett.* **69**, 2026 (1992).
- [18] A. Kosowsky, M. S. Turner, and R. Watkins, *Phys. Rev. D* **45**, 4514 (1992).
- [19] M. Kamionkowski, A. Kosowsky, and M. S. Turner, *Phys. Rev. D* **49**, 2837 (1994).
- [20] C. Cutler and K. S. Thorne, in *Proceedings, 16th International Conference on General Relativity and Gravitation: Durban, South Africa, July 15–21, 2001* (World Scientific, Singapore; River Edge, NJ, 2013), pp. 72–111.
- [21] C. Grojean and G. Servant, *Phys. Rev. D* **75**, 043507 (2007).
- [22] S. J. Huber and T. Konstandin, *J. Cosmol. Astropart. Phys.* **09** (2008) 022.
- [23] C. Caprini, R. Durrer, and G. Servant, *Phys. Rev. D* **77**, 124015 (2008).
- [24] C. Caprini, R. Durrer, and G. Servant, *Phys. Rev. D* **77**, 124015 (2008).
- [25] K. Nakayama, S. Saito, Y. Suwa, and J. Yokoyama, *Phys. Rev. D* **77**, 124001 (2008).
- [26] J. Kehayias and S. Profumo, *J. Cosmol. Astropart. Phys.* **03** (2010) 003.
- [27] D. J. H. Chung and P. Zhou, *Phys. Rev. D* **82**, 024027 (2010).
- [28] L. Krauss, S. Dodelson, and S. Meyer, *Science* **328**, 989 (2010).
- [29] J. R. Espinosa, T. Konstandin, J. M. No, and G. Servant, *J. Cosmol. Astropart. Phys.* **06** (2010) 028.
- [30] E. Greenwood and P. M. Vaudrevange, [arXiv:1011.5881](https://arxiv.org/abs/1011.5881).
- [31] J. M. No, *Phys. Rev. D* **84**, 124025 (2011).
- [32] C. Wainwright, S. Profumo, and M. J. Ramsey-Musolf, *Phys. Rev. D* **84**, 023521 (2011).
- [33] R. Durrer and J. Hasenkamp, *Phys. Rev. D* **84**, 064027 (2011).
- [34] R. Saito and S. Shirai, *Phys. Lett. B* **713**, 237 (2012).
- [35] M. Hindmarsh, S. J. Huber, K. Rummukainen, and D. J. Weir, *Phys. Rev. Lett.* **112**, 041301 (2014).
- [36] W. Buchmüller, V. Domcke, K. Kamada, and K. Schmitz, *J. Cosmol. Astropart. Phys.* **10** (2013) 003.
- [37] B. J. Vlcek, Ph. D. thesis, Wisconsin U., Milwaukee, 2013 [[arXiv:1308.5347](https://arxiv.org/abs/1308.5347)].
- [38] N. Okada and Q. Shafi, [arXiv:1311.0921](https://arxiv.org/abs/1311.0921).
- [39] D. G. Figueroa, *J. High Energy Phys.* **11** (2014) 145.
- [40] A. Kamada and M. Yamada, *Phys. Rev. D* **91**, 063529 (2015).
- [41] T. Kalaydzhyan and E. Shuryak, *Phys. Rev. D* **91**, 083502 (2015).
- [42] P. Schwaller, *Phys. Rev. Lett.* **115**, 181101 (2015).
- [43] M. Chala, G. Nardini, and I. Sobolev, *Phys. Rev. D* **94**, 055006 (2016).
- [44] R. Jinno and M. Takimoto, [arXiv:1604.05035](https://arxiv.org/abs/1604.05035).
- [45] M. Kakizaki, S. Kanemura, and T. Matsui, *Phys. Rev. D* **92**, 115007 (2015).
- [46] K. Hashino, M. Kakizaki, S. Kanemura, and T. Matsui, *Phys. Rev. D* **94**, 015005 (2016).
- [47] A. Klein, E. Barausse, A. Sesana, A. Petiteau, E. Berti, S. Babak, J. Gair, S. Aoudia, I. Hinder, F. Ohme, and B. Wardell, *Phys. Rev. D* **93**, 024003 (2016).
- [48] C. Caprini, M. Hindmarsh, S. Huber, T. Konstandin, J. Kozaczuk, G. Nardini, J. M. No, A. Petiteau, P. Schwaller, G. Servant, and D. J. Weir, *J. Cosmol. Astropart. Phys.* **04** (2016) 001.
- [49] P. S. B. Dev and A. Mazumdar, *Phys. Rev. D* **93**, 104001 (2016).
- [50] J. Jaeckel, V. V. Khoze, and M. Spannowsky, *Phys. Rev. D* **94**, 103519 (2016).
- [51] M. Artymowski, M. Lewicki, and J. D. Wells, [arXiv:1609.07143](https://arxiv.org/abs/1609.07143).
- [52] A. Addazi, [arXiv:1607.08057](https://arxiv.org/abs/1607.08057).
- [53] P. Huang, A. J. Long, and L.-T. Wang, *Phys. Rev. D* **94**, 075008 (2016).
- [54] K. Hashino, M. Kakizaki, S. Kanemura, P. Ko, and T. Matsui, [arXiv:1609.00297](https://arxiv.org/abs/1609.00297).
- [55] G. M. Harry (LIGO Scientific Collaboration), *Classical Quantum Gravity* **27**, 084006 (2010).
- [56] J. Aasi *et al.* (LIGO Scientific Collaboration), *Classical Quantum Gravity* **32**, 074001 (2015).
- [57] D. V. Martynov *et al.* (LIGO Scientific Collaboration), *Phys. Rev. D* **93**, 112004 (2016).
- [58] B. P. Abbott *et al.* (VIRGO, LIGO Scientific Collaborations), *Phys. Rev. Lett.* **116**, 131102 (2016).
- [59] S. Ghosh, A. Kundu, and S. Ray, *Phys. Rev. D* **93**, 115034 (2016).
- [60] D. O'Connell, M. J. Ramsey-Musolf, and M. B. Wise, *Phys. Rev. D* **75**, 037701 (2007).
- [61] M. Gonderinger, Y. Li, H. Patel, and M. J. Ramsey-Musolf, *J. High Energy Phys.* **01** (2010) 053.
- [62] J. Elias-Miro, J. R. Espinosa, G. F. Giudice, H. M. Lee, and A. Strumia, *J. High Energy Phys.* **06** (2012) 031.
- [63] O. Lebedev, *Eur. Phys. J. C* **72**, 2058 (2012).
- [64] G. F. Giudice and H. M. Lee, *Phys. Lett. B* **694**, 294 (2011).
- [65] A. Salvio and A. Mazumdar, *Phys. Lett. B* **750**, 194 (2015).

- [66] A. Salvio and A. Mazumdar, *Phys. Lett. B* **755**, 469 (2016).
- [67] A. Mazumdar and J. Rocher, *Phys. Rep.* **497**, 85 (2011).
- [68] J. Elias-Miro, J. R. Espinosa, G. F. Giudice, G. Isidori, A. Riotto, and A. Strumia, *Phys. Lett. B* **709**, 222 (2012).
- [69] S. Alekhin, A. Djouadi, and S. Moch, *Phys. Lett. B* **716**, 214 (2012).
- [70] G. Degrossi, S. Di Vita, J. Elias-Miro, J. R. Espinosa, G. F. Giudice, G. Isidori, and A. Strumia, *J. High Energy Phys.* **08** (2012) 098.
- [71] I. Masina, *Phys. Rev. D* **87**, 053001 (2013).
- [72] Z. Xing, H. Zhang, and S. Zhou, *Phys. Rev. D* **86**, 013013 (2012).
- [73] C. Balázs, A. Mazumdar, E. Pukartas, and G. White, *J. High Energy Phys.* **01** (2014) 073.
- [74] R. Jinno, K. Nakayama, and M. Takimoto, *Phys. Rev. D* **93**, 045024 (2016).
- [75] H. H. Patel and M. J. Ramsey-Musolf, *J. High Energy Phys.* **07** (2011) 029.
- [76] M. Quiros, in *Finite temperature field theory and phase transitions* (1999), p. 187–259, <https://inspirehep.net/record/494058>.
- [77] A. K. Das, *Finite Temperature Field Theory* (World Scientific, New York, 1997), ISBN 9789810228569, 9789814498234.
- [78] A. H. Guth and S. H. H. Tye, *Phys. Rev. Lett.* **44**, 631 (1980).
- [79] S. R. Coleman, *Phys. Rev. D* **15**, 2929 (1977); **16**, 1248(E) (1977).
- [80] S. Akula, C. Balázs, and G. A. White, *Eur. Phys. J. C* **76**, 681 (2016).
- [81] M. S. Turner, E. J. Weinberg, and L. M. Widrow, *Phys. Rev. D* **46**, 2384 (1992).
- [82] C. J. Hogan, *Phys. Lett.* **133B**, 172 (1983).
- [83] J. T. Giblin and E. Thrane, *Phys. Rev. D* **90**, 107502 (2014).
- [84] P. John and M. G. Schmidt, *Nucl. Phys.* **B598**, 291 (2001); **B648**, 449(E) (2003).
- [85] R. Jinno and M. Takimoto, *Phys. Rev. D* **95**, 024009 (2017).
- [86] E. Thrane and J. D. Romano, *Phys. Rev. D* **88**, 124032 (2013).
- [87] S. K. Kang and J. Park, *J. High Energy Phys.* **04** (2015) 009.
- [88] F. Staub, *Comput. Phys. Commun.* **185**, 1773 (2014).
- [89] CMS Collaboration, CERN Technical Report No. CMS-PAS-HIG-12-045, 2012.
- [90] S. Profumo, M. J. Ramsey-Musolf, C. L. Wainwright, and P. Winslow, *Phys. Rev. D* **91**, 035018 (2015).
- [91] S. Inoue, G. Ovanessian, and M. J. Ramsey-Musolf, *Phys. Rev. D* **93**, 015013 (2016).

# Effective field theory, electric dipole moments and electroweak baryogenesis

---

## 8.1 Introductory remarks

Effective field theory allows to build physics models from bottom-up by including higher and higher dimensional interactions in the Lagrangian approximating better and better an ultraviolet complete theory. This technique is also used to make the scope of experimental constraints more model independent [123, 124, 125]. They have been used for example in applying dark matter direct and indirect detection constraints [126]. Unfortunately, some of these effective operators were used outside the range of validity of effective field theory [127]. This motivated the use of simplified models which minimally extend the Standard Model particle content [128, 129, 130, 131, 132, 133]. (Simplified models can also be viewed as a lowest order effective field theory that, by adding more effective operators, begins to asymptote the complete model.) There has been little done on effective field theory in the study of electroweak baryogenesis. As such one needs to explore the basic framework before discussing questions of the range of validity and ultraviolet completion.

The strength of the experimental constraints on CP violating effective operators due mostly to negative searches for permanent electric dipole moments is impressive – constraining some operators up to the multi TeV level [134, 135, 136, 137]. This motivates an effective field theory approach that attempts to broaden the scope on these limits. However, successful electroweak baryogenesis requires not only new sources of CP violation, but new weak scale physics to catalyse a phase transition. In principle, these two conditions could have a unified explanation – say one extra particle. I consider the more general case where they are unrelated. In this case, the many possibilities that could catalyse a strongly first order electroweak phase transition is a peripheral concern and it is more practical to sweep such details under the rug and instead parametrize the details of the phase transition.

When I calculate the baryogenesis produced by some test operators I find that surprisingly, the scale of CP violation can be quite high if the conditions of the phase transition are ideal (generally a very strongly first order phase transition, a thin bubble wall propagating at a slow speed). A second surprising finding is that

when one sweeps details of the physics that leads to a strongly first order phase transition under a rug, the degeneracy of certain dimension 6 operators is lifted. For such claims to be verified one will eventually need to look at the UV completion of such operators to see if one can avoid contributions from the heavy physics from becoming Boltzmann suppressed. With these issues in mind I nonetheless present a rigorous step toward linking EDM constraints to baryogenesis calculations in a model independent way.

## 8.2 Declaration for thesis chapter 8

### Declaration by candidate

In the case of the paper present contained in chapter 8, the nature and extent of my contribution was as follows:

Publication	Nature of contribution	Extent of contribution
8	Came up with idea, numerical implementation, analytic demonstration of key concepts in the paper, wrote large parts of the paper and contributed to discussions throughout.	50%

The following coauthors contributed to the work. If the coauthor is a student at Monash, their percentage contribution is given:

Author	Nature of contribution	Extent of contribution
Csaba Balazs	Involved with writeup. Contributed to discussions throughout	
Jason Yue	Worked heavily on EDM calculations, write up and contributed to discussions throughout.	

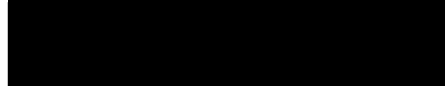
The undersigned hereby certify that the above declaration correctly reflects the nature and extent of the candidate and co-authors' contributions to this work.

**Signatures:**

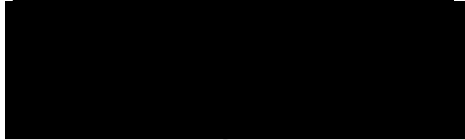
Graham White



Csaba Balazs



Jason Yue



**Date:**

3.04.2017

### **8.3 Published material for chapter 8: Effective field theory, electric dipole moments and electroweak baryogenesis**

Begins overleaf

# Effective field theory, electric dipole moments and electroweak baryogenesis

Csaba Balazs,<sup>a</sup> Graham White<sup>a</sup> and Jason Yue<sup>b,c</sup>

<sup>a</sup>*ARC Centre of Excellence for Particle Physics at the Terascale School of Physics and Astronomy, Monash University, Victoria 3800, Australia*

<sup>b</sup>*Department of Physics, National Taiwan Normal University, Taipei 116, Taiwan*

<sup>c</sup>*ARC Centre of Excellence for Particle Physics at the Terascale, School of Physics, The University of Sydney, NSW 2006, Australia*

*E-mail:* [csaba.balazs@monash.edu](mailto:csaba.balazs@monash.edu), [graham.white@monash.edu](mailto:graham.white@monash.edu), [jason.yue@ntnu.edu.tw](mailto:jason.yue@ntnu.edu.tw)

**ABSTRACT:** Negative searches for permanent electric dipole moments (EDMs) heavily constrain models of baryogenesis utilising various higher dimensional charge and parity violating (CPV) operators. Using effective field theory, we create a model independent connection between these EDM constraints and the baryon asymmetry of the universe (BAU) produced during a strongly first order electroweak phase transition. The thermal aspects of the high scale physics driving the phase transition are parameterised by the usual kink solution for the bubble wall profile. We find that operators involving derivatives of the Higgs field yield CPV contributions to the BAU containing derivatives of the Higgs vacuum expectation value (vev), while non-derivative operators lack such contributions. Consequently, derivative operators cannot be eliminated in terms of non-derivative operators (via the equations of motion) if one is agnostic to the new physics that leads to the phase transition. Thus, we re-classify the independent dimension six operators, restricting ourselves to third generation quarks, gauge bosons and the Higgs. Finally, we calculate the BAU (as a function of the bubble wall width and the cutoff) for a derivative and a non-derivative operator, and relate it to the EDM constraints.

**KEYWORDS:** Cosmology of Theories beyond the SM, CP violation, Effective field theories, Thermal Field Theory

ARXIV EPRINT: [1612.01270](https://arxiv.org/abs/1612.01270)

---

**Contents**

<b>1</b>	<b>Introduction</b>	<b>1</b>
<b>2</b>	<b>Removing redundancies of operators with derivative coupling to the Higgs</b>	<b>3</b>
<b>3</b>	<b>Operators classification</b>	<b>5</b>
<b>4</b>	<b>Electroweak baryogenesis with higher dimensional operators</b>	<b>5</b>
4.1	Constructing new CPV sources with higher dimensional operators	5
4.2	Contributions from $\mathcal{O}_{t1}$ vertices	7
4.3	Contributions from $\mathcal{O}_{DD}$ vertices	8
4.4	Calculating the baryon asymmetry	9
<b>5</b>	<b>EDM constraints</b>	<b>10</b>
<b>6</b>	<b>Numerical results and discussion</b>	<b>12</b>
6.1	Space-time dependent cutoff	16
<b>7</b>	<b>Conclusions</b>	<b>17</b>

---

**1 Introduction**

The Higgs boson discovered at the Large Hadron Collider (LHC) [1, 2] closely resembles that of the Standard Model (SM). This rules out the mechanism of electroweak baryogenesis (cf. [3] and references therein for a pedagogical review) within the SM because with a Higgs mass of 125 GeV [4] the electroweak phase transition (EWPT) does not provide a sufficient departure from equilibrium [5]. The SM also falls short in the amount of charge (C) and charge-parity (CP) violation to generate the observed baryon asymmetry of the universe (BAU) [6, 7]. These two facts alone are enough to motivate the existence of new physics responsible for baryon asymmetry.

Physics models entailing new particles or interactions can introduce charge-parity violating (CPV) phases to assist explaining the observed BAU [8] via electroweak baryogenesis. The use of effective field theories (EFTs) allows one to test a large class of models without adhering to a specific model or framework. This greatly facilitates the connection with experimental constraints. Under this motivation, we consider an extension of the Standard Model by effective dimension six operators. To achieve electroweak baryogenesis, one typically utilises two such higher dimensional operators<sup>1</sup> to simultaneously generate enough

---

<sup>1</sup>For an approach where EWBG is achieved without adding particle content to the SM nor invoking higher dimensional operators, see [9].

$CP$  violation and a strongly first order phase transition (SFOPT) at the electroweak scale (cf. [10–12] and references therein). Considerable amount of literature have been devoted to generate sufficient CPV via dimension six operators [13–16], whilst evading ever tighter constraints from searches for permanent electric dipole moments (EDMs). Similarly, studies of a SFOPT catalysed by dimension six operators [17, 18] (particularly applied to top-Higgs sector [19, 20]) place a bound of  $\Lambda \lesssim 800$  GeV on the scale of new physics that could boost the strength of the phase transition [21].

In this work, we argue that it possible to build a relatively direct bridge between the EDM constraints on a higher dimensional operator and the maximal baryon asymmetry produced by such an operator by assuming a strongly first order phase transition (which is parametrised by the bubble wall width, velocity, etc.) [22–25]. This bridge can be used to then classify the UV completion(s) corresponding to the EFT (for some examples see [26–29]).<sup>2</sup> While building the above bridge, we point out that the degeneracy between certain higher dimensional operators is lifted. Usually, derivative operators are traded to non-derivative ones via the classical equations of motion. However, such degeneracy may be broken in BAU calculations since the CPV sources corresponding to these operators have different dependencies on the assumed profile of the space-time varying vacuum. It is necessary then to extend the higher dimensional  $CP$  violating operator basis (cf. e.g. [31–33]) that is capable of generating the baryon asymmetry.

The most promising operators for BAU generation are those that contain at least one Higgs field to accommodate  $CP$  violating interactions with a space-time varying bubble wall as well as a strongly coupled SM field, i.e. a top quark or a gauge boson. The resonant enhancement of such interaction during the electroweak phase transition becomes the most efficient mode for baryogenesis. Consequently, two qualitatively different operators are chosen within the new catalogue of the operators presented in this paper to demonstrate the aforementioned bridge. One of the operators chosen is normally considered redundant due to the equations of motion. It involves a derivative coupling to the Higgs and the result is an increased sensitivity to the width of the electroweak bubble wall. The respective baryon asymmetries are calculated show that current EDM measurements can meaningfully constrain the available parameter space.

The structure of this paper is outlined as follows. In section 2 we demonstrate that the redundancy between various operators is lost during the electroweak phase transition. We then catalogue the full set of  $CP$  violating dimension six operators that are candidates for producing the BAU via the electroweak mechanism in section 3. The  $CP$  violating sources are calculated using the closed time path formalism in section 4, with their respective EDM constraints derived subsequently in section 5. We present resulting BAU in section 6 before briefly discussing the possibility of space-time varying masses of heavy particles in section 6.1. Finally we conclude with section 7.

---

<sup>2</sup>See [30] for an approach of connecting EFTs and UV complete models in the context of Higgs flavour violation.

## 2 Removing redundancies of operators with derivative coupling to the Higgs

A successful explanation of the BAU necessarily fulfils the three Sakharov conditions [34]:

- (1) baryon number violation,
- (2) charge and charge-parity violation, and
- (3) departure from thermal equilibrium.

In electroweak baryogenesis, the  $SU(2)$  sphalerons are responsible for meeting the first condition as the anomalous baryon number violating processes become unsuppressed at high temperature. In the SM, the second condition is met through a  $CP$  violating phase in the Cabibbo-Kobayashi-Maskawa (CKM) matrix, but it is too feeble to provide enough baryon asymmetry. The third condition also fails in the SM as the Higgs mass is too heavy to catalyse a strongly first order electroweak phase transition.

The second and third conditions can be satisfied within the SMEFT framework by adding higher dimensional operators to the SM Lagrangian

$$\mathcal{L} = \mathcal{L}_{\text{SM}} + \frac{c_{CPV}}{\Lambda_{CPV}^2} \mathcal{O}_{D=6,CPV} + \sum_{n,m \in \mathbb{N}} \frac{c_{n,m}}{\Lambda_m^n} \mathcal{O}_{\Delta V, D=4+n}^{(m)}, \quad (2.1)$$

where  $\mathcal{O}_{D=6,CPV}$  is an operator<sup>3</sup> contributing to both the BAU as well as EDMs, and the set of operators  $\mathcal{O}_{\Delta V, D=4+n}^{(m)}$  ensure that the EWPT is strongly first order (see for example [10, 11]). In general, the  $\mathcal{O}_{D=6,CPV}$  operator may contain derivatives, and there can be a single or several  $\mathcal{O}_{\Delta V, D=4+n}^{(m)}$  operators, each possibly with a different cutoff scales.

Usually, the classical equations of motion are used to eliminate derivative operators as redundant. However, we will show in this section qualitatively (numerically in a subsequent section) that one should exercise caution when eliminating derivative operators with EOMs for baryon asymmetry calculations within the EFT framework. The reason for this is because the Sakharov conditions are met only if *both* the operators  $\mathcal{O}_{\Delta V, D=4+n}^{(m)}$  and  $\mathcal{O}_{D=6,CPV}$  exist. For a concrete example consider an example operator of the class  $\mathcal{O}_{D=6,CPV}$

$$\mathcal{O}_{DD} = \bar{Q}_L t_R D_\mu D^\mu H. \quad (2.2)$$

The derivatives on the Higgs in the above operator can be typically eliminated by making use of the field equations

$$D_\mu D^\mu H = -\frac{\partial \mathcal{L}_{\text{SM}}}{\partial H^\dagger} + \mathcal{O}\left(\frac{1}{\Lambda}\right). \quad (2.3)$$

Explicitly, one can use the classical equations of motion to rewrite  $\mathcal{O}_{DD}$  as

$$\begin{aligned} \frac{1}{\Lambda^2} \mathcal{O}_{DD} &= \frac{1}{\Lambda^2} \bar{Q}_L t_R D_\mu D^\mu H \\ &\rightarrow \frac{1}{\Lambda^2} \bar{Q}_L t_R \left( \frac{\partial \mathcal{L}_{\text{SM}}}{\partial H^\dagger} + \frac{\partial}{\partial H^\dagger} \sum_{n,m} \frac{c_{n,m}}{\Lambda_m^n} \mathcal{O}_{\Delta V, D=4+n}^{(m)} + \dots \right). \end{aligned} \quad (2.4)$$

---

<sup>3</sup>We note that one can in principle have many such operators. The approach we adopt here is to inspect each one separately as a sole source of CPV (in addition to the CKM phase).

After substituting in the SM Lagrangian and evaluating the derivatives, the operator  $\mathcal{O}_{DD}$  reads

$$\begin{aligned} \mathcal{O}_{DD} = & \bar{Q}_L H t_R \left( \mu^2 - \lambda H^\dagger H \right) - (\bar{Q}_L t_R)_i \epsilon^{ij} (\bar{L} Y_e e_R)_j \\ & - (\bar{Q}_L t_R)_i \epsilon^{ij} (\bar{u}_R Y_u^\dagger Q)_j - (\bar{Q}_L t_R)_i \epsilon^{ij} (\bar{Q}_i Y_d^\dagger d_R)_j + \mathcal{O} \left( \frac{1}{\Lambda^2} \right). \end{aligned} \quad (2.5)$$

In EDM calculations, operators suppressed by  $\Lambda^{-n}$  can be safely neglected in eq. (2.4). The use of the equations of motion to relate different operators is justified in this context since a hierarchy of scale is established between the constant Higgs vacuum expectation value (vev),  $\langle H(x) \rangle = v$ , and the cutoff  $\Lambda$ .

In BAU calculations, however, the  $CP$  violating sources typically depend on the derivative of the space-time varying vacuum during the phase transition. For example, for the supposedly degenerate operators shown in eq. (2.4), one can derive the  $CP$  violating sources to lowest order in the inverse cutoff:<sup>4</sup>

$$\begin{aligned} S_{\mathcal{O}_{DD}}^{CP} & \sim \frac{1}{\Lambda^2} [v(x) \partial_t (\partial_\mu \partial^\mu v(x)) - \partial_t v(x) (\partial_\mu \partial^\mu v(x))], \\ S_{\mathcal{O}_{\partial V/\partial H}}^{CP} & \sim \frac{1}{\Lambda^2} \left[ v(x) \partial_t \left( \frac{\partial V_{SM}}{\partial H} \Big|_{v(x)} \right) - \partial_t v(x) \left( \frac{\partial V_{SM}}{\partial H} \Big|_{v(x)} \right) \right] + \mathcal{O} \left( \frac{1}{\Lambda^4} \right). \end{aligned} \quad (2.6)$$

One can immediately see that the two expressions do not agree in general. This is made explicit when a specific form for the Higgs profile of  $v(x)$  is introduced to describe bubble formation during the electroweak phase transition. The profile is a stationary field configuration in the finite temperature effective action which interpolates the false vacuum to the true vacuum. Assuming an  $O(3)$  symmetry, the *bounce solution* takes the form:

$$v(z) \approx \frac{v(T)}{2} \left[ 1 + \tanh \left( \frac{z}{L_w} \right) \right]. \quad (2.7)$$

Here,  $L_w$  measures the width of the bubble wall and  $z$  parametrises the distance perpendicular to the wall. With both  $L_w$  and  $v(T)$  determined by the operators  $\mathcal{O}_{\Delta V, D=4+n}^{(m)}$ , there are no free parameters left in eq. (2.7). Using eq. (2.7) in eq. (2.6) does not yield the same result, not even approximately. This is due to the fact that  $S_{\mathcal{O}_{DD}}^{CP}$  and  $S_{\mathcal{O}_{\partial V/\partial H}}^{CP}$  have different dependencies on  $L_w$  and  $v(T)$ . Specifically, the CPV source resulting from the operator with derivative coupling to the Higgs,  $\mathcal{O}_{DD}$ , has a cubic sensitivity to the bubble wall width whereas the non-derivative operator has a quartic sensitivity to the value of  $v(T)$ . The strength of the CPV source due to the CPV operators then become very sensitive to the exact structure of the set of operators  $\mathcal{O}_{\Delta V, D=4+n}^{(m)}$  rather than the  $\mathcal{O}(\Lambda^{-4})$  sensitivity that occurs in EDM calculations.

For each  $\mathcal{O}_{D=6, CPV}$ , one could in principle consider every single possibility for the set  $\mathcal{O}_{\Delta V, D=4+n}^{(m)}$  and their Wilson coefficients to calculate  $L_w$  and  $v(T)$ . However, by ignoring the precise structure of  $\mathcal{O}_{\Delta V, D=4+n}^{(m)}$  and instead leaving  $L_w$  and  $v(T)$  as free parameters, we can then draw as direct a bridge as possible between BAU calculations and EDM limit.

<sup>4</sup>The reader is referred to (4.8) for the explicit form of the sources.

The result is that redundancy between derivative and non-derivative operators is lifted. This is due to the sensitivity of  $CP$  violating sources to  $\mathcal{O}_{\Delta V, D=4+n}^{(m)}$  being much sharper than the expected  $\Lambda^{-4}$  sensitivity. This behaviour is attributed to the derivative structure of the operators and the changing the profile of the vev during the EWPT as controlled by  $L_w$  and  $v(T)$ .

### 3 Operators classification

In this section, we classify and count the operators involving derivative couplings with Higgs which can no longer be considered redundant. In electroweak baryogenesis, the SM fields whose contribution to the BAU are suppressed by small Yukawa couplings can be neglected. This means that only the left handed third generation quark doublet, the right-handed top, the Higgs and gauge bosons need be considered. With the symbolic meanings of  $\psi$ ,  $D$ ,  $F$  and  $H$  applied to fermions, derivative operators, (dual) field strength tensors and Higgs operators respectively, one should obtain 12 operator classes, 8 of which involve the Higgs

$$\begin{aligned}
 & H^6, \quad H^4 D^2, \quad H^2 D^4, \quad F H^2 D^2, \quad \psi^2 H^3, \quad F^2 H^2, \quad \psi^2 H^2 D, \quad \psi^2 H D^2, \quad \psi^2 H F, \\
 & F^2 D^2, \quad \psi^4, \quad \psi^2 D F, \quad F^3.
 \end{aligned}
 \tag{3.1}$$

In order for the contributions to the BAU be resonantly enhanced, a  $CP$  violating operator must involve at least one space-time varying Higgs operator and one other field. Terms with single  $H$  cannot appear without a  $\psi^2$  combination to cancel the  $SU(2)$  charge. Therefore, terms such as  $F D^2 H$  should not appear. Under these constraints the possible classes of operators are

$$H^4 D^2, \quad H^2 D^4, \quad \psi^2 H^3, \quad F H^2 D^2, \quad F^2 H^2, \quad \psi^2 H^2 D, \quad \psi^2 H D^2, \quad \psi^2 H F.
 \tag{3.2}$$

We take the  $CP$ -odd operators from [31], while the  $CP$ -even analogue is given in [32] (see also [33, 35].) We list in table 1 the operators satisfying the above constraints. We find 34 in total that fulfil all of our constraints, including 19 with higher derivative couplings that are usually considered redundant. We considered operators with  $D_\mu D^2$  and not  $D_\mu D^2$  as the latter can be formed by taking the sum of the first operator and an operator involving the field strength tensor. We will select two qualitatively different operators for an extensive study — one with a second derivative coupling,  $\mathcal{O}_{DD}$ , and one with no derivative couplings  $\mathcal{O}_{t1}$ .

## 4 Electroweak baryogenesis with higher dimensional operators

### 4.1 Constructing new CPV sources with higher dimensional operators

When the Higgs field develops a space-time varying vacuum expectation value,  $v(x)$ , there are operators which interfere with the standard top quark vev insertion diagram to give exotic new sources of  $CP$  violation. We use the closed time path (CTP) formalism [37–41] to calculate  $CP$  violating source terms for two operators which facilitate resonantly enhanced  $CP$  violating interactions with the bubble wall.

$H^2 D^4$		$H^4 D^2$	
$\mathcal{O}_{H^2 D^4}^{(1)}$	$(D^4 H^\dagger) H$	$\mathcal{O}_{H^4 D^2}^{(1a)}$	$(H^\dagger H) H^\dagger D^2 H$
$\mathcal{O}_{H^2 D^4}^{(2)}$	$(D^2 D_\mu H^\dagger) D^\mu H$	$\mathcal{O}_{H^4 D^2}^{(2a)}$	$(H^\dagger H) D^\mu H^\dagger D_\mu H$
$\mathcal{O}_{H^2 D^4}^{(3a)}$	$(D^2 H^\dagger)(D^2 H)$	$\mathcal{O}_{H^4 D^2}^{(2b)}$	$(H^\dagger \overleftrightarrow{D}^\mu H)(H^\dagger \overleftrightarrow{D}_\mu H)$
$\mathcal{O}_{H^2 D^4}^{(3b)}$	$(D^\mu D^\nu H^\dagger)(D_\mu D_\nu H)$		

$\psi^2 H^3$		$\psi^2 H^2 D$		$\psi^2 H D^2$	
$\mathcal{O}_{t1}$	$(H^\dagger H) (\overline{Q}_L \tilde{H} t_R)$	$\mathcal{O}_{Hq}^{(1)}$	$(H^\dagger i \overleftrightarrow{D}_\mu H) (\overline{Q}_L \gamma^\mu Q_L)$	$\mathcal{O}_{\sigma DD}$	$(\overline{Q}_L \sigma^{\mu\nu} t_R) D_\mu D_\nu \tilde{H}$
		$\mathcal{O}_{Hq}^{(3)}$	$(H^\dagger i \overleftrightarrow{D}_\mu^i H) (\overline{Q}_L \gamma^\mu \tau^i Q_L)$	$\mathcal{O}_{\sigma DD}$	$(\overline{Q}_L \sigma^{\mu\nu} \overleftrightarrow{D}_\mu t_R) D_\nu \tilde{H}$
		$\mathcal{O}_{Ht}$	$(H^\dagger i \overleftrightarrow{D}_\mu H) (\overline{t}_R \gamma^\mu t_R)$	$\mathcal{O}_{DD}$	$(\overline{Q}_L t_R) D^\mu D_\mu \tilde{H}$
				$\mathcal{O}_{DtDH}$	$(\overline{Q}_L \overleftrightarrow{D}_\mu t_R) D^\mu \tilde{H}$

$F^2 H^2$		$\psi^2 H F$		$F H^2 D^2$	
$\mathcal{O}_{HG}$	$(H^\dagger H) G_{\mu\nu}^a G^{a\mu\nu}$	$\mathcal{O}_{tG}$	$(\overline{Q}_L \sigma^{\mu\nu} T^a t_R) \tilde{H} G_{\mu\nu}^a$	$\mathcal{O}_{D^2 HW}^{(1)}$	$W_{\mu\nu}^i (D^\mu H^\dagger) \tau^i (D^\nu H)$
$\mathcal{O}_{H\tilde{G}}$	$(H^\dagger H) G_{\mu\nu}^a \tilde{G}^{a\mu\nu}$	$\mathcal{O}_{tW}$	$(\overline{Q}_L \sigma^{\mu\nu} \tau^i t_R) \tilde{H} W_{\mu\nu}^i$	$\mathcal{O}_{D^2 HW}^{(2)}$	$D^\mu W_{\mu\nu}^i (H^\dagger \overleftrightarrow{D}^{i,\nu} H)$
$\mathcal{O}_{HW}$	$(H^\dagger H) W_{\mu\nu}^i W^{i\mu\nu}$	$\mathcal{O}_{tB}$	$(\overline{Q}_L \sigma^{\mu\nu} t_R) \tilde{H} B_{\mu\nu}$	$\mathcal{O}_{D^2 H\tilde{W}}^{(1)}$	$\tilde{W}_{\mu\nu}^i (D^\mu H^\dagger) \tau^i (D^\nu H)$
$\mathcal{O}_{H\tilde{W}}$	$(H^\dagger H) W_{\mu\nu}^i \tilde{W}^{i\mu\nu}$			$\mathcal{O}_{D^2 H\tilde{W}}^{(2)}$	$D^\mu \tilde{W}_{\mu\nu}^i (H^\dagger \overleftrightarrow{D}^{i,\nu} H)$
$\mathcal{O}_{HB}$	$(H^\dagger H) B_{\mu\nu} B^{\mu\nu}$			$\mathcal{O}_{D^2 BH}^{(1)}$	$B_{\mu\nu} (D^\mu H^\dagger) (D^\nu H)$
$\mathcal{O}_{H\tilde{B}}$	$(H^\dagger H) B_{\mu\nu} \tilde{B}^{\mu\nu}$			$\mathcal{O}_{D^2 BH}^{(2)}$	$D^\mu B_{\mu\nu} (H^\dagger \overleftrightarrow{D}^\nu H)$
$\mathcal{O}_{HWB}$	$(H^\dagger \tau^i H) W_{\mu\nu}^i B^{\mu\nu}$			$\mathcal{O}_{D^2 \tilde{B}H}^{(1)}$	$\tilde{B}_{\mu\nu} (D^\mu H^\dagger) (D^\nu H)$
$\mathcal{O}_{H\tilde{W}B}$	$(H^\dagger \tau^i H) \tilde{W}_{\mu\nu}^i B^{\mu\nu}$			$\mathcal{O}_{D^2 \tilde{B}H}^{(2)}$	$D^\mu \tilde{B}_{\mu\nu} (H^\dagger \overleftrightarrow{D}^\nu H)$

**Table 1.** List of dimension six operators based on [36] involving at least one Higgs and one other field that is either a Standard Model gauge boson or a top quark. Since redundancies due to the equations of motion are no longer applicable, one has to be cautious with the classes involving (i) two derivatives acting on a Higgs field and (ii) one derivative acting on either a gauge field or a fermion field. Here we follow the definition that  $H^\dagger i \overleftrightarrow{D}_\mu H := i H^\dagger (D_\mu - \overleftarrow{D}_\mu) H$  and  $H^\dagger i \overleftrightarrow{D}_\mu^i H := i H^\dagger (\tau^i D_\mu - \overleftarrow{D}_\mu \tau^i) H$ .

We also use the vev-insertion approximation (VIA) where the BAU production is dominated by physics in front of the advancing bubble wall. This is valid when the vev is small compared to both the nucleation temperature and the mass splitting of particles that produce the resonant CPV sources. The effective degrees of freedom are then those belonging in the mass eigenbasis of the symmetric (unbroken) phase. Their interactions with the space-time varying vevs are treated perturbatively under such approximation. One could perform a resummation to all orders in the vevs following the techniques in [42, 43]. As a simplification, we ignore the hole modes in the quark plasma [44–46]. The effects of mixing with multiparticle states in the thermal bath as well as resummation will also be left to a later, more precise numerical study. Under these assumptions, the quark propagator reads

$$S^\lambda(x-y) = \int \frac{d^4k}{(2\pi)^4} e^{-ik \cdot (x-y)} g_F^\lambda(k_0, \mu_{t_{L/R}}) \rho(k_0, k) (\not{k} + m), \quad (4.1)$$

where  $\rho(k_0, k)$  is the density of states and

$$\begin{aligned} g_F^>(x) &= 1 - n_F(x), \\ g_F^<(x) &= -n_F(x), \end{aligned} \quad (4.2)$$

with  $n_F(x) = (e^{\beta x} + 1)^{-1}$ .

We will consider two exotic operators,  $\mathcal{O}_{t11}$  and  $\mathcal{O}_{DD}$ . The first can be treated in the usual way by defining the self energy as

$$\Sigma_{\text{tot}}(x, y) = \left( y_t v(x) + \frac{c_i}{\Lambda^2} v(x)^3 \right) \left( y_t^* v(y) + \frac{c_i^*}{\Lambda^2} v(y)^3 \right) S_{t_R}(x, y), \quad (4.3)$$

whereas the  $\mathcal{O}_{DD}$  term has a derivative coupling. For simplicity we will ignore interactions with gauge bosons. Making the replacements  $H(x) \rightarrow v(x)$ , the self energy is

$$\Sigma_{\text{tot}}(x, y) = \left( y_t v(x) + \frac{c_i}{\Lambda^2} \partial_\mu \partial^\mu v(x) \right) \left( y_t^* v(y) + \frac{c_i^*}{\Lambda^2} \partial_\mu \partial^\mu v(y) \right) S_{t_R}(x, y). \quad (4.4)$$

The  $CP$  conserving term to lowest order in  $\Lambda^{-1}$  for both operators is just the usual resonant relaxation term arising from interactions between the top and the space-time varying vacuum. The term  $v(x)v(y)$  is then expanded near  $y = x$  taking the lowest order term. In this case the lowest order is the zeroth order and we find

$$\begin{aligned} \Gamma_t = N_C \frac{|y_t|^2}{2\pi^2 T} v(x)^2 \int_0^\infty \frac{k^2 dk}{\omega_L \omega_R} \text{Im} \left[ (\mathcal{E}_L \mathcal{E}_R + k^2) \left( \frac{h_F(\mathcal{E}_L) + h_F(\mathcal{E}_R)}{\mathcal{E}_L + \mathcal{E}_R} \right) \right. \\ \left. - (\mathcal{E}_L \mathcal{E}_R^* - k^2) \left( \frac{h_F(\mathcal{E}_L) + h_F(\mathcal{E}_R^*)}{\mathcal{E}_R^* - \mathcal{E}_L} \right) \right]. \end{aligned} \quad (4.5)$$

## 4.2 Contributions from $\mathcal{O}_{t1}$ vertices

The  $CP$  conserving relaxation term up to  $O(\Lambda^{-2})$  just produces the following correction to the Standard Model

$$\Gamma_t \mapsto \left( 1 + \left| \frac{c_i}{\Lambda^2} \right| v(x)^2 \right) \Gamma_t. \quad (4.6)$$

For the new  $CP$  violating source we expand to first order in  $z = x$ . The result is

$$\text{Im} \left[ \frac{c_i y_t^*}{\Lambda^2} \right] [v(x)^3 v(y) - v(x)v(y)^3] \mapsto \text{Im} \left[ \frac{c_i y_t^*}{\Lambda^2} \right] (z-x)^\mu v(x)^3 \partial_\mu v(x). \quad (4.7)$$

Only the zeroth component contributes under the assumption of spatial isotropy. Let us also ignore the bubble wall curvature and work in the rest frame of the bubble wall  $z = |v_w t - x|$ . The time derivative of the vev profile is then a spatial derivative times the wall velocity. In line with the VIA, we assume that the variation of bubble wall with respect to  $z$  is sufficiently gentle near the phase boundary [47]. Solving the contour integrals we find

$$\begin{aligned} S_{\mathcal{O}_{DD}}^{\mathcal{CP}} &= 2 \frac{v_w N_C}{\pi^2} \text{Im} \left[ \frac{c_i y_t^*}{\Lambda^2} \right] v(x)^3 v'(x) \int_0^\infty \frac{k^2 dk}{\omega_L \omega_R} \text{Im} \left[ (\mathcal{E}_L \mathcal{E}_R + k^2) \left( \frac{n_f(\mathcal{E}_L) - n_F(-\mathcal{E}_R)}{(\mathcal{E}_L + \mathcal{E}_R)^2} \right) \right. \\ &\quad \left. + (\mathcal{E}_L \mathcal{E}_R^* - k^2) \left( \frac{n_f(\mathcal{E}_L) - n_F(\mathcal{E}_R^*)}{(\mathcal{E}_R^* - \mathcal{E}_L)^2} \right) \right] \\ &= 2 \frac{v_w N_C}{\pi^2} \text{Im} \left[ \frac{c_i y_t^*}{\Lambda^2} \right] v(x)^3 v'(x) I[m_{t_L}, m_{t_R}, \Gamma_{t_R}, \Gamma_{t_L}, \Lambda], \end{aligned} \quad (4.8)$$

where we have implicitly defined the function  $I[\cdot]$  for notational convenience.

### 4.3 Contributions from $\mathcal{O}_{DD}$ vertices

The  $\mathcal{O}_{DD}$  operator requires some care since it involves a derivative coupling to the Higgs. Once again, we replace the Higgs field with a space-time varying vacuum and expanding the vacuum near  $z = x$ . The correction to the SM  $CP$  conserving relaxation term comes from the zeroth order term in the expansion

$$\Gamma_t \mapsto \left( 1 + \left| \frac{c_i}{\Lambda^2 v(x)} \right| v''(x) \right) \Gamma_t. \quad (4.9)$$

Note that the correction to the relaxation term involves the second derivative of the vev. The usual practice in solving these transport equations is to linearise the differential equations which means assuming the relaxation terms are a constant value in the broken phase. There are some ambiguity in this procedure in that the correction to the above relaxation term varies quite rapidly with  $x$  when  $x \lesssim L_w$  before going to zero. We therefore linearise the transport equations by setting this correction to its average value between  $[0, L_w]$ . This will be a somewhat a conservative assumption as this correction will not relax the number densities at all far from the bubble wall.

The  $CP$  violating source term, involving the third derivative of the Higgs coming from the next to leading order expansion around  $z = x$ , is given by

$$S_{\mathcal{O}_{DD}}^{\mathcal{CP}} = \frac{v_w N_C}{\pi^2} \text{Im} \left[ \frac{c_i y_t^*}{\Lambda^2} \right] [v'''(x)v(x) - v''(x)v'(x)] I[m_{t_L}, m_{t_R}, \Gamma_{t_R}, \Gamma_{t_L}, \Lambda]. \quad (4.10)$$

The derivative coupling causes the operator to be much more sensitive to the bubble width than the  $CP$  violating sources arising from  $\mathcal{O}_{t1}$ , or two Higgs doublet models which all have the  $CP$  violating source controlled by the first derivative of the vev. We note that there is

a danger that the VIA approximation becomes cruder for derivative couplings particularly when the bubble wall becomes very thin. Nonetheless, we expect the qualitative result that the source has an increased sensitivity to the wall width to be true even if one uses Wigner functional methods, as it comes from the derivative coupling to the space-time varying vev itself, rather than our approximation scheme.

#### 4.4 Calculating the baryon asymmetry

When calculating the BAU, we make the usual assumption that gauge interactions are very fast and that in the VIA the chemical potential for the  $W^\pm$  bosons vanishes as in the symmetric phase. We ignore interactions with particle species whose interactions are suppressed by small coupling constants. Specifically, the number densities we consider are the following linear combinations

$$\begin{aligned} Q &= n_{t_L} + n_{b_L}, \\ T &= n_{t_R}, \\ H &= n_{H^+} + n_{H^0}. \end{aligned} \tag{4.11}$$

Systematically calculating the sources for each self energy term involving the above particle species leads to a network of coupled transport equations. Using the usual relationship  $n_i = k_i \mu_i T^2/6$  we can then relate the chemical potentials to the number densities. For operator  $\mathcal{O}_X$  with  $X \in \{DD, t1\}$  these are

$$\begin{aligned} \partial_\mu Q^\mu &= \Gamma_M \left( \frac{T}{k_T} - \frac{Q}{k_Q} \right) + \Gamma_Y \left( \frac{T}{k_T} - \frac{Q}{k_Q} - \frac{H}{k_H} \right) - 2\Gamma_{SS}\mathcal{U}_5 - S_{\mathcal{O}_X}^{\mathcal{CP}}, \\ \partial_\mu T^\mu &= -\Gamma_M \left( \frac{T}{k_T} - \frac{Q}{k_Q} \right) - \Gamma_Y \left( \frac{T}{k_T} - \frac{Q}{k_Q} - \frac{H}{k_H} \right) + \Gamma_{SS}\mathcal{U}_5 + S_{\mathcal{O}_X}^{\mathcal{CP}}, \\ \partial_\mu H^\mu &= \Gamma_Y \left( \frac{T}{k_T} - \frac{Q}{k_Q} - \frac{H}{k_H} \right), \end{aligned} \tag{4.12}$$

where

$$\mathcal{U}_5 = \left( \frac{2Q}{k_Q} - \frac{T}{k_T} + \frac{9(Q+T)}{k_B} \right), \tag{4.13}$$

and the three body Yukawa rates,  $\Gamma_Y$ , are derived in reference [48]. Neglecting the bubble wall curvature we can reduce the problem to a one dimensional one by changing variables to the rest frame of the bubble wall  $z = |v_w t - x|$ . We then use the diffusion approximation to write  $\nabla \cdot \mathbf{J} = \nabla^2 n$  thus reducing the problem to a set of coupled differential equations in a single space-time variable. We do not use the usual simplification that the strong sphaleron and three body Yukawa rates are fast compared to a diffusion time as it has been shown that this assumption can cause an underestimate of the baryon asymmetry in an example model (the MSSM) by a factor of  $O(100)$ . While such an analysis has not been done in the SM+X, we consider it worth solving the transport analytically using the techniques in [49]. In the broken phase the solution is

$$X(z) = \sum_{i=1}^6 x_1 A_X(\alpha_i) e^{-\alpha_i z} \left( \int_0^z dy, e^{-\alpha_i y} S_{\mathcal{O}_X}^{\mathcal{CP}}(y) \right), \tag{4.14}$$

and in the symmetric phase we have

$$X(z) = \sum_{i=1}^6 A_{X,s} y_i e^{\gamma_i z}, \quad (4.15)$$

where  $X \in \{Q, T, H\}$ . The procedure for how to derive  $\alpha_i, \beta_i, x_i, y_i$  and  $A_X(\alpha_i)$  is given in [49]. From these solutions one can then define the left handed number density  $n_L(z) = Q_{1L} + Q_{2L} + Q_{3L} = 5Q + 4T$ . The baryon number density,  $\rho_B$ , satisfies the equation [50, 51]

$$D_Q \rho_B''(z) - v_w \rho_B'(z) - \Theta(-z) \mathcal{R} \rho_B = \Theta(-z) \frac{n_F}{2} \Gamma_{ws} n_L(z), \quad (4.16)$$

where  $n_F$  is the number of fermion families. The relaxation parameter is given by

$$\mathcal{R} = \frac{15}{4} \Gamma_{ws}, \quad (4.17)$$

where  $\Gamma_{ws} \approx 120 \alpha_W^5 T$  [52–54]. The baryon asymmetry of the universe,  $Y_B$  is then given by

$$Y_B = -\frac{n_F \Gamma_{ws}}{2\kappa_+ D_Q S} \int_{-\infty}^0 e^{-\kappa_- x} n_L(x) dx, \quad (4.18)$$

where

$$\kappa_{\pm} = \frac{v_w \pm \sqrt{v_w^2 + 4D_Q \mathcal{R}}}{2D_Q}, \quad (4.19)$$

and the entropy density is

$$s = \frac{2\pi^2}{45} g_* T^3. \quad (4.20)$$

## 5 EDM constraints

New sources of  $CP$ -violation in the Higgs sector are necessary to realise electroweak baryogenesis. These sources, however, are severely constrained via their contributions to the electric dipole moments (EDMs) of electron, neutron, molecules and atoms. A direct connection between EDMs and electroweak baryogenesis have been suggested in [22, 23]. The sensitivity of these low energy observables owes to contributions from operator mixing and threshold corrections as high scale physics is run down and integrated out. The present experimental constraints are summarised in table 2, showing that the electron EDM gives the most stringent bound since it is weakly sensitive to hadronic uncertainties. This bound is obtained from measurements using polar molecule thorium monoxide (ThO) [55]. We therefore focus on contributions to electron EDMs (eEDM) and delay a more comprehensive and systematic treatment to a future study that will include other dimension six operators (cf. e.g. [16, 19, 20, 56, 57]).

The dipole moment  $d_\psi$  corresponding to a charged fermion  $\psi$  is identified as the coefficient of the five dimensional operator in the effective Lagrangian

$$\mathcal{L}_{\text{EDM}} = -id_f \bar{\psi} \gamma^5 \sigma^{\mu\nu} \psi F_{\mu\nu}. \quad (5.1)$$

As argued before, one is led to focus on the top-Higgs sector in electroweak baryogenesis

Type	Molecule/Atom	Bounds
Paramagnetic	$^{205}\text{Tl}$	$ d_{\text{Tl}}  < 1.6 \times 10^{-27} e \text{ cm}$ [58]
Diamagnetic	$^{199}\text{Hg}$	$ d_{\text{Hg}}  < 6.2 \times 10^{-30} e \text{ cm}$ [59]
Neutron	$n$	$ d_n  < 3.0 \times 10^{-26} e \text{ cm}$ [60, 61]
Electron (ThO)	$e$	$ d_e  < 8.7 \times 10^{-29} e \text{ cm}$ [55]

**Table 2.** Current limits on electric dipole moments of the electron ( $e$ ), neutron ( $n$ ), mercury ( $^{199}\text{Hg}$ ) and thallium ( $^{205}\text{Tl}$ ) atoms at 90% C.L.

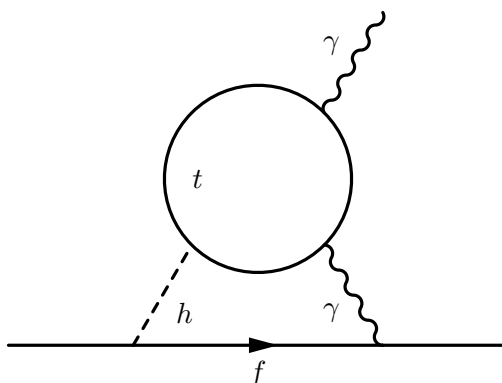


**Figure 1.** Two-loop Barr-Zee diagrams contributing to the electron EDM.

due to the  $\mathcal{O}(1)$  coupling. At the non-derivative level,  $CP$  violation interactions of this sort are encoded in

$$\begin{aligned} \mathcal{L} \supset & -m_t \bar{t}_L t_R - \frac{y_t}{\sqrt{2}} e^{i\xi} h \bar{t}_L t_R + h.c., \\ & = -m_t \bar{t}_L t_R - \frac{y_t}{\sqrt{2}} \bar{t} t h (\cos \xi + i\gamma^5 \sin \xi), \end{aligned} \tag{5.2}$$

where  $t_L, t_R, h$  are assumed to be in their mass eigenstate and  $m_t = 173 \text{ GeV}$  is the physical top mass. In addition,  $y_t$  parametrises the magnitude of the top-Higgs coupling, and  $\xi$  its  $CP$  phase. In the SM one has  $y_t = y_t^{SM} := \sqrt{2}m_t/v$  and  $\xi = 0$ . If there is  $CP$  violation in the top-Higgs coupling ( $\xi \neq 0$ ) it induces contributions to  $d_e$  via two-loop Barr-Zee type diagram [62] as shown figure 1. Such contribution is given by<sup>5</sup>

$$\frac{d_e}{e} = \frac{16}{3} \frac{\alpha}{(4\pi)^3} \frac{m_e}{y_t^{SM} y_e^{SM} v^2} \left[ y_e^S y_t^P f_1 \left( \frac{m_t^2}{m_h^2} \right) + y_e^P y_t^S f_2 \left( \frac{m_t^2}{m_h^2} \right) \right], \tag{5.3}$$

where the loop functions  $f_{1,2}$  are defined in [16, 65]. We add that other degrees of freedom (not present in our analysis), e.g. charged Higgs boson, may interact with the top quark to give sizable contribution to the EDM via the same the Barr-Zee type diagram. This have been studied in detail in the context of two Higgs doublet models [66–69].

Firstly we discuss how the  $\mathcal{O}_{t1}$  operator leads to  $CP$  violating top-Higgs coupling of the form (5.2) by expansion of the  $H$  operator around its vev. With  $H = \frac{1}{\sqrt{2}}(0, v + h)^T$ ,

<sup>5</sup>See [63] (based on [64]) for a more pedagogical discussion of the derivation.

this leads to

$$\begin{aligned}
 \mathcal{L} \supset & - \left( \alpha + \frac{c_{t1}}{\Lambda^2} H^\dagger H \right) \bar{Q}_L \tilde{H} t_R + h.c. \\
 & = - \underbrace{\frac{1}{\sqrt{2}} \left( \alpha + c_{t1} \frac{v^2}{\Lambda^2} \right)}_{m_t e^{i\xi_m}} v \bar{t}_L t_R - \underbrace{\left( \alpha + 3c_{t1} \frac{v^2}{\Lambda^2} \right)}_{y_t e^{i\xi_t}} \frac{h}{\sqrt{2}} \bar{t}_L t_R + h.c.. \quad (5.4)
 \end{aligned}$$

These operators are brought into their mass basis by a field redefinition  $t_R \mapsto e^{-i\xi_m} t_R$ . In such case, the physical  $CP$  phase can be identified with  $\xi_t - \xi_m$ .

In case of the  $\mathcal{O}_{DD}$  operator, the top-Higgs interaction contains a derivative. In principle, this contributes to  $d_e$  through the same two-loop diagram, shown in figure 1, and one can derive an analogue of (5.3) with the momentum dependent top-Higgs vertex. Differing from the discussion of the baryon production during the EWPT, the Higgs vev here corresponds to the one well after the EWPT and is hence not space-time dependent. It is valid then to use classical EOMs to recast  $\mathcal{O}_{DD}$  in terms of derivative free operators as in equation (2.5).

The dominant constraints on  $\mathcal{O}_{DD}$  come from from the first term of (2.5), since four-fermion operators do not lead to sensitive observables [20]. Following the previous steps, one obtains

$$\begin{aligned}
 \mathcal{L} \supset & - \left[ \alpha + \frac{c_{DD}}{\Lambda^2} (\mu^2 - \lambda H^\dagger H) \right] \bar{Q}_L \tilde{H} t_R + h.c. \quad (5.5) \\
 & = - \underbrace{\frac{1}{\sqrt{2}} \left( \alpha + \frac{c_{DD}}{\Lambda^2} \left( \mu^2 - \frac{1}{2} \lambda v^2 \right) \right)}_{m_t e^{i\xi_m}} v \bar{t}_L t_R - \underbrace{\left[ \alpha + \frac{c_{DD}}{\Lambda^2} \left( \mu^2 - \frac{3}{2} \lambda v^2 \right) \right]}_{y_t e^{i\xi_t}} \frac{h}{\sqrt{2}} \bar{t}_L t_R + h.c..
 \end{aligned}$$

In both of these cases, one assumes a generic coefficient  $\alpha \in \mathbb{C}$  for the dimension-four top Yukawa coupling  $\bar{Q}_L \tilde{H} t_R$ . Making the assumption that  $CP$ -violation comes only from the  $d = 6$  operators and that the scale of the operator is set by the cutoff, one sets  $\text{Im}(\alpha) = 0$  and  $c_{DD,t1} = e^{i\phi_{CP}}$ . The value of  $\alpha$  is chosen to absorb the effects of the  $\mathcal{O}_{DD,t1}$  and to reproduce  $m_t = 173 \text{ GeV}$ . Currently, we take  $\mu^2 = m_h^2$  and  $\mu^2 = \lambda v^2$  but we note that this relation can be modified by pure Higgs effective operators such as  $(H^\dagger H)^3$ . Figure 2 shows the contributions of the  $\mathcal{O}_{t1}$  and  $\mathcal{O}_{DD}$  operators to the electron EDM as a function of the cutoff scale  $\Lambda$ . For the former, operator a strong dependence on the  $CP$  phase of the higher dimensional operator is observed. Particularly, a cutoff of  $\Lambda \gtrsim 3600 \text{ GeV}$  is required to remain consistent with the current constraints  $\phi_{CP} = \pi/2$ , but is relaxed to  $\Lambda \gtrsim 3000 \text{ GeV}$  for  $\phi_{CP} = \pi/4$ . The electron EDM bound on the latter operator is weaker, with the cutoff scale roughly required to be  $\Lambda \gtrsim 1 \text{ TeV}$  for both  $CP$  phases. One should keep in mind that when interpreting these results, one assumes a pure scalar electron Yukawa coupling with its SM value (cf. [70] and references therein for discussions on experimental constraints of such coupling).

## 6 Numerical results and discussion

We plot the BAU produced by the new  $CP$  violating sources resulting from the operators  $\mathcal{O}_{DD}$  and  $\mathcal{O}_{t1}$  in figure 3 and figure 4 respectively. We set the nucleation temperature to

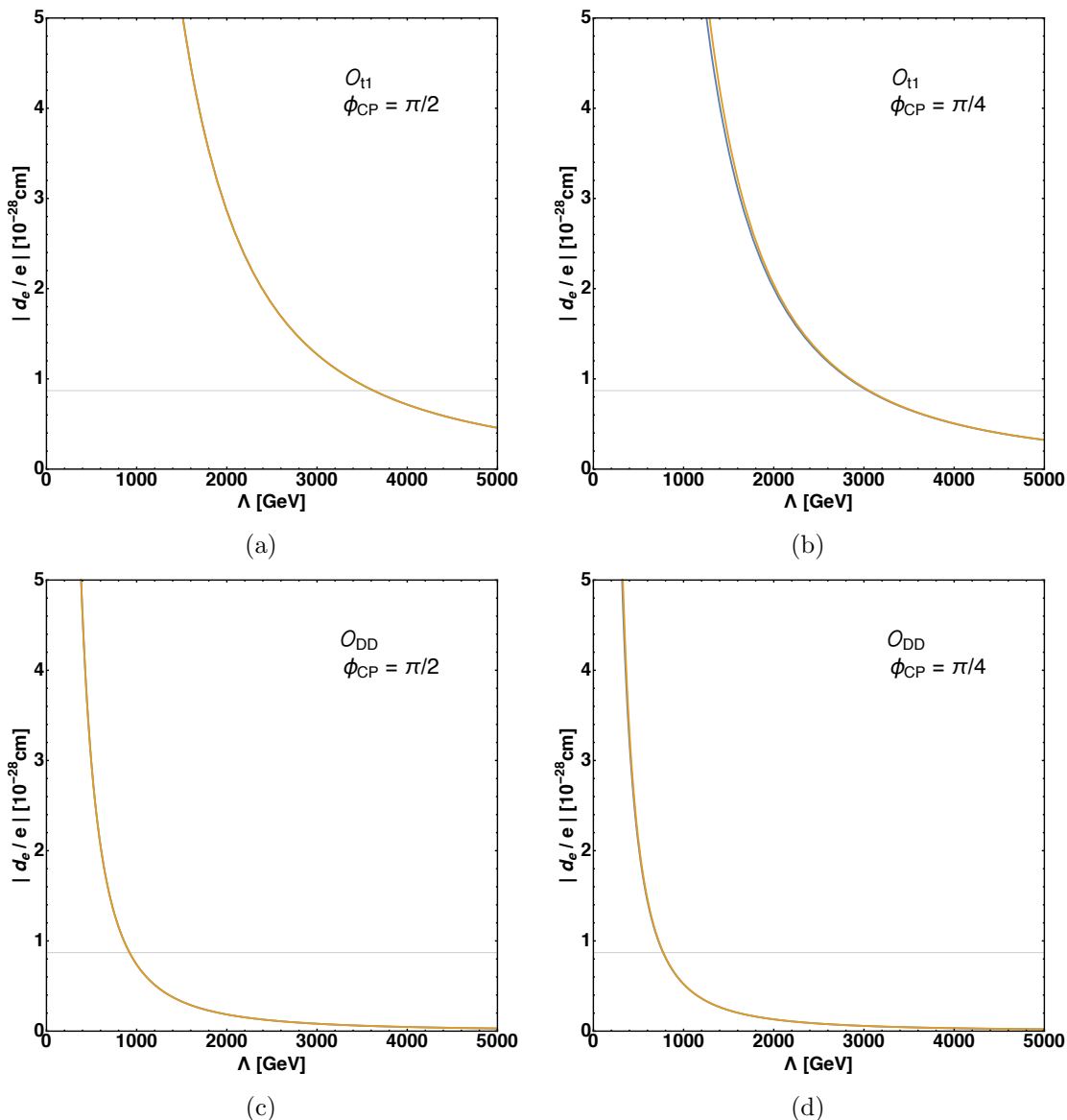


**Figure 2.** Two loop contribution to the electron electric dipole moment via a top quark due to the  $\mathcal{O}_{t1}$  and  $\mathcal{O}_{DD}$  operators. Here  $\phi_{CP}$  denotes the phase  $c_{DD,t1} = e^{i\phi_{CP}}$  of the Wilson coefficient appearing in front of the operator. The horizontal line corresponds to the experimental limit.

$T_n = 100$  GeV and the  $CP$  violating phase  $\phi_{CP} = \pi/2$  such that new coupling constants are  $c_{DD,t1} = i$  (cf. section 5). We then set the value of the vev deep within the broken phase to obtain two different values of the order parameter  $\gamma := v(T)/T$ . The first value is the minimal value of unity — since this is the approximate condition for a strongly first order phases transition necessary to sufficiently suppress sphaleron interactions deep in the broken phase thereby preserving the baryon number. The higher value is  $\gamma = 2$  since this is an approximate maximum value for  $\gamma$  during the electroweak phase transition for a critical temperature  $T_c \geq 100$  [71]. Generically, a smaller value of the wall velocity produces a larger

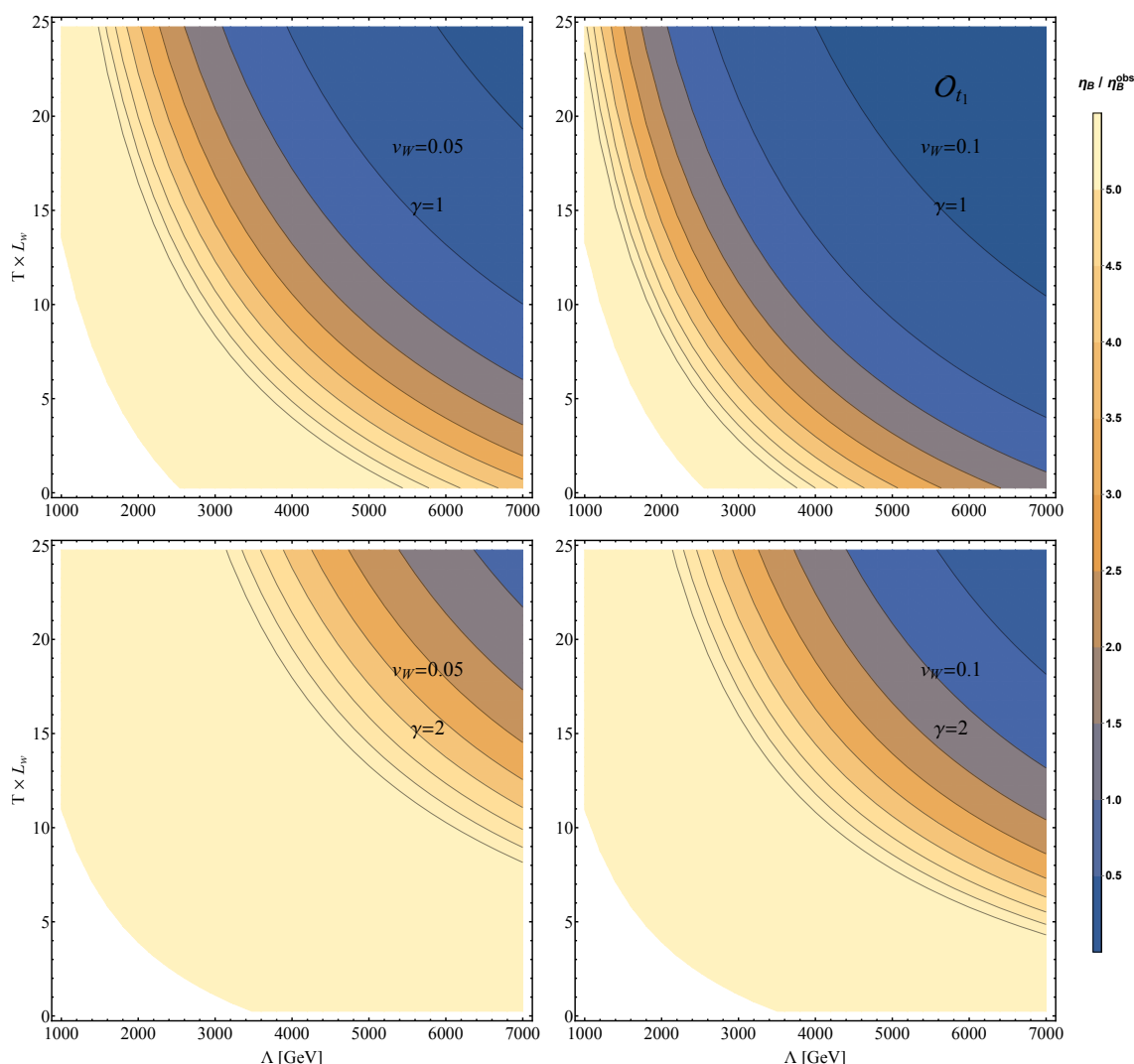


**Figure 3.** The baryon asymmetry due to the  $CP$  violating operator  $\mathcal{O}_{t1}$  in the plane of the bubble wall width vs. cutoff ( $L_w, \Lambda$ ). The dependence on  $L_w$  is relatively gentle.

BAU as does a larger value of  $\gamma$  which is expected given that the  $CP$  violating sources are all proportional to  $\gamma$  to some power. One should note that the Standard Model with a light Higgs has a larger wall velocity. The wall velocity can be suppressed by additional particles in the plasma which might also be heavy enough to justify an effective field theory approach. Therefore, we can once again parametrise our ignorance of such particles just by keeping the wall velocity as a free parameter and setting it to values 0.05 and 0.1. As explained in section 5, the minimum cutoff for the operator  $\mathcal{O}_{DD}$  is about a TeV whereas the minimum cutoff for the  $\mathcal{O}_{t1}$  operator is significantly higher, about 3.5 TeV, due to its effect on the top quark Yukawa.

As expected, the baryon asymmetry due to the operator  $\mathcal{O}_{DD}$  is very sensitive to the bubble wall width. In both cases, a thin bubble wall is favoured with a large proportion of

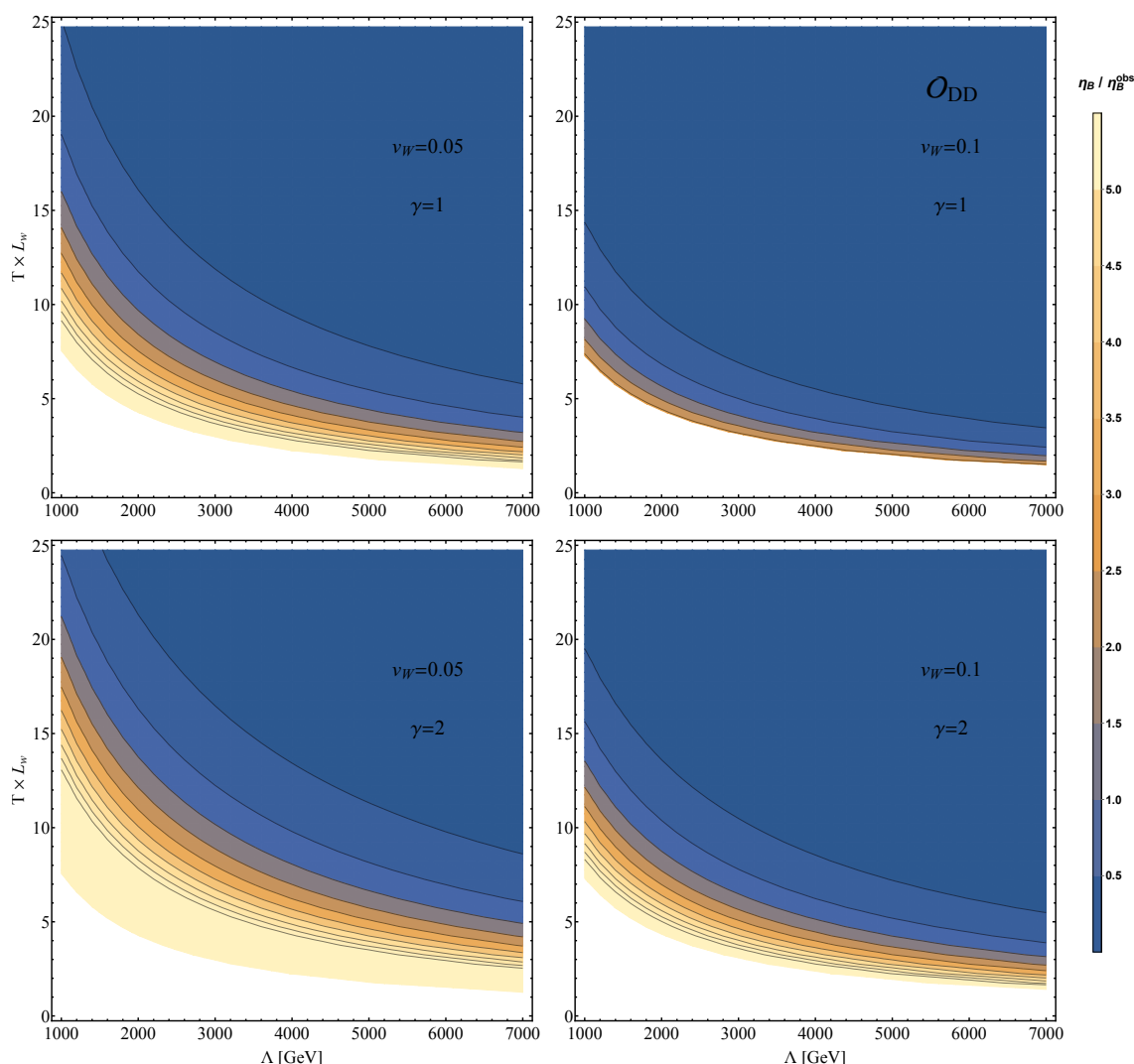


**Figure 4.** The baryon asymmetry due to the  $CP$  violating operator  $\mathcal{O}_{DD}$  in the plane of the bubble wall width vs. cutoff ( $L_w, \Lambda$ ). The dependence on  $L_w$  is quite steep.

the parameter space already ruled out. However, the baryon asymmetry diverges quickly for very small values of  $L_w$  for the operator  $\mathcal{O}_{DD}$ . It would be very interesting to see how strongly this effect persists when one goes beyond the VIA by using techniques described in [42, 43].

Remarkably the BAU can be produced by the  $\mathcal{O}_{t1}$  operator with extremely large values of the cutoff if the wall width and velocity are small but the order parameter  $\gamma$  is large. This is due to the fact that the  $CP$  violating source scales as  $v(T)^4/\Lambda^2$  so the suppression due to the cutoff is not as severe as it is for the  $\mathcal{O}_{DD}$  operator. This also means that the BAU for operator  $\mathcal{O}_{t1}$  is more sensitive to the value of  $v(T)$ . However, explaining the baryon asymmetry with the  $\mathcal{O}_{t1}$  operator is not viable with about a 6-fold increase in the minimal value of  $\Lambda$  (or equivalently  $\Lambda/|c_i|$ ). This means that this operator may be completely ruled

out as a sole explanation to the BAU in the foreseeable future if EDM searches improve in sensitivity by about an order of magnitude or measurements of the top quark Yukawa coupling become moderately more accurate. There is of course the caveat that the baryon asymmetry has some moderate dependence on the nucleation temperature.

Not all baryon number produced during the electroweak phase transition is preserved until the phase transition is finished. The fraction that is preserved has a double exponential dependence on the strength of the order parameter  $v(T_c)/T_c$ . So for an order parameter of  $v(T_c)/T_c \approx 0.75$  one might need to produce as much as 10 times of the observed baryon asymmetry [72]. Including the effects of washout, with detailed calculations of the sphaleron energy, we leave to an interesting future project.

### 6.1 Space-time dependent cutoff

Within the approach of effective field theory, we approximate the propagators of heavy particles by the inverse of their mass squared. If a particle acquires some of its mass via symmetry breaking, the mass of the heavy particle inherits a space-time dependence via the vev of the other field such that

$$\frac{1}{\Lambda^2} \rightarrow \frac{1}{\Lambda_0^2(T) + \Delta\Lambda^2(x)} := \frac{\kappa(x)}{\Lambda_0^2(T) + v^2(x)}. \tag{6.1}$$

Here  $\kappa(x)$  is a space-time dependent function absorbing the effects of heavy physics which the EFT is ignorant of. An example for such situation is an EFT for sparticles in supersymmetry that have a soft mass but acquire some contribution to their masses from the vacuum expectation value of the Higgs.

In this section, we argue that a space-time dependent cutoff is not necessarily fatal for an effective field theory, although we do not claim that our treatment is comprehensive. For example, we do not discuss any subtleties that may arise from the fact that the space-time varying cutoff is defined within a particular frame of reference (although comfort ourselves with the fact that temperature is also defined within a particular reference frame). For the effective field theory to remain valid  $\Lambda_0$  has to be high enough to justify the new physics it represents to be heavy enough. Since CPV source terms generically will depend on the derivative of  $\Lambda$ , one could ask if it is in principle possible that such a term can boost the baryon asymmetry. The answer is typically no in the case where  $\Lambda_0(T)$  is large enough as corrections to the  $CP$  violating source will be of the order

$$\frac{1}{\Lambda^4(x)} \frac{\partial}{\partial x} [\Delta\Lambda^2(x)]. \tag{6.2}$$

Finally, we briefly consider the case where we definitely do not expect effective field theory to work when  $\Lambda_0(T) \rightarrow 0$ . Using intuition about the generic behaviour of space-time varying functions during the electroweak phase transition (such as CPV phases, vevs and variation of the ratio of vevs  $\beta(x)$ ) we can make an *ansatz* to parametrise our ignorance of the new physics

$$\kappa(x) = \kappa_0 + \frac{\Delta\kappa}{2} \left[ 1 + \tanh\left(\frac{x}{L_w}\right) \right]. \tag{6.3}$$

Suppose we have the case where our  $D = 6$  operator that we test is  $\mathcal{O}_{t1}$  which is acquired by integrating out a heavy Higgs in a two Higgs doublet model. If we set  $\Lambda_0$  to zero<sup>6</sup> the  $CP$  violating source we get is

$$S_{\mathcal{O}_{t1}}^{\mathcal{CP}} = v^2(x)\dot{\kappa}(x)\text{Im}[y_t c_i^*]I(m_{t_L}, m_{t_R}, \Gamma_{t_L}, \Gamma_{t_R}, \Lambda(x_i)) . \quad (6.4)$$

Here  $\Lambda(x_i)$  is the cutoff evaluated at a single space-time point for simplicity. This is, of course, the most ambiguous part of this discussion. We can compare the above to the two Higgs doublet model where one gets

$$S_{2HDM}^{\mathcal{CP}} = v^2(x)\dot{\beta}(x)\text{Im}[y_{t1}y_{t2}^*]I(m_{t_L}, m_{t_R}, \Gamma_{t_L}, \Gamma_{t_R}) . \quad (6.5)$$

Remarkably, the effective field theory framework reproduces much of the structure of the UV complete theory in a case where we had no right to expect this.

One should not, however, take the comparisons between the above two CPV sources too literally. If we replaced the cutoff with the mass of the second Higgs doublet we would acquire coefficients with complicated dependence on parameters beyond the SM. This is expected since the heavy physics that produces  $\mathcal{O}_{t1}$  is not unique and the EFT framework is necessarily somewhat ignorant of the UV completion. What is remarkable here is that the EFT framework produces the correct dependence on the masses and thermal widths of the top quark, including resonance effects, the correct dependence on the vev profiles, the top Yukawa coupling as well as the variation of the space-time dependence of the heavy physics all in a scenario where the EFT framework is expected to be crude. While this may be coincidental, it would be interesting for future work to ascertain how well the effective field theory works in calculating the BAU for a variety of models where  $\Lambda_0(T)$  is small.

## 7 Conclusions

The growing sensitivity of electric dipole moment searches is increasingly constraining the parameter space of baryogenesis models. Consequently, in the near future various electroweak baryogenesis models will be either confirmed or ruled out by EDM searches. The number of baryogenesis models, however, is rendering the application of experimental bounds (including EDM limits) on each model impractical. This necessitates a model independent, direct connection between EDM constraints and BAU calculations. In this work, we studied such a connection using the framework of an effective field theory.

Examining the connection between dimension six effective operators and the BAU, we found that the conventional degeneracy is broken between operators containing derivatives of the Higgs field and their counterparts related by the equation of motion. According to the naïve CPV analysis, higher order contributions which arises when derivative operators are traded to non-derivative ones, can be safely neglected since they are suppressed by the cutoff scale. When calculating the BAU, however, operators containing a derivative of the Higgs field yield a CPV contribution to baryogenesis that involves the derivative of the Higgs vev. If one trades these operators to non-derivative ones then one completely changes the nature

---

<sup>6</sup>This is physically unrealistic as there is always a thermal mass mass but done for illustrative purposes.

of the CPV contribution to baryogenesis. The removal of  $\mathcal{O}_{\Delta V, D=4+n}^{(m)}$  due to power-counting arguments in the EOMs when relating  $\mathcal{O}_{D=6, \text{CPV}}$  with SM operators is problematic as a rapidly varying Higgs wall profile destabilises the hierarchy between the vev and cutoff scale.

After re-classifying dimension six effective operators, we selected two simple dimension six operators (one containing a derivative and the other not) and calculated the respective baryon asymmetry. We also subjected these operators to EDM constraints, thereby directly connecting the effect of the EDM constraints to the amount of baryon asymmetry these operators can yield. Finally, we discussed the possibility of the effective cutoff being space-time dependent and showed that the effective field theory approach captures the bulk of the correct physics even when we expect it to be a crude approximation.

We stress that the baryon asymmetry calculated from the normally neglected dimension six operators involving derivative coupling to the Higgs is more sensitive to the bubble dynamics of the EWPT. The approach we suggest does not apply to more complicated scenarios such as multistep phase transitions (cf. e.g. [73]). Also, more work needs to be done analysing these operators using the full Wigner functional approach presented in references [74]. Nonetheless, we have made a step toward a more general test of the electroweak baryogenesis paradigm.

## Acknowledgments

We like to thank W. Denkers, J. de Vries, Nodoka Yamanaka, Michael Schmidt and Chuan-Ren Chen for useful discussions. This work was partially supported by the Australian Research Council. JY will like to particularly thank Archil Kobakhidze for supporting this work during his transitional period.

**Open Access.** This article is distributed under the terms of the Creative Commons Attribution License ([CC-BY 4.0](https://creativecommons.org/licenses/by/4.0/)), which permits any use, distribution and reproduction in any medium, provided the original author(s) and source are credited.

## References

- [1] ATLAS collaboration, *Observation of a new particle in the search for the Standard Model Higgs boson with the ATLAS detector at the LHC*, *Phys. Lett. B* **716** (2012) 1 [[arXiv:1207.7214](https://arxiv.org/abs/1207.7214)] [[INSPIRE](#)].
- [2] CMS collaboration, *Observation of a new boson at a mass of 125 GeV with the CMS experiment at the LHC*, *Phys. Lett. B* **716** (2012) 30 [[arXiv:1207.7235](https://arxiv.org/abs/1207.7235)] [[INSPIRE](#)].
- [3] G.A. White, *A pedagogical introduction to electroweak baryogenesis*, *IOP Concise Physics*, Morgan & Claypool, (2016) [[INSPIRE](#)].
- [4] ATLAS and CMS collaborations, *Combined measurement of the Higgs boson mass in pp collisions at  $\sqrt{s} = 7$  and 8 TeV with the ATLAS and CMS experiments*, *Phys. Rev. Lett.* **114** (2015) 191803 [[arXiv:1503.07589](https://arxiv.org/abs/1503.07589)] [[INSPIRE](#)].
- [5] K. Rummukainen, M. Tsy-pin, K. Kajantie, M. Laine and M.E. Shaposhnikov, *The universality class of the electroweak theory*, *Nucl. Phys. B* **532** (1998) 283 [[hep-lat/9805013](https://arxiv.org/abs/hep-lat/9805013)] [[INSPIRE](#)].

- [6] M.B. Gavela, P. Hernández, J. Orloff and O. Pene, *Standard Model CP-violation and baryon asymmetry*, *Mod. Phys. Lett. A* **9** (1994) 795 [[hep-ph/9312215](#)] [[INSPIRE](#)].
- [7] T. Konstandin, T. Prokopec and M.G. Schmidt, *Axial currents from CKM matrix CP-violation and electroweak baryogenesis*, *Nucl. Phys. B* **679** (2004) 246 [[hep-ph/0309291](#)] [[INSPIRE](#)].
- [8] PLANCK collaboration, P.A.R. Ade et al., *Planck 2015 results. XIII. Cosmological parameters*, *Astron. Astrophys.* **594** (2016) A13 [[arXiv:1502.01589](#)] [[INSPIRE](#)].
- [9] A. Kobakhidze, L. Wu and J. Yue, *Electroweak baryogenesis with anomalous Higgs couplings*, *JHEP* **04** (2016) 011 [[arXiv:1512.08922](#)] [[INSPIRE](#)].
- [10] D. Bödeker, L. Fromme, S.J. Huber and M. Seniuch, *The baryon asymmetry in the Standard Model with a low cut-off*, *JHEP* **02** (2005) 026 [[hep-ph/0412366](#)] [[INSPIRE](#)].
- [11] L. Fromme and S.J. Huber, *Top transport in electroweak baryogenesis*, *JHEP* **03** (2007) 049 [[hep-ph/0604159](#)] [[INSPIRE](#)].
- [12] F.P. Huang, P.-H. Gu, P.-F. Yin, Z.-H. Yu and X. Zhang, *Testing the electroweak phase transition and electroweak baryogenesis at the LHC and a circular electron-positron collider*, *Phys. Rev. D* **93** (2016) 103515 [[arXiv:1511.03969](#)] [[INSPIRE](#)].
- [13] J. Engel, M.J. Ramsey-Musolf and U. van Kolck, *Electric dipole moments of nucleons, nuclei and atoms: the Standard Model and beyond*, *Prog. Part. Nucl. Phys.* **71** (2013) 21 [[arXiv:1303.2371](#)] [[INSPIRE](#)].
- [14] T. Chupp and M. Ramsey-Musolf, *Electric dipole moments: a global analysis*, *Phys. Rev. C* **91** (2015) 035502 [[arXiv:1407.1064](#)] [[INSPIRE](#)].
- [15] Y.T. Chien, V. Cirigliano, W. Dekens, J. de Vries and E. Mereghetti, *Direct and indirect constraints on CP-violating Higgs-quark and Higgs-gluon interactions*, *JHEP* **02** (2016) 011 [[arXiv:1510.00725](#)] [[INSPIRE](#)].
- [16] J. Brod, U. Haisch and J. Zupan, *Constraints on CP-violating Higgs couplings to the third generation*, *JHEP* **11** (2013) 180 [[arXiv:1310.1385](#)] [[INSPIRE](#)].
- [17] A. Noble and M. Perelstein, *Higgs self-coupling as a probe of electroweak phase transition*, *Phys. Rev. D* **78** (2008) 063518 [[arXiv:0711.3018](#)] [[INSPIRE](#)].
- [18] C. Delaunay, C. Grojean and J.D. Wells, *Dynamics of non-renormalizable electroweak symmetry breaking*, *JHEP* **04** (2008) 029 [[arXiv:0711.2511](#)] [[INSPIRE](#)].
- [19] V. Cirigliano, W. Dekens, J. de Vries and E. Mereghetti, *Is there room for CP-violation in the top-Higgs sector?*, *Phys. Rev. D* **94** (2016) 016002 [[arXiv:1603.03049](#)] [[INSPIRE](#)].
- [20] V. Cirigliano, W. Dekens, J. de Vries and E. Mereghetti, *Constraining the top-Higgs sector of the Standard Model effective field theory*, *Phys. Rev. D* **94** (2016) 034031 [[arXiv:1605.04311](#)] [[INSPIRE](#)].
- [21] C. Grojean, G. Servant and J.D. Wells, *First-order electroweak phase transition in the Standard Model with a low cutoff*, *Phys. Rev. D* **71** (2005) 036001 [[hep-ph/0407019](#)] [[INSPIRE](#)].
- [22] K. Fuyuto, J. Hisano and E. Senaha, *Toward verification of electroweak baryogenesis by electric dipole moments*, *Phys. Lett. B* **755** (2016) 491 [[arXiv:1510.04485](#)] [[INSPIRE](#)].
- [23] S.J. Huber, M. Pospelov and A. Ritz, *Electric dipole moment constraints on minimal electroweak baryogenesis*, *Phys. Rev. D* **75** (2007) 036006 [[hep-ph/0610003](#)] [[INSPIRE](#)].

- [24] J. Shu and Y. Zhang, *Impact of a CP-violating Higgs sector: from LHC to baryogenesis*, *Phys. Rev. Lett.* **111** (2013) 091801 [[arXiv:1304.0773](#)] [[INSPIRE](#)].
- [25] X. Zhang and B.L. Young, *Effective Lagrangian approach to electroweak baryogenesis: Higgs mass limit and electric dipole moments of fermion*, *Phys. Rev. D* **49** (1994) 563 [[hep-ph/9309269](#)] [[INSPIRE](#)].
- [26] F.P. Huang and C.S. Li, *Electroweak baryogenesis in the framework of the effective field theory*, *Phys. Rev. D* **92** (2015) 075014 [[arXiv:1507.08168](#)] [[INSPIRE](#)].
- [27] P.H. Damgaard, A. Haarr, D. O'Connell and A. Tranberg, *Effective field theory and electroweak baryogenesis in the singlet-extended Standard Model*, *JHEP* **02** (2016) 107 [[arXiv:1512.01963](#)] [[INSPIRE](#)].
- [28] N. Bernal, F.-X. Josse-Michaux and L. Ubaldi, *Phenomenology of WIMPy baryogenesis models*, *JCAP* **01** (2013) 034 [[arXiv:1210.0094](#)] [[INSPIRE](#)].
- [29] C. Zhang, N. Greiner and S. Willenbrock, *Constraints on non-standard top quark couplings*, *Phys. Rev. D* **86** (2012) 014024 [[arXiv:1201.6670](#)] [[INSPIRE](#)].
- [30] J. Herrero-Garcia, N. Rius and A. Santamaria, *Higgs lepton flavour violation: UV completions and connection to neutrino masses*, *JHEP* **11** (2016) 084 [[arXiv:1605.06091](#)] [[INSPIRE](#)].
- [31] J.M. Yang and B.-L. Young, *Dimension-six CP-violating operators of the third family quarks and their effects at colliders*, *Phys. Rev. D* **56** (1997) 5907 [[hep-ph/9703463](#)] [[INSPIRE](#)].
- [32] K. Whisnant, J.-M. Yang, B.-L. Young and X. Zhang, *Dimension-six CP conserving operators of the third family quarks and their effects on collider observables*, *Phys. Rev. D* **56** (1997) 467 [[hep-ph/9702305](#)] [[INSPIRE](#)].
- [33] J.A. Aguilar-Saavedra, *A minimal set of top-Higgs anomalous couplings*, *Nucl. Phys. B* **821** (2009) 215 [[arXiv:0904.2387](#)] [[INSPIRE](#)].
- [34] A.D. Sakharov, *Violation of CP invariance, c asymmetry and baryon asymmetry of the universe*, *Pisma Zh. Eksp. Teor. Fiz.* **5** (1967) 32 [*JETP Lett.* **5** (1967) 24] [*Sov. Phys. Usp.* **34** (1991) 392] [*Usp. Fiz. Nauk* **161** (1991) 61] [[INSPIRE](#)].
- [35] D. Nomura, *Effects of top-quark compositeness on Higgs boson production at the LHC*, *JHEP* **02** (2010) 061 [[arXiv:0911.1941](#)] [[INSPIRE](#)].
- [36] B. Grzadkowski, M. Iskrzynski, M. Misiak and J. Rosiek, *Dimension-six terms in the Standard Model Lagrangian*, *JHEP* **10** (2010) 085 [[arXiv:1008.4884](#)] [[INSPIRE](#)].
- [37] P.C. Martin and J.S. Schwinger, *Theory of many particle systems. 1*, *Phys. Rev.* **115** (1959) 1342 [[INSPIRE](#)].
- [38] J.S. Schwinger, *Brownian motion of a quantum oscillator*, *J. Math. Phys.* **2** (1961) 407 [[INSPIRE](#)].
- [39] L.V. Keldysh, *Diagram technique for nonequilibrium processes*, *Zh. Eksp. Teor. Fiz.* **47** (1964) 1515 [*Sov. Phys. JETP* **20** (1965) 1018] [[INSPIRE](#)].
- [40] K.-C. Chou, Z.-B. Su, B.-L. Hao and L. Yu, *Equilibrium and nonequilibrium formalisms made unified*, *Phys. Rept.* **118** (1985) 1 [[INSPIRE](#)].
- [41] K.T. Mahanthappa, *Multiple production of photons in quantum electrodynamics*, *Phys. Rev.* **126** (1962) 329 [[INSPIRE](#)].

- [42] V. Cirigliano, C. Lee, M.J. Ramsey-Musolf and S. Tulin, *Flavored quantum Boltzmann equations*, *Phys. Rev. D* **81** (2010) 103503 [[arXiv:0912.3523](#)] [[INSPIRE](#)].
- [43] V. Cirigliano, C. Lee and S. Tulin, *Resonant flavor oscillations in electroweak baryogenesis*, *Phys. Rev. D* **84** (2011) 056006 [[arXiv:1106.0747](#)] [[INSPIRE](#)].
- [44] H.A. Weldon, *Dynamical holes in the quark-gluon plasma*, *Phys. Rev. D* **40** (1989) 2410 [[INSPIRE](#)].
- [45] H.A. Weldon, *Structure of the quark propagator at high temperature*, *Phys. Rev. D* **61** (2000) 036003 [[hep-ph/9908204](#)] [[INSPIRE](#)].
- [46] V.V. Klimov, *Spectrum of elementary Fermi excitations in quark gluon plasma*, *Sov. J. Nucl. Phys.* **33** (1981) 934 [*Yad. Fiz.* **33** (1981) 1734] [[INSPIRE](#)].
- [47] C. Lee, V. Cirigliano and M.J. Ramsey-Musolf, *Resonant relaxation in electroweak baryogenesis*, *Phys. Rev. D* **71** (2005) 075010 [[hep-ph/0412354](#)] [[INSPIRE](#)].
- [48] V. Cirigliano, M.J. Ramsey-Musolf, S. Tulin and C. Lee, *Yukawa and tri-scalar processes in electroweak baryogenesis*, *Phys. Rev. D* **73** (2006) 115009 [[hep-ph/0603058](#)] [[INSPIRE](#)].
- [49] G.A. White, *General analytic methods for solving coupled transport equations: from cosmology to beyond*, *Phys. Rev. D* **93** (2016) 043504 [[arXiv:1510.03901](#)] [[INSPIRE](#)].
- [50] M. Carena, M. Quirós, M. Seco and C.E.M. Wagner, *Improved results in supersymmetric electroweak baryogenesis*, *Nucl. Phys. B* **650** (2003) 24 [[hep-ph/0208043](#)] [[INSPIRE](#)].
- [51] J.M. Cline, M. Joyce and K. Kainulainen, *Supersymmetric electroweak baryogenesis*, *JHEP* **07** (2000) 018 [[hep-ph/0006119](#)] [[INSPIRE](#)].
- [52] D. Bödeker, G.D. Moore and K. Rummukainen, *Chern-Simons number diffusion and hard thermal loops on the lattice*, *Phys. Rev. D* **61** (2000) 056003 [[hep-ph/9907545](#)] [[INSPIRE](#)].
- [53] G.D. Moore and K. Rummukainen, *Classical sphaleron rate on fine lattices*, *Phys. Rev. D* **61** (2000) 105008 [[hep-ph/9906259](#)] [[INSPIRE](#)].
- [54] G.D. Moore, *Sphaleron rate in the symmetric electroweak phase*, *Phys. Rev. D* **62** (2000) 085011 [[hep-ph/0001216](#)] [[INSPIRE](#)].
- [55] ACME collaboration, J. Baron et al., *Order of magnitude smaller limit on the electric dipole moment of the electron*, *Science* **343** (2014) 269 [[arXiv:1310.7534](#)] [[INSPIRE](#)].
- [56] L. Bian, T. Liu and J. Shu, *Cancellations between two-loop contributions to the electron electric dipole moment with a CP-violating Higgs sector*, *Phys. Rev. Lett.* **115** (2015) 021801 [[arXiv:1411.6695](#)] [[INSPIRE](#)].
- [57] A. Crivellin, S. Najjari and J. Rosiek, *Lepton flavor violation in the Standard Model with general dimension-six operators*, *JHEP* **04** (2014) 167 [[arXiv:1312.0634](#)] [[INSPIRE](#)].
- [58] B.C. Regan, E.D. Commins, C.J. Schmidt and D. DeMille, *New limit on the electron electric dipole moment*, *Phys. Rev. Lett.* **88** (2002) 071805 [[INSPIRE](#)].
- [59] W.C. Griffith, M.D. Swallows, T.H. Loftus, M.V. Romalis, B.R. Heckel and E.N. Fortson, *Improved limit on the permanent electric dipole moment of  $^{199}\text{Hg}$* , *Phys. Rev. Lett.* **102** (2009) 101601 [[INSPIRE](#)].
- [60] J.M. Pendlebury et al., *Revised experimental upper limit on the electric dipole moment of the neutron*, *Phys. Rev. D* **92** (2015) 092003 [[arXiv:1509.04411](#)] [[INSPIRE](#)].

- [61] C.A. Baker et al., *An improved experimental limit on the electric dipole moment of the neutron*, *Phys. Rev. Lett.* **97** (2006) 131801 [[hep-ex/0602020](#)] [[INSPIRE](#)].
- [62] S.M. Barr and A. Zee, *Electric dipole moment of the electron and of the neutron*, *Phys. Rev. Lett.* **65** (1990) 21 [*Erratum ibid.* **65** (1990) 2920] [[INSPIRE](#)].
- [63] N. Yamanaka, *Analysis of the electric dipole moment in the R-parity violating supersymmetric Standard Model*, Ph.D. thesis, Osaka U., Springer, Japan, (2013) [[INSPIRE](#)].
- [64] N. Yamanaka, T. Sato and T. Kubota, *A reappraisal of two-loop contributions to the fermion electric dipole moments in R-parity violating supersymmetric models*, *Phys. Rev. D* **85** (2012) 117701 [[arXiv:1202.0106](#)] [[INSPIRE](#)].
- [65] D. Stöckinger, *The muon magnetic moment and supersymmetry*, *J. Phys. G* **34** (2007) R45 [[hep-ph/0609168](#)] [[INSPIRE](#)].
- [66] R.G. Leigh, S. Paban and R.M. Xu, *Electric dipole moment of electron*, *Nucl. Phys. B* **352** (1991) 45 [[INSPIRE](#)].
- [67] T. Abe, J. Hisano, T. Kitahara and K. Tobioka, *Gauge invariant Barr-Zee type contributions to fermionic EDMs in the two-Higgs doublet models*, *JHEP* **01** (2014) 106 [*Erratum ibid.* **04** (2016) 161] [[arXiv:1311.4704](#)] [[INSPIRE](#)].
- [68] M. Jung and A. Pich, *Electric dipole moments in two-Higgs-doublet models*, *JHEP* **04** (2014) 076 [[arXiv:1308.6283](#)] [[INSPIRE](#)].
- [69] D. Bowser-Chao, D. Chang and W.-Y. Keung, *Electron electric dipole moment from CP-violation in the charged Higgs sector*, *Phys. Rev. Lett.* **79** (1997) 1988 [[hep-ph/9703435](#)] [[INSPIRE](#)].
- [70] W. Altmannshofer, J. Brod and M. Schmaltz, *Experimental constraints on the coupling of the Higgs boson to electrons*, *JHEP* **05** (2015) 125 [[arXiv:1503.04830](#)] [[INSPIRE](#)].
- [71] S. Profumo, M.J. Ramsey-Musolf and G. Shaughnessy, *Singlet Higgs phenomenology and the electroweak phase transition*, *JHEP* **08** (2007) 010 [[arXiv:0705.2425](#)] [[INSPIRE](#)].
- [72] H.H. Patel and M.J. Ramsey-Musolf, *Baryon washout, electroweak phase transition and perturbation theory*, *JHEP* **07** (2011) 029 [[arXiv:1101.4665](#)] [[INSPIRE](#)].
- [73] H.H. Patel and M.J. Ramsey-Musolf, *Stepping into electroweak symmetry breaking: phase transitions and Higgs phenomenology*, *Phys. Rev. D* **88** (2013) 035013 [[arXiv:1212.5652](#)] [[INSPIRE](#)].
- [74] S. Tulin and P. Winslow, *Anomalous B meson mixing and baryogenesis*, *Phys. Rev. D* **84** (2011) 034013 [[arXiv:1105.2848](#)] [[INSPIRE](#)].



## Chapter 9

---

# Conclusions and future work

---

Electroweak baryogenesis is a field where there is a large amount of work to be done. There is only one numerical toolkit available publicly which only covers a few of the calculations need [106]. There has been limited work on multistep phase transitions [11]. There is also much work to be done on examining the baryogenesis compatible parameter space of popular BSM models. Very little work has been done in the context of effective field theory to directly use experimental limits to confine higher dimensional CP violating operators. This in particular is a sub-field in its infancy as the validity range and scope of EFT requires study. The scale of new physics in preliminary studies was found to be surprisingly high. Nonetheless if these theoretical questions can be answered it presents an exciting opportunity to directly link EDM constraints to baryogenesis calculations. Finally, gravitational waves provide an exciting new direction to test physics at energy not otherwise accessible on Earth through colliders.

In this thesis I have focused energy on each of these directions with an eye to the bigger picture of particle cosmology. Having said that, there is much work to be done in each of these directions. On the effective field theory front, one needs to thoroughly examine the validity limits of effective field theory as has been done for dark matter. Furthermore the fate of operator degeneracies needs to be understood on a deeper level. Finally there needs to be a systematic study of all CP violating higher dimensional operators in the Standard Model and in the case of extended scalar sectors.

In the case of testing baryogenesis within existing particle physics models, in some soon to be published work, I examine the charged transport dynamics during the electroweak phase transition in the NMSSM. In this work I find that the baryon asymmetry can be very different if the singlet acquires a vacuum expectation value before or during the electroweak phase transition. Furthermore, others [97] have found that the parameter  $\Delta\beta$ , which the baryon asymmetry is proportional to, can be an order of magnitude higher in the NMSSM compared to its MSSM value. There is ample motivation to perform a scan where the transport dynamics and the properties of the phase transition are examined simultaneously. Such a work naturally ties into the need for better numerical tools. I am in the process with several collaborators of developing a numerical toolkit that has enough flexibility to perform multiple baryogenesis calculations: from phase transitions, to EDMs, to deriving and solving coupled transport equations.

In the case of extending the vanilla electroweak baryogenesis scenario to multi-step phase transitions, again, very little has been done before this thesis. I have some soon to be published work where I look at the case where  $SU(3)_C$  is spontaneously broken and then restored through the addition of leptoquark scalars. I demonstrate that this is still a testable framework and secondly that the baryon asymmetry can be produced during the colour break phase transition. A nice extension to the work done here would be to explore the experimental signatures more deeply. For instance, two step phase transitions can leave relic charge asymmetries. In the case I test the charge asymmetry is many orders of magnitude lower than current observational bounds. Perhaps there is a scenario where this asymmetry is large enough to be testable in the near future. Secondly anomalous violation of lepton flavour violation was recently explained through the leptoquark representation I used [138]. Understanding the impact on flavour physics of the colour breaking paradigm would be a rich extension to our project and there is already evidence that such a leptoquark might exist.

Finally gravitational wave detectors provide a useful avenue to test the whole multistep paradigm. This is particularly important as the key phase transition that catalyzes the production of a baryon asymmetry might involve scalar particles far too heavy to be seen by either this or the next generations of particle colliders but might be detectable through gravitational wave detectors. Ligo is sensitive to cosmic phase transitions at an unusual energy scale but it is expected to be sensitive to relic gravitational backgrounds from cosmic phase transitions many decades earlier. I have written the first work outlining a physical motivation for a cosmic phase transition at such a scale but if there are other physical motivations that would be worth exploring.

---

# Bibliography

---

- [1] Luis Alvarez-Gaume, J. Polchinski, and Mark B. Wise. Minimal Low-Energy Supergravity. *Nucl. Phys.*, B221:495, 1983.
- [2] Nima Arkani-Hamed, Savas Dimopoulos, and G. R. Dvali. The Hierarchy problem and new dimensions at a millimeter. *Phys. Lett.*, B429:263–272, 1998.
- [3] Lisa Randall and Raman Sundrum. A Large mass hierarchy from a small extra dimension. *Phys. Rev. Lett.*, 83:3370–3373, 1999.
- [4] N. Arkani-Hamed, A. G. Cohen, E. Katz, and A. E. Nelson. The Littlest Higgs. *JHEP*, 07:034, 2002.
- [5] Peter W. Graham, David E. Kaplan, and Surjeet Rajendran. Cosmological Relaxation of the Electroweak Scale. *Phys. Rev. Lett.*, 115(22):221801, 2015.
- [6] Nima Arkani-Hamed, Tao Han, Michelangelo Mangano, and Lian-Tao Wang. Physics opportunities of a 100 TeV proton–proton collider. *Phys. Rept.*, 652:1–49, 2016.
- [7] Graham Albert White. *A Pedagogical Introduction to Electroweak Baryogenesis*. IOP Concise Physics. Morgan Claypool, 2016.
- [8] Alan H. Guth. The Inflationary Universe: A Possible Solution to the Horizon and Flatness Problems. *Phys. Rev.*, D23:347–356, 1981.
- [9] Ashutosh V. Kotwal, Michael J. Ramsey-Musolf, Jose Miguel No, and Peter Winslow. Singlet-catalyzed electroweak phase transitions in the 100 TeV frontier. *Phys. Rev.*, D94(3):035022, 2016.
- [10] Chiara Caprini et al. Science with the space-based interferometer eLISA. II: Gravitational waves from cosmological phase transitions. *JCAP*, 1604(04):001, 2016.
- [11] Satoru Inoue, Grigory Ovanesyan, and Michael J. Ramsey-Musolf. Two-Step Electroweak Baryogenesis. *Phys. Rev.*, D93:015013, 2016.
- [12] P. S. Bhupal Dev and A. Mazumdar. Probing the Scale of New Physics by Advanced LIGO/VIRGO. *Phys. Rev.*, D93(10):104001, 2016.

- [13] Antony Lewis and Anthony Challinor. Weak gravitational lensing of the cmb. *Phys. Rept.*, 429:1–65, 2006.
- [14] Maxim Markevitch, A. H. Gonzalez, D. Clowe, A. Vikhlinin, L. David, W. Forman, C. Jones, S. Murray, and W. Tucker. Direct constraints on the dark matter self-interaction cross-section from the merging galaxy cluster 1E0657-56. *Astrophys. J.*, 606:819–824, 2004.
- [15] R. Bernabei et al. Investigation on light dark matter. *Mod. Phys. Lett.*, A23:2125–2140, 2008.
- [16] D. S. Akerib et al. Results from a search for dark matter in the complete LUX exposure. *Phys. Rev. Lett.*, 118(2):021303, 2017.
- [17] Andi Tan et al. Dark Matter Results from First 98.7 Days of Data from the PandaX-II Experiment. *Phys. Rev. Lett.*, 117(12):121303, 2016.
- [18] Nima Arkani-Hamed and Juan Maldacena. *Cosmological Collider Physics*. 2015.
- [19] A. Matyja et al. Observation of  $B^0 \rightarrow D^{*-} \tau^+ \nu(\tau)$  decay at Belle. *Phys. Rev. Lett.*, 99:191807, 2007.
- [20] I. Adachi et al. Measurement of  $B \rightarrow D^{(*)} \tau \nu$  using full reconstruction tags. In *Proceedings, 24th International Symposium on Lepton-Photon Interactions at High Energy (LP09): Hamburg, Germany, August 17-22, 2009*, 2009.
- [21] J. P. Lees et al. Evidence for an excess of  $\bar{B} \rightarrow D^{(*)} \tau^- \bar{\nu}_\tau$  decays. *Phys. Rev. Lett.*, 109:101802, 2012.
- [22] J. P. Lees et al. Measurement of an Excess of  $\bar{B} \rightarrow D^{(*)} \tau^- \bar{\nu}_\tau$  Decays and Implications for Charged Higgs Bosons. *Phys. Rev.*, D88(7):072012, 2013.
- [23] Michel Davier, Andreas Hoecker, Bogdan Malaescu, and Zhiqing Zhang. Reevaluation of the Hadronic Contributions to the Muon  $g-2$  and to  $\alpha(M_Z)$ . *Eur. Phys. J.*, C71:1515, 2011. [Erratum: *Eur. Phys. J.* C72,1874(2012)].
- [24] Michael E. Peskin and Daniel V. Schroeder. *An Introduction to quantum field theory*. 1995.
- [25] C. Balazs, Marcela Carena, A. Menon, D. E. Morrissey, and C. E. M. Wagner. The Supersymmetric origin of matter. *Phys. Rev.*, D71:075002, 2005.
- [26] Stephen P. Martin. A Supersymmetry primer. 1997. [Adv. Ser. Direct. High Energy Phys. 18,1(1998)].
- [27] Philip W. Anderson. Plasmons, Gauge Invariance, and Mass. *Phys. Rev.*, 130:439–442, 1963.
- [28] Peter W. Higgs. Broken Symmetries and the Masses of Gauge Bosons. *Phys. Rev. Lett.*, 13:508–509, 1964.

- [29] F. Zwicky. Die Rotverschiebung von extragalaktischen Nebeln. *Helv. Phys. Acta*, 6:110–127, 1933. [Gen. Rel. Grav.41,207(2009)].
- [30] V. C. Rubin, N. Thonnard, and W. K. Ford, Jr. Rotational properties of 21 SC galaxies with a large range of luminosities and radii, from NGC 4605 /R = 4kpc/ to UGC 2885 /R = 122 kpc/. *Astrophys. J.*, 238:471, 1980.
- [31] Vera C. Rubin and W. Kent Ford, Jr. Rotation of the Andromeda Nebula from a Spectroscopic Survey of Emission Regions. *Astrophys. J.*, 159:379–403, 1970.
- [32] M. S. Roberts and A. H. Rots. Comparison of Rotation Curves of Different Galaxy Types. *aap*, 26:483–485, August 1973.
- [33] G. Hinshaw et al. Nine-Year Wilkinson Microwave Anisotropy Probe (WMAP) Observations: Cosmological Parameter Results. *Astrophys. J. Suppl.*, 208:19, 2013.
- [34] Gerard Jungman, Marc Kamionkowski, and Kim Griest. Supersymmetric dark matter. *Phys. Rept.*, 267:195–373, 1996.
- [35] L. Dolan and R. Jackiw. Symmetry Behavior at Finite Temperature. *Phys. Rev.*, D9:3320–3341, 1974.
- [36] Gian Francesco Giudice. Naturally Speaking: The Naturalness Criterion and Physics at the LHC. 2008.
- [37] Sidney R. Coleman and J. Mandula. All Possible Symmetries of the S Matrix. *Phys. Rev.*, 159:1251–1256, 1967.
- [38] Steven Weinberg. *The quantum theory of fields. Vol. 3: Supersymmetry*. Cambridge University Press, 2013.
- [39] H. Baer and X. Tata. *Weak scale supersymmetry: From superfields to scattering events*. Cambridge University Press, 2006.
- [40] P Labelle. *Supersymmetry DeMYSTiFieD*. McGraw Hill, 2010.
- [41] Ulrich Ellwanger, Cyril Hugonie, and Ana M. Teixeira. The Next-to-Minimal Supersymmetric Standard Model. *Phys. Rept.*, 496:1–77, 2010.
- [42] Howard E. Haber and Ralf Hempfling. Can the mass of the lightest Higgs boson of the minimal supersymmetric model be larger than  $m(Z)$ ? *Phys. Rev. Lett.*, 66:1815–1818, 1991.
- [43] A. Arbey, M. Battaglia, A. Djouadi, F. Mahmoudi, and J. Quevillon. Implications of a 125 GeV Higgs for supersymmetric models. *Phys. Lett.*, B708:162–169, 2012.
- [44] Csaba Balazs, Andy Buckley, Daniel Carter, Benjamin Farmer, and Martin White. Should we still believe in constrained supersymmetry? *Eur. Phys. J.*, C73:2563, 2013.

- [45] Ali Cici, Zerrin Kirca, and Cem Salih Un. Light Stops and Fine-Tuning in MSSM. 2016.
- [46] Graham G. Ross, Kai Schmidt-Hoberg, and Florian Staub. Revisiting fine-tuning in the MSSM. 2017.
- [47] Stefan Liebler, Stefano Profumo, and Tim Stefaniak. Light Stop Mass Limits from Higgs Rate Measurements in the MSSM: Is MSSM Electroweak Baryogenesis Still Alive After All? *JHEP*, 04:143, 2016.
- [48] Rouzbeh Allahverdi, Bhaskar Dutta, and Anupam Mazumdar. Probing the parameter space for an MSSM inflation and the neutralino dark matter. *Phys. Rev.*, D75:075018, 2007.
- [49] Sayantan Choudhury, Anupam Mazumdar, and Supratik Pal. Low & High scale MSSM inflation, gravitational waves and constraints from Planck. *JCAP*, 1307:041, 2013.
- [50] Keith A. Olive and Marco Peloso. The Fate of SUSY flat directions and their role in reheating. *Phys. Rev.*, D74:103514, 2006.
- [51] Arindam Chatterjee and Anupam Mazumdar. Tuned MSSM Higgses as an inflaton. *JCAP*, 1109:009, 2011.
- [52] Kari Enqvist and Anupam Mazumdar. Cosmological consequences of MSSM flat directions. *Phys. Rept.*, 380:99–234, 2003.
- [53] Rouzbeh Allahverdi, Kari Enqvist, Juan Garcia-Bellido, and Anupam Mazumdar. Gauge invariant MSSM inflaton. *Phys. Rev. Lett.*, 97:191304, 2006.
- [54] R. Jeannerot. Inflation in supersymmetric unified theories. *Phys. Rev.*, D56:6205–6216, 1997.
- [55] J. C. Bueno Sanchez, Konstantinos Dimopoulos, and David H. Lyth. A-term inflation and the MSSM. *JCAP*, 0701:015, 2007.
- [56] G. F. Giudice and A. Romanino. Split supersymmetry. *Nucl. Phys.*, B699:65–89, 2004. [Erratum: *Nucl. Phys.*B706,487(2005)].
- [57] Takeo Moroi and Lisa Randall. Wino cold dark matter from anomaly mediated SUSY breaking. *Nucl. Phys.*, B570:455–472, 2000.
- [58] Joakim Edsjo and Paolo Gondolo. Neutralino relic density including coannihilations. *Phys. Rev.*, D56:1879–1894, 1997.
- [59] John R. Ellis, Keith A. Olive, Yudi Santoso, and Vassilis C. Spanos. Supersymmetric dark matter in light of WMAP. *Phys. Lett.*, B565:176–182, 2003.
- [60] John R. Ellis, Toby Falk, and Keith A. Olive. Neutralino - Stau coannihilation and the cosmological upper limit on the mass of the lightest supersymmetric particle. *Phys. Lett.*, B444:367–372, 1998.

- [61] Howard Baer and Michal Brhlik. Neutralino dark matter in minimal supergravity: Direct detection versus collider searches. *Phys. Rev.*, D57:567–577, 1998.
- [62] Utpal Chattopadhyay, Achille Corsetti, and Pran Nath. WMAP constraints, SUSY dark matter and implications for the direct detection of SUSY. *Phys. Rev.*, D68:035005, 2003.
- [63] Jonathan L. Feng, Arvind Rajaraman, and Fumihiro Takayama. SuperWIMP dark matter signals from the early universe. *Phys. Rev.*, D68:063504, 2003.
- [64] M. E. Gomez, George Lazarides, and C. Pallis. Supersymmetric cold dark matter with Yukawa unification. *Phys. Rev.*, D61:123512, 2000.
- [65] Toby Falk, Keith A. Olive, and Mark Srednicki. Heavy sneutrinos as dark matter. *Phys. Lett.*, B339:248–251, 1994.
- [66] Ian Affleck and Michael Dine. A New Mechanism for Baryogenesis. *Nucl. Phys.*, B249:361–380, 1985.
- [67] P. John and M. G. Schmidt. Do stops slow down electroweak bubble walls? *Nucl. Phys.*, B598:291–305, 2001. [Erratum: *Nucl. Phys.*B648,449(2003)].
- [68] P. A. R. Ade et al. Planck 2013 results. XVI. Cosmological parameters. *Astron. Astrophys.*, 571:A16, 2014.
- [69] James M. Cline. Baryogenesis. In *Les Houches Summer School - Session 86: Particle Physics and Cosmology: The Fabric of Spacetime Les Houches, France, July 31-August 25, 2006*, 2006.
- [70] A D Sakharov. Violation of CP invariance, C asymmetry, and baryon asymmetry of the universe. *J. Exper. Theor. Phys.*, 5:24–7, 1967.
- [71] A D Sakharov. Violation of CP invariance, C asymmetry, and baryon asymmetry of the universe. *Sov. Phys Usp.*, 34:392–3, 1991.
- [72] David E. Morrissey and Michael J. Ramsey-Musolf. Electroweak baryogenesis. *New J. Phys.*, 14:125003, 2012.
- [73] Mark Trodden. Electroweak baryogenesis. *Rev. Mod. Phys.*, 71:1463–1500, 1999.
- [74] Kimmo Kainulainen, Tomislav Prokopec, Michael G. Schmidt, and Steffen Weinstock. Semiclassical force for electroweak baryogenesis: Three-dimensional derivation. *Phys. Rev.*, D66:043502, 2002.
- [75] Kimmo Kainulainen, Tomislav Prokopec, Michael G. Schmidt, and Steffen Weinstock. First principle derivation of semiclassical force for electroweak baryogenesis. *JHEP*, 06:031, 2001.
- [76] Julian S. Schwinger. Brownian motion of a quantum oscillator. *J. Math. Phys.*, 2:407–432, 1961.

- [77] Kalyana T. Mahanthappa. Multiple production of photons in quantum electrodynamics. *Phys. Rev.*, 126:329–340, 1962.
- [78] Pradip M. Bakshi and Kalyana T. Mahanthappa. Expectation value formalism in quantum field theory. 1. *J. Math. Phys.*, 4:1–11, 1963.
- [79] Pradip M. Bakshi and Kalyana T. Mahanthappa. Expectation value formalism in quantum field theory. 2. *J. Math. Phys.*, 4:12–16, 1963.
- [80] L. V. Keldysh. Diagram technique for nonequilibrium processes. *Zh. Eksp. Teor. Fiz.*, 47:1515–1527, 1964. [Sov. Phys. JETP20,1018(1965)].
- [81] Kuang-chao Chou, Zhao-bin Su, Bai-lin Hao, and Lu Yu. Equilibrium and Nonequilibrium Formalisms Made Unified. *Phys. Rept.*, 118:1, 1985.
- [82] Ashok K. Das. *Finite Temperature Field Theory*. World Scientific, New York, 1997.
- [83] Peter Millington and Apostolos Pilaftsis. Perturbative nonequilibrium thermal field theory. *Phys. Rev.*, D88(8):085009, 2013.
- [84] Steven Weinberg. Gauge and Global Symmetries at High Temperature. *Phys. Rev.*, D9:3357–3378, 1974.
- [85] Sidney R. Coleman and Erick J. Weinberg. Radiative Corrections as the Origin of Spontaneous Symmetry Breaking. *Phys. Rev.*, D7:1888–1910, 1973.
- [86] Michael Dine, Robert G. Leigh, Patrick Y. Huet, Andrei D. Linde, and Dmitri A. Linde. Towards the theory of the electroweak phase transition. *Phys. Rev.*, D46:550–571, 1992.
- [87] Mariano Quiros. Finite temperature field theory and phase transitions. In *Proceedings, Summer School in High-energy physics and cosmology: Trieste, Italy, June 29-July 17, 1998*, pages 187–259, 1999.
- [88] Sidney R. Coleman. The Fate of the False Vacuum. 1. Semiclassical Theory. *Phys. Rev.*, D15:2929–2936, 1977. [Erratum: *Phys. Rev.*D16,1248(1977)].
- [89] Curtis G. Callan, Jr. and Sidney R. Coleman. The Fate of the False Vacuum. 2. First Quantum Corrections. *Phys. Rev.*, D16:1762–1768, 1977.
- [90] Andrei D. Linde. Fate of the False Vacuum at Finite Temperature: Theory and Applications. *Phys. Lett.*, B100:37–40, 1981.
- [91] Andrei D. Linde. Decay of the False Vacuum at Finite Temperature. *Nucl. Phys.*, B216:421, 1983. [Erratum: *Nucl. Phys.*B223,544(1983)].
- [92] Christopher Lee, Vincenzo Cirigliano, and Michael J. Ramsey-Musolf. Resonant relaxation in electroweak baryogenesis. *Phys. Rev.*, D71:075010, 2005.
- [93] Vincenzo Cirigliano, Michael J. Ramsey-Musolf, Sean Tulin, and Christopher Lee. Yukawa and tri-scalar processes in electroweak baryogenesis. *Phys. Rev.*, D73:115009, 2006.

- [94] Daniel J. H. Chung, Bjorn Garbrecht, Michael.J. Ramsey-Musolf, and Sean Tulin. Supergauge interactions and electroweak baryogenesis. *JHEP*, 12:067, 2009.
- [95] Sean Tulin and Peter Winslow. Anomalous  $B$  meson mixing and baryogenesis. *Phys. Rev.*, D84:034013, 2011.
- [96] J. E. Camargo-Molina, B. O’Leary, W. Porod, and F. Staub. Vevacious: A Tool For Finding The Global Minima Of One-Loop Effective Potentials With Many Scalars. *Eur. Phys. J.*, C73(10):2588, 2013.
- [97] Jonathan Kozaczuk, Stefano Profumo, Laurel Stephenson Haskins, and Carroll L. Wainwright. Cosmological Phase Transitions and their Properties in the NMSSM. *JHEP*, 01:144, 2015.
- [98] Vincenzo Branchina, Emanuele Messina, and Marc Sher. Lifetime of the electroweak vacuum and sensitivity to Planck scale physics. *Phys. Rev.*, D91:013003, 2015.
- [99] Peter Brockway Arnold. Can the Electroweak Vacuum Be Unstable? *Phys. Rev.*, D40:613, 1989.
- [100] Andrey Shkerin and Sergey Sibiryakov. On stability of electroweak vacuum during inflation. *Phys. Lett.*, B746:257–260, 2015.
- [101] Luigi Delle Rose, Carlo Marzo, and Alfredo Urbano. On the fate of the Standard Model at finite temperature. *JHEP*, 05:050, 2016.
- [102] Jaume Garriga, Alexander Vilenkin, and Jun Zhang. Non-singular bounce transitions in the multiverse. *JCAP*, 1311:055, 2013.
- [103] Stefano Profumo, Michael J. Ramsey-Musolf, Carroll L. Wainwright, and Peter Winslow. Singlet-catalyzed electroweak phase transitions and precision Higgs boson studies. *Phys. Rev.*, D91(3):035018, 2015.
- [104] Stefano Profumo, Lorenzo Ubaldi, and Carroll Wainwright. Singlet Scalar Dark Matter: monochromatic gamma rays and metastable vacua. *Phys. Rev.*, D82:123514, 2010.
- [105] Peter John. Bubble wall profiles with more than one scalar field: A Numerical approach. *Phys. Lett.*, B452:221–226, 1999.
- [106] Carroll L. Wainwright. CosmoTransitions: Computing Cosmological Phase Transition Temperatures and Bubble Profiles with Multiple Fields. *Comput. Phys. Commun.*, 183:2006–2013, 2012.
- [107] Georges Aad et al. Observation of a new particle in the search for the Standard Model Higgs boson with the ATLAS detector at the LHC. *Phys. Lett.*, B716:1–29, 2012.
- [108] Serguei Chatrchyan et al. Observation of a new boson at a mass of 125 GeV with the CMS experiment at the LHC. *Phys. Lett.*, B716:30–61, 2012.

- [109] Hiren H. Patel and Michael J. Ramsey-Musolf. Baryon Washout, Electroweak Phase Transition, and Perturbation Theory. *JHEP*, 07:029, 2011.
- [110] Hsin-Chia Cheng and Ian Low. TeV symmetry and the little hierarchy problem. *JHEP*, 09:051, 2003.
- [111] B. P. Abbott et al. Observation of Gravitational Waves from a Binary Black Hole Merger. *Phys. Rev. Lett.*, 116(6):061102, 2016.
- [112] Sichun Sun. Inflationary electroweak/particle phase transitions and new classical gravitational waves on CMB. In *Proceedings, 2nd LeCosPA Symposium: Everything about Gravity, Celebrating the Centenary of Einstein's General Relativity (LeCosPA2015): Taipei, Taiwan, December 14-18, 2015*, pages 168–174, 2017.
- [113] Ariel Megevand and Santiago Ramirez. Bubble nucleation and growth in very strong cosmological phase transitions. 2016.
- [114] Ville Vaskonen. Electroweak baryogenesis and gravitational waves from a real scalar singlet. 2016.
- [115] Michał Artymowski, Marek Lewicki, and James D. Wells. Gravitational wave and collider implications of electroweak baryogenesis aided by non-standard cosmology. 2016.
- [116] Wei Chao, Huai-Ke Guo, and Jing Shu. Gravitational Wave Signals of Electroweak Phase Transition Triggered by Dark Matter. 2017.
- [117] Iason Baldes. Gravitational waves from the asymmetric-dark-matter generating phase transition. 2017.
- [118] David Alejandro Tamayo Ramírez. *Gravitational Waves in Decaying Vacuum Cosmologies*. PhD thesis, Sao Paulo U., 2015.
- [119] Fa Peng Huang and Xinmin Zhang. Probing the hidden gauge symmetry breaking through the phase transition gravitational waves. 2017.
- [120] Michele Maggiore. Gravitational wave experiments and early universe cosmology. *Phys. Rept.*, 331:283–367, 2000.
- [121] Marc Kamionkowski, Arthur Kosowsky, and Michael S. Turner. Gravitational radiation from first order phase transitions. *Phys. Rev.*, D49:2837–2851, 1994.
- [122] Arthur Kosowsky, Michael S. Turner, and Richard Watkins. Gravitational radiation from colliding vacuum bubbles. *Phys. Rev.*, D45:4514–4535, 1992.
- [123] Makoto Kobayashi and Toshihide Maskawa. CP Violation in the Renormalizable Theory of Weak Interaction. *Prog. Theor. Phys.*, 49:652–657, 1973.
- [124] Sidney R. Coleman and Sheldon L. Glashow. High-energy tests of Lorentz invariance. *Phys. Rev.*, D59:116008, 1999.
- [125] B. Grzadkowski, M. Iskrzynski, M. Misiak, and J. Rosiek. Dimension-Six Terms in the Standard Model Lagrangian. *JHEP*, 10:085, 2010.

- [126] A. Liam Fitzpatrick, Wick Haxton, Emanuel Katz, Nicholas Lubbers, and Yiming Xu. The Effective Field Theory of Dark Matter Direct Detection. *JCAP*, 1302:004, 2013.
- [127] Giorgio Busoni, Andrea De Simone, Enrico Morgante, and Antonio Riotto. On the Validity of the Effective Field Theory for Dark Matter Searches at the LHC. *Phys. Lett.*, B728:412–421, 2014.
- [128] Asher Berlin, Dan Hooper, and Samuel D. McDermott. Simplified Dark Matter Models for the Galactic Center Gamma-Ray Excess. *Phys. Rev.*, D89(11):115022, 2014.
- [129] Jalal Abdallah et al. Simplified Models for Dark Matter and Missing Energy Searches at the LHC. 2014.
- [130] Matthew R. Buckley, David Feld, and Dorival Goncalves. Scalar Simplified Models for Dark Matter. *Phys. Rev.*, D91:015017, 2015.
- [131] Oliver Buchmueller, Matthew J. Dolan, Sarah A. Malik, and Christopher McCabe. Characterising dark matter searches at colliders and direct detection experiments: Vector mediators. *JHEP*, 01:037, 2015.
- [132] Jalal Abdallah et al. Simplified Models for Dark Matter Searches at the LHC. *Phys. Dark Univ.*, 9-10:8–23, 2015.
- [133] Philip Harris, Valentin V. Khoze, Michael Spannowsky, and Ciaran Williams. Constraining Dark Sectors at Colliders: Beyond the Effective Theory Approach. *Phys. Rev.*, D91:055009, 2015.
- [134] Jonathan Engel, Michael J. Ramsey-Musolf, and U. van Kolck. Electric Dipole Moments of Nucleons, Nuclei, and Atoms: The Standard Model and Beyond. *Prog. Part. Nucl. Phys.*, 71:21–74, 2013.
- [135] Yingchuan Li, Stefano Profumo, and Michael Ramsey-Musolf. A Comprehensive Analysis of Electric Dipole Moment Constraints on CP-violating Phases in the MSSM. *JHEP*, 08:062, 2010.
- [136] Oleg Lebedev and Maxim Pospelov. Electric dipole moments in the limit of heavy superpartners. *Phys. Rev. Lett.*, 89:101801, 2002.
- [137] Timothy Chupp and Michael Ramsey-Musolf. Electric Dipole Moments: A Global Analysis. *Phys. Rev.*, C91(3):035502, 2015.
- [138] Peter Cox, Alexander Kusenko, Olcyr Sumensari, and Tsutomu T. Yanagida. SU(5) Unification with TeV-scale Leptoquarks. 2016.

□